

UNCLASSIFIED

MARION MARCIETTA ENERGY SYSTEMS LIBRARIES



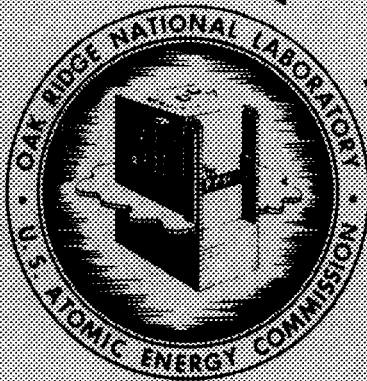
3 4456 0250821 2

CENTRAL RESEARCH LIBRARY
DOCUMENT COLLECTION

ORNL-2309
Physics and Mathematics
TID-4500 (13th ed.)

Cof 4

CONFERENCE ON NEUTRON PHYSICS BY TIME-OF-FLIGHT
HELD AT GATLINBURG, TENNESSEE
NOVEMBER 1 AND 2, 1956



CENTRAL RESEARCH LIBRARY
DOCUMENT COLLECTION
LIBRARY LOAN COPY
DO NOT TRANSFER TO ANOTHER PERSON
If you wish someone else to see this document, send in name with document and the library will arrange a loan.

OAK RIDGE NATIONAL LABORATORY

OPERATED BY

UNION CARBIDE NUCLEAR COMPANY

A Division of Union Carbide and Carbon Corporation



POST OFFICE BOX X · OAK RIDGE, TENNESSEE

UNCLASSIFIED

Printed in USA. Price 1.00 cents. Available from the

Office of Technical Services
U. S. Department of Commerce
Washington 25, D. C.

LEGAL NOTICE

This report was prepared as an account of Government sponsored work. Neither the United States, nor the Commission, nor any person acting on behalf of the Commission:

- A. Makes any warranty or representation, express or implied, with respect to the accuracy, completeness, or usefulness of the information contained in this report, or that the use of any information, apparatus, method, or process disclosed in this report may not infringe privately owned rights; or
- B. Assumes any liabilities with respect to the use of, or for damages resulting from the use of any information, apparatus, method, or process disclosed in this report.

As used in the above, "person acting on behalf of the Commission" includes any employee or contractor of the Commission to the extent that such employee or contractor prepares, handles or distributes, or provides access to, any information pursuant to his employment or contract with the Commission.

UNCLASSIFIED

ORNL-2309

Contract No. W-7405-eng-26

PHYSICS DIVISION

CONFERENCE ON NEUTRON PHYSICS BY TIME-OF-FLIGHT

HELD AT GATLINBURG, TENNESSEE

NOVEMBER 1 AND 2, 1956

DATE ISSUED

JUN 12 1957

OAK RIDGE NATIONAL LABORATORY
Operated by
UNION CARBIDE NUCLEAR COMPANY
A Division of Union Carbide and Carbon Corporation
Post Office Box X
Oak Ridge, Tennessee

MARTIN MARIETTA ENERGY SYSTEMS LIBRARIES



3 4456 0250821 2

UNCLASSIFIED

UNCLASSIFIED

ORNL-2309
Physics and Mathematics
TID-4500 (13th ed.)

INTERNAL DISTRIBUTION

1. C. E. Center
2. Biology Library
3. Health Physics Library
- 4-6. Central Research Library
7. Reactor Experimental Engineering Library
- 8-19. Laboratory Records Department
20. Laboratory Records, ORNL R.C.
21. A. M. Weinberg
22. L. B. Emler (K-25)
23. J. P. Murray (Y-12)
24. J. A. Swartout
25. E. H. Taylor
26. E. D. Shipley
27. E. J. Murphy
28. M. L. Nelson
29. A. H. Snell
30. A. Hollaender
31. K. Z. Morgan
32. F. L. Culler
33. M. T. Kelley
34. E. M. King
35. E. O. Wollan
36. D. W. Cardwell
37. A. S. Householder
38. L. D. Roberts
39. R. B. Briggs
40. R. N. Lyon
41. W. C. Koehler
42. E. P. Blizard
43. M. E. Rose
44. G. E. Boyd
45. W. H. Sullivan
46. R. W. Stoughton
47. C. E. Winters
48. W. H. Jordan
49. E. C. Campbell
50. D. S. Billington
51. M. A. Bredig
52. R. S. Livingston
53. C. P. Keim
54. F. C. Maienschein
55. C. E. Clifford
56. R. C. Block
57. C. D. Susano
58. C. J. Borkowski
59. M. J. Skinner
60. M. K. Wilkinson
61. J. W. Cable
62. P. M. Reyling
63. H. W. Schmitt
64. W. M. Good
65. G. C. Williams
66. J. L. Fowler
67. G. T. Trammell
68. J. R. McNally, Jr.
69. J. L. Gabbard
70. R. A. Charpie
71. E. P. Wigner (consultant)
72. G. G. Slaughter
73. Eugene Guth
74. R. W. Peelle
75. P. R. Bell
76. G. G. Kelley
77. C. C. Harris
78. H. G. MacPherson
79. P. H. Stelson
80. J. E. Sherwood
81. W. Zobel
82. R. B. Murray
83. H. B. Willard
84. J. Schenck
85. J. H. Neiler
86. J. A. Harvey
87. C. F. Barnett
88. N. H. Lazar
89. R. R. Dickison
90. A. Simon
91. J. H. Gibbons
92. J. J. Pinajian
93. S. Bernstein
94. H. A. Bethe (consultant)
95. ORNL - Y-12 Technical Library,
Document Reference Section

EXTERNAL DISTRIBUTION

96. R. F. Bacher, California Institute of Technology
97. Division of Research and Development, AEC, ORO
- 98-672. Given distribution as shown in TID-4500 (13th ed.) under Physics and Mathematics category (100 copies - OTS)

UNCLASSIFIED

FOREWORD

A conference on neutron physics by time-of-flight was held at Gatlinburg, Tennessee, November 1 and 2, 1956. The program consisted of talks by invited speakers and contributed remarks from participants. The subject matter covered new experimental results and the interpretation of resonance parameters, elastic and inelastic scattering, and fission.

A complete stenotypic record was made at the time of the conference, and it forms the basis of the following report of the proceedings. Since the verbatim record was 465 pages long, with 190 slides, the program committee subsequently requested each speaker to reduce the length of his contribution. Most of the speakers revised their talks in compliance and often added a little additional pertinent information. Where appropriate, most of the discussion has been incorporated into the talk itself. Questions and discussion arising merely from misunderstandings have been deleted. The final responsibility for any inaccuracies or errors rests with the editors.

The conference was organized by a committee consisting of A. H. Snell, chairman, W. M. Good, and J. A. Harvey. The expert assistance of D. D. Cowen was indispensable to the smooth functioning of the meeting, and the hospitality of Union Carbide Nuclear Company is gratefully acknowledged.

The Editors:

R. C. Block
W. M. Good
J. A. Harvey
H. W. Schmitt
G. T. Trammell

CONTENTS

SESSION I. EXPERIMENTAL AND THEORETICAL LOW-ENERGY NEUTRON PHYSICS

Welcome	3
A. M. Weinberg Oak Ridge National Laboratory	
Nuclear Size by Potential-Scattering Cross Sections	5
K. K. Seth Brookhaven National Laboratory	
Ratio of Neutron Width to Level Spacing.....	10
R. L. Zimmerman Brookhaven National Laboratory	
Gamma Radiation from Resonance Neutron Capture in Mercury	13
H. H. Landon and E. R. Rae Brookhaven National Laboratory	
Studies on the Resonances in U^{238} Using the High-Resolution Nevis Synchrocyclotron Neutron Velocity Spectrometer	19
W. W. Havens, Jr., J. Rainwater, S. Desjardins, and J. Rosen Columbia University	
Analysis of Nevis Neutron Time-of-Flight Data on Silver Resonance Levels by Recently Improved Techniques	27
E. Melkonian Columbia University	
Neutron Resonance Parameters of Eu^{151} and Eu^{153}	38
J. A. Harvey and R. C. Block Oak Ridge National Laboratory	
Performance and Some Results from the Harwell Neutron Spectrometer Based on the Linear Electron Accelerator	41
E. Bretscher Atomic Energy Research Establishment, Harwell	
Contributions of Neutron Time-of-Flight Experimentation to Low-Energy Neutron Physics	48
D. J. Hughes Brookhaven National Laboratory	
Results and Theory of Resonance Absorption	59
E. P. Wigner Princeton University	
Nucleon Densities in a Diffuse-Boundary Independent-Particle Model.....	71
A. E. S. Green Florida State University	
SESSION II. ELASTIC AND INELASTIC NEUTRON SCATTERING	
Inelastic Scattering of Fast Neutrons in Rhodium and Niobium.....	77
M. A. Rothman Bartol Research Foundation	

Inelastic Scattering from Tantalum, Tungsten, and Gold	84
J. S. Levin and L. Cranberg Los Alamos Scientific Laboratory	
Gamma Rays from Inelastic Scattering by Zr ⁹⁴ and Pt ¹⁹⁴	90
R. B. Day Los Alamos Scientific Laboratory	
Time-of-Flight Neutron Scattering with the Brookhaven National Laboratory Small Cyclotron.....	95
C. O. Muehlhause Brookhaven National Laboratory	
Back-Angle Elastic Scattering with 14-Mev Neutrons	97
C. Wong, J. D. Anderson, C. C. Gardner, and M. P. Nakada University of California Radiation Laboratory, Livermore	
Elastic and Inelastic Scattering of Fast Neutrons.....	103
R. V. Smith Westinghouse Research Laboratory	
Comments on Neutron Scattering.....	108
H. Feshbach Massachusetts Institute of Technology	
SESSION III. EXPERIMENTAL AND THEORETICAL LOW- AND INTERMEDIATE-ENERGY NEUTRON PHYSICS	
Widths and Spacings of Nuclear Resonance Levels	113
A. M. Lane Atomic Energy Research Establishment, Harwell	
Fluctuations in Average Neutron Cross Sections.....	124
P. A. Egelstaff Atomic Energy Research Establishment, Harwell	
Discussion on Cross-Section Measurements in the keV Region	129
R. E. Coté	129
Argonne National Laboratory	
W. W. Havens, Jr.	130
Columbia University	
J. H. Gibbons	130
Oak Ridge National Laboratory	
H. W. Newson	138
Duke University	
The Oak Ridge National Laboratory Fast-Chopper Program.....	145
R. C. Block Oak Ridge National Laboratory	
Isolation of Cyclotron Beam Bunches for Neutron Spectroscopy	146
J. E. Draper Brookhaven National Laboratory	

New System for Fast-Neutron Cross-Section Measurements	148
L. Cranberg, W. P. Aiello, R. K. Beauchamp, H. J. Lang, J. S. Levin, and J. E. Midgley Los Alamos Scientific Laboratory	
Harwell Superchopper	153
P. A. Egelstaff Atomic Energy Research Establishment, Harwell	
SESSION IV. EXPERIMENTAL AND THEORETICAL FISSION PHYSICS	
Anomalies and Regularities in Fission	157
J. A. Wheeler Princeton University	
Problems and Progress in Measuring Cross Sections of Fissile Nuclei.....	167
L. M. Bollinger Argonne National Laboratory	
Low-Energy Fission Measurements of Pu^{240}	179
B. R. Leonard, E. J. Seppi, and W. J. Friesen Hanford Atomic Products Operation, General Electric Company	
Asymmetry of Resonance Levels in Fissile Target Nuclei	182
P. A. Egelstaff and N. Pattenden Atomic Energy Research Establishment, Harwell	
Initial Results on the Fission Cross Section of U^{233}	184
L. G. Miller, R. M. Brugger, and R. G. Fluharty Phillips Petroleum Company	
Fission and Capture Cross Section of U^{235} for Slow Neutrons	187
F. J. Shore and V. L. Sailor Brookhaven National Laboratory	
Velocities of Coincident Pairs of Fragments in the Spontaneous Fission of Cf^{252}	188
J. S. Fraser and J. C. D. Milton Atomic Energy of Canada Limited, Chalk River	
Resonance Parameters of U^{235}	192
R. B. Schwartz Brookhaven National Laboratory	
LIST OF PARTICIPANTS	197

•
•

•
•

•
•

SESSION I

EXPERIMENTAL AND THEORETICAL LOW-ENERGY NEUTRON PHYSICS

WELCOME

A. M. Weinberg
Director, Oak Ridge National Laboratory

A. M. WEINBERG: I should like to welcome you most sincerely on behalf of the Oak Ridge National Laboratory of the Union Carbide Nuclear Company and the Oak Ridge office of the Atomic Energy Commission. We hope that your stay here will be a pleasant one.

My purpose in taking these few minutes to talk to you is in some sense perhaps one of subversion; namely, I think that these will be the only remarks that will be made during the conference which speak to the question of the relevance of what you are doing and of the matters which you will discuss here to other than purely scientific issues. The fact of the matter is that in two fields, astrophysics and reactor physics, the questions of the resonance structure of fissionable nuclei and of other nuclei have suddenly taken on an importance which perhaps had not been originally foreseen, and I will take just one moment to indicate how this comes about.

Those of you who listened to Professor Gamow's talk last night recognized the generally held view nowadays as to how elements, at least many elements, are manufactured; that is, that they are manufactured in much the same way that we manufacture isotopes in the man-made reactors, except that these reactors in which the elements are manufactured are not man-made. They are God-made, and they are stars rather than reactors, and instead of being thermal-neutron reactors they are resonance-neutron reactors.

I refer to the fact that in many of the stars the temperatures reach the order of 10 keV, and hence the elements produced under these circumstances are produced by the absorption of 10-keV neutrons. The probability of absorption and, therefore, the inverse probability of the formation of elements are consequently determined by the average neutron cross section of the elements in the kilovolt region.

I realize that there are some difficulties in this view, but I quote it as being the one that is generally held and the one that the reactor physicists have found to be the most intriguing, since it indicates, if you like, that when God

decided to manufacture man he also put into man the device for manufacturing elements in much the same way that God himself manufactures elements; namely, we put the target nuclei into our reactors; he puts them into his star resonance reactors. But the point remains that the strength functions and cross sections in this region apparently have very high relevance to astrophysics at the present.

For the same reason, the strength functions and details of the cross sections become more and more important in application to reactor problems, for the reason that more and more of the reactors which we are dealing with nowadays are small, compact reactors, devices which in order to be made small must have a large fraction of fissionable material, and, therefore, they are devices in which the average neutron spectrum tends to be pushed up into the resonance region. In consequence one finds more and more, in the reactor literature, very direct use being made of the detailed and general information which is coming out of the vast amount of time-of-flight work which is being done today.

Perhaps the most recent use of this information is a question which many of you may have seen discussed in the newspapers. You are probably all acquainted with the fact that there is proposed a large-scale fast reactor to be built near Detroit, and there seems to be some objection to the building of this fast reactor on the grounds that it cannot be demonstrated completely unequivocally that it will have a negative temperature coefficient, and I need not mention to you what the consequences of its having a positive temperature coefficient might be.

It is rather interesting that at least two of the distinguished participants in this purely scientific conference (I refer to Dr. Lane and Dr. Feshbach) have been involved in the question of estimating the temperature coefficient for such fast resonance reactors, and in both cases the information which they have had to use has been information on the statistics of the levels, the spacing, the strength functions, and similar quantities both for the fissionable and the nonfissionable materials.

Well, as I said, I think this is probably the only time in the next two days that anybody will talk to you about the relevance of what you are doing to the applied rather than the basic part of nuclear science, and so I thought I would take four of my five minutes to state my views on the matter.

I should like to repeat that we are very pleased that all of you have been able to find your way to Gatlinburg, although not without some travail, and we hope that you have a pleasant time here in Gatlinburg.

NUCLEAR SIZE BY POTENTIAL-SCATTERING CROSS SECTIONS

K. K. Seth
Brookhaven National Laboratory

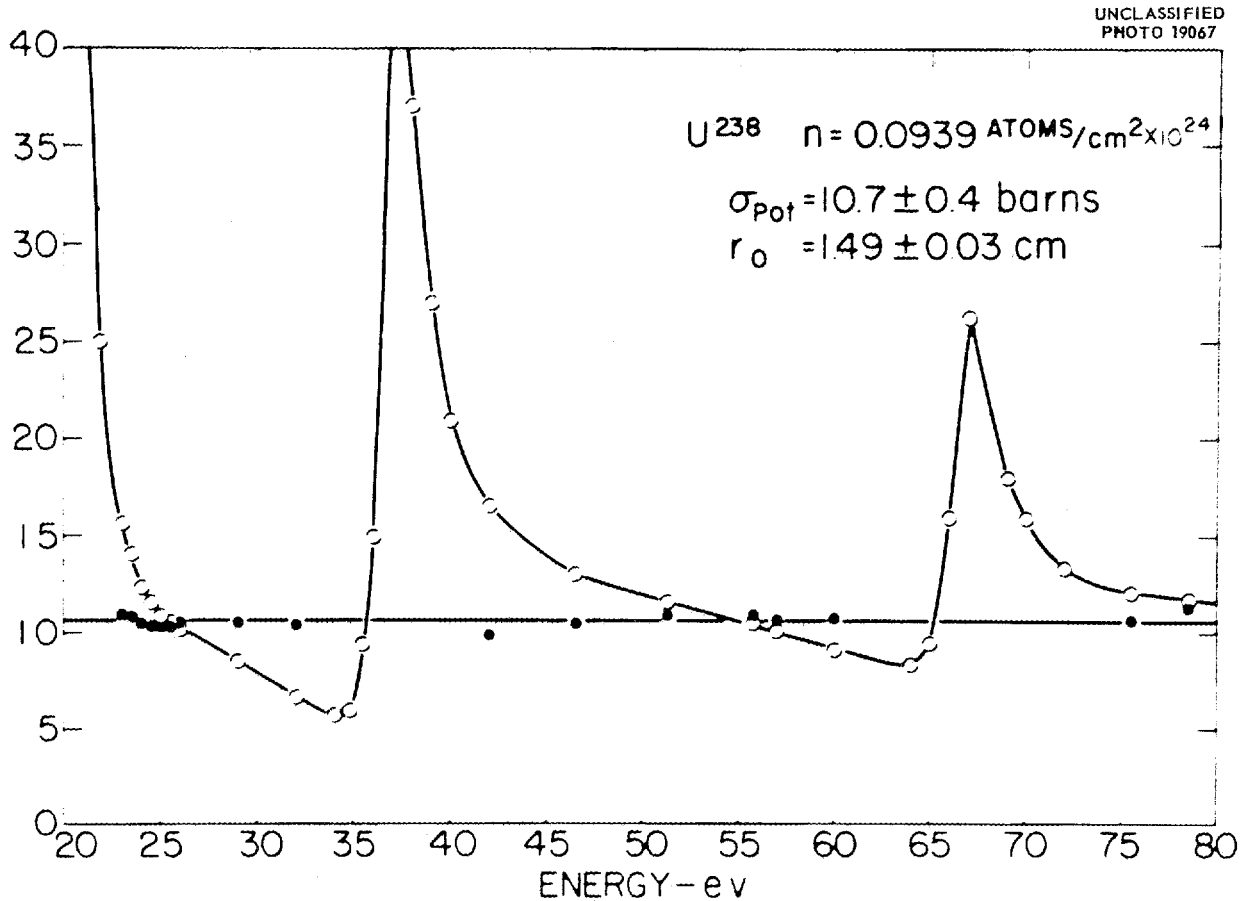
K. K. SETH: This talk is divided into two parts; the first, in which I propose to describe how a systematic and accurate determination of neutron potential-scattering cross section, σ_p , has been made for various elements, employing the Brookhaven fast chopper, and the second in which I propose to describe how we have salvaged a measure of nuclear size out of it.

It may be noted that I have preferred to use the comparatively vague term "nuclear size" rather than "nuclear radius." This is so because I believe the use of the latter term at this stage of the game is fraught with the grave danger of dragging one into embarrassing controversy.

At Brookhaven we have used two different methods to determine σ_p in two different energy ranges;

the so-called "between-resonances" method in the ev range, and the "averaging" method in the kev range.

The "between-resonances" method makes use of the simple fact that in the low-energy region (1 to 100 ev) potential scattering is observed between resonances but is affected by the interference of potential and resonance scattering, their amplitudes being added coherently. In cases where the parameters of adjoining resonances are known with reasonable accuracy, such contributions can be calculated and can be subtracted from the measured total cross section in this region. This was done for thirteen elements (from $A = 89$ to 238). Slide 1 shows the results of a typical analysis of this type. The single-level



Slide 1. Total Cross Section of U^{238} .

Breit-Wigner formula was used to calculate the contribution of resonance scattering and interference scattering to the total cross section, σ_T . The remarkably constant cross section (solid circles) obtained by subtraction of this contribution from σ_T (open circles) is a good proof of the soundness of this procedure. Table 1 lists the results of this method for the other elements investigated so far.

The second or so-called "averaging" method is based on the measurement of average transmission, T_{av} , for kev neutrons for different sample thicknesses, n . This is facilitated by the fact that, at kev energies, the chopper loses most of its resolution anyway, and the measurement of σ_T with a wide channel width automatically yields T_{av} rather than T .

The theoretical basis of the method deserves some mention. In a hypothetical element with no resonance structure, potential scattering is the only way of removing neutrons from the incident

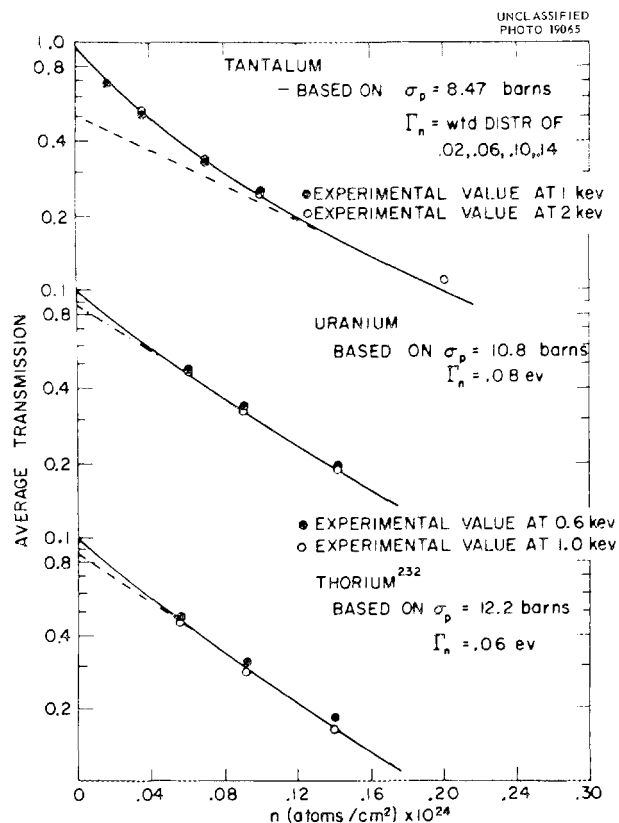
beam, so that $T = \exp(-n\sigma_p)$. Thus the slope of a logarithmic plot of transmission vs thickness, $d \ln T/dn$, is equal to σ_p . In any real case, however, the element has a resonance structure with its characteristic strength function, $\langle \Gamma_n^0/D \rangle$, and the above simple relation no longer holds true. In such a case one has to consider the effect of resonances in some detail.

Consider, then, a plot of $\log T_{av}$ vs n (Slide 2). It starts at $T_{av} = 1$ for $n = 0$, in any case. Then it has an initial slope greater than σ_p , because, in addition to potential scattering, resonances are also effective in removing neutrons selectively from the beam. As n increases, however, the steepness of the curve gradually decreases. This is because each additional thickness of sample does not remove neutrons to the same extent — simply because it sees fewer and fewer of them at each stage. Very soon all neutrons at the exact resonance energy, E_0 , are removed, and $T = 0$ at E_0 . Any further increase in n does not affect

Table 1. Potential-Scattering Cross Sections and Scattering Lengths for 13 Elements

Element	σ_p (barns)	R' (cm)
		$\times 10^{-13}$
Y	7.3 ± 0.5	7.6 ± 0.3
Zr	7.3 ± 0.6	7.6 ± 0.3
Nb	6.2 ± 0.1	7.02 ± 0.05
Ag	$6.2 \pm 0.4^*$	$6.90 \pm 0.25^*$
Sn	4.35 ± 0.05	5.90 ± 0.03
Te	4.9 ± 0.3	6.2 ± 0.2
Ta	8.45 ± 0.8	8.2 ± 0.4
	$8.5 \pm 0.8^*$	$8.25 \pm 0.4^*$
Au	11.8 ± 1.0	9.8 ± 0.3
Tl	9.8 ± 0.8	8.85 ± 0.4
Pb	11.3 ± 0.2	9.5 ± 0.1
Bi	10.2 ± 0.8	9.0 ± 0.4
Th	11.8 ± 0.7	9.7 ± 0.3
	$12.2 \pm 0.8^*$	$9.85 \pm 0.3^*$
U	10.7 ± 0.4	9.25 ± 0.2
	$10.8 \pm 0.5^*$	$9.27 \pm 0.2^*$

*Values obtained by the "averaging" method.



Slide 2. Average Transmissions of Tantalum, Uranium, and Th²³² for Varying Sample Thicknesses.

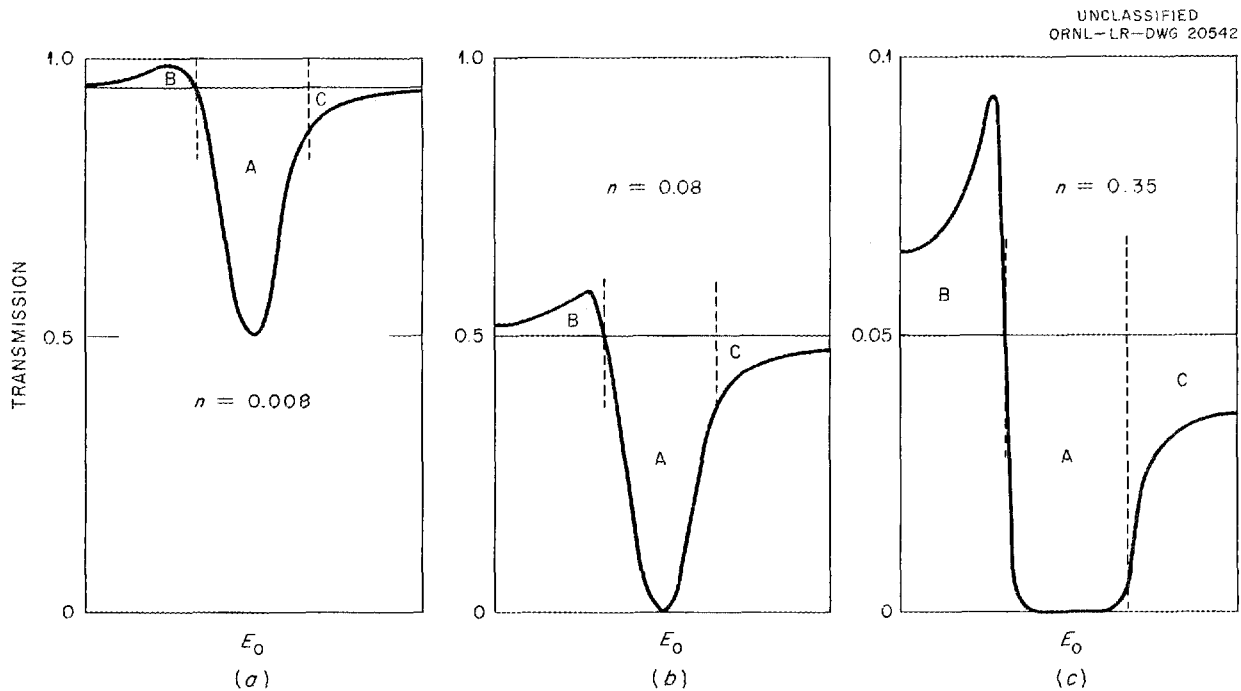
neutrons at E_0 , because none are left to be affected, and potential scattering once again remains the only way of removing neutrons from the beam. The slope of the $\log T_{av}$ vs n plot therefore levels off to σ_p .

The slope henceforth would remain equal to σ_p , were it not for the so-called "window effect." This effect arises from the fact that the Breit-Wigner resonance is not symmetrical about E_0 , but looks like Slide 3a. The resonance dip, A, in a transmission plot is accompanied by a window, B, and a tail, C, on either side. As the sample thickness increases, the normalized areas in A, B, and C increase proportionately only as long as the stage shown in Slide 3b is not reached. After this, the proportionality is disturbed as the resonance starts "blackening out" (Slide 3c), that is, the growth of the main body, A, is stunted by the physical limit $T = 0$, while that of parts B and C is not. Still in general B and C continue to balance each other, their contributions to the total area being nearly equal and opposite. However, soon the tail, C, also starts feeling the effect of the so-called blackening out, but the window remains free to grow relative to the transmission resulting from σ_p . The curve $\log T_{av}$ vs n of Slide 2 there-

fore gradually assumes a slope less steep than σ_p . This is scarcely noticeable in the lower two curves. In the top curve for tantalum it is slightly more obvious, because the solid theoretical curve was calculated using a distribution of Γ_n^0 's, as indicated, rather than an average value. Of course in any case the effect becomes more pronounced for a greater value of Γ_n^0 .

The results of these experiments on tantalum, silver, thorium, and uranium are included in Table I and are seen to agree very well with the results of the "between-resonances" method. This is not surprising, since in essence the two methods are equivalent. In the first case we remove the resonance contribution by calculating and subtracting it. In the second case we do it by letting the initial thickness of the sample remove the resonance neutrons. What is worth noting, however, is that the agreement exists, in spite of the fact that the two experiments are done in different energy regions. This casts serious doubt on the suggestion sometimes ventured that potential scattering might be an energy-dependent phenomenon.

Let us now turn our attention to what this measurement of σ_p might mean. In classical terms, σ_p



Slide 3. The Transmission of a Sample Undergoing a Breit-Wigner Resonance for Varying Sample Thicknesses.

corresponds to the cross section for scattering from a hard sphere of the same radius, R , as the nucleus. Thus for s -wave neutrons, $\sigma_p = 4\pi R^2$. It is well known, however, that a real nucleus is not exactly a hard, impenetrable sphere - it is to an extent absorbing as well. Such a nucleus is the subject of two equivalent models, Wigner's giant-resonance model and the less abstruse cloudy-crystal-ball model of Feshbach, Porter, and Weisskopf.

Feshbach, Porter, and Weisskopf, in their latest calculations,¹ replace the nucleus by a rounded-edge partially absorbing potential well of the form:

$$V = \frac{-V_0(1 + i\xi)}{1 + \exp[2(r - R)/d]}$$

¹V. F. Weisskopf, *Physica* 22, 952 (1956).

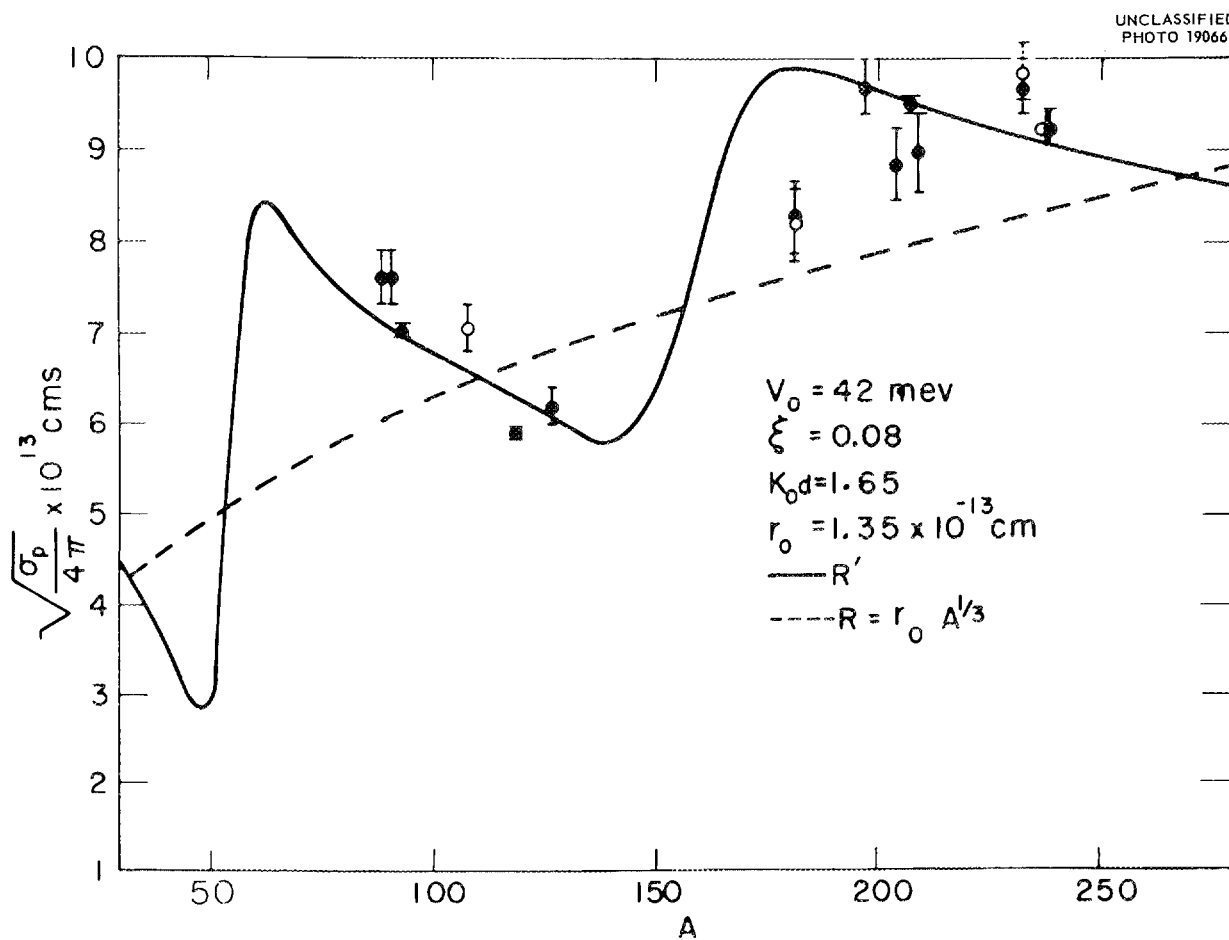
Here the symbols have their usual meaning; and their best-fit values, derived from total cross sections, angular distributions, and $\langle \Gamma_n^0/D \rangle$, are those in Slide 4. According to this model,

$$\sigma_p = 4\pi R'^2,$$

where

$$R' = R \left(1 + \frac{r_{aa}}{K_\alpha R} \right).$$

Here r_{aa} is the weakly energy-dependent contribution of faraway levels and R' is a scattering length which possesses a resonance structure for a weakly absorbing nucleus. The theoretical ratio R'/R is rather insensitive to the choice of well parameters (with a weak dependence through the combination $V_0 R^2$) and hence, for a given



Slide 4. Experimentally Determined Nuclear Radii Compared to the Prediction of the Diffuse-Edge Complex-Well-Potential Model.

experimental value of R' , may be expected to lead to rather reliable values of the nuclear radius R .

Slide 4 shows the theoretical curve (based on the 42-Mev-deep well, with $r_0 = 1.35 \times 10^{-13}$ cm and the values of other parameters as fixed by various data on neutron scattering) and also the experimental results, full circles representing values obtained by the "between-resonances" method and open circles those by the "averaging" method (see also Table 1). As already pointed out, it is seen that the results of the two methods agree very well. It may be noted that at the moment the errors on individual points are much greater than would be desirable. However, one conclusion is easily drawn. The experimental points show much better qualitative agreement with the theoretical R' curve (with maxima and minima) than with the uniform-radius R curve (dashed), which is also shown in Slide 4.² The magnitude of the experimental errors and the lack of enough points limit the usefulness of this experiment at present, but we hope that, in time, it will have important bearing in assessing the over-all soundness of the cloudy-crystal-ball model, and even in the choice of certain parameters. It may also be expected to shed some direct light on the importance of nuclear deformations, on shell effects in heavy nuclei, and on the relationship between the different measurements of nuclear "radii."

Amongst some obviously interesting and unexplained facts, I might mention the rather large differences in σ_p between neighboring nuclei like Ag^{107} and Ag^{109} or bismuth, lead, and thallium. However, preliminary calculations of McVoy and others show that nuclear deformations might have a very noticeable effect on R' in certain regions of A .

In conclusion, let me mention that though the tentative value, $r_0 = 1.35 \times 10^{-13}$ cm, used here is admittedly different from the Hofstadter charge

²Radii of four other elements have been determined since this talk was given, and, as pointed out by the author in a paper presented at the American Physical Society at New York [*Bull. Am. Phys. Soc.* 2, 42 (1957)], the results are consistent with the above remarks.

radius, $r_0 = 1.07 \times 10^{-13}$ cm, this should cause no great concern. On the basis of very elementary reasoning, one expects nuclear force or channel radius to be larger than nuclear charge radius. However, one also expects (based on a theory due to Drell) this difference to be reduced as one goes to relativistic energies. Some preliminary experiments of Cool *et al.* at Brookhaven on the absorption cross sections of various elements for 970-Mev π^- mesons give them $r_0 = 1.13 \times 10^{-13}$ cm, while some cosmic-ray experiments in the region around 20 Bev seem to lead to $r_0 \approx 1.10 \times 10^{-13}$ cm. This is all very hopeful.

E. GUTH: I should like to use the occasion to make a quick, rather short comment of general interest. Your results are compared with the cloudy-crystal-ball model with the diffuse-edge potential. In general you find the statement in the literature that agreement with the square well may not be so good, but if you diffuse it, it will get better. It seems to me that maybe there is a slight misunderstanding. If you diffuse the edge, it can play a role only with the low-energy scattering. It does not play much of a role with the high-energy scattering. The same is true for the bound states which were investigated by Alex Green. It made a difference only in the low-energy limits and not in the higher-energy limits, and therefore it seems to me that comparison with the square well should be almost as good as with the diffuse well.

Since one of the chief originators of the cloudy-crystal-ball model, Herman Feshbach, is our Chairman, I am glad to ask him to correct any statement that I have made with which he does not agree.

H. FESHBACH: Well, I don't want to open up a debate on the cloudy crystal ball at the moment. One remark I want to make is that I believe that the s states would be affected, and these experiments are on s states.

The other remark I would make is that we are still playing with the parameters that Seth mentioned to see how they will fit the entire panorama of scattering, elastic scattering, total cross section, etc., and the diffuse edge is very essential for this. We are now going up into several Mev, and these are still not our best fit.

RATIO OF NEUTRON WIDTH TO LEVEL SPACING

R. L. Zimmerman
Brookhaven National Laboratory

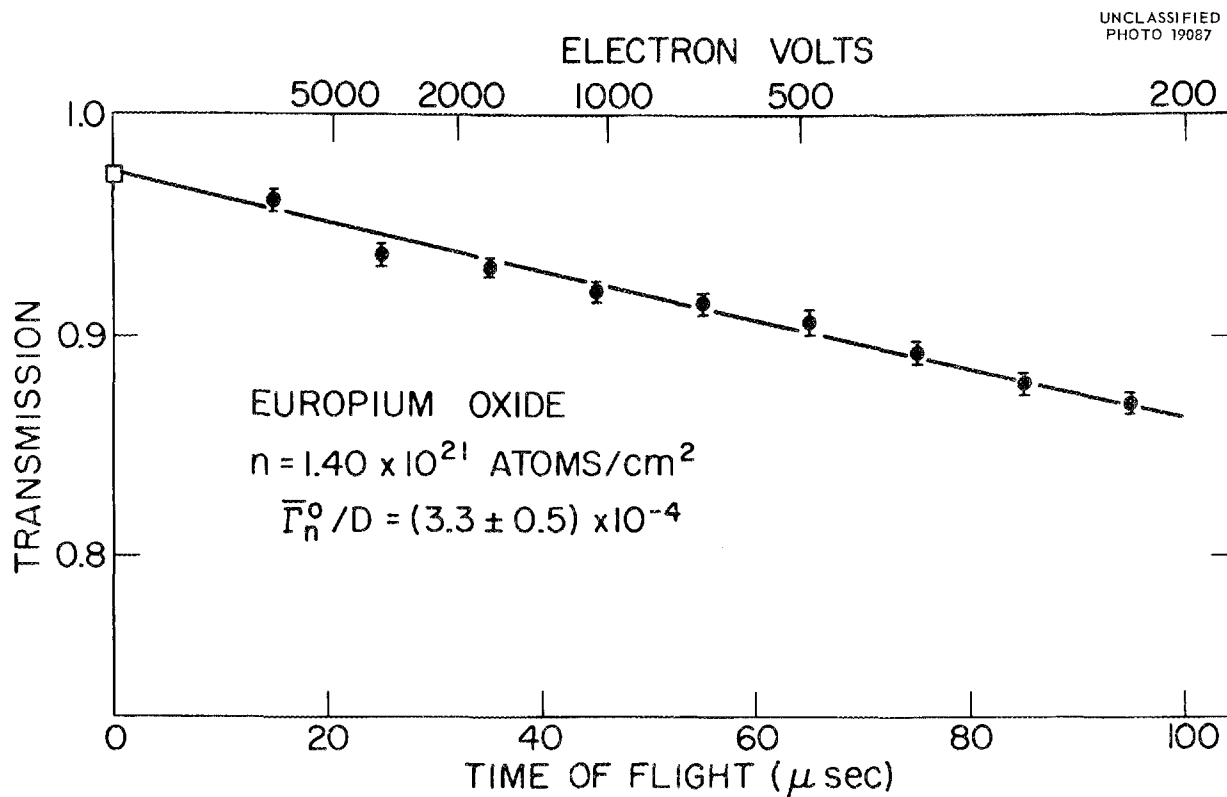
R. L. ZIMMERMAN: The Brookhaven fast chopper has been used in two methods of measuring the neutron strength function, $\langle \Gamma_n^0/D \rangle$. For several years we have measured total neutron cross sections in the electron-volt region, where individual resonances are resolved. The parameters of each resonance were obtained by detailed analysis. The first method of getting $\langle \Gamma_n^0/D \rangle$ consisted of averaging these parameters of individual resonances in a given isotope over as wide an energy region as we could cover while still resolving individual resonances.

In addition, during the past year we have been exploiting another method, in which we measure the total neutron cross section in the kilovolt energy region, where individual levels are not resolved and the cross section is an average over the contributions of many levels.

Slide 1 shows the experimental data for europium. Our flight path is 20 m, so that 46 μ sec corresponds to 1000 ev. The errors shown on the points are the statistical errors only. Not shown are the errors arising from fluctuations in the number and strength of levels over which a given point is averaged, but these errors are negligible for all but the points at long time of flight.

The square symbol denotes the fraction of the neutrons taken out of the beam by potential scattering in europium oxide. (In separate experiments we will use this point to determine the potential scattering; however, in such experiments the sample thickness will be larger, and some knowledge of $\langle \Gamma_n^0/D \rangle$ will be used to make the extrapolation to zero time of flight.)

The fraction of neutrons taken out of the beam by resonances is simply $2.8tn \langle \Gamma_n^0/D \rangle$, where



Slide 1. Europium Oxide Transmission in the kev Region.

t is the time of flight in microseconds and n is the sample thickness. The constant is independent of energy. It follows that the method consists of taking the slope of the transmission in the kilovolt energy region. No absolute accuracy is required in the data.

In order that we are not restricted to analytically thin samples where there is no self-protection by the larger resonances, a small correction is made involving the transmission and the level spacing. Corrections are typically smaller than 1% of the observed transmission, even at the longer times of flight.

Slide 2 shows the experimentally measured values of $\langle \Gamma_n^0/D \rangle$ plotted against the atomic weight of the isotopes we used. The solid curve is a calculation made by Charles Porter using a diffuse-surface cloudy-crystal-ball model,

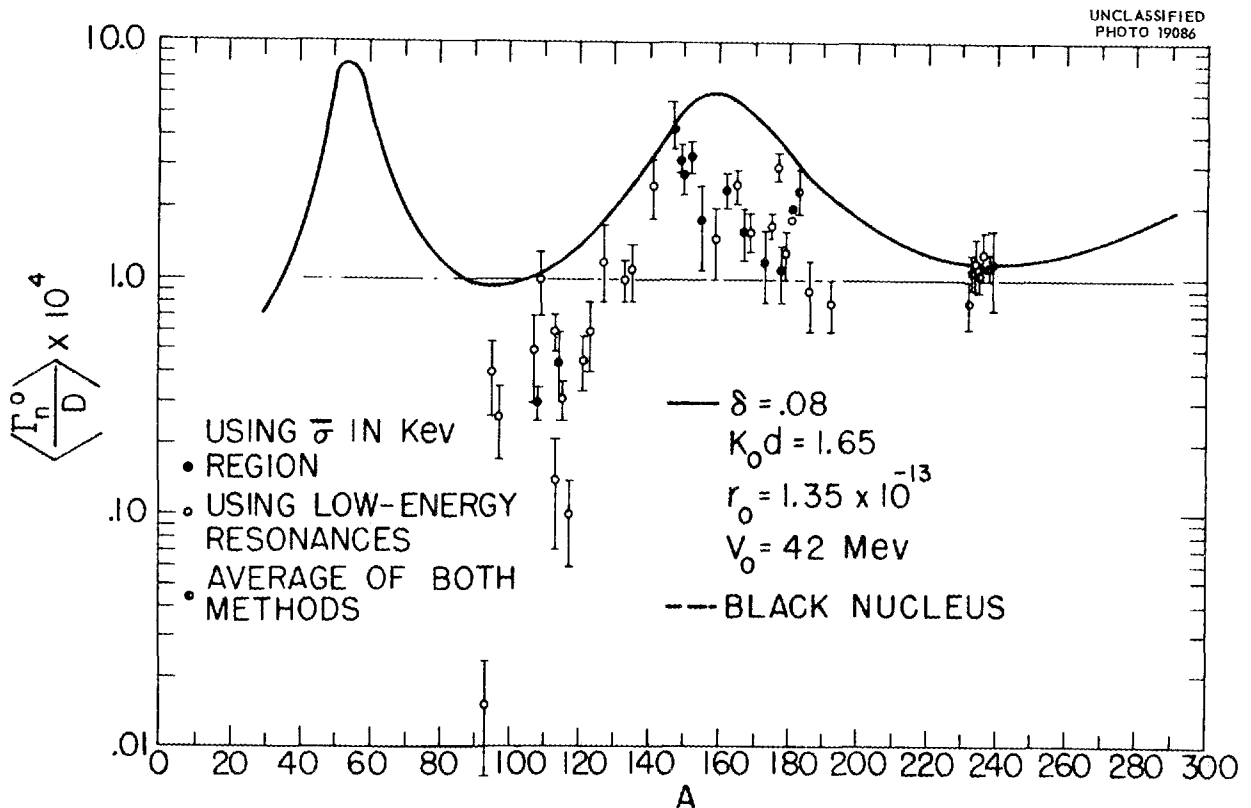
$$V = \frac{-V_0(1 + i\zeta)}{1 + \exp[2(r - R)/d]}$$

with the parameters shown in the caption.

The general nature of the variation of $\langle \Gamma_n^0/D \rangle$ with atomic weight is confirmed by this calculation but there seems to be a significant asymmetry in values on either side of the peak that is not obtained even with other possible values of the cloudy-crystal-ball parameters.

H. FESHBACH: I will try to discuss the parameters in the cloudy-crystal-ball diffuse-surface potential to which both Zimmerman and Seth referred. It is, of course, an attractive well. Zeta is the part that tells you the complex part of the potential, and we again make the assumption that both the complex and the real part of the potential have the same spatial distribution. The spatial distribution is given by a Wigner well, and the diffuseness of the surface is measured by d .

By varying the parameters we can change the theoretical curve in Slide 2, but it will be very hard to get a decrease of a factor of five, which



Slide 2. Experimentally Measured Strength Functions Compared to Strength Functions Calculated from a Diffuse-Edge Complex Well Potential.

is needed in the region of $A = 100$, without destroying the fit at other atomic weights.

E. GUTH: In spite of the fact that the cloudy crystal ball is a very nice tool, I believe that you should not push the agreement to disagreement by comparing the experiment too closely with its theoretical predictions.

A. M. WEINBERG: Do the experimental data about $A = 55$ also fall below the theoretical curve?

R. L. ZIMMERMAN: The data that we have on it from other laboratories overlapped with the theoretical peak, but the errors were quite large.

H. GOLDSTEIN: Do you make the assumption that the radiation width is large compared to the neutron width?

R. L. ZIMMERMAN: No assumptions like that are made. The derivation of the formula is very simple and involves only the total width and the peak cross section as a product which, except for the energy term, is exactly proportional to Γ_n .

P. A. EGELSTAFF: Last year, using our fast chopper, we made a very similar set of measurements, using the average over many resonances and the intercept at zero time of flight to get the nuclear radius. In these measurements it was necessary to apply just these corrections you have been talking about. As far as I can see from the curves we have seen this morning, the agreement between our measurements and yours is very good. But I should like to ask Dr. Zimmerman if he has made a detailed comparison.

R. L. ZIMMERMAN: We have made checks with data from other laboratories and the agreement is good.

H. W. NEWSON: The points which fall very low around $A = 100$ are in a region where the p -wave contribution is very high. Could some of the discrepancy come from confusing the s - and p -wave resonances? A p -wave resonance is very narrow, and if you assumed that it was an s -wave resonance it would give you an error in that direction.

P. A. EGELSTAFF: On the subject of the p -wave contribution, we had to consider this very carefully

in our work, because we went slightly higher than 2 kev. It turned out that in the region between 80 and 100 there is a p -wave contribution. It is essential to allow for this if you are going to get the correct results. The s -wave contribution falls off with increasing energy in this energy region, and this is offset by the rising p -wave contribution. So, in effect, the two tend to cancel out.

R. L. ZIMMERMAN: I might point out that a lot of the points in this low region around $A = 100$ have been determined by counting resonances at quite low energies. So we can be more certain that we are dealing with s -wave resonances. By the same token, we can only count a very few resonances and the errors are large.

H. H. LANDON: Isn't that question the same as the question as to whether or not you are missing very small resonances?

P. A. EGELSTAFF: I think the question of missing small levels is irrelevant to the measurement of Γ_n^0/D . In the resonance-counting method, you have essentially an averaging method. You are averaging out all the Γ_n 's, and, if you miss a level, you measure its Γ_n in the next one, and you get the total of the area and divide it by the total energy. This is essentially an averaging method identical to the kilovolt averaging method that has been described. In either of the cases, you have added in all the neutron waves, whether they are large or small.

H. FESHBACH: I think that the conclusion is that in the low-energy resonance region the narrow widths do not introduce an error, and this is important because the particular point that is under discussion is the low-energy point.

H. W. NEWSON: I should like to say that my reasoning was based on work at much higher energies, and the p -wave contribution comes in very strongly in that region. However, some of these rather low energy resonances could still be p -waves, and that would have this same effect on the curve.

GAMMA RADIATION FROM RESONANCE NEUTRON CAPTURE IN MERCURY

H. H. Landon and E. R. Rae
Brookhaven National Laboratory

H. H. LANDON: One of the more pressing problems in low-energy, that is, resonance-energy, neutron physics has been the determination of the spins associated with the individual sharp resonances in the compound nucleus, particularly the determination of the spin of more than one resonance in a single isotope. The problem is, of course, in principle straightforward. An accurate determination of the total cross section yields essentially all of the parameters of a resonance except the statistical weight factor, which involves the spin.

If one can measure accurately, in addition to the total cross section, the resonance scattering cross section, an unambiguous choice of parameters is possible. This has, of course, been the stumbling block. Since one desires to measure a scattering cross section which is large, one is led to choose those isotopes with strong resonances. It is just these isotopes, however, which on the average can be expected to have large spacings of levels and, consequently, few available resonances in the region of high neutron flux and high detector efficiency.

One is led to very difficult measurements which must be made with high precision to enable an unambiguous choice of spin to be made. Let me refer you to the crystal-spectrometer results for the well-known strong first levels in gold, silver, indium, samarium, tellurium, etc. The effort expended to establish one resonance in these cases has been considerable. Recently very encouraging results have been obtained at Harwell for the particular case of silver by Rae, Collins, Lynn, and Wiblin. However, the techniques are, and will remain, difficult and time consuming even with the higher-flux pulsed machines. For some time, then, we have wished to know what could be achieved by somewhat different approaches, utilizing differences in the decay schemes of the compound nucleus which might depend upon spin. We have known for some time, for example, that the population of the ground state and of the isomeric states near ground varies, depending upon the resonance of the compound nucleus in which capture occurs.

One would certainly expect that the capture-gamma-ray spectrum would change depending upon

spin, although it has been evident for some time that such changes are not always obvious and easy to measure. The Yale linear-electron-accelerator group has been studying these changes, utilizing the low-energy gamma rays which presumably are associated with transitions between the low-lying excited states.

The best that can be hoped for from these measurements is that a general division of the measured property into two distinct groups might be achieved from which the spin might be inferred if the spin of one resonance could be established. We have felt, however, that, if one could choose individual gamma rays (presumably those of high energy, which must originate at the capturing state) and establish the multipolarity of these, one would have a direct attack upon the problem of the spin of the compound state. One needs for this, of course, rather special knowledge of the capture-gamma-ray spectra, of which measurements themselves have been difficult. In particular, it has been the situation that the spectra have been unknown for just those cases for which the density of the capturing levels near the capturing state is interestingly large. It is, of course, just the complexity of the decay scheme, caused by the close spacing of levels, which has made the problem so difficult for Kinsey and Motz and many of the others who are working in the field.

The interesting results achieved in the USSR, which appeared at the time of the Geneva conference, aroused our interest in two cases, samarium and mercury. Mercury is particularly interesting, as a look at the Russian results indicates. Let us consider in the conventional way the energy-level diagram of the compound nucleus Hg^{200} . We are considering Hg^{200} since the capture in Hg^{199} , which produces this isotope, dominates the thermal capture in mercury. If we consider the levels in this compound nucleus which are associated with this capture in Hg^{199} , we find that there is a level which is at a negative energy of about -2 ev, and then there is a series of three virtual levels which we can see. These have been established at least tentatively by Bollinger to be in this compound nucleus.

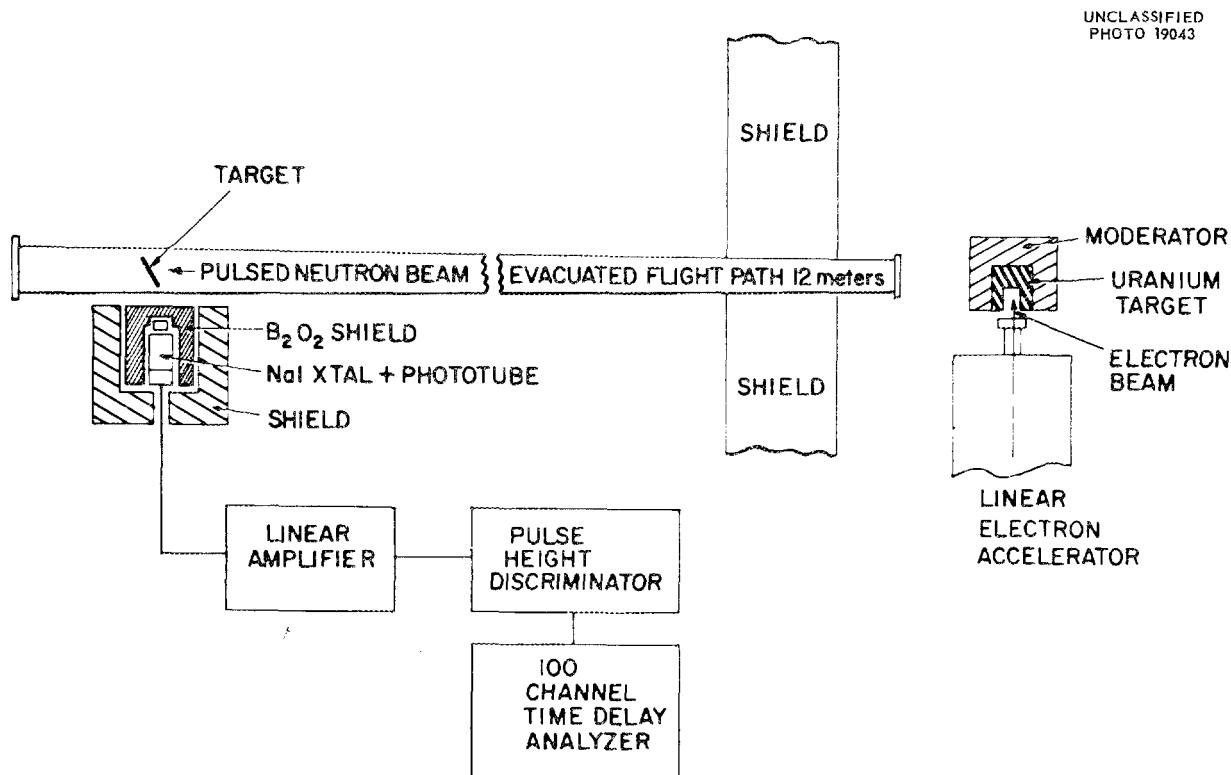
Near the ground state, the level structure has been established, not only by the Russians and by Kinsey in early work, but also by decay from Tl^{200} . The ground state is, of course, 0^+ . The first excited state is 2^+ , and this comes at about 0.37 Mev. The next state, which is also thought to be 2^+ (it is not important for this consideration), occurs at 0.95 Mev. There is another state that the Russians say is at 1.1 Mev, and the next state is at 1.59 Mev.

The binding energy, that is, this total difference, has been established by the Russians to be 8.03 Mev, and no transition has the full binding energy. Since the even-even ground state is 0^+ , this establishes the spin of the capturing state as most likely 0^+ . The other possible state that one can form by *s*-wave neutron capture is, of course, 1^- . The zero-zero transition is strictly forbidden.

The presence, then, of an 8-Mev direct ground-state transition which has the *E1* speed and intensity would unambiguously establish the spin of that state as 1^- . This is just the situation we

have been looking for. The problem of detecting an 8-Mev gamma ray with good efficiency and resolution is not particularly easy, but the problem is further simplified by the existing scheme of the low-lying states. Transitions, it turns out, to all three of these states from the 0^- state are extremely weak. The first really strong transition is a 6.4-Mev transition to the 1.6-Mev state. This is strong, approximately 10%, and is thought, then, to be *E1*. We have, therefore, set up in this experiment to detect just the presence of those 8-Mev gamma rays which might be associated with the virtual levels that we can excite in the compound nucleus.

The equipment is shown in Slide 1. Here we have the linear electron accelerator at $13\frac{1}{2}$ Mev, producing a pulsed neutron beam down an evacuated 12-m flight path. Our target is mercury oxide, and we have actually three such detectors as the one illustrated, essentially in parallel. These are shielded from scattered neutrons. We have examined the background which comes from the target by a



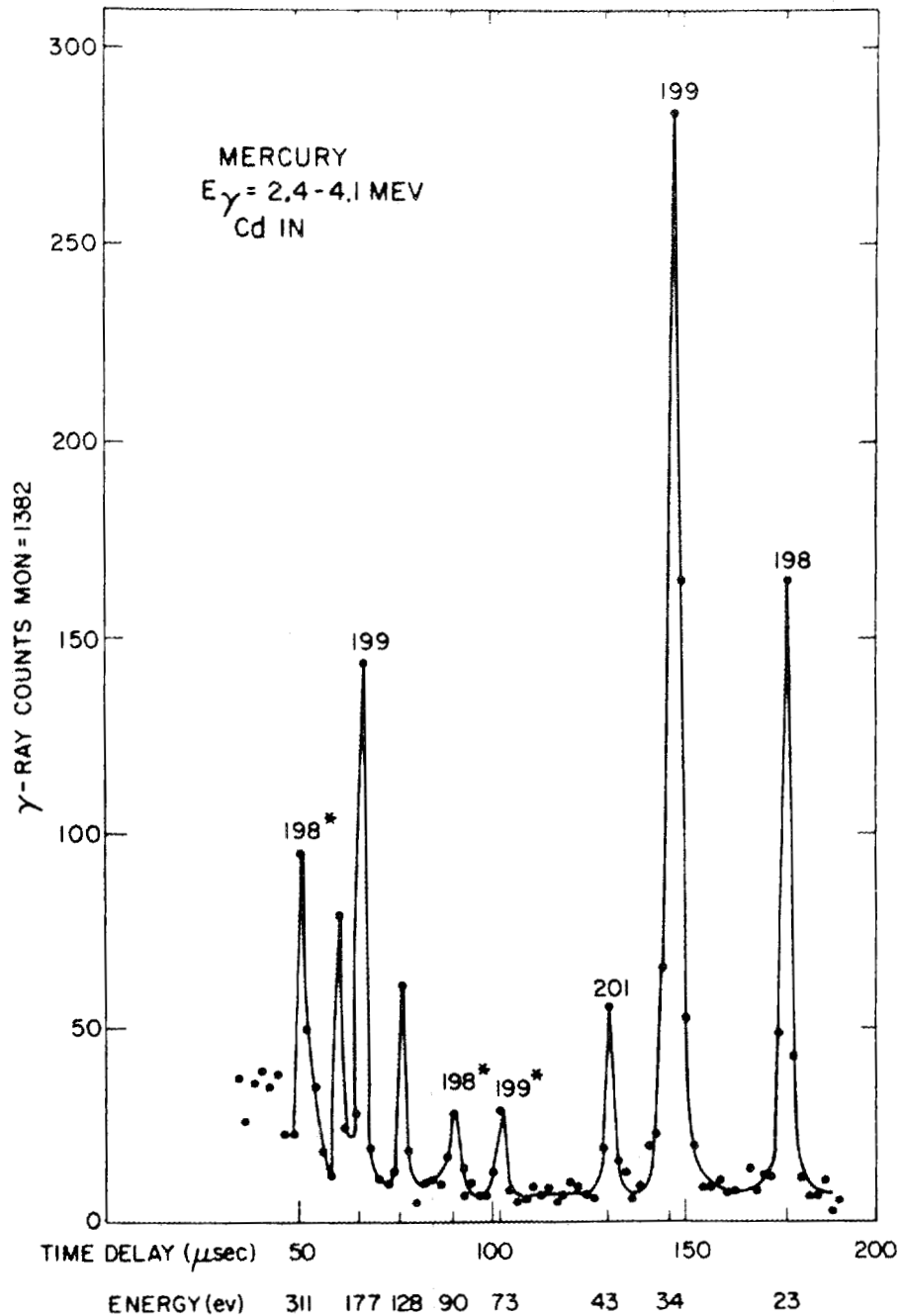
Slide 1. Schematic View of Capture-Gamma Apparatus.

number of means. (I won't go into that.) We take the pulse from the detector, put it through a linear amplifier, and then use pulse-height discrimination. For the time being it has only been single-channel discrimination. Then we put it through a 100-channel time analyzer to analyze for the energy of the neutron which caused the gamma ray. This is

to establish in which of the virtual states capture has taken place.

Slide 2 is a picture of what one observes if he sets the single-channel analyzer to accept gamma rays between 2.4 and 4.1 Mev. You see a very distinct resonance structure. The resonance that we are concerned with is the strong one at 34 ev.

UNCLASSIFIED
PHOTO 19044



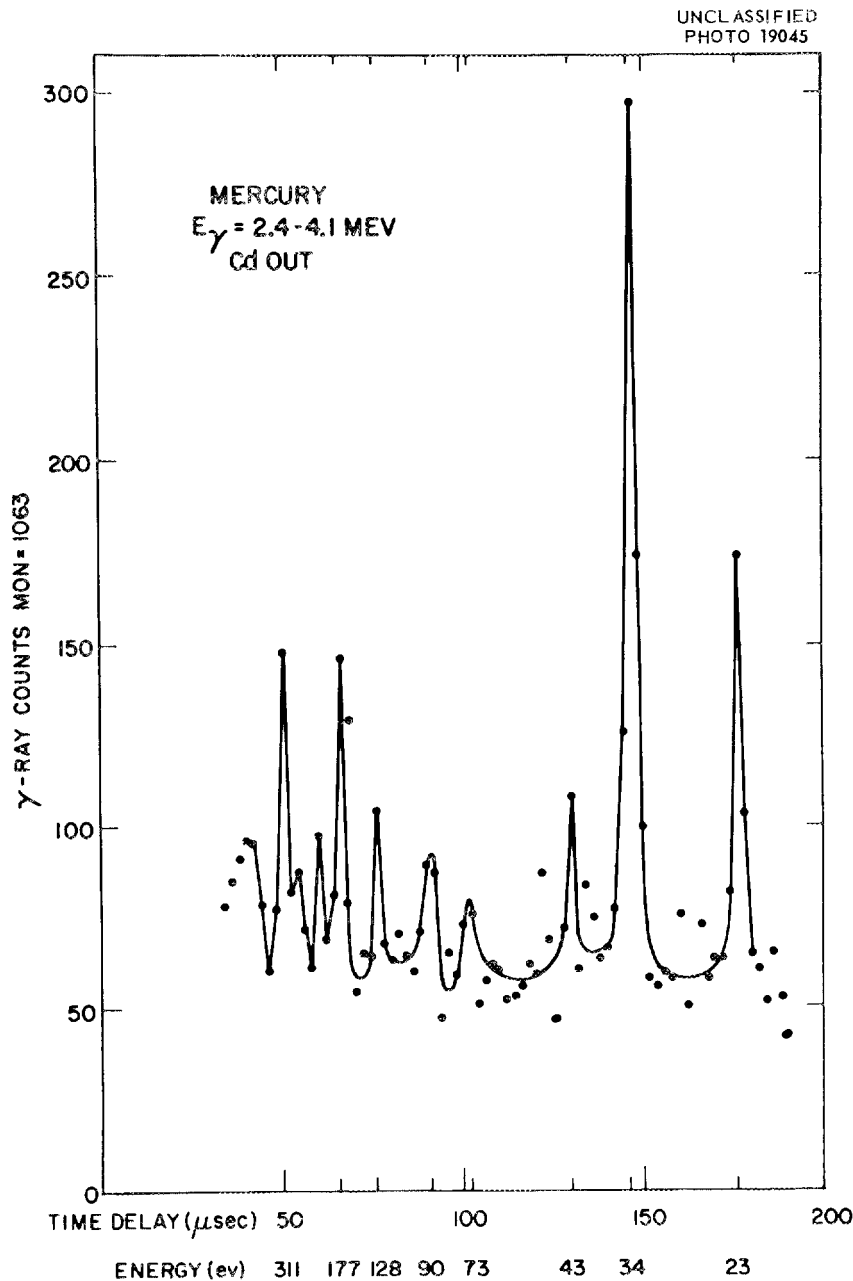
Slide 2. Capture-Gamma-Ray Spectrum from Mercury at an Incident-Neutron Energy of 34 ev With Cadmium in the Neutron Beam.

There are two others which we can also see but for which the statistics are still poor. I won't report on the results for these.

What we do, then, is simply to increase the bias on the single-channel analyzer successively and to look for what we hope to be the disappearance of some of these levels while the others remain. What we would expect to have in the ideal case

of a single isotope is that half the levels, or some number of levels, disappear before the others do.

The problem is, then, one of comparing the intensity associated with the 34-ev resonance with that due to the capture which takes place in the negative energy resonance. To do this we have simply done the following: Rather than timing at very long times, we simply count those gamma-ray pulses (see Slide 3) which occur when cadmium is



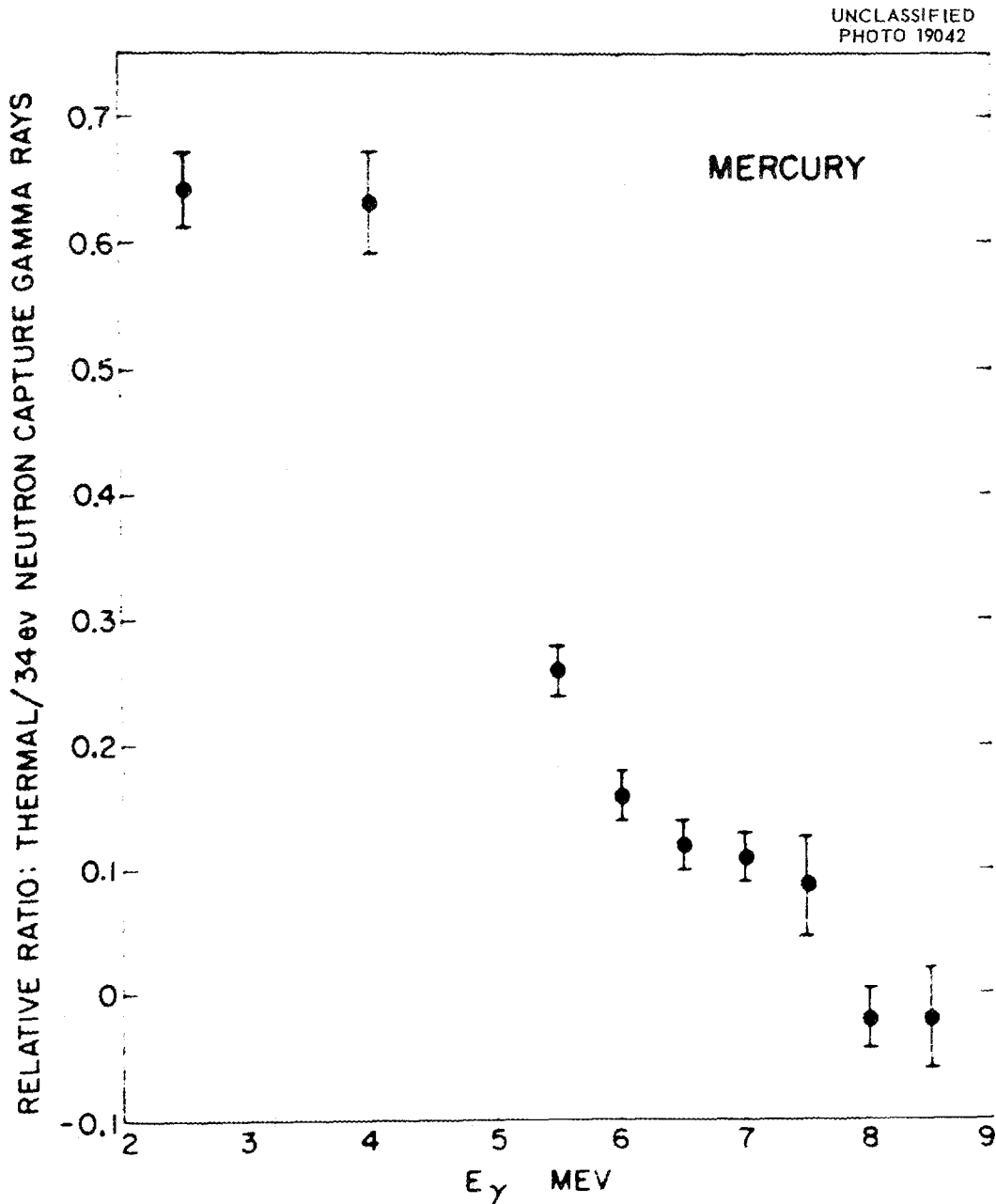
Slide 3. Capture-Gamma-Ray Spectrum from Mercury at an Incident-Neutron Energy of 34 ev With Cadmium Not in the Neutron Beam.

taken out of the beam. These are due to the gamma rays associated with the capture of thermal neutrons from the previous burst. We then take a ratio of the intensity in the peak to an average background and look for variations in that ratio. The results are shown in Slide 4.

Indeed, there is a variation. It is difficult to establish the energy scale here. We would expect that the ratio should drop off at the edge of this

level, 6.4 Mev, and it seems to drop off higher than that. We should no longer see any of the 34-ev level after 8 Mev. We do see it at 9 Mev. This means that our energy scale is probably wrong by about 1 Mev.

In a separate experiment, Rae has looked at the total gamma-ray spectrum from a single level, using what amounts in effect to a multichannel analyzer. The details I shall omit. The spectra do, indeed,



Slide 4. Relative Ratio of Thermal- to 34-ev-Neutron Capture Gamma Rays.

seem to have different end points. The normalization in this case has to be done rather carefully. We can say, however, that at least the 34-ev level seems to give the harder radiation.

Finally let me conclude that this has an interesting application. If one can separate out those gamma rays above 6.5 Mev after one has set the bias sufficiently high to eliminate all the resonances due to one spin state, then one can compare the relative intensity of the remaining levels and from this get the distribution of the relative partial radiation widths. Furthermore, since one does select the exit channel by this means, one should presumably see interference between resonances again showing up, whereas these interferences have been washed out in the normal spectrum.

I should like to thank the Harwell people for the opportunity to work with them for a month last summer.

H. FESHBACH: I wonder if you would again tell us what the conclusion is that one reaches when one finds that the radiation from the 34-ev level is harder than the radiation from the negative-energy level.

H. H. LANDON: We would then say that the spin of that level must be the spin associated with a 1^- state. It is capturing in the parallel spin state, as opposed to the antiparallel.

H. PALEVSKY: I should like to ask a question with regard to your last statement about interference. If you could pick out the same spin states in capture, is it necessarily true that you would get interference between these states?

H. H. LANDON: If one looks only at those gamma rays which occur to the ground state, then one selects only the exit channel, and one should then see interference.

H. FESHBACH: What is interfering with what?

H. H. LANDON: It would then be the partial width for the emission of this gamma ray to the ground state from one resonance interfering with the same partial width from a nearby level. The amplitude for this emission from this state would interfere with the similar amplitude for the emission of the same gamma ray from the adjacent state. It is similar to the fission problem, where, if you limit the exit channel, you should, indeed, observe interference. This is going to be very hard, of course, because you are going to have to pick two resonances which are close together.

M. E. ROSE: What is the basis for the minus parity of Hg^{199} ? Is that experimental evidence, or is it the shell-model assignment?

H. H. LANDON: I presume it is the shell-model assignment.

A. M. LANE: Although the presence of the strong transition to the ground state does certainly seem to indicate a 1^- spin, the absence of a strong transition to the ground state does not indicate a 0^- spin.

H. H. LANDON: This is perfectly true, but in this case the presence of the radiation assigns a spin of 1^- , but not vice versa.

A. M. LANE: But if the transition is also absent to the 2^+ level, that certainly increases the probability that the spin is 0^- .

E. C. CAMPBELL: I should like to ask about an experimental detail. It looks as if this experiment is particularly susceptible to the possibility of summing pulses. I presume that you have taken this into account, although you didn't mention it.

H. H. LANDON: Yes, that was a worry. The detection efficiency for a single gamma ray is very small, and if you then require that two of them combine, this is, indeed, very small.

H. L. SCHULTZ: Landon mentioned that we were looking at low-energy capture-gamma-ray spectra, and I just want to point out some recent results in this connection.

Earlier indications pointed to the fact that, in a number of cases where we looked at gamma rays, these low-energy capture-gamma-ray spectra did vary between the resonances. In particular there were two cases, tantalum and indium. Originally it was found in the tantalum, for example, that the 13-ev resonance did not show a 260-kev transition which was very prominent in the other two low-lying resonances. Likewise, in indium the 1-ev resonance did not show a 560-kev line which was indicated in the two higher resonances. Well, the point is that since then we have made fairly accurate absolute intensity measurements, and these apparent differences have apparently disappeared.

When one takes into account such matters as the depression of peaks due to the effect of resolution and carefully considers how many neutrons are absorbed in the resonance, then one finds that, in these two cases at least, the low-lying capture-gamma-ray spectra seem to be quite similar. However, more recent work has indicated again that the higher-energy transitions do vary between the various resonances.

STUDIES ON THE RESONANCES IN U^{238} USING THE HIGH-RESOLUTION NEVIS SYNCHROCYCLOTRON NEUTRON VELOCITY SPECTROMETER

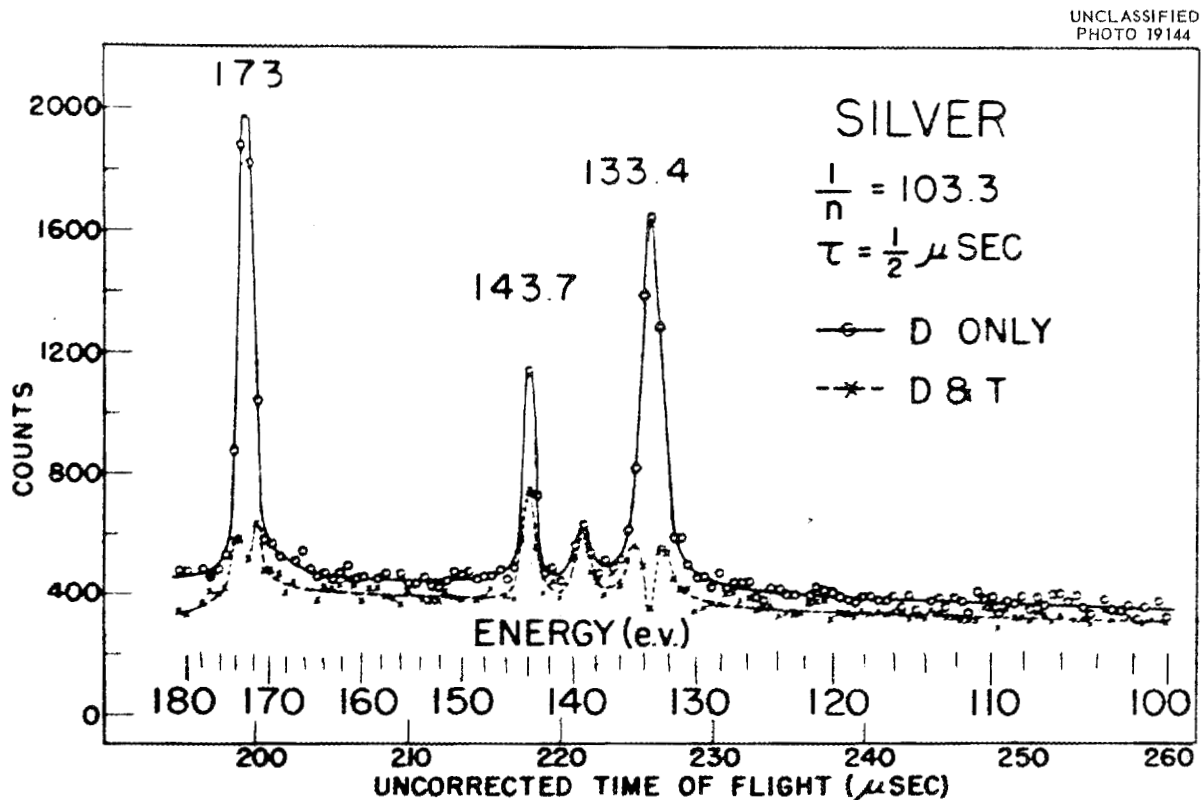
W. W. Havens, Jr. J. Rainwater S. Desjardins J. Rosen
Columbia University

W. W. HAVENS, JR.: When I prepared the abstract of this talk, I expected to have full analyses of about 30 resonances in U^{238} . However, I am the victim of the machine age. In the early days, resonances were analyzed one by one, but nowadays all the data are punched on cards and processed in a machine, and you don't have any results until you have all the results.

This time the machine broke down, and our results came out as gibberish. We found the mistake not in the data but in the computing machine, and consequently it has had to be run over again. So I have no results on U^{238} , except for positions of levels. I will show some of our recent Nevis results and point out some of the interesting features of these. I am going to give some of the results on tantalum, silver, and U^{238} . Rainwater

has shown some of the tantalum and silver results before, but the U^{238} results are new.

Slide 1 shows some of our results on silver. I chose this slide, out of many which show a large number of resonances, because of the particular energy region covered. I should like to point out the fairly small resonance at 139 ev, which I will stress when we look at the results on tantalum. These data are experimental counts observed with our detection method. We are counting the gamma rays that are emitted immediately after neutron capture. There is a background of somewhere around 400, and the highest peak at 173 ev runs to 2000 counts over the background. However, the small peak at 139 ev has an intensity of only 650 counts over the background. This illustrates the necessity of obtaining good statistics on runs like this.



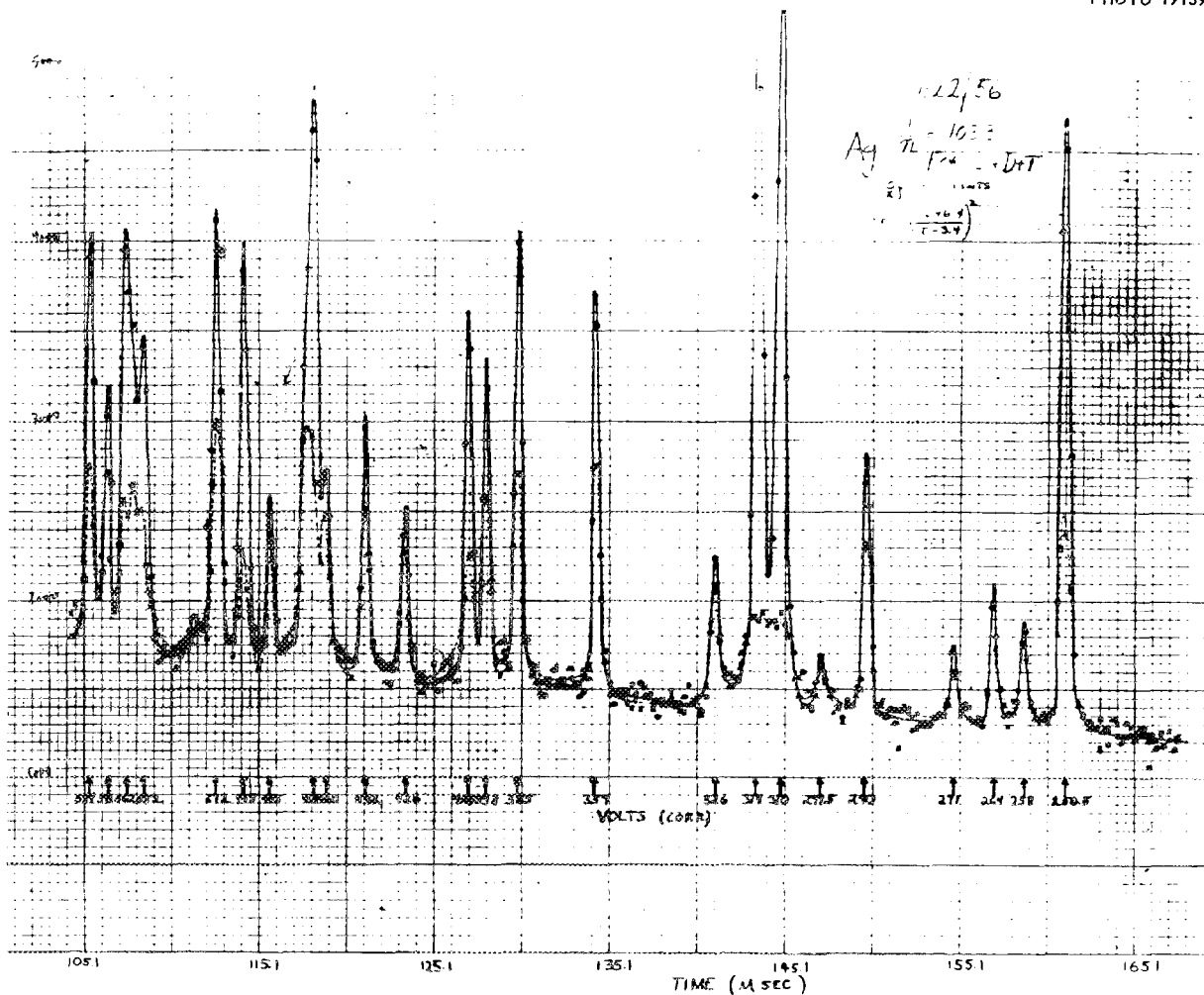
Slide 1. Neutron Time-of-Flight Spectrum of Silver from 100 to 180 ev.

Slide 2 shows higher-energy resonances in silver. The interesting part here is that published results begin to lose resonances at 88 ev. This run goes from 250 ev up to 584 ev. You can see that at about 500 ev we are not resolving the resonances. I am not going to quote a resolution width, but I will say that our principal spread in energy is due to the detector. These data were taken with $\frac{1}{4}$ - μ sec channels at a distance of 35 m. We have two sets of results here, one with a detector only, and then a dotted curve which has both a detector of the material being studied and another sample, in front of the detector, which absorbs the resonance neutrons.

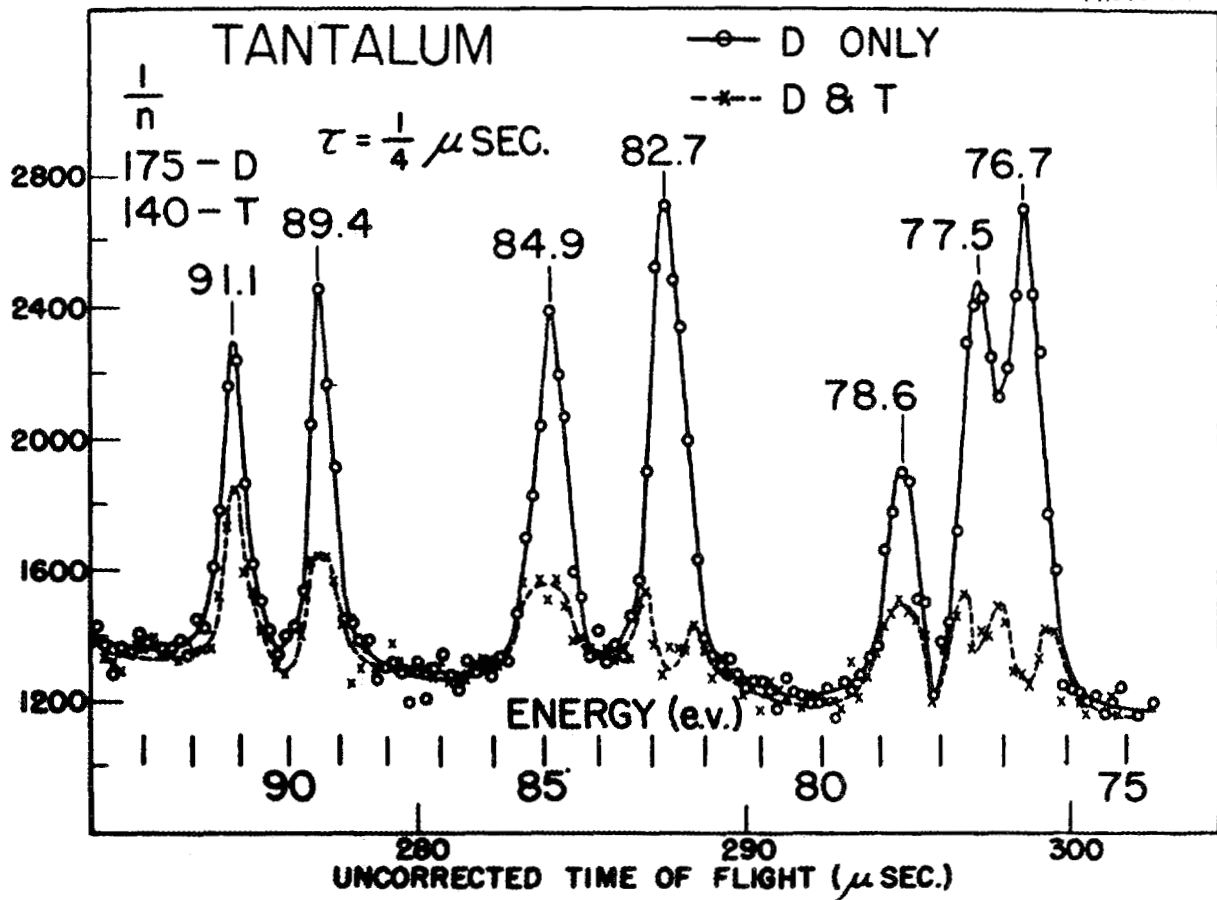
Slide 3 shows results on tantalum. This slide shows three levels at 76.7, 77.5, and 78.6 ev, which were shown as one level at 76.9 ev in the most recently published results.

Slide 4 shows our most recent results on tantalum. We have somewhere around 9000 counts at the peak of the largest resonance. The number of resonances from 170 to 250 ev has also increased substantially. There are small peaks which have a total of 1000 counts. When the statistics were poorer, we didn't dare call these resonances. However, when there are a sufficiently large number of counts, these little peaks become very definite. This illustrates that we may be missing resonances.

UNCLASSIFIED
PHOTO 19139



Slide 2. Neutron Time-of-Flight Spectrum of Silver from 250 to 584 ev.



Slide 3. Neutron Time-of-Flight Spectrum of Tantalum from 75 to 94 eV.

I should like to call attention to the close level spacing between 190 eV and about 250 eV. The level spacing here seems to be quite a bit smaller than the average. There is no point to our studying energies higher than 250 eV in tantalum, because of the small level spacing.

Slide 5 shows some recent results on cadmium which were taken in about $\frac{1}{2}$ hr. With our present resolution, there is no point in studying cadmium resonances above about 230 eV, because the levels would not be separated. The statistics here are very poor, and more running time is required to see the small levels.

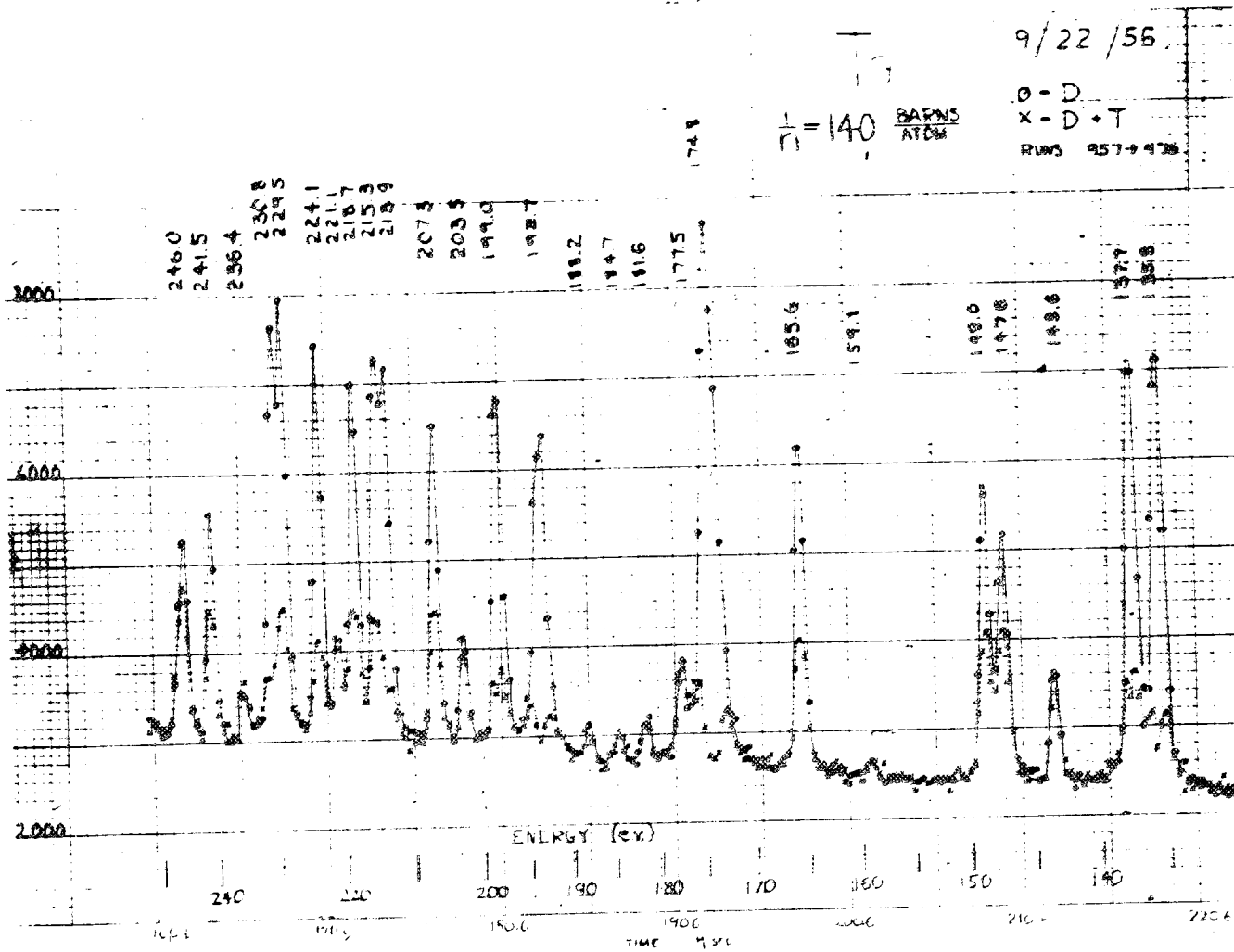
Slide 6 shows the higher-energy resonance structure in U^{238} . The maximum number of counts in a resonance is 8500. We have observed all the resonances reported by the Brookhaven group.

Above 290 eV, levels which the Brookhaven group report as single are resolved into more than one level. We begin to miss levels at about 600 eV.

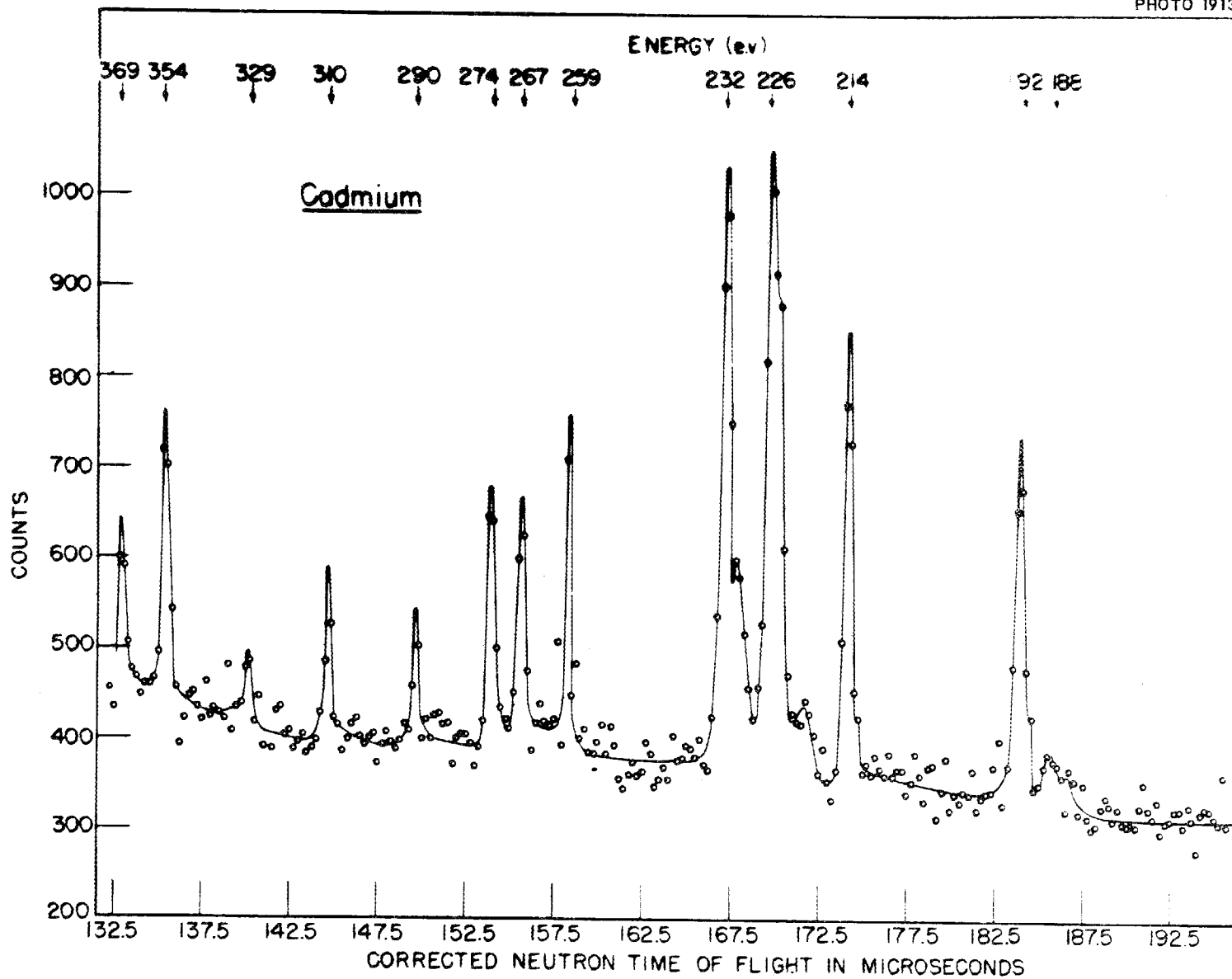
Slide 7 shows the number of levels below a given energy as a function of the energy. The Brookhaven group gave an average level spacing of 18 ± 2 eV, which, in the low-energy region, agrees very well with our data. From this curve it looks as if we might also be missing levels above 300 eV. Higher statistical accuracy will show whether or not we are still missing levels.

Slide 8 shows the results on tantalum. The MTR group stopped resolving levels at 63 eV. There is a mistake in this slide. The average level spacing of 7.8 eV refers to the average spacing per spin state. Since there are two spin states possible, the average spacing should be

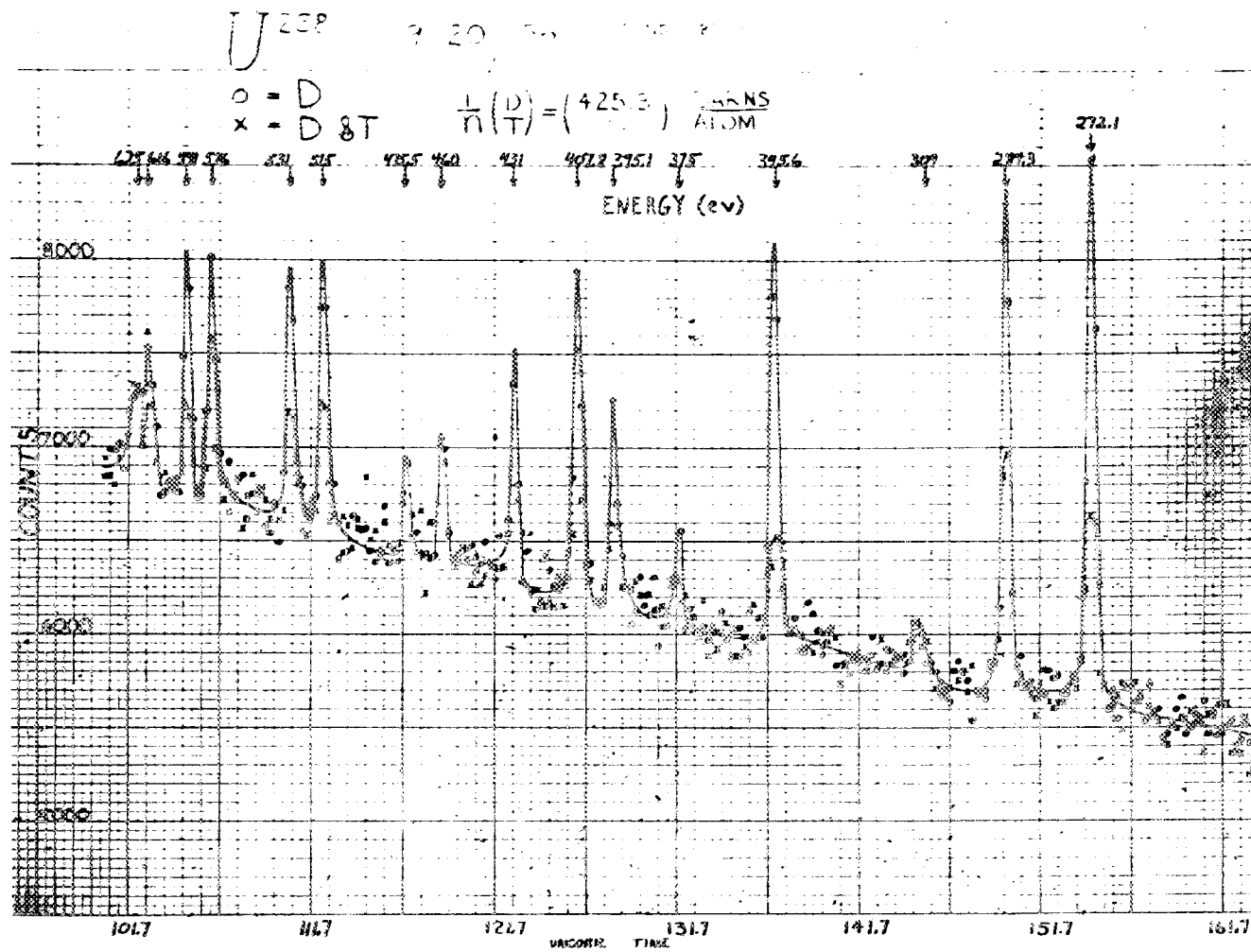
UNCLASSIFIED
PHOTO 19133

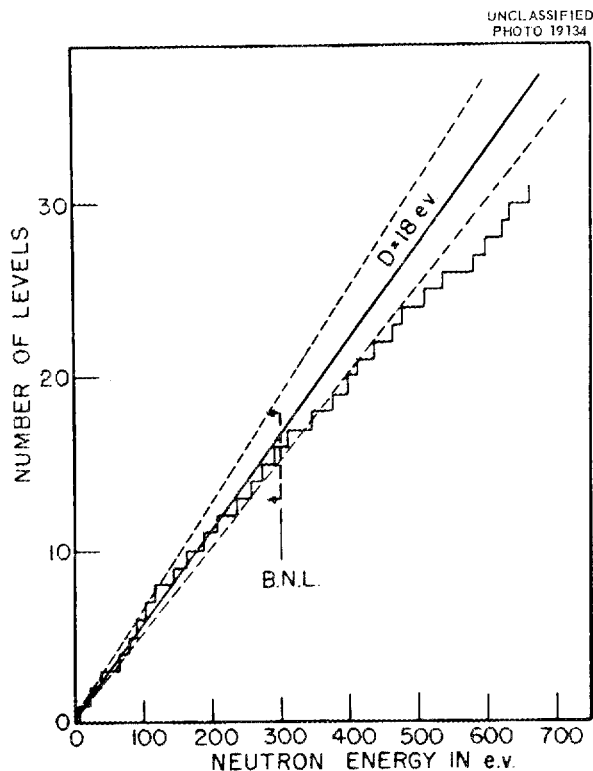


Slide 4. Neutron Time-of-Flight Spectrum of Tantalum from 130 to 250 ev.



Slide 5. Neutron Time-of-Flight Spectrum of Cadmium from 180 to 370 ev.



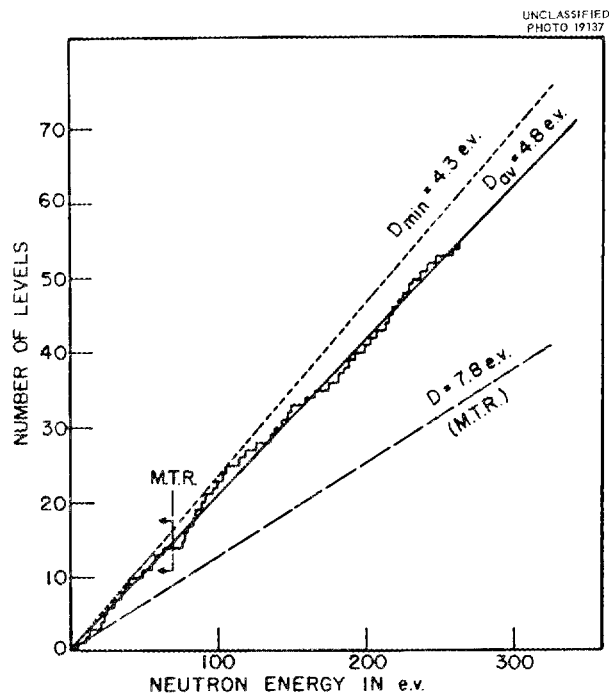


Slide 7. Neutron Energy Level Distribution in U^{238} .

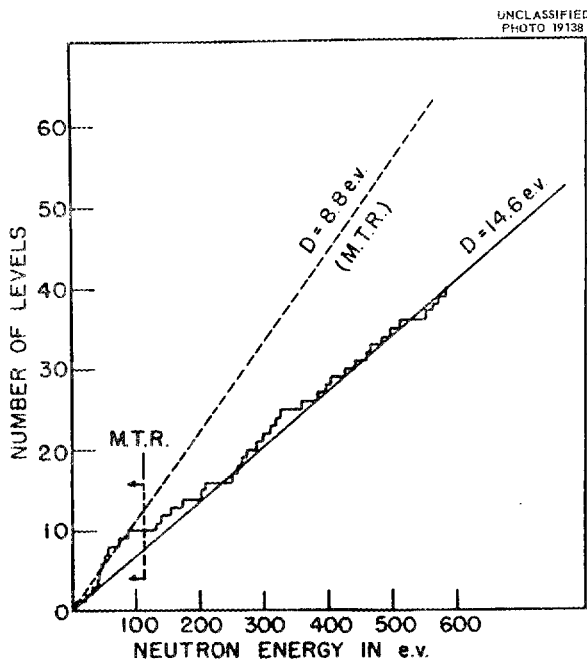
3.9 e.v. The minimum level spacing we obtain from this curve is 4.3 e.v, and the average level spacing is 4.8 e.v. There were 54 levels observed, and I think now you can see that there are some statistical fluctuations in level density.

Slide 9 shows the same results for silver. These data definitely show that there are fluctuations in level density. The first ten levels have an average spacing of 8.8 e.v. However, there is no observable level in silver between 88 and 138 e.v. On the basis of these data, the average level spacing for the first 600 e.v is 14.6 e.v if we are not missing any levels. These data indicate that the average level density for the first 100 e.v is considerably higher than for the first 600 e.v.

One encouraging aspect of our apparatus was observed during the last run. We were experimenting with our detector bias, which had always been set to reject 2.2-Mev gamma rays. In early runs, the peak-to-valley ratio of our curves decreased rapidly as the detector bias was decreased.



Slide 8. Neutron Energy Level Distribution in Ta^{181} .



Slide 9. Neutron Energy Level Distribution in Normal Silver.

However, when the bias was decreased recently, the signal-to-background ratio did not change appreciably. Our final counting rate was a little higher than 1 count per second per $\frac{1}{4}$ - μ sec detector channel. At this counting rate we were being limited by the time resolution of our time analyzer. How much further the intensity can be increased cannot be determined until our time analyzer is improved.

L. M. BOLLINGER: In the past you have shown cases in which you missed resonances because they were largely scattering.

W. W. HAVENS, JR.: This is true. It is for this reason we cannot say that we have seen all the levels.

L. M. BOLLINGER: Yet in the case of uranium some of the levels which I happen to know are largely scattering seem to show up.

W. W. HAVENS, JR.: Every level that the Brookhaven group reported was observed. Some of the peaks were very small, and we had to obtain good statistics before we could see these levels. If you look at our previous results, the small levels were lost in the background. I have hopes that as we improve the statistics we will be able to see smaller and smaller levels.

A. M. WEINBERG: The U^{238} distribution of levels that you showed indicates that they are not really random. What is the situation on testing of the distribution for its randomness? A casual look indicates that 20 ev seems to come in very regularly.

W. W. HAVENS, JR.: I haven't done any testing for randomness. As we have improved the statistics, we have always seen more levels. I haven't plotted the probability distribution.

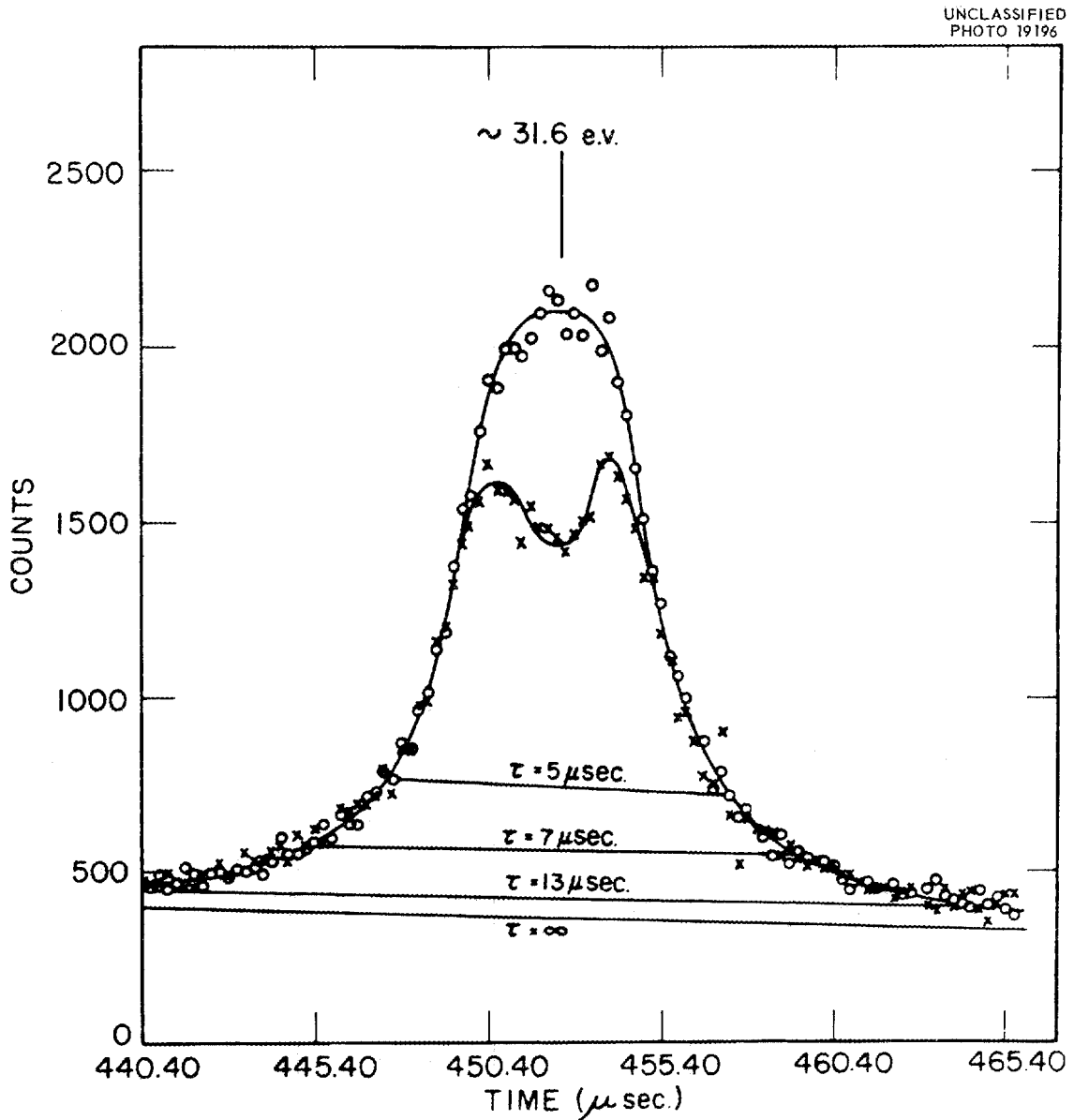
ANALYSIS OF NEVIS NEUTRON TIME-OF-FLIGHT DATA ON SILVER RESONANCE LEVELS BY RECENTLY IMPROVED TECHNIQUES

E. Melkonian
Columbia University

E. MELKONIAN: This is a study of some of our Nevis cyclotron data on the low energy levels of silver to get more accurate resonance parameters. One of the main difficulties in the interpretation of these data is the proper choice of the background to be subtracted from the observed counting rate. The main innovation of this paper is the develop-

ment of a method of analysis in which the choice of an arbitrary background leads to the same results that would have been obtained if the correct, but unknown, background had been used in the first place.

Slide 1 shows typical data in the neighborhood of a resonance level in silver, taken at 35.2 m with



Slide 1. Level in Silver at 31.6 ev.

the Nevis neutron velocity spectrometer at low energies where well-isolated levels are defined by many points. The "circle" points were taken by detecting the capture gamma rays emitted by silver placed at the detector position. The "x" points were taken with an additional sample of silver in a transmission position. We are considering here only data represented by the circles.

Since the counting rate represented by the circles is proportional to $(1 - \text{transmission})$, one method of analysis which has been used (and which will be used here) is to treat the observed curve as though it were an inverted transmission curve and to perform the usual area analysis. However, counting rates corresponding to zero transmission and to unity transmission must first be identified before such a procedure can be carried out. For the particular level and sample ($1/n = 103.3$ barns per atom) under consideration, $n\sigma_0 \gg 1$, so that the peak counting rate corresponds to zero transmission. Finding the location of unity transmission is complicated by the presence of experimental background, as well as by potential scattering and contributions from other levels which have nothing to do with the level under consideration. Sometimes, the location of the background (and hence $T = 1$) can be obtained by considering the counting rate far from the level. However, this is frequently unreliable and not always possible, so that a more general method is desired.

Because of this, we have developed a new approach, in which knowledge of the background is not necessary. Instead, an arbitrary background, subject only to limitations to be given, is chosen, and the subsequent procedure automatically gives the results which would have been obtained had the true background been used. In Slide 1, the line marked $\tau = 13 \mu\text{sec}$ appears to be a reasonable background ($\tau = 13$ means that the background line intersects the data at points $13 \mu\text{sec}$ on each side of the resonance time of flight). Application of the procedure to be described shows that the true background is given by the line marked $\tau = \infty$, and gives results corresponding to it.

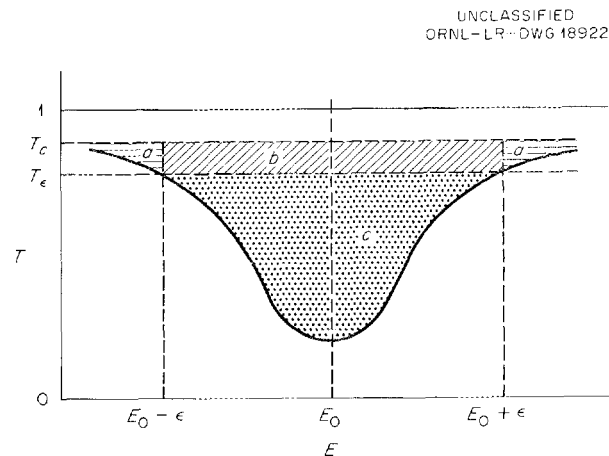
Before proceeding to describe this new method, two comments are necessary. First, we have been trying to analyze the data of Slide 1 in terms of an inverted transmission curve. In fact, it is simpler to think in terms of a transmission dip, and the

following derivation will be based on transmission. Second, since the Breit-Wigner equations are given in terms of energies and not time of flight, the derivation will be made on an energy basis, and time-of-flight data must be converted to an energy basis before application of this method. Since applications are made over small ranges of energy (several times Γ) compared with the resonance energy E_0 , the equation

$$\frac{\Delta E}{E} = 2 \frac{\Delta t}{t}$$

is sufficiently accurate, and the " $1/v$ " term may be neglected.

With these in mind, we refer to Slide 2, which shows a typical transmission dip, where T_c is the transmission arising from potential scattering, contributions from other levels, and background (as in the case of capture-gamma data). What is desired for an area analysis is the area above the transmission dip after the entire curve has been divided by T_c . Since the value of T_c is presumed unknown, we pick an arbitrary transmission T_{E_t} which intersects the transmission curve at $E_0 + \epsilon$ and $E_0 - \epsilon$. The desired total area, $A_{ED'}$ above



Slide 2. A Typical Experimental Transmission Curve of a Sample Undergoing Resonance.

the corrected curve can then be written as the sum of partial contributions from regions *a*, *b*, and *c*:

$$\frac{A_{ED}}{\Delta} = \frac{A'_{ED}}{\Delta} \cdot \frac{1}{T_c} + 2 \frac{\epsilon}{\Delta} \left(1 - e^{-n\sigma_0 \psi(\epsilon)} \right) + \quad (c) \quad (b)$$

$$+ 2 \int_{\epsilon/\Delta}^{\infty} \left(1 - e^{-n\sigma_0 \psi(E-E_0)} \right) d \left(\frac{E-E_0}{\Delta} \right), \quad (a)$$

where A'_{ED} is the observed partial area for region *c*, and Δ is the Doppler width. Since

$$T_\epsilon = T_c e^{-n\sigma_0 \psi(\epsilon)},$$

the above equation can be rewritten as

$$\frac{A_{ED}}{\Delta} = \frac{A'_{ED}}{\Delta T_\epsilon} + \left(\frac{2\epsilon}{\Delta} - \frac{A'_{ED}}{\Delta T_\epsilon} \right) \left(1 - e^{-n\sigma_0 \psi(\epsilon)} \right) + \quad I \quad II$$

$$+ 2 \int_{\epsilon/\Delta}^{\infty} \left(1 - e^{-n\sigma_0 \psi(E-E_0)} \right) d \left(\frac{E-E_0}{\Delta} \right). \quad III$$

If ϵ is chosen such that

$$\frac{\epsilon}{\Delta} \geq 3.5 \text{ and } \frac{\epsilon}{\Gamma} \geq 10,$$

and if the experimental resolution is perfect for $|E - E_0| \geq 3.5 \epsilon$, then the terms II and III, which are to be added to $A'_{ED}/\Delta T_\epsilon$ to make up for the contributions of regions *a* and *b* and for the fact that T_ϵ was used instead of $T_{c\epsilon}$ become functions only of the quantities $m \equiv n\sigma_0 \Gamma^2/\Delta^2$ and ϵ/Δ . (The condition on ϵ/Δ must be met exactly for this method to be valid. The condition on ϵ/Γ ensures that the calculation is good to 1%, and smaller values of ϵ/Γ may be used with the error $\sim (\Gamma/\epsilon)^2$.) It is thus possible to express A_{ED}/Δ in terms only of ϵ/Δ and m in addition to the observed quantity $A'_{ED}/\Delta T_\epsilon$. Slides 3, 4, and 5 give graphs useful in performing these calculations and correspond, respectively, to terms I, II, and III. Given

the observed quantities A'_{ED} , ϵ , and $T_{c\epsilon}$ as well as Δ , the analysis procedure is: (1) Select a value of $m \equiv n\sigma_0 \Gamma^2/\Delta^2$, and with the aid of Slides 4 and 5 compute terms II and III, respectively. Add to $A'_{ED}/\Delta T_\epsilon$ to get A_{ED}/Δ . (2) For these values of m and A_{ED}/Δ , read Δ/Γ from Slide 3. (3) Choose other values of m , and deduce for each a value of Δ/Γ in the same way. This procedure gives essentially a relationship between $\sigma_0 \Gamma^2$ and Γ , which is the maximum amount of information that a single area determination can give. Additional information is needed to get a second relationship between $\sigma_0 \Gamma^2$ and Γ so that the values of σ_0 and Γ , separately, may be determined.

This procedure has been applied to the data of Slide 1, giving the results (circles) shown in Slide 6. (The resonance-energy values are only nominal, and there are some discrepancies in the labels.) Two other choices of background have been included (crosses and squares). The reason for obtaining three distinct curves is that the Doppler broadening is still operative at the cutoff points, giving dependence upon the shape of the wings of the resonance level. If the data and procedure were perfectly accurate, the intersection of the three curves would give the values of σ_0 and Γ . However, although the intersection gives approximately correct values, these should not be taken too seriously because of the very sensitive dependence upon experimental errors. Data from the MTR and from BNL-325 are included for comparison. It is to be noted that these results are definitely lower. This same procedure has been applied to five other silver levels, usually with higher results than obtained by other experimenters. We attribute this in part to the fact that, without the use of the present method, backgrounds are generally picked too large (refer to Slides 1 and 7). Results for two more levels are shown in Slides 7, 8, and 9. Table 1 gives a summary of results on the six levels of silver which were considered.

R. L. MACKLIN: Would you say that this method was sensitive to the shape in the wings?

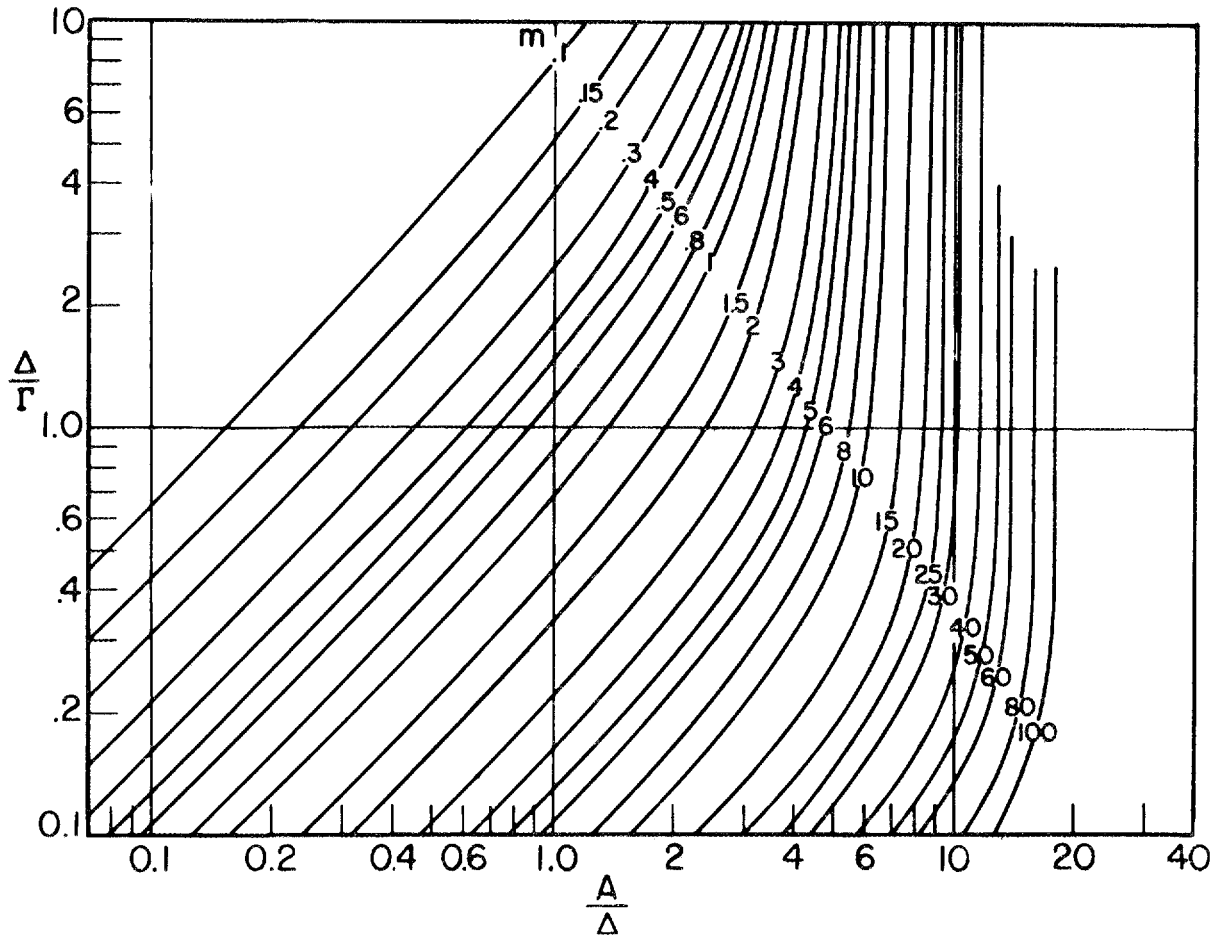
E. MELKONIAN: Yes, it is sensitive.

R. L. MACKLIN: So you are really combining area analysis with wing shape?

E. MELKONIAN: Yes, you are, in a way. The shape comes in because of the Doppler effect. If the Doppler effect were negligible, then these three curves would be the same. However, this

$$\frac{A}{\Delta} = \int_{-\infty}^{\infty} (1 - e^{-n\sigma_0\psi(E)}) d\frac{E}{\Delta}$$

$$m \equiv n\sigma_0 \frac{\Gamma^2}{\Delta^2}$$

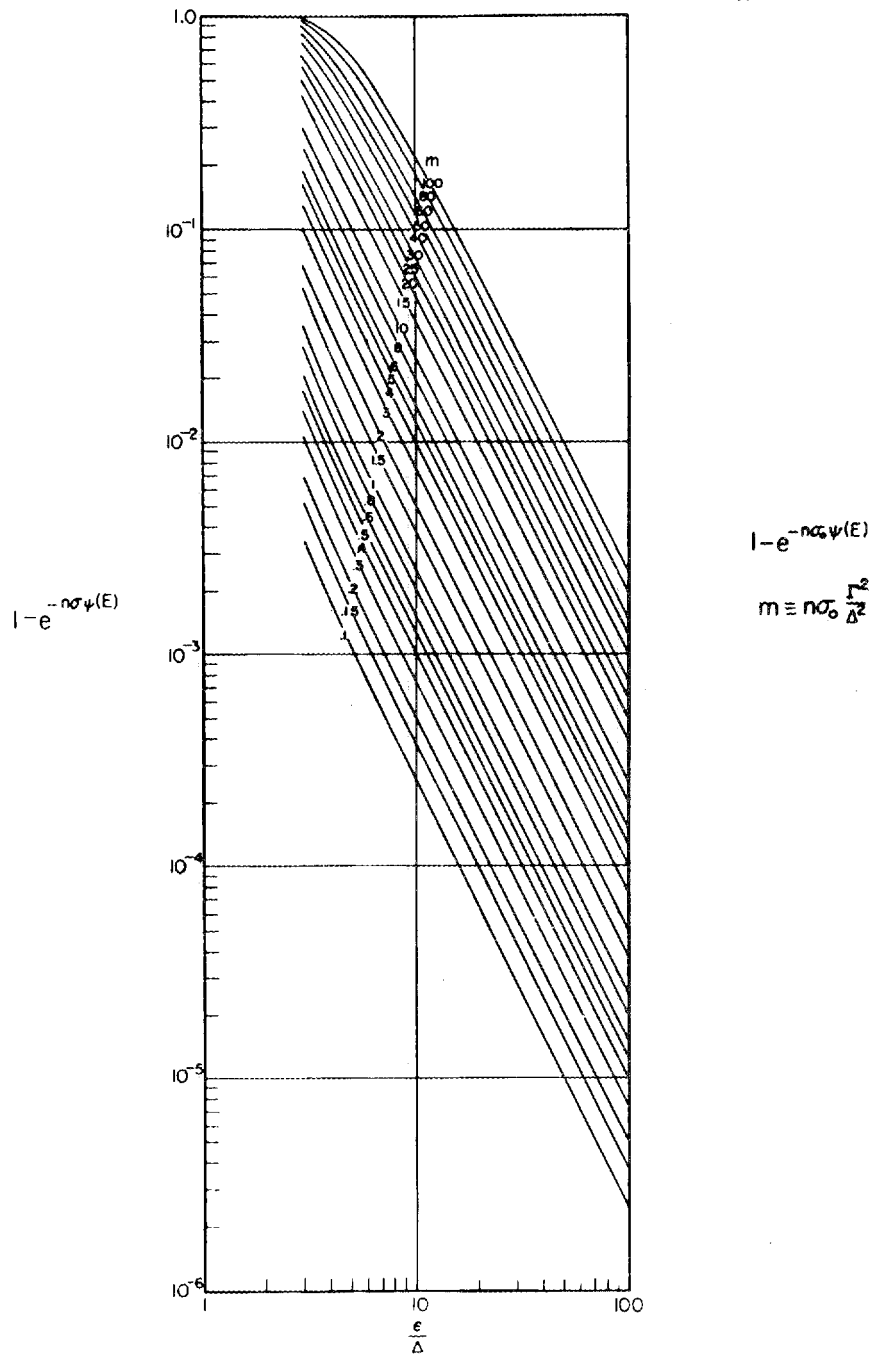


Slide 3. Graph for Calculation of $\sigma_0\Gamma^2$ in the Analysis of Resonance Levels (See Text).

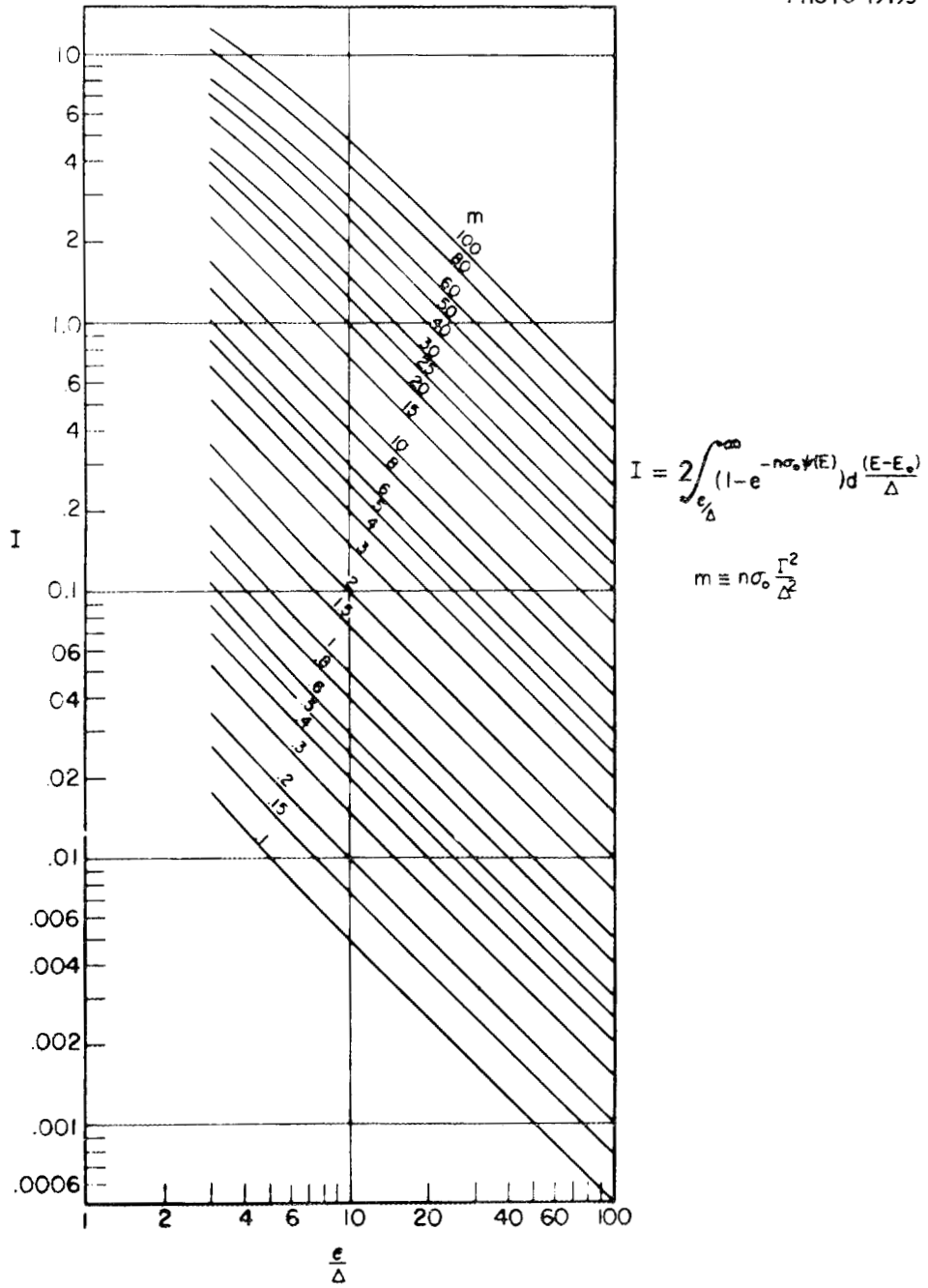
shape dependence may not be as useful as it would seem at first sight, since the point of intersection of the several curves is very sensitive to small experimental errors, because of the small angle of intersection.

R. G. FLUHARTY: I should like to ask a question about what effect this analysis has on the potential scattering that you obtain between the resonances.

E. MELKONIAN: This has been applied, at the moment, only to Nevis data, where things like potential scattering just go right into the experimental background. There is no way of distinguishing them. If you had a transmission curve, the "background" transmission would be due to the potential scattering plus contributions from some other levels.

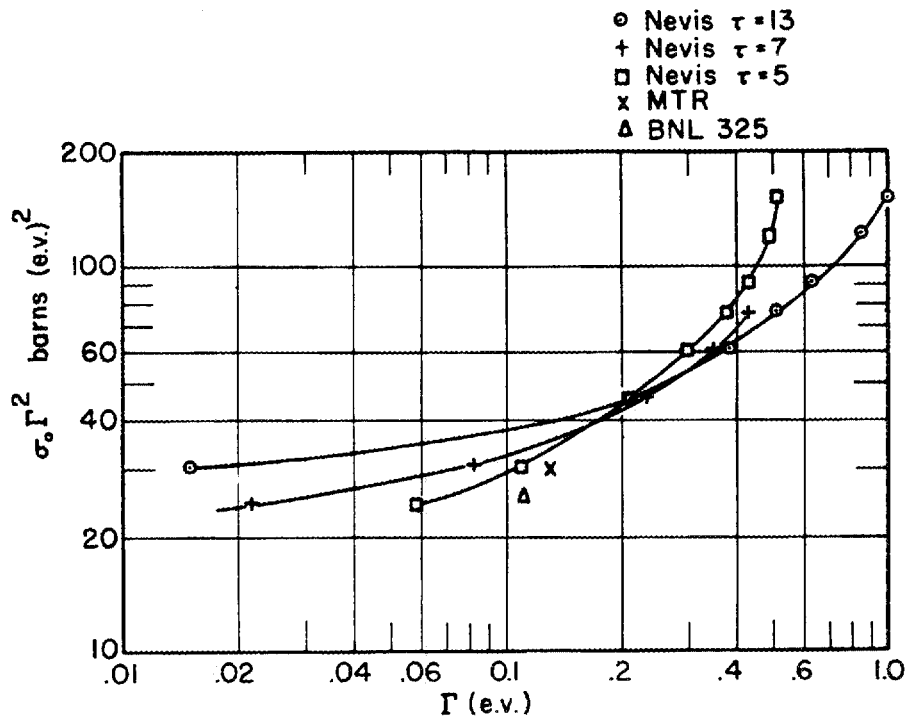


Slide 4. Graph for Calculation of Term II in the Analysis of Resonance Levels (See Text).



Slide 5. Graph for Calculation of Term III in the Analysis of Resonance Levels (See Text).

Ag 30.5 e.v. LEVEL



Slide 6. Analysis of Level in Silver at 30.5 e.v.

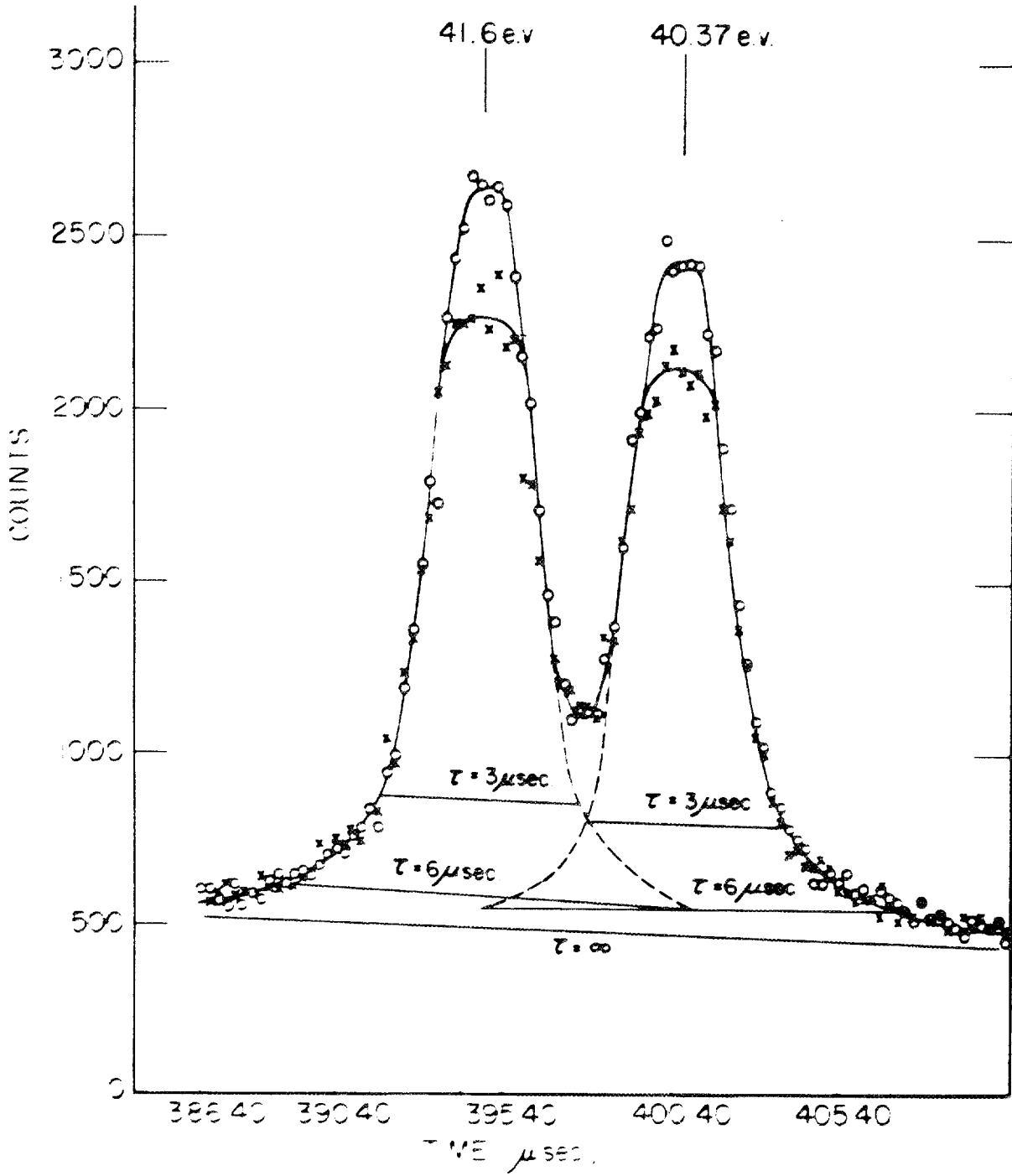
Table 1. Summary of Results on Six Levels in Silver^a

E_0	30.5	40.5	41.6	51.6	55.9	71.2
Δ (e.v.)	0.18	0.20	0.20	0.22	0.23	0.26
τ (μ sec)	13.0	6.0	6.0	4.8	3.75	5.0
ϵ (e.v.)	1.90	1.28	1.24	1.41	1.25	2.39
ϵ/Δ	10.56	6.40	6.22	6.40	5.42	9.21
$A'_{ED}/\Delta T_\epsilon$	6.022	4.192	4.092	5.884	4.554	5.82
T_ϵ/T_c for $\Gamma = 0.15$ e.v.	0.97	0.96	0.96	0.90	0.93	0.97
$\sigma_0 \Gamma^2$ for $\Gamma = 0.05$ e.v.	35	13	14	76	28	58
= 0.1 e.v.	39	18	20	82	35	65
= 0.2 e.v.	45	27	28	92	50	77
= 0.4 e.v.	62		50	118	76	100
MTR ^b Γ (e.v.)	0.13	0.14	0.14	0.13	0.24	0.094
$\sigma_0 \Gamma^2$	30	16	18	58	38	38
BNL-325 Γ (e.v.)	0.11	0.14 ^c	0.14 ^c	0.15	0.16 ^c	0.18 ^c
$\sigma_0 \Gamma^2$	26	18 ^c	20 ^c	65	36 ^c	69 ^c

^aBased on the element with normal isotopic mixture.

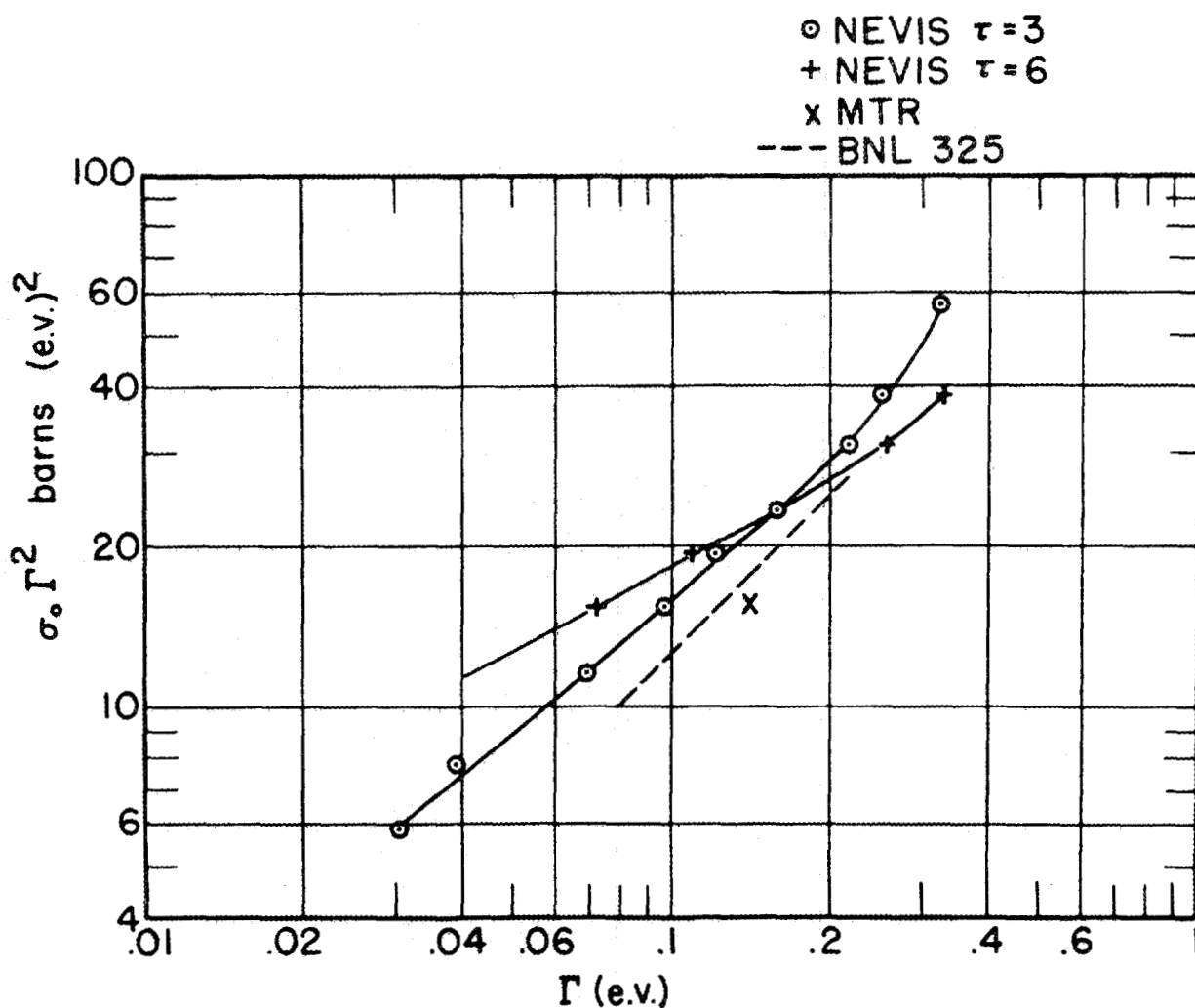
^bR. G. Fluharty, F. B. Simpson, and O. D. Simpson, *Phys. Rev.* **103**, 1778 (1956).

^cBased on $\Gamma_\gamma = 0.135$ e.v.



Slide 7. Levels in Silver at 41.6 and 40.37 e.v.

Ag 40.5 e.v. LEVEL



Slide 8. Analysis of Level in Silver at 40.5 e.v.

R. G. FLUHARTY: Then with your parameters you could apply this to the transmission data and presumably get a value for the potential scattering?

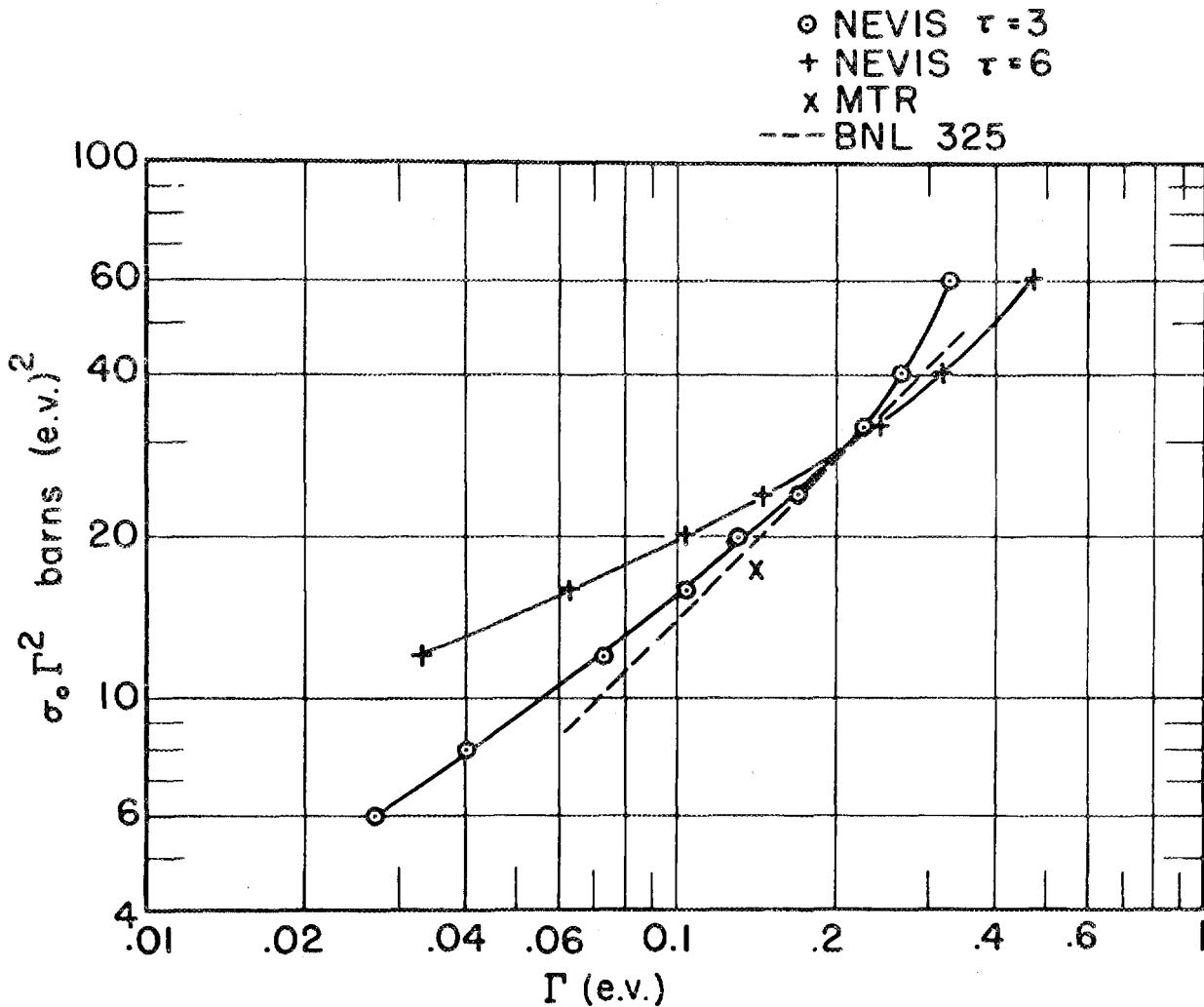
E. MELKONIAN: Yes, if you had transmission data. We don't have transmission data with "flat" detectors. "Self-indication" transmission measurements, such as ours, are not useful in the wings of the resonance, because the detection efficiency becomes so small.

H. PALEVSKY: I would like to get clear what you have here. As I understand it, you are just getting $\sigma_0 \Gamma^2$ by this method. Now can you use the

same method, say with thin samples, and therefore get the parameters out, or would this method just work to get $\sigma_0 \Gamma^2$?

E. MELKONIAN: There are two points. The one point was the slight wing sensitivity. So, to some extent you have two curves which give σ_0 and Γ separately, with considerable amplification of experimental error. But generally this method would apply to any thickness of sample, and application to a thin sample would give thin-sample results, that is, essentially, $\sigma_0 \Gamma$.

Ag 41.6 e.v. LEVEL



Slide 9. Analysis of Level in Silver at 41.6 ev.

H. PALEVSKY: Have you gotten any parameters from your silver down where you say you can get them out by using this method in a thick and a thin sample?

E. MELKONIAN: I guess I didn't make it very plain that one of the basic difficulties of a capture-gamma-type measurement is that you don't know what zero transmission corresponds to unless you have a thick sample. In principle, one could alternate a thick and a thin sample and use the thick sample to get the zero-transmission counting rate. Such measurements have not yet been done carefully enough. But from one run alone one cannot

analyze data unless a thick sample is used. The levels above 72 ev were not analyzed in this manner, because it was not clearly established that the peak counting rates corresponded to zero transmission. However, this method is not limited by these considerations, which are faults of the capture-gamma method.

D. G. HURST: If the gamma cascades vary with the resonances, will this affect the background that you subtract?

W. W. HAVENS, JR.: I can give an answer to that one. If we analyzed thin samples, that would be true, but that is why all the analyses have been

applied to thick samples. Each resonance is normalized to its own thick-sample value. You see, we normalized to the peak for the thick sample, and when you have the thick sample you know that all neutrons at the peak have interacted with the sample; therefore, at the peak your transmission is zero. We do not try to go from resonance to resonance, but each resonance is normalized to itself by the total number of counts for a thick sample.

J. E. DRAPER: Since this seems to depend on the detailed shape in the wings, I wonder whether

the $1/v$ term is negligible, and also whether the interference in scattering would influence this.

E. MELKONIAN: These factors would have to be considered for each level separately, I would suppose. At sufficiently high energies the change in energy from one side to the other is small enough so that the $1/v$ -term variation is negligible. The effect of scattering interference is expected to be small, since in the wings, where the interference is most pronounced, the sample becomes thin and the counting rate depends only upon the capture cross section. This might become important in cases of extremely thick samples.

NEUTRON RESONANCE PARAMETERS OF Eu^{151} AND Eu^{153}

J. A. Harvey and R. C. Block
Oak Ridge National Laboratory

J. A. HARVEY: I should like to report on the measurements that we have made recently on resonances in Eu^{151} and Eu^{153} . We were interested in determining the level spacings and the strength functions of these two nuclides. Earlier transmission and activation measurements with natural europium up to a few ev by the Brookhaven crystal-spectrometer group suggested that the level spacing of Eu^{151} was about half that of Eu^{153} . Since separated isotopes became available a few months ago, we decided that we would check the earlier identifications and extend the data to higher energies to see if this difference in level spacing was significant.

The strength functions (the ratio, $\overline{\Gamma_n^0}/D$) of Eu^{151} and Eu^{153} were predicted from the cloudy-crystal-ball model to be about 4×10^{-4} and 5×10^{-4} , respectively (see Slide 2 of Zimmerman's paper). However, it was suggested that the strength functions of these two nuclides might be considerably reduced due to their spheroidal shape. Since the quadrupole moment of Eu^{153} is twice that of Eu^{151} and, hence, its distortion from sphericity is greater, its strength function should be reduced more than that of Eu^{151} . Hence, we wanted to determine the strength functions of these two nuclides using the enriched isotopes.

We have made transmission measurements with several different sample thicknesses of enriched isotopes with the Oak Ridge fast chopper up to 10 ev. The Eu^{151} sample was enriched to 91.9%, and the Eu^{153} sample was enriched to 95%. The transmission curves of the samples have been corrected for the few per cent impurity of the other isotope. The transmission data have been analyzed using the standard area method with several sample thicknesses for each isotope. We have found that the previously reported resonances at 1.76, 3.35, 3.84, 4.83, 7.47, and 8.90 ev are each two resonances with a resonance in each isotope. For example, in addition to the previously reported resonance at 1.76 ev in Eu^{153} there is also a resonance at 1.84 ± 0.02 ev in Eu^{151} . Also, in addition to the resonance assigned to Eu^{151} at 3.35 ev there is also a small resonance at 3.28 ± 0.03 ev in Eu^{153} . The resonance at 3.84 ev has been resolved into

two resonances, one in Eu^{151} at 3.72 ev and one in Eu^{153} at 3.94 ev. This shows the need of running separated isotopes. We have identified and measured the parameters of all the resonances from 1 to 10 ev, and our conclusions on level spacings and strength functions are based on these data.

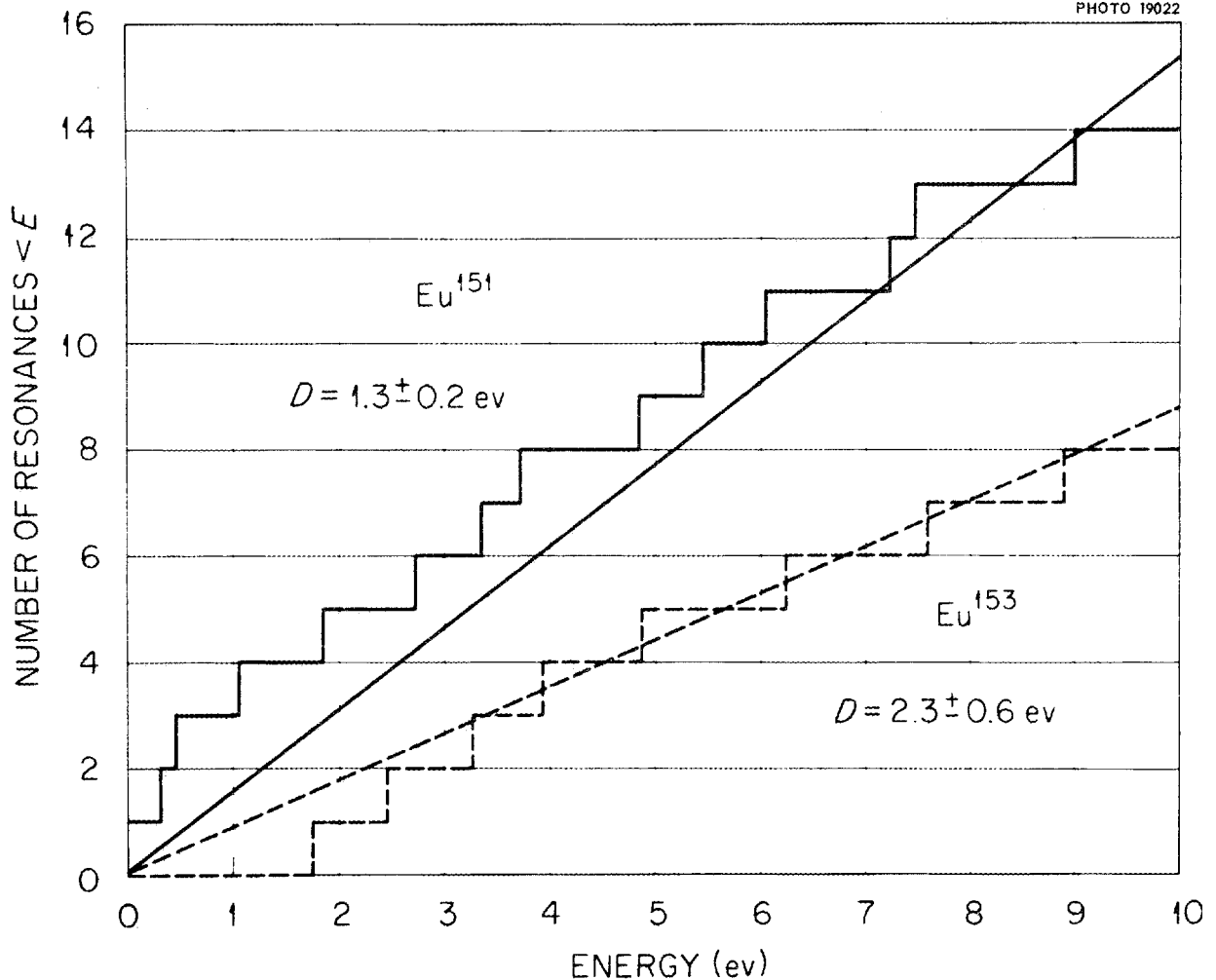
Slide 1 shows the plot of the number of levels versus energy up to 10 ev. The straight lines represent the average level spacings computed from the number of resonances in each isotope up to 10 ev. A 10% correction was applied for the number of small resonances that we estimated would have been missed, assuming a Porter-Thomas distribution of neutron widths. Assuming that the level spacings of the two spin states are equal, the level spacings per spin state are 2.3 ± 0.6 ev for Eu^{153} and 1.3 ± 0.2 ev for Eu^{151} (including the three resonances in Eu^{151} below 1 ev).

The strength functions of these nuclides were determined from the data up to 10 ev. A 2% correction was applied to correct for the small resonances that we estimated would have been missed. The strength functions from the data up to 10 ev are $(1.7 \pm 0.6) \times 10^{-4}$ for Eu^{153} and $(3.1 \pm 0.8) \times 10^{-4}$ for Eu^{151} . Although the errors are quite large, we feel that the difference is significant and that the strength function of Eu^{153} is less than that of Eu^{151} . This is the effect that was expected, since the quadrupole moment of Eu^{153} is twice that of Eu^{151} , and, hence, its strength function would be reduced more than that of Eu^{151} because of the greater nuclear distortion.

A. M. WEINBERG: According to the views expressed by Professor Gamow, the abundances should come in inverse ratio to strength function. Do you remember the abundances of the two isotopes?

J. A. HARVEY: The abundance of Eu^{153} (52.2%) is only slightly more than that of Eu^{151} (47.8%), and, hence, although the effect is small, it is at least in the right direction.

R. L. ZIMMERMAN: Maybe it is appropriate to present some preliminary data from the Brookhaven fast-chopper group in which we measured the strength functions for the separated isotopes of europium both by the averaging method which I



Slide 1. The Number of Observed Eu^{151} and Eu^{153} Levels $< E$ as a Function of Neutron Energy.

described and by counting the levels. In the case of Eu^{153} we measured 16 resonances up to 24 ev, and in the case of Eu^{151} 20 resonances up to 18 ev. The measured strength functions in the kev energy region agree with the low-energy measurements within the errors. The weight averages of the two methods give values for the strength functions of $(2.7 \pm 0.5) \times 10^{-4}$ for Eu^{151} and $(2.7 \pm 0.6) \times 10^{-4}$ for Eu^{153} . The value obtained from measurements in the kev energy region with natural europium was $(3.3 \pm 0.6) \times 10^{-4}$.

The level spacings per spin state over the energy range mentioned earlier are 3.0 ± 0.6 ev for Eu^{153}

and 1.8 ± 0.4 ev for Eu^{151} . So there is a definite difference in spacing.

J. A. HARVEY: I think the values for the level spacings from BNL and ORNL are certainly in agreement and indicate that the level spacings of the two nuclides are significantly different. However, the situation is not definite with regard to the strength functions.

H. H. LANDON: We have been interested in europium for a long time as one of the best cases in which we could get careful measurements of several radiation widths. I should like to point out that radiation widths have been measured with

the BNL crystal spectrometer for several of these resonances in europium that you have been talking about, and they seem to separate into two groups. In Eu^{151} , one group has a radiation width of about 93 mev (milli-electron volts), and the other group has a radiation width of about 70 mev. Since there are two spin states, it looks as though the radiation widths may differ depending on the spin state of the resonance. We have also one very good measurement of a radiation width in Eu^{153} of 89 mev.

If we identify this value in Eu^{153} with the same spin state that corresponds to the value of 93 mev in Eu^{151} , there does not seem to be a strong dependence of radiation width on level spacing.

J. A. HARVEY: However, if this value in Eu^{153} corresponds to the value of 70 mev in Eu^{151} , then there is a dependence. This is in the direction that the smaller level spacing of Eu^{151} produces smaller radiation widths.

PERFORMANCE AND SOME RESULTS FROM THE HARWELL NEUTRON SPECTROMETER BASED ON THE LINEAR ELECTRON ACCELERATOR

E. Bretscher
Atomic Energy Research Establishment, Harwell

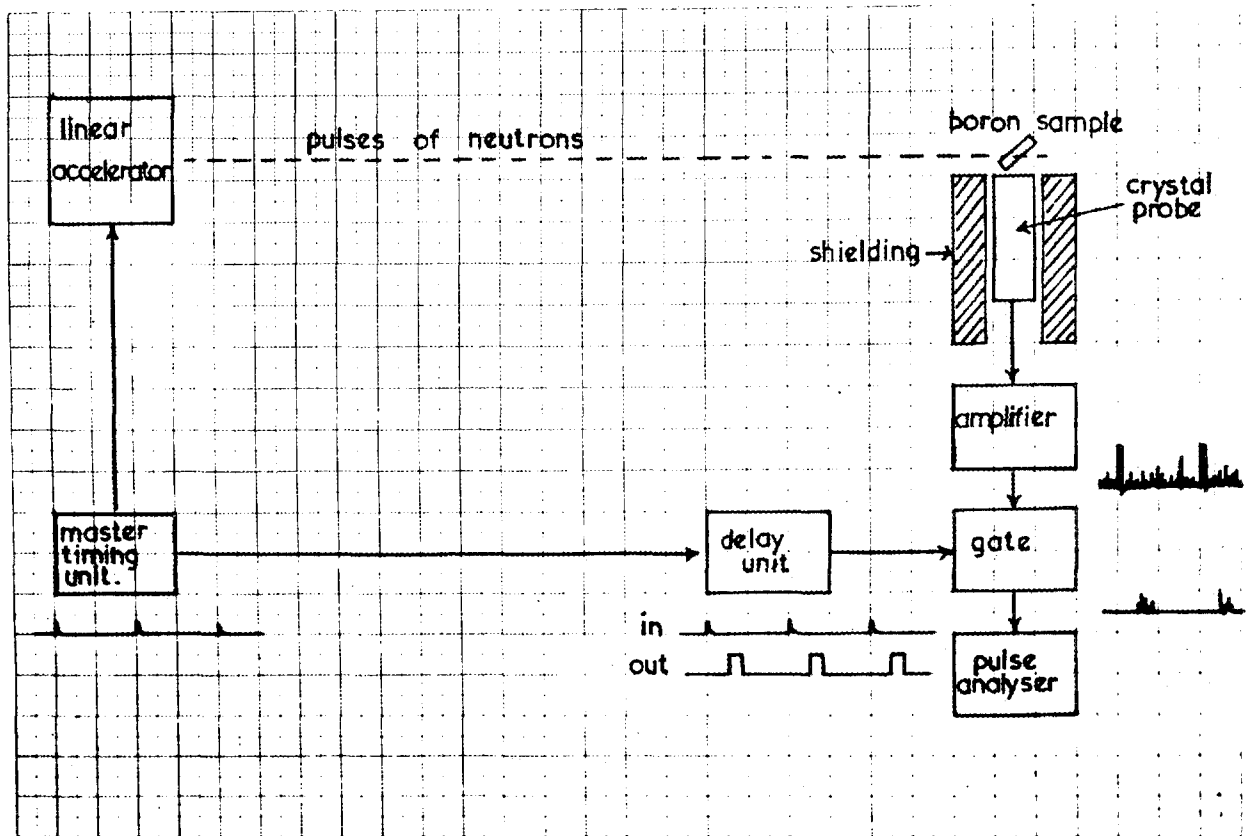
E. BRETSCHER: I have been asked to say something of the work and of the instrument which we have through the development of a pulsed neutron source based on a high-current linear electron accelerator at Harwell. This instrument is rather unique, and I think that, up till now, we were the only physicists who had such a neutron spectrometer.

In some respects this talk does not fit in with what has been said up till now, because we have mostly been concerned with results and their interpretation by theory. However, I have been asked by the organizers of this conference to give a survey of this field, and so you have to expect a change in what is coming.

First of all, I am not directly in charge of this work; the neutron-spectrometer group is led by Mr. E. R. Wiblin, and he has, as collaborators, Dr. E. R. Rae, Dr. E. R. Collins, Mr. J. E. Lynn, and Mr. J. E. Evans.

Let us first look at the experimental setup as a whole. You will see on the first slide the linear accelerator with the flight path and a detector station for, in this case, the observation of the neutron-capture gamma rays. You note that the linear accelerator and the time gates are controlled by a master oscillator. We have several flight paths of up to 60 m length, so that several experiments can be done at the same time.

UNCLASSIFIED
PHOTO 19163



Slide 1. Schematic Diagram of Apparatus for the Study of Neutron-Capture Gamma Rays.

I will now give you a few details of this machine and begin with the linear electron accelerator. In Slide 2 we have a wave guide into which we inject electrons at 50 kev energy. At the same time a radar pulse supplied by a magnetron enters and travels down the corrugated guide. To be successful in accelerating electrons, one has to match the speed of the radar pulses to the increasing velocity of the electrons. This is done by increasing the diameter of the corrugations and thus the speed of electromagnetic pulses down the wave guide. To secure a high intensity, the electrons are kept on the axis of the accelerator by a magnetic field parallel to it. The instrument at present in use has the following characteristics:

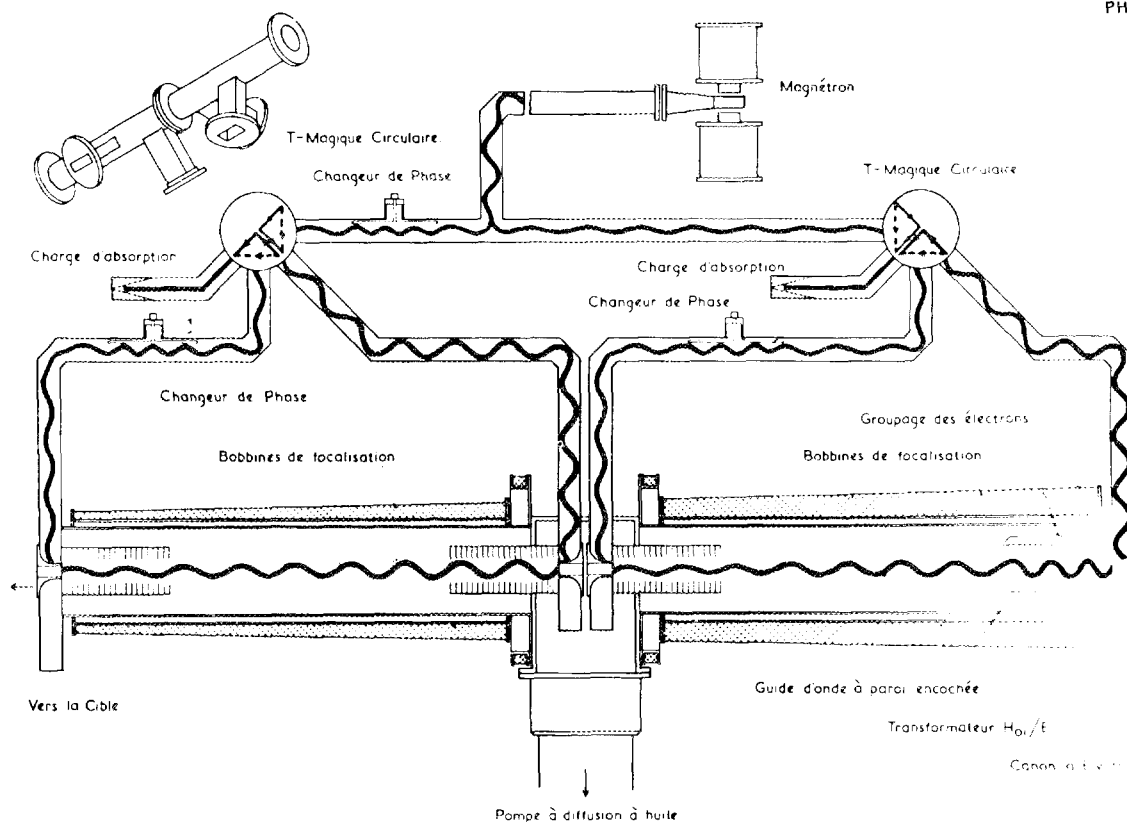
Mean current for maximum duty cycle	30 μ a
Magnetron frequency	3000 Mc
Magnetron power (in pulse)	2 Mw

Electron energy (for load below)	14 Mev
Pulse length: choice of	2, 1, 0.5, 0.25 μ sec
Repetition rate (max.)	500 cps
Current in pulse	30 ma

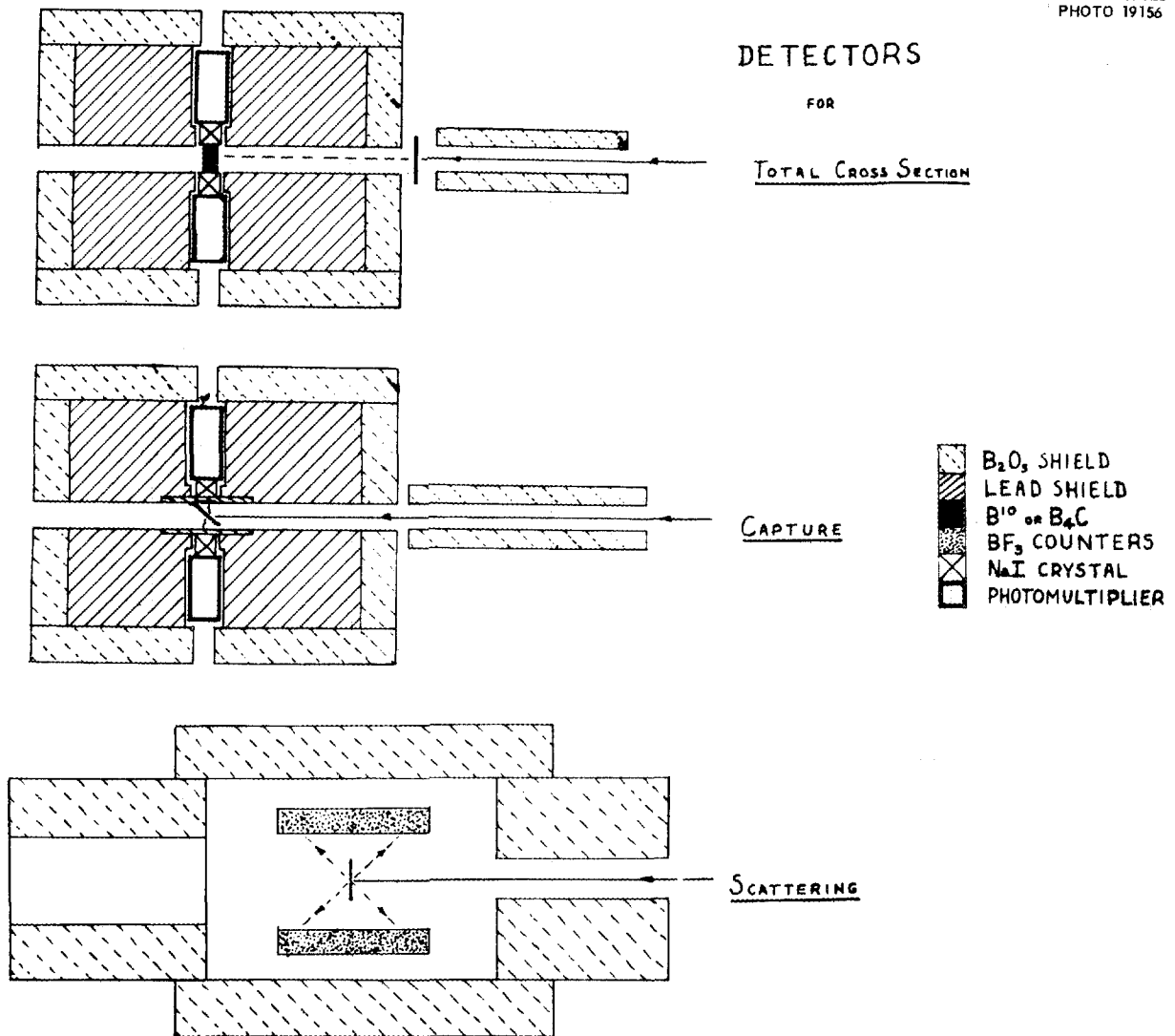
The wave guide is subdivided into two independent sections fed by the same magnetron. The total length of the accelerator is 6 m. Any electromagnetic energy left over at the end of the guide length is fed back into the circuit instead of being attenuated in a dummy load. The electron beam leaves the wave guide through a window and enters a uranium block, where the brems-radiation is produced and the neutrons are released. This target is surrounded by suitable amounts of moderator.

Turning to the detectors, we use the following arrangements (Slide 3) for the determination of the total, capture, and scattering cross sections. Here you will note that in the case of total cross sections all the neutrons are absorbed by a thick

UNCLASSIFIED
PHOTO 19157



Slide 2. Schematic Diagram of the Acceleration of Electrons in a Linear Accelerator with Dual Feed.



Slide 3. Detector Arrangement Used for Total, Capture, and Scattering Cross-Section Measurements.

block of B¹⁰, from which the 480-kev gamma is emitted and detected with the help of several NaI crystals. A similar setup can be used to measure the gamma-ray spectrum due to capture of neutrons into various resonances. The B¹⁰ is then replaced by the specimen to be studied. This arrangement allows us to use for total cross sections a resolution of about 0.004 $\mu\text{sec}/\text{m}$ at 1 kev.

I should now like to say something about the results, and I will refer to a study of the silver resonances which has been carried out by Rae and Lynn and which was reported in a preliminary communication at the Amsterdam Conference.

Our aim in the past has been, not so much to perform a lot of transmission measurements, but to study some cases carefully and to obtain as complete a set of resonance parameters as possible. The aim, therefore, is to measure Γ , Γ_n , Γ_γ , and g , the spin statistical factor. The area method was applied to the case of silver, though with some other elements the shape method has been used. The observations result, after correcting for Doppler effect and thickness, in the determination of the following quantities: $\sigma_0 I^\gamma$, $\sigma_{0c} I^\gamma$, $\sigma_{0sc} I^\gamma$ for thin and $\sigma_0 I^{\gamma 2}$ for thick samples, where the subscripts 0, 0c, 0sc refer to the resonance total,

capture, or scattering cross section. These experimental values are connected with the desired parameters as:

- (1) $\sigma_0 \Gamma = a \cdot g \cdot \Gamma_n$,
- (2) $\sigma_0 \Gamma^2 = a \cdot g \cdot \Gamma_n \cdot \Gamma$,
- (3) $\sigma_{0sc} = a \cdot g \cdot \Gamma_n^2 / \Gamma$,
- (4) $\sigma_{0c} = a \cdot g \cdot \Gamma_n \cdot \Gamma_\gamma / \Gamma = a \cdot g \cdot \Gamma_n (\Gamma - \Gamma_n) / \Gamma$,

with

$$a = 4\pi\lambda^2,$$

$$g = \frac{l+1}{2l+1} \text{ or } \frac{l}{2l+1} \text{ for the two spin states,}$$

$$l = \text{spin of target nucleus.}$$

The experimental results are contained on the left side of the four above equations and overdetermine the three parameters desired: g , Γ , Γ_n . The correct value of g can be found in a neat way, due to Dr. Rae, as follows: Let us plot Γ_n against Γ for each of the four equations, with the appropriate value at the left side divided by $a \cdot g$, and let us do this separately for each of the two possible values of g . This has been done on Slide 4 for the case of the 5.22-eV resonance of Ag^{109} . On the left you see the four curves for $g = 1/4$, and on the right those

for $g = 3/4$. The result points most spectacularly to the value $g = 3/4$ as the correct one and to $J = 1$ as the spin of the compound nucleus.

The results in the case of silver have been collected in Table I. Out of eight resonances, six have spin $l + 1/2$, two have $l - 1$. It seems, if one is prepared to say anything from these small numbers, that the frequency ratio of the two spin states is $(l + 1)/l$. Further, one can say that Γ_γ seems approximately constant and independent of J (for discussion of Brink's theory about this see Dr. Lane's talk).

In Slide 5, one result is shown in the high-energy region in the case of Na^{23} , where the parameters for the 2.85-keV resonance could essentially be obtained from shape measurements, as a high resolution of $0.25 \mu\text{sec}$ at 60 m path was used. The parameters are:

$$\sigma_0 = 370 \pm 5 \text{ barns,}$$

$$\Gamma = 405 \pm 12 \text{ ev,}$$

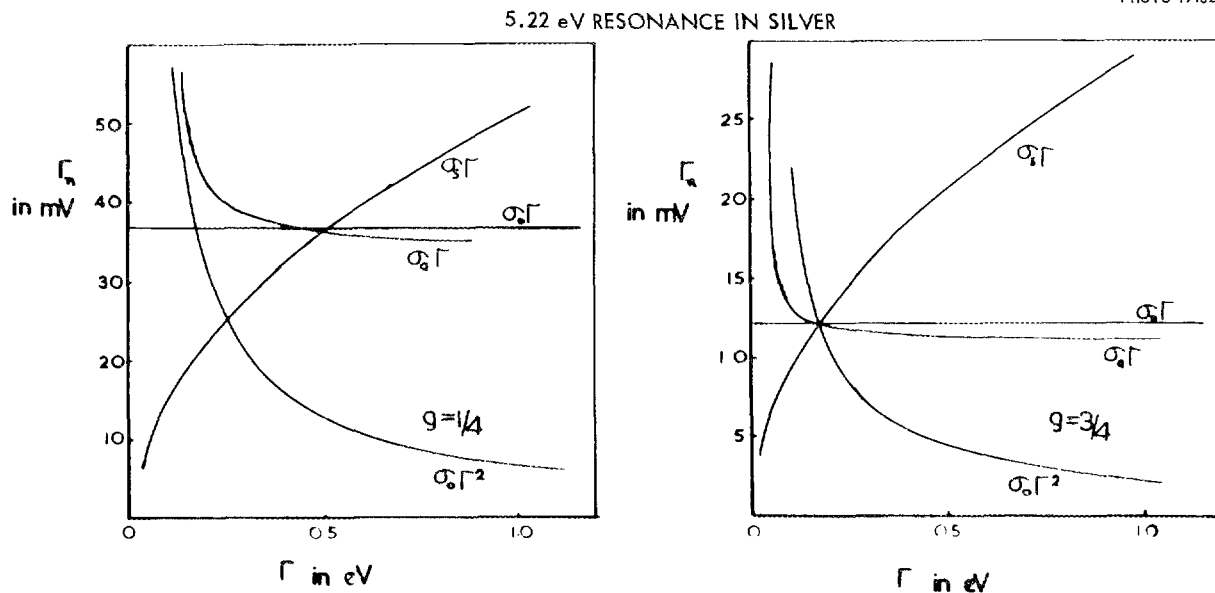
$$\sigma_p = 2.75 \text{ barns,}$$

$$J = 1.$$

There seems to be a disagreement here, in respect to Γ , between us and the U.S.A.

Finally, I would like to say something about the new machine we are soon setting up and what it will do.

UNCLASSIFIED
PHOTO 19162



Slide 4. Graphic Method of Determining the Statistical Spin Factor.

Table 1. Resonance Parameters for Silver

E_0 (ev)	Isotope	Γ (mev)*	Γ_n (mev)*	Γ_γ (mev)*	Spin
5.22	109	170 ± 11	12.1 ± 0.33	158 ± 11	1
16.3	107	150 (140)	12 (4)	138 (136)	0 (1)
30.7	109	149 ± 13	6.7 ± 0.43	142 ± 13	1
41, 42	107, 109	142 ± 19	5.0 ± 0.40	137 ± 19	1
45	107	~200	-	~200	-
51.8	107	157 ± 16	20.8 ± 0.94	136 ± 16	1
56	109	180 ± 11	36.3 ± 1.4	144 ± 11	0
71	109	190 ± 6	27.8 ± 0.65	162 ± 6	1
88	109	158 ± 21	18.3 ± 1.4	140 ± 21	0

*Milli-electron volts.

As you know, once one has an instrument one always wants a bigger and better one. The Metropolitan Vickers Company in Manchester have developed high-current machines and were willing to build a bigger accelerator for us. The new machine is expected to deliver at 28 Mev a current of about 1 amp in the pulse; it will produce with a small load 35-Mev electrons. Otherwise the specifications are similar to those of the present one, though the pulse repetition frequency has gone up to 750 cps. The maximum target power will increase to 42 kw. The neutron production rate of the present machine is about 10^{14} neutrons per second (during pulse); the new one will be about $(1 \text{ to } 5) \times 10^{16}$ neutrons per second. The x rays are produced in a flowing mercury target, and the neutrons are emitted from a uranium block which stands behind it. The x-ray production has been estimated to be 250,000 r/min at 1 m in the forward direction. The instrument has a large number of flight paths and will be used, besides for nuclear physics, for the study of lattice spectra and other problems.

There has always been in the back of our minds the hope that we might increase the source strength for our time-of-flight equipment with the help of a multiplicative assembly of fissile material, a device christened a "booster." It is now under construction and will, we hope, be available in the second half of 1957. There is a water-cooled core of U^{235} with a mercury target as x-ray source and natural uranium as neutron source; we have reduced

our original high multiplication to the value of about 10 to 15, which brings our source strength to 5×10^{16} to 5×10^{17} neutrons per second in the pulse. The above multiplication has been chosen to avoid the formation of a long tail in the $\frac{1}{4}$ - μ sec neutron burst due to neutrons returning late to the core from the tamper or moderator and starting a chain again. Thus we still have a pulse length of 0.25 μ sec at our disposal. This is advantageous for the resolution, as it is well known that it is better to cut the pulse length than to increase the length of flight path.

J. L. FOWLER: How do you dissipate the energy in the booster?

E. BRETSCHER: Cooling with water.

H. L. SCHULTZ: Might I inquire what the status of this new machine is?

E. BRETSCHER: The machine is just now being erected.

H. L. SCHULTZ: Has any test been made on achieving 1 amp current in any part of the machine, say one section?

E. BRETSCHER: No, the firm is under obligation to provide an ampere, and it is a matter of collecting the electrons over a rather large angle from the source. They have only obtained $\frac{3}{4}$, but I do not think there are any difficulties really in achieving this.

H. GOLDSTEIN: I am very much interested in this sodium resonance which you showed in one of the slides, and I have a number of questions. One

is that, on the slide you showed, there appeared to be an asymmetric curve which had been fitted to the shape of the observed transmission resonance. I was wondering what assumption had been made about the interference with the potential scattering. There seemed to be no dip shown. Do you just assume that there is no such interference?

E. BRETSCHER: I am sorry I do not know at the moment which value they used, but they included potential scattering.

A. M. WEINBERG: Could you say a word about what is the ultimate limitation in the average number of neutrons you will get from a machine of this sort? Is it the heating of the target, or what do you conceive will ultimately limit the production rate? Let me say the reason I ask this question is, when you get a neutron production of this order, then a device like this begins to be competitive with reactors.

E. BRETSCHER: It is a pulsed reactor.

A. M. WEINBERG: What is the maximum duty cycle you can probably get on a machine of this sort?

E. BRETSCHER: Well, I think it is probably a matter of money and the amount we want to invest to start with. Let me say if we could increase the production rate by a factor of ten, then the cooling of the target would be rather difficult. We would have to figure it out, but I believe it is something like 10 or 20 kw in the booster. I do not remember exactly.

A. M. WEINBERG: I think that 5×10^{16} , if I did not make a mistake, corresponds to a reactor at about 1,000 kw.

E. BRETSCHER: This is correct. When we include the duty cycle, that is 1 kw mean.

A. M. WEINBERG: How much do you think you could increase the duty cycle if you did not have your multiplier there at all, if it were not a matter of cooling? Is there something in the electronics of the device which makes it impossible to go to more than 0.001 duty cycle?

E. BRETSCHER: I suppose the limit in the electric part is, of course, the current. As soon as one goes to a really high current one gets space charges, and then the beam spreads. It would also be hard to get a sufficiently large cathode emission and collect all the electrons.

J. J. MENY: Our experience with recent work indicates that probably the most real limitation today on the duty cycle of the radio-frequency oscillator is the klystron.

E. BRETSCHER: How limiting is that?

J. J. MENY: About 10^{-3} is approximately the duty cycle. The reactor people still do not have to go out of business quite yet. I think I can assure you of that.

E. BRETSCHER: This new machine consists of six sections, instead of only two as did the old one, and each is run by a 6-megavolt klystron. Another feature which is very interesting is the high conversion rate of the electrical energy into the beam, when you consider how much energy investment one has in the cyclotron with the magnetic field. In our machine, if I remember correctly, one can get up to 85% of the radar energy which is fed into the accelerator coming out as kinetic energy of the electrons.

E. GUTH: How much better is uranium than beryllium as a target?

E. BRETSCHER: In the 28-Mev region one gets, of course, nearly the whole integral over the range of the giant resonance in U^{238} , and in beryllium the cross section goes down. Beryllium is good enough for a few million electron volts gamma energy.

W. M. GOOD: Is the sample size that is used here such that it is practical to use separated isotopes for total-cross-section measurements?

E. BRETSCHER: The full advantage of this machine is best obtained with large samples. For small samples, we rather consider using Egelstaff's superchopper.

CONTRIBUTIONS OF NEUTRON TIME-OF-FLIGHT EXPERIMENTATION TO LOW-ENERGY NEUTRON PHYSICS

D. J. Hughes
Brookhaven National Laboratory

D. J. HUGHES: In the low-energy region we have been accumulating data for a long enough time now that we certainly ought to be at the stage where we can sort of look at this great accumulation and ask where we are going and what we are going to do with it all. We are not really quite at that stage in the higher-energy region at present, but there the instruments have been getting a lot better, new techniques have been devised, and so really a lot of new results will be coming out. Also in the higher-energy region the millimicrosecond timing techniques mean that a lot of things are just beginning now, so that it isn't really the time to look at that part of the field and ask whither are we drifting. But we can certainly do that with the low-energy region.

If we first of all look at what has been happening in this lower-energy region from the side of the instruments themselves, I think it is fair to say that things have not been changing extremely rapidly. That is, at a meeting of this type two years ago we probably would have been talking about resolving powers of the order of 0.06 or 0.07 $\mu\text{sec}/\text{m}$. Well, I think the best we do now is maybe better than that by two or two and one-half times, and that isn't really a tremendous increase in resolving power.

If we ask what instrument is doing the best, are people doing better, say, with fast choppers, mechanical velocity selectors, or linear accelerators, then I think the interesting thing is that it is still about neck and neck. It was that way about two years ago, and it still seems to be about the same. I think the reason is that, while it is true that improvements have been made in pulsed accelerators and the methods of using them, it is also true that higher fluxes have become available over about the last two years in reactors. The choppers themselves haven't improved tremendously; all you can do is spin something so fast that it just about flies apart. Materials haven't become stronger in the last two years, but fluxes in reactors have become quite a bit higher, and, of course, this flux can be used up in order to get better resolution simply by putting the detector farther away. However, as you all know, you use up a factor of 10 or

100 in flux awfully fast if you try to improve resolution just by pushing the detectors farther away.

If we look at the detecting instruments, the analyzing instruments, the techniques of analysis, and so on, there I don't really believe that things have advanced extremely rapidly. Perhaps really no great advances are needed. That is, people now have 1000-channel timing analyzers. There does not seem to be any particular problem with them. It seems possible to get the data written down on punch cards or typed out on long sheets of paper.

The method of analyzing all these data in order to get parameters has really not changed greatly. If we are speaking only of total cross sections, the problems are rather well worked out for getting the parameters of resonances.

There is a problem, however, that is getting to be more and more acute — how to handle all the numbers. When 1000 channels are run simultaneously, 24 hr a day, 7 days a week, then the numbers pile up, and I think all of the people who are on the receiving end of this kind of data have the same problem of deciding just how to handle it all.

There is another type of analysis, really almost another instrument problem, and that is how to get information on things other than just the total cross section. There, really valiant efforts have been going on for a number of years. But if you look at the compilations you will find that there still are not very many results available from measurements other than total cross sections.

It is a little hard to say just what the reason is for this situation. Probably the fundamental reason is again that these other types of measurements, the partial cross sections, are just tough to do. Quite a few people have made measurements of scattered neutrons, have made measurements of capture gamma rays, but when it comes right down to the business of getting parameters out of the measurements, there still are not very many real parameters reported from this kind of work. It is important to push that kind of work, and I think all the effort that can be put into it is certainly worth while.

I should like now to talk a little about the results in terms of how good they are or how finished they are, and a little about the relationship to theory, and here let's make a split between the nonfissionable nuclei and the fissionable nuclei.

First, if we look at the nonfissionable nuclei, say at the great lists of parameters, obviously the problem is what are people going to do with all of these high-resolution instruments in, say, three, four, or five years. I mean that so many parameters are being measured that we might just as well quit. In a sense that is true. My guess would be that the main findings are known. You can almost say that the principal facts of the behavior of parameters of levels are reasonably well known. The field is sort of staked out. In a very negative way, it is just a matter of measuring some more parameters to fill in the details. But I don't think that is really the right way to say it. It is true that the gross aspects of the behavior of parameters of levels are known, and you can say that the things that are yet to be measured are details, but, on the other hand, it does not mean that they are unimportant, because it may be that just these details are the things that are crucial as far as a particular theory is concerned.

So now let's look at what we know about parameters very briefly, just to see whether these conclusions are true or not. For instance, we know pretty well that the radiation widths are constant from level to level within a single nucleus, and that throughout the atomic weight table the radiation widths vary rather slowly. There are some peaks at magic numbers, but they are supposed to be there. Those peaks can be correlated with other discontinuities, such as discontinuities in binding energy. The absolute magnitude of the radiation widths, however, is quite far from the theoretical estimate. When we say that radiation widths are *about* constant, then it is important to know *how* constant. The reason that they are constant is that there are many possible final states for radiation emission, but we would like to know *how many* final states; therefore it is important to know if the radiation width is *exactly* the same from level to level, or does it vary by 5%, or 10%, or 15%. This fact would have a direct bearing on the number of possible final states that are available.

Another possibility is slight differences in radiation widths from level to level, depending on the spin. It is possible that there are really two groups of gamma-ray widths, but that they are close enough

together so we don't see the difference. There may be other differences in the radiation, not so much the radiation width, but in the details of the capture gamma rays emitted in each level. This again is a thing that takes very careful work. It is not just a measurement of a few more parameters. They have to be measured extremely well.

Then if we go to the neutron widths, there again the story is the same. We can say: Well, after all, everybody knows that the neutron widths have a very wide range in size, and furthermore that they are about exponential in their size distribution, or maybe sort of halfway between exponential and the Porter-Thomas distribution. But again the same story is true. We don't know exactly. It does seem important, in order to compare with theory, to know just what the distribution is. That is not a matter of just measuring twice as many levels. It means measuring a lot more levels, maybe ten times as many levels, and measuring them very accurately.

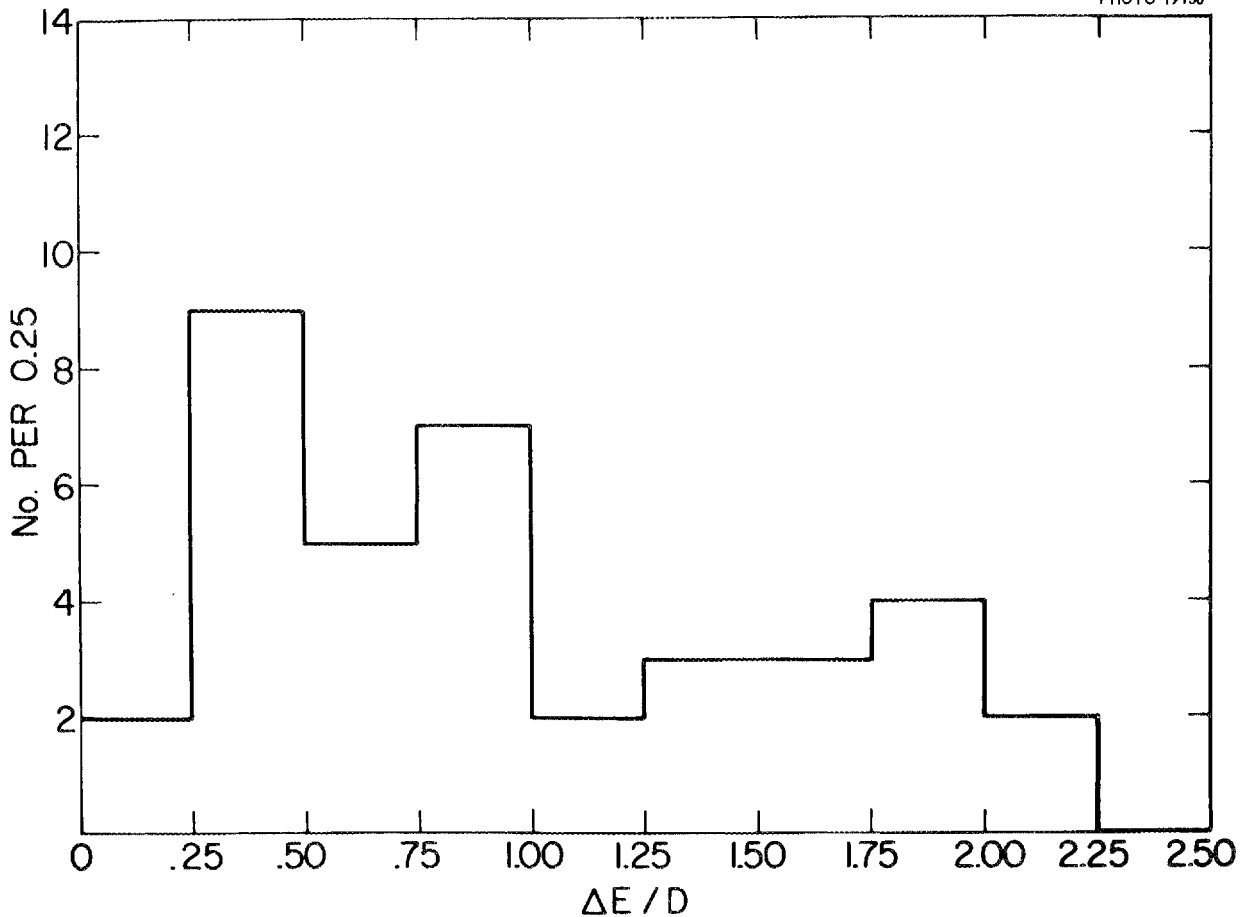
If we go beyond the widths for a moment to the matter of spacing of levels, the story is again the same. Levels are spaced *almost* at random. We are not sure whether they are exactly at random or not.

Slide 1 is a reasonably recent picture of the differential distribution of the levels in some even-even nuclides. A random distribution, of course, would be exponential on this rectangular plot, and you can see that the distribution, within rather poor statistics, is consistent with being exponential except for the smallest spacing.

Those of us at Brookhaven, plus Jack Harvey at Oak Ridge, have done a lot of thinking about various experimental effects that could mess up the thing for small spacings, but we are pretty well convinced, ourselves, that experimental effects might bring this up somewhat, but that there remains a real shortage of small spacings. That is, to summarize the situation, you would say that for most of the spacings the distribution is random, but there does seem to be an effect of repulsion. Levels don't want to be extremely close together.

Again here it obviously takes extremely careful work to try to settle this problem. It gets more complicated when we don't limit ourselves to even-even nuclides. Things get somewhat more complicated then. So again the situation is the same. We need more work and very careful work.

Now we have talked about the radiation width, the neutron width, and spacings, and for all of these things we have a good general picture but



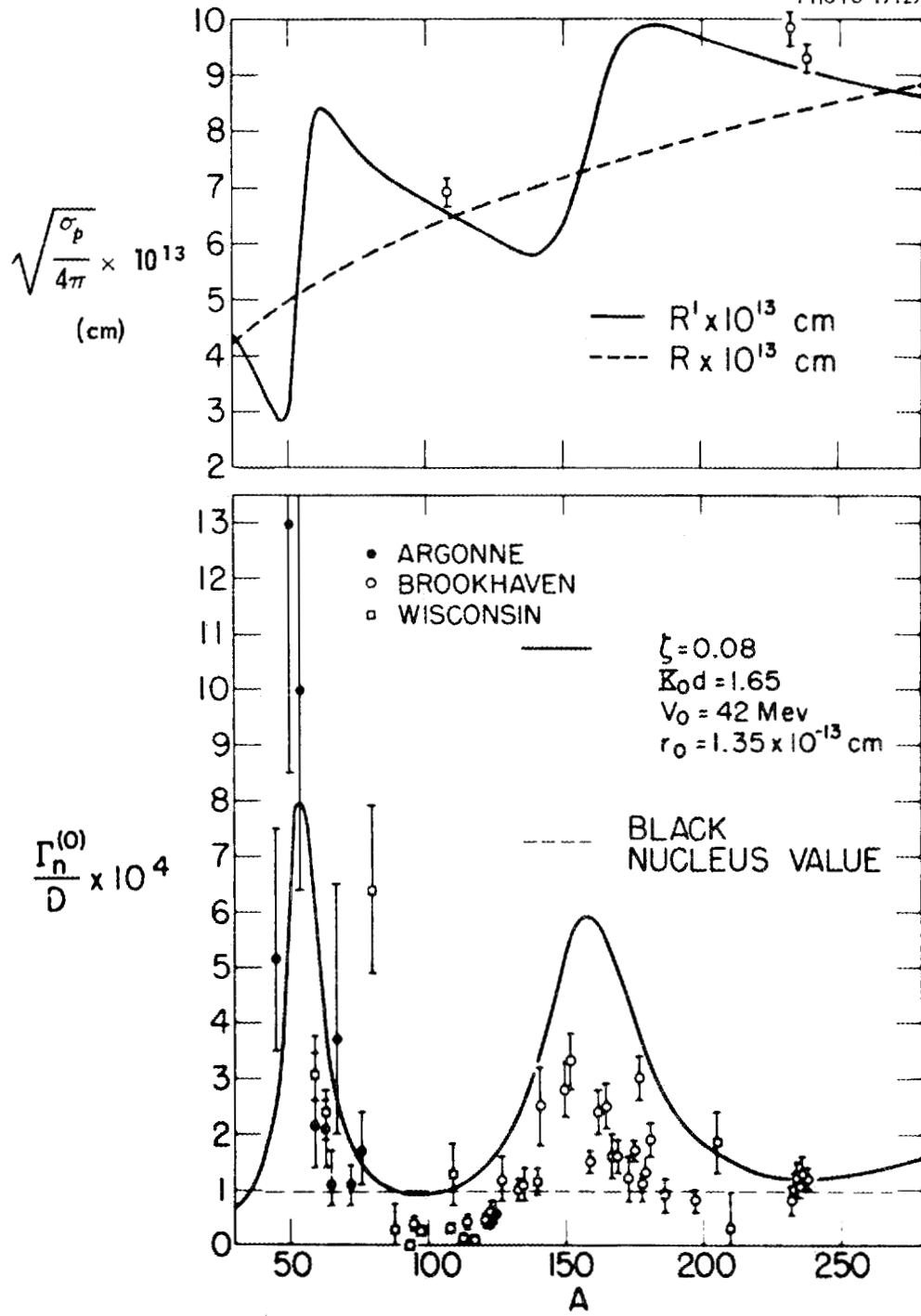
Slide 1. Differential Distribution of Spacings (Th^{232} , U^{234} , U^{236} , U^{238}).

we don't have the last word. If we want to compare these results with theory, the most interesting thing at the moment is to see how these results compare with current nuclear models.

Slide 2 was prepared at Brookhaven about the first of July to be shown by Weisskopf at the Amsterdam meeting on the third of July. It represents a lot of calculations and quite a few experimental points. You probably think that you have seen these curves before, but I would bet you haven't. They are the results of calculations carried out at MIT over the last ten months or so, in which the cloudy-crystal-ball model was modified by including a diffuse edge. These are the so-called zero-energy results, the "strength function," that is, the $\bar{\Gamma}_n^0/D$ ratio, which gives the probability of formation of the compound nucleus, and the

apparent size of the nucleus to a slow neutron. In this computation, R is the distance out to the halfway point of the potential, and the R that was used is $1.35A^{1/3} \times 10^{-13}$ cm. That was the quantity that best fitted the proton-scattering data. The way the computation was done was to fix as many of the parameters as possible right at the beginning so there would not be too many to play with later on. So the r_0 of 1.35×10^{-13} cm was fixed by the proton-scattering data at the start.

The quantity R' appears in the equation for the potential scattering, which says that the potential scattering is $4\pi(R')^2$. Thus you can say that R' is the apparent size of the nucleus to a slow neutron. The value of ζ , you see, is now 0.08, and you probably remember a value of 0.03. A sloping boundary allows the neutron to enter the nucleus



Slide 2. Experimentally Measured Strength Functions and Nuclear Radii Compared to Predictions of the Diffuse-Edge Complex-Well Model.

much better. That increases the compound-nucleus formation at one of these peaks. To bring it down it is necessary to make the nucleus blacker again, thus increasing ζ .

If you remember the situation a few months ago, the experimental points for the strength function at $A = 100$ were much lower than the value for the black nucleus, about 10^{-4} . However, out around atomic weights of 230 to 240 the experimental points were about equal to the black-nucleus prediction. It was hoped that putting in the diffuse boundary would raise the theoretical curve at $A = 240$, but that it would not raise it very much at $A = 100$. Well, it produced that effect, but only very slightly, the major discrepancy remaining.

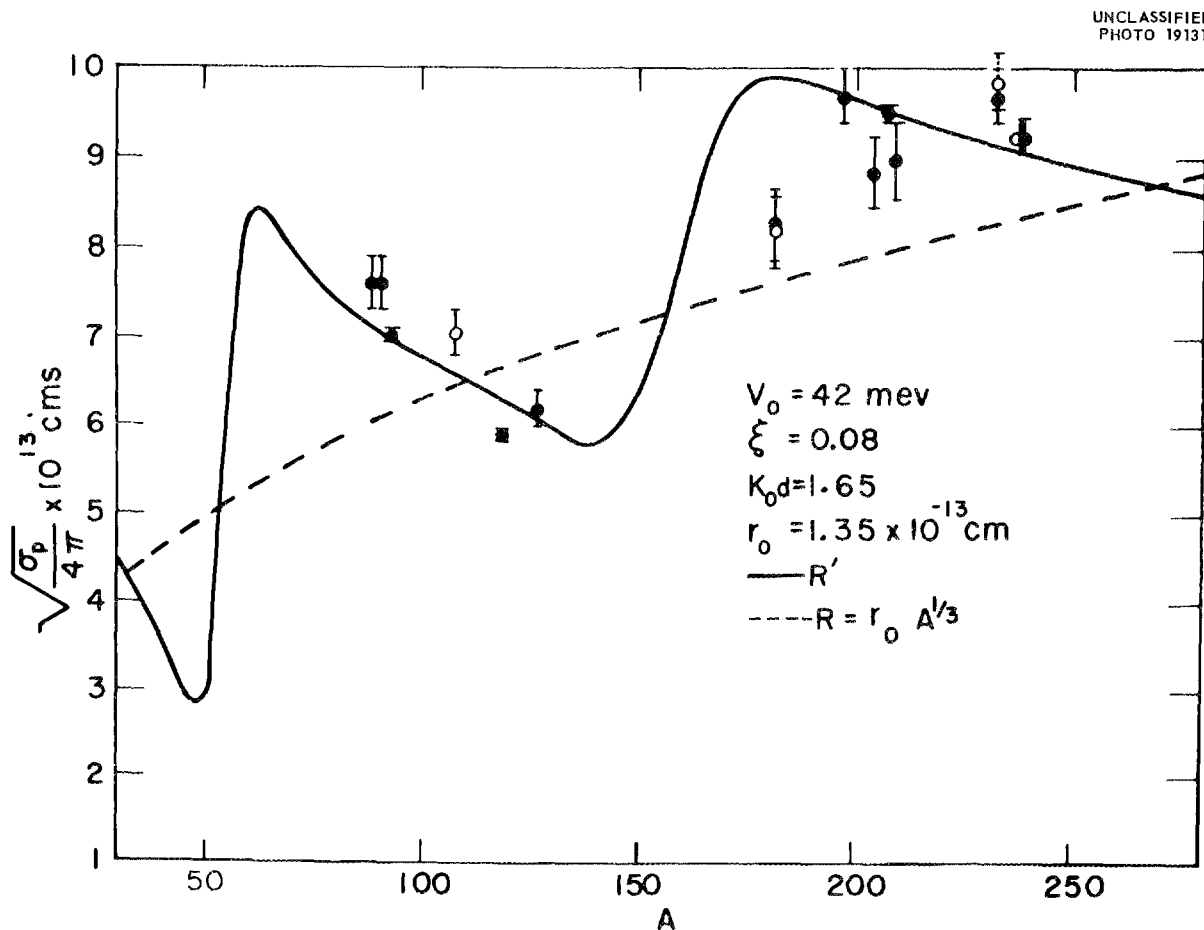
As for this wavy behavior of the apparent radius, R' , there were only a few experimental points available at the time of the calculation that really

could be trusted. So we really can't say much about this radius curve.

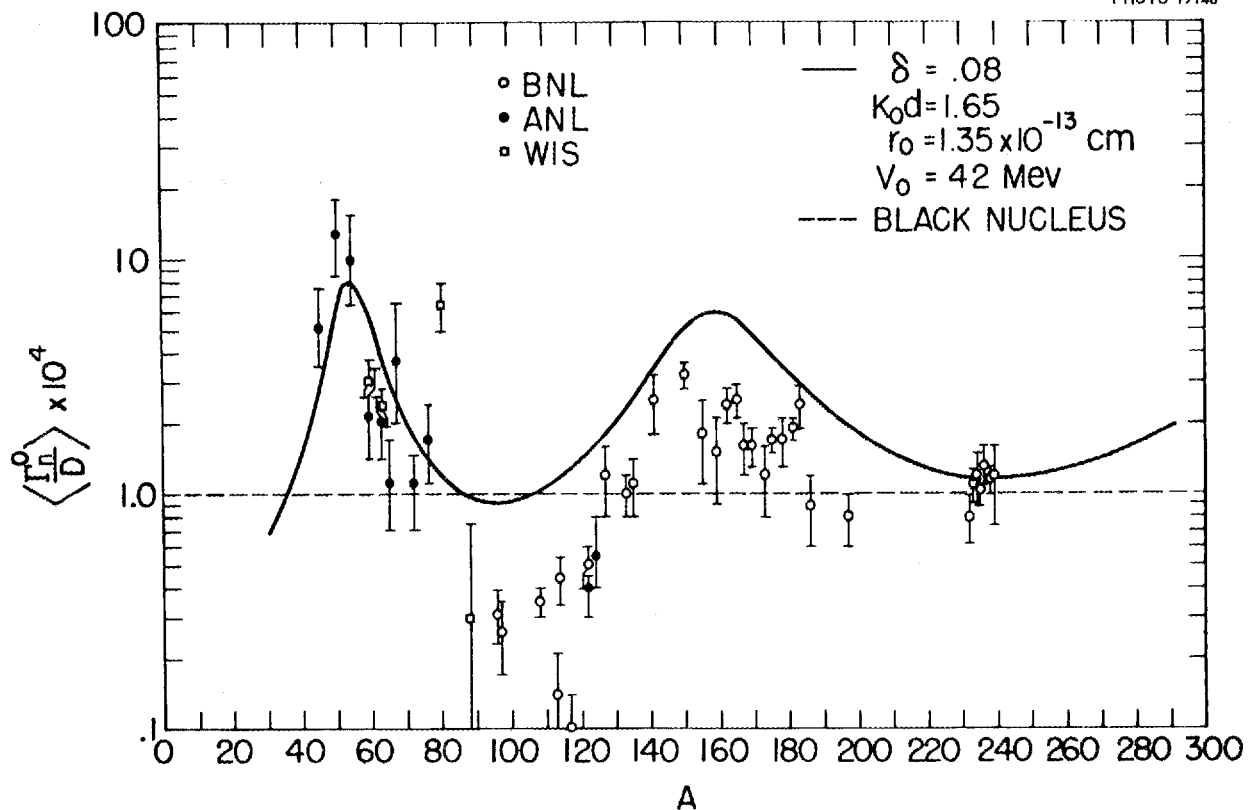
What I should like to do now is to show you two figures containing more recent results.

Slide 3 shows some of the more recent points on radii that seem to substantiate this cloudy-crystal-ball effect, but again it looks as if things are not nearly as good as they should be.

On Slide 4 we have combined various results to get the best values throughout, and we now have the work for lighter nuclei from Argonne and Wisconsin. There are also some more recent points as compared to slide 2. The discrepancy, which I think is a real one, now looks quite definite. In other words, you would say that certainly for $A > 60$ the theoretical curve is just too high. That is, neutrons, when they hit nuclei like these ($A \sim 100$), just don't form the compound nucleus



Slide 3. Experimentally Determined Nuclear Radii Compared to the Prediction of the Diffuse-Edge Complex-Potential-Well Model.



Slide 4. Experimentally Determined Strength Functions Compared to the Prediction of the Diffuse-Edge Complex-Well-Potential Model.

readily. The fact that something is off by a big ratio, I think, is important, and it means that the model in its present shape does not reproduce the results and needs still further modification of some type. The status of comparison with theory is similar to all the other things I mentioned. You would certainly say that there is a definite "wavy" effect, so there is truth to the cloudy crystal ball, but even the best calculations don't check the experimental points accurately. Now there may be some additional effect not included in the calculation. It may be that there are odd-even effects in the strength function. It may be that nuclei of the same atomic weight but of different quadrupole moments have different values of I_n^0/D , but to answer such questions requires much more careful work.

Now let's turn to the fissionable materials. Here the situation is different in that we cannot state that for the fissionable materials things are pretty well sketched out and it is just a matter of filling

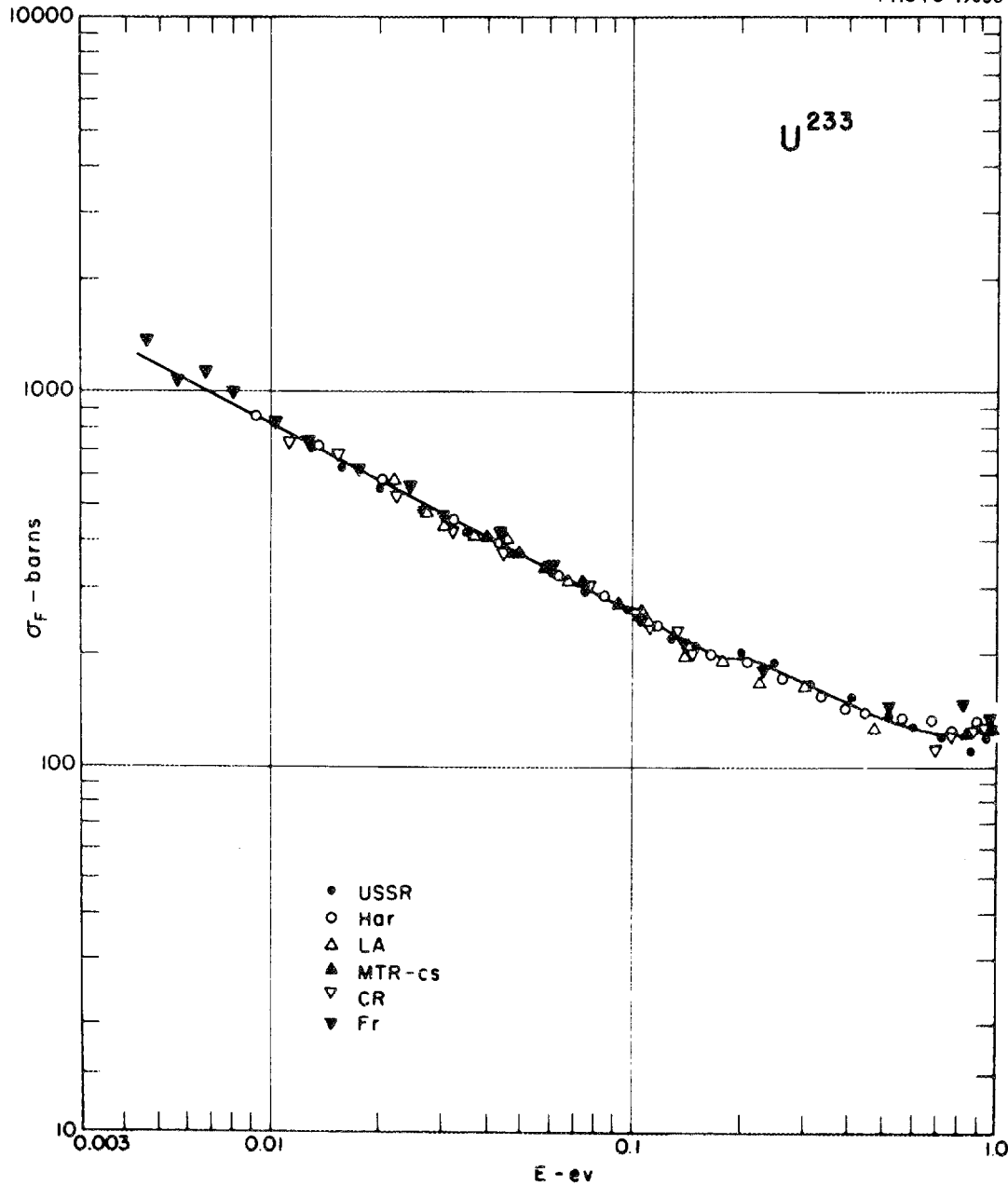
in the details. There are still some very fundamental things we don't know. There are recent theories, for instance, that would have it that all the levels, say of U^{235} , have the same spin, and the levels of the other spins just aren't there, or they may be so different we don't even recognize them as levels. You see, there are no problems like that for the nonfissionable materials. We pretty well know what a level looks like, we know that pure radiation levels don't interfere with each other, we know that scattering levels do interfere with each other; but we don't even know those simple things for the fissionable materials.

I don't know why the fissionable materials seem to be so much harder to do. Just the fact that fission is there I don't think is enough reason to make it so tough, because even on the total cross section alone of fissionable nuclides there still is quite a bit of disagreement. That is, we really don't know just how many levels there are in a given energy region for sure.

I want to illustrate that by talking a little about what things are like at Brookhaven, where we collect cross sections. We will take U^{233} , which is a reasonably important isotope, and lots of people have worked on it. We are making a list of the levels in U^{233} , but can hardly get to zero because we are not sure of the negative levels. But leaving

that out for a minute, we are soon stuck because for a long time people thought these funny wiggles at 0.2 eV (Slide 5) didn't mean anything. Especially if the work had been done with a crystal spectrometer, people would say: "It is a second order effect, and we will leave it out." But at Geneva the Russians pointed out quite forcefully that they

UNCLASSIFIED
PHOTO 19063

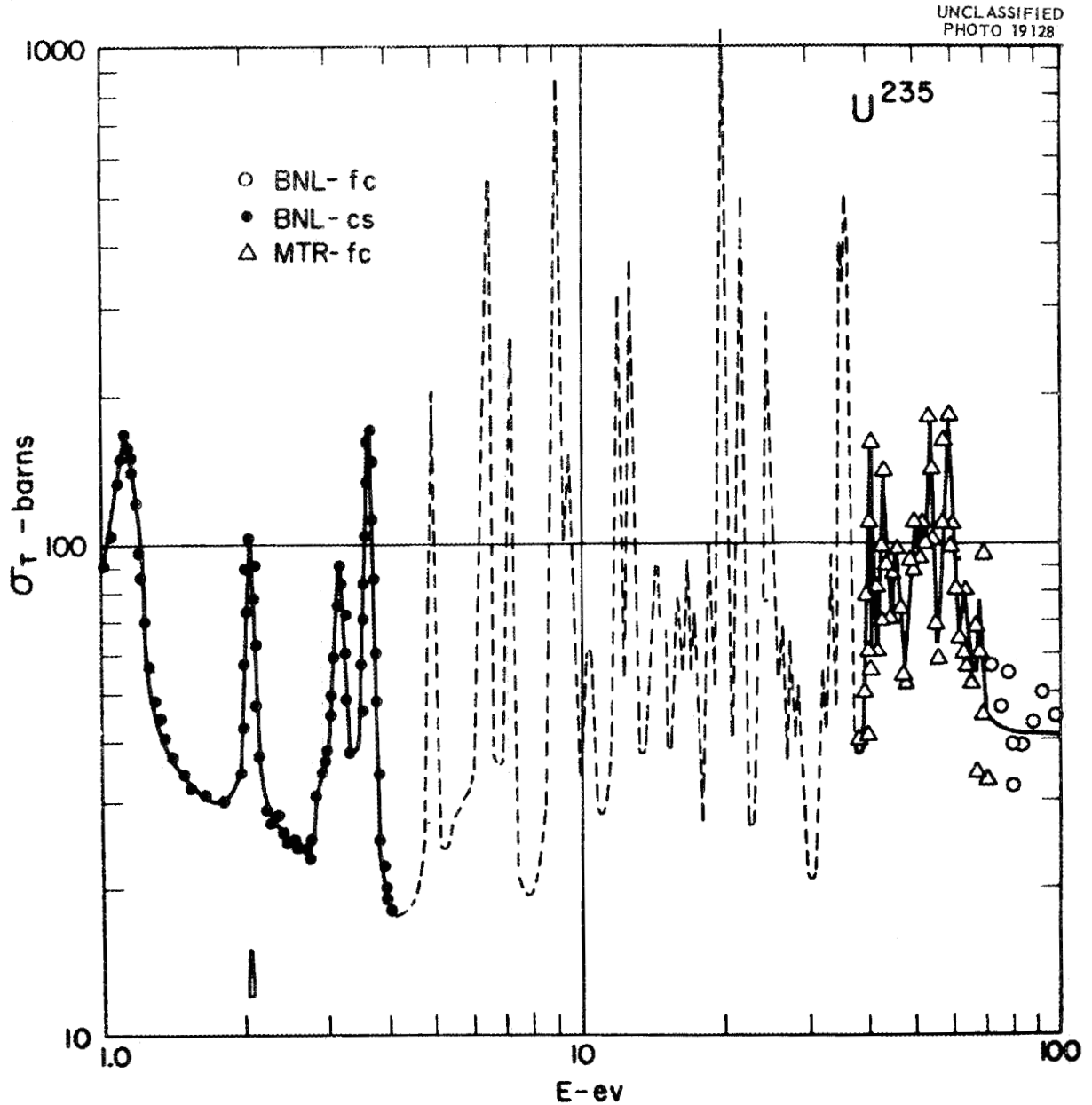


Slide 5. Total Cross Section of U^{233} .

really thought there was a level there, and when you begin to put data together from various countries, then you begin to believe that there really is a resonance at about 0.2 ev in U^{233} and so we have to try to decide what the parameters are.

Well, of all the isotopes, you would say we ought to know most about U^{235} . It is the most important isotope, and everybody works on it quite a lot. But

again the agreement is not very good at all. There is disagreement even on the first few levels (Slide 6), partly again because there are one, two, or three negative levels. We don't know quite what their parameters are. Again, is a small asymmetry a level, or is it an interference effect? The question of the presence or the absence of interference in U^{235} is a messy thing. If we assume that radiation



Slide 6. Total Cross Section of U^{235} .

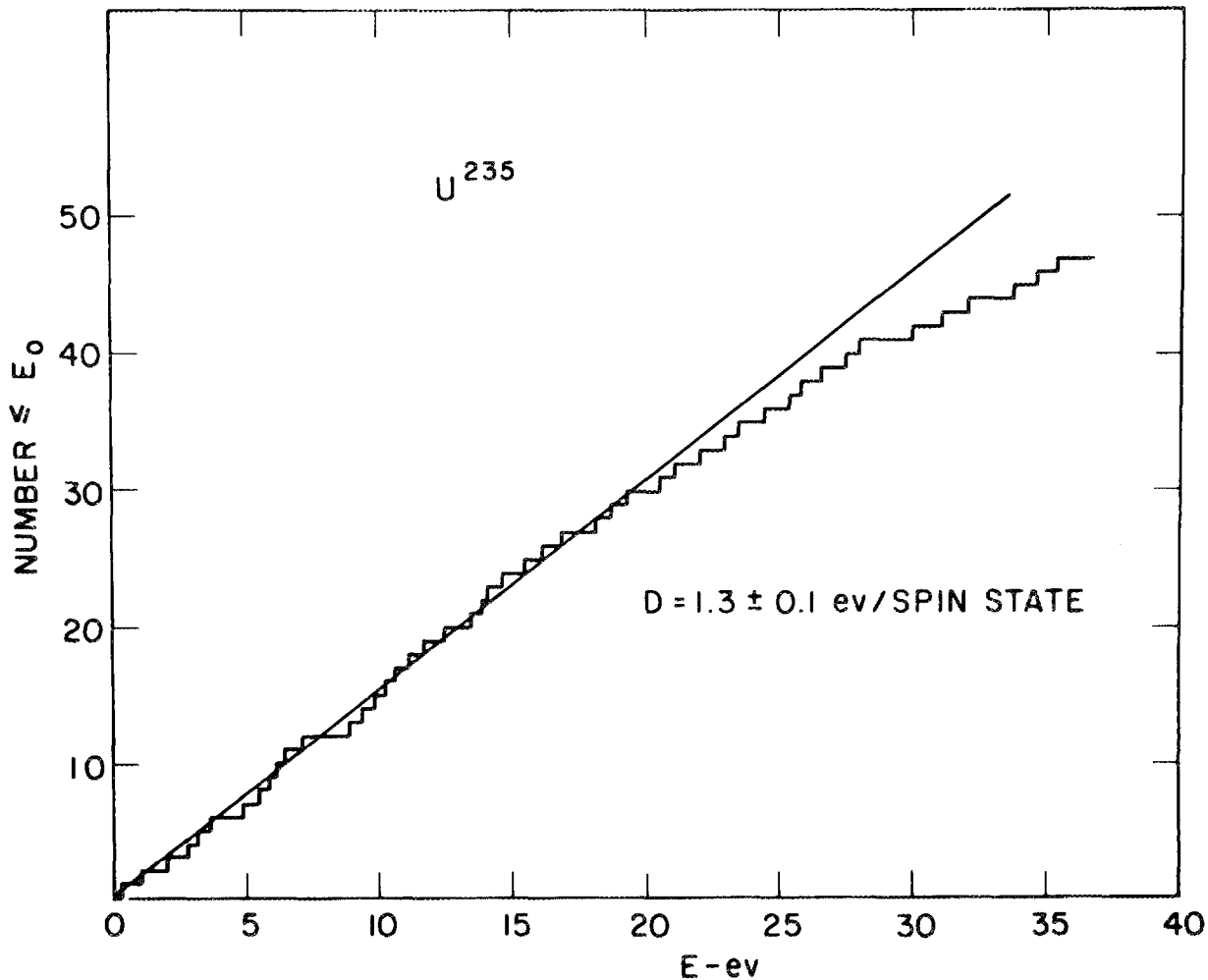
widths don't interfere and that fission widths do interfere completely, and then compute what the interference effect should be like, they don't agree quantitatively with the experimental curve. If the computed interference effects are too big, then we can of course say: Well, maybe they partially interfere. Maybe there are five or six channels; therefore only some part of the fission cross section would interfere. But, of course, then there are so many parameters available that almost any curve could be fitted by assuming a certain fraction of interference.

Of course, then the danger would be that you would be taking wiggles and saying that they are real levels. By putting in enough parameters, you

could explain it away as an interference effect. You would be missing a real level by calling it interference. It makes it extremely difficult to decide even how many levels there are.

Slide 7 is simply a plot of the number of levels as a function of neutron energy. This is the rate at which levels appear in U^{235} , starting at zero energy. You see, the levels are not regular in spacing. So the way they appear is with a sort of wobble, but the general behavior of this thing is linear. In other words, the level spacing is given by the slope of the curve, so the average level spacing calculated in the region 0 to 5 ev is the same as at 10 to 15 ev. This seems to be important, especially when we recall how rapidly the resolving

UNCLASSIFIED
PHOTO 19127



Slide 7. The Number of U^{235} Levels $< E_0$ as a Function of Neutron Energy.

power gets bad with increasing neutron energy. The resolving power changes very fast, and yet we find the same number of levels per electron volt until we get up to about 20 ev. Then decreasing resolution makes this thing drop off, but it is a little hard to see how we could be missing small levels at low energy. You are almost forced to the conclusion, from a plot like this, that you are finding essentially all of the levels in the linear region, here 0 to 20 ev.

Now I should like to make a plea that everybody work really hard on the fissionable materials, and, more than that, I think it is important not just to measure a lot of things and report numbers, but really to sit down and worry about why the numbers don't agree with the numbers that some other person has measured -- whether really all the levels have been found or not; whether really interference is there or not -- and do a good quantitative job of it. I feel strongly about this because right at the moment we are trying to make a reasonably well-thought-out, well-evaluated list of parameters in these fissionable isotopes, and need careful work.

I will just give you some numbers without telling you precisely what they are, so that nobody will recognize whose results they are. Here is a level at 15 ev, and the fission width is reported at 160 mev (milli-electron volts) from one laboratory and as 400 mev from another. Then there are a couple of levels that are found in several laboratories but not in another where supposedly the resolution was better. Then there are some neutron or fission widths -- I won't mention which -- 61 mev from a particular laboratory, 17 mev from another; and finally a neutron width of 3 mev from one laboratory and 0.4 mev from another. Now I don't want to make too much of a point of it all, but it should be possible to measure things and to get values that agree better than that. I don't mean that these are easy. As I said before, I am not really quite sure why these fissionable materials are so difficult, but that is the way the numbers come out.

It may be that if we look at europium, say, which has about the same level spacing as U^{235} , and, say, five different laboratories measure europium, and we compare the numbers, the disagreement will be rather bad also. But somehow I don't feel that way. I don't know just why it is, but I feel that in other materials we don't have too much trouble averaging numbers. We can at least recog-

nize that the people are looking at the same levels. With some of the fissionable materials we say: He must be looking at another level. It could not possibly be the same.

So I want to end up by just sort of making a plea for really careful work and by saying that the field has changed. It is not the way it was some years ago, when it was important just to find a few levels and to get some idea what the neutron widths were and what the radiation widths were. I say that it is important now to get these finer details filled in, to get some good quantitative results, and I say that the standards are set really by the theory and by the things we are going to use the data for. The standards are quite high, and I would say that this is the thing that will separate the men from the boys.

R. E. SEGEL: Getting back to this fitting of the data to the theory or to the theories, as I understand it you pick your parameters, such as the nuclear radius, from the experiments at different energy regions. Is it not possible that these parameters vary with energy?

D. J. HUGHES: I think Feshbach can best discuss the procedure that was followed.

H. FESHBACH: I want to make just a few comments about what Hughes has said. First of all, about the fitting of the experiments by the theory, we did not just use the zero-energy data.

We used essentially the data which include total cross sections, angular distributions, and inelastic scattering as far as we can manage it, and so on, in the energy range from zero to 3 Mev, from nuclei starting with lithium and going up to europium. This is not the final fit by any means. We are not at all satisfied with this particular one.

I would like to make some comments about the philosophy of this whole business. We do not intend, as a matter of fact we are sure it is impossible, to fit everything at every corner. I think that all we are interested in doing is getting a sort of over-all view of the panorama. That is, if you take a picture of these three-dimensional plots, and you put them at a sufficiently great distance, you know that the theory and experiment will look alike; but if, in fact, you look at a particular peak or a particular place, they, of course, do not agree. There are various possible places where things mix in that indicate that this must be so.

For example, the assumption of a simple law of radius with A is certainly much oversimplified,

and there is no reason there should not be fluctuations away from that, and so on and so forth. I don't want to belabor that point. Does that answer your question?

R. E. SEGEL: Well, the feeling I got from the data that Hughes presented was that the agreement was pretty horrible. Now would you say, from what you are trying to do, that it isn't pretty horrible?

H. FESHBACH: I think it is pretty wonderful. Let's put it another way. If we really want to do any element separately, we can get a set of parameters that will fit each element separately, and we can, therefore, map the whole thing and give you a plot of nuclear radius versus atomic weight and versus energy, but I think it would be a waste of time. We have already done some calculations with zero energy with different values of ζ and different values of $K_0 d$, that is, of the width of the diffuse edge; and none of these will give this low region for the strength function near $A = 100$. The only thing that did give the low region was the square well, the original calculation. If you want to, you can have a square well at $A = 100$ and a diffuse well somewhere else. But this gives you some idea as to why we don't want it in too much detail.

Finally, I want to wind up by asking Hughes a question. Is there any correlation between the neutron widths and the level spacings — that is to say, if you find a region in which the level spacing is wide, is the neutron width big — or are they statistically independent?

D. J. HUGHES: We have looked into that question rather carefully by plotting the spacing at a particular level against the width of that level — well, we have plotted the thing in all kinds of ways looking for some correlation, and there isn't any correlation at all as far as we can see.

H. FESHBACH: Well, I was just concerned because, in a way, if there were a correlation, then very small widths might go with very small spacings, for example, and that might explain some of the reasons for the missing levels.

D. J. HUGHES: That is one reason we looked into it, but we are quite sure there is no correlation.

I just want to add something to what you said. I didn't mean to imply at all that the fitting had only to do with Slide 2 that I showed. I realize it sounded that way. The philosophy that you mentioned of not trying to fit things in great detail was certainly borne out by Weisskopf at the Amsterdam meeting. It was quite interesting, because Porter had been trying hard to get everything to fit. Weisskopf spread the philosophy very strongly at Amsterdam that it is really not sensible to compute and compute and put in more parameters. It is much better to think about the fundamentals of what is going on in the nucleus and to try to get a good foundation for the whole thing.

E. P. WIGNER: We have tried to give another explanation, and it is that the sum of the widths of all the levels between two single-particle levels is equal to the width of a single-particle level. Let me say this again because the sentence was long and complicated: Let us consider an approximation in which a single-particle picture is valid. In the single-particle picture there are very few levels, very far from each other, and these levels are extremely wide because they are single-particle levels. They are just unbelievably wide. In the actual nucleus we do not have these levels, but they are replaced by just hundreds and hundreds of levels very closely spaced. The sum of the neutron widths of these levels is the same as the original width of this level.

A. WATTENBERG: I would like to ask the theoreticians what may be a very naive question but which bears on this spacing in detail. That is, are all levels going to be repulsed from one another, or can you have levels attracted so that they coalesce?

E. P. WIGNER: Well, I don't know. According to theory, the levels which have different J 's don't influence each other at all, and this, I think, is generally accepted. I think it should be equally generally accepted that levels with the same J repel each other. I will talk about this later, and I will go into this in some detail.

RESULTS AND THEORY OF RESONANCE ABSORPTION

E. P. Wigner
Princeton University

E. P. WIGNER: The detailed and elaborate nature of the experimental results presented here is most gratifying. It is my impression that the agreement of theory with experiment is now perhaps less close than it appeared before. This gives me renewed confidence that this will remain for some time an interesting subject.

It was, originally, my intention to review both the formal and the more problematic parts of the subject. I found, however, that the second part could be treated only in a very perfunctory fashion if any attention is given to the first. The detailed results which were presented today on resonance absorption make it desirable to review the formal theory, and my address will be largely confined to this subject.

The formal theory of resonance is by now quite old; it is largely the work of L. Eisenbud. His original objective was the calculation of the collision matrix. However, it was much easier to calculate something else, now called the derivative matrix. If you look at the various channels emerging from the black box called the nucleus, you can much more easily establish a connection between the value of the wave function in a channel and the derivatives of the wave function in all the channels than between the amplitudes of the incoming and outgoing waves. Of course, the physical situation is that you have in one channel an incoming wave and in all other channels outgoing waves. What you really want to know is the intensity of the outgoing waves if the intensity of the incoming wave in one particular channel, usually in the neutron channel, is unity. However, the expression for this is complicated, and the expression for the connection between the value of the wave function and the derivative of the wave function is simple:

$$(1) \quad v_\lambda = \sum_{s, \mu} \frac{\gamma_{s\lambda} \gamma_{s\mu}}{E_s - E} d_\mu .$$

In Eq. 1, the sum is to be extended over the infinite number of levels, s , with energies E_s . The energy of the system is E . The subscripts λ , μ refer to the channels. The squares of the γ 's are called the reduced widths; $\gamma_{s\lambda}$ is the value at the

channel radius of channel λ of the eigenfunction of the Hamiltonian whose eigenvalue is E_s . This eigenfunction is normalized and satisfies certain boundary conditions at the channel radii, but it will not be necessary to discuss these in detail. The quantities v_λ and d_μ are the value of the wave function in channel λ and its derivative in channel μ , respectively.

There are two observations which present themselves in connection with Eq. 1. First, this equation contains an infinite number of parameters, and it would appear that almost every experimental result can be represented by it. If this were actually the case, the formula would be entirely useless. The second observation is that Eq. 1 does not even give us what we want. It gives us something that we don't want, namely, the value of the wave function; but we want the outgoing wave. It is true, however, that if we know the value of the wave function and the derivative of the wave function, since we can continue with the wave function outside the nucleus, it is in principle possible to calculate everything. This "in principle" is, of course, the "catch," because if something can be calculated in principle it may yet be very far from being calculated.

In practice one uses approximations instead of the infinite series (Eq. 1). I should mention in passing that it is not true at all that any function can be approximated by the infinite series in Eq. 1.

The first point which I wish to make refers to these approximations. It is customary to use as an approximation a single term of Eq. 1. I should like to persuade you that this is not a good idea. It is not a good idea because it obscures the fact that the expression connecting the value of the wave function with the derivative of the wave function somewhere in the channel depends on the point where you consider the value and the derivative of the wave function. This point is called the boundary of the internal region. In this regard, the derivative matrix is quite different from the collision matrix, which gives the amplitude of the outgoing wave in terms of the amplitude of the incoming wave. The amplitude of the outgoing wave is the same no matter where you take it. Once the wave has started to go out of the black

box, it will continue to go out, and its amplitude will not change along the channel. However, the value of the wave function and the derivative of the wave function are not of this nature. It seems to be desirable to use such an approximation for Eq. 1 which will have the *same analytic form* no matter where we place the boundary of the internal region (i.e., no matter at which point we express the value of the wave function in terms of its derivative), at least if the solutions of the wave equation can be considered to be energy independent within the region where we are inclined to place this boundary. The analytic form of the R matrix will then remain the same within the energy region considered, no matter where we place the boundary – again within the region considered.

An approximation to Eq. 1 which satisfies this condition is, for instance,

$$(1a) \quad v_\lambda = \sum_{\mu} \left(r_{\lambda\mu} + \frac{\gamma_{0\lambda} \gamma_{0\mu}}{E_0 - E} \right) d_{\mu},$$

which is obtained from Eq. 1 by keeping only one term (except for replacing its index s by 0) and replacing all others by an energy-independent term. The approximation, Eq. 1a, will be good in the neighborhood of E_0 , but this neighborhood will be wider than if one neglected the $s \neq 0$ terms of Eq. 1 entirely, rather than replacing them by an energy-independent term.

The fact that the analytical form of the connection 1a is indeed independent of the choice of the boundary of the internal region can be seen most easily by calculating, by means of Eq. 1a, a quantity which is independent of such a choice. Such a quantity is, for instance, the matrix Q which expresses the coefficients g_{μ} of the irregular solution G_{μ} in channel μ in terms of the coefficients f_{ν} of the regular solutions F_{ν} :

$$(2) \quad g_{\mu} = \sum_{\nu} Q_{\mu\nu} f_{\nu}.$$

Under the assumption made in Eq. 1a, the $Q_{\mu\nu}$ have the form:

$$(2a) \quad Q_{\mu\nu} = q_{\mu\nu} + \frac{1}{E_0 - E} \gamma_{\mu} \gamma_{\nu},$$

where $q_{\mu\nu}$ is symmetric, $q_{\mu\nu} = q_{\nu\mu}$, just as $r_{\mu\nu} = r_{\nu\mu}$ is symmetric. Since regular and irregular solutions remain regular and irregular, respectively, all over the channel outside the region of inter-

action, the $Q_{\mu\nu}$ are independent of the choice of the boundary of the internal region. This becomes evident also if one expresses the collision matrix S in terms of Q :

$$(2b) \quad S = \frac{1 + iQ}{1 - iQ},$$

a formula which is given here only for the sake of reference.

The connection between the quantities in Eqs. 2a and 1a is:

$$(3) \quad \sum_{\nu} q_{\mu\nu} G'_{\nu} r_{\nu\eta} + F'_{\mu} r_{\mu\eta} - q_{\mu\eta} G_{\eta} - F_{\mu} \delta_{\mu\eta} = 0.$$

There are as many linear equations for the $r_{1\eta}$, $r_{2\eta}$, ... as there are such quantities, since Eq. 3 is valid for every channel μ . The F , G , F' , G' are the values and the radial derivatives of the regular and irregular solutions in the channel indicated by their index, taken at the boundary of the internal region. One sees that the r will depend on this boundary even though the q do not. On the other hand, the r will be energy independent if this holds both for the q and the quantities F , G , F' , G' . The expressions for the γ are:

$$(3a) \quad \gamma_{\mu} = \sum_{\nu} q_{\mu\nu} G'_{\nu} \gamma_{0\nu} + F'_{\mu} \gamma_{0\mu},$$

while

$$(3b) \quad E_0 = \mathcal{E} - \sum_{\mu} G'_{\mu} \gamma_{\mu} \gamma_{0\mu},$$

and the same remarks apply with respect to the dependence of the $\gamma_{0\nu}$ and E_0 on the position of the internal region's boundary and on energy E as were made in connection with the r . It may be remarked, again solely for the sake of reference, that the preceding equations follow from:

$$(4) \quad Q = (F - F'R)(G'R - G)^{-1},$$

where F , G , F' , G' are commuting matrices (in our case diagonal matrices with diagonal elements F_{μ} , G_{μ} , etc.) which satisfy the equation:

$$(4a) \quad F'G - FG' = 1.$$

Then if:

$$(4b) \quad R = r + (E_0 - E)^{-1} (\gamma_0 \times \gamma_0),$$

where r is a (real) symmetric matrix, Q becomes:

$$(5) \quad Q = q + (\mathcal{E} - E)^{-1} (\gamma \times \gamma),$$

where (the γ^2 are not the reduced widths, the γ_0^2 are):

$$(5a) \quad q = (F - F'r) (G'r - G)^{-1},$$

$$(5b) \quad \gamma = (qG' + F') \gamma_0,$$

$$(5c) \quad \mathcal{E} = E_0 + [\gamma_0 \cdot (G'qG' + F'G') \gamma_0],$$

and q is symmetric. Conversely, if Q has the form given by Eq. 5, R will have the form of Eq. 4b, with r , γ_0 , and E_0 being given by the last three equations. Hence, R for one set of boundaries of the internal region can be expressed in terms of R for another set of boundaries, and it will remain of the form of Eq. 4b with energy-independent r , γ_0 , E_0 as long as the r , γ_0 , E_0 of the R from which one started are energy independent and as long as the same holds for the two sets of F , G , F' , G' . The verification of Eqs. 5 is lengthy but simple. It is given in the Appendix.

Another approximation to Eq. 1, the form of which is independent of the choice of the boundary of the internal region, has the form given by Eq. 1a with the further stipulation, however, that r also commute with F , G , F' , G' , that is, that it be a diagonal matrix in our case. Then Eq. 3 or Eq. 5a shows that q will be a diagonal matrix also. The great advantage of this approximation is that Eqs. 3 can be solved at once:

$$(6) \quad q_{\mu\nu} = - \frac{F_{\mu} - F'_{\mu} r_{\mu\mu}}{G_{\mu} - G'_{\mu} r_{\mu\mu}} \delta_{\mu\nu},$$

so that Q and the cross sections can be obtained very easily. In particular, the collision matrix and the cross sections are given by the following formulas:

$$(6a) \quad S_{\mu\nu} = \frac{2i\beta_{\mu}\beta_{\nu}}{\mathcal{E} - E - i\sum\beta_{\lambda}\gamma_{\lambda}}, \quad \text{for } \mu \neq \nu,$$

$$(6b) \quad S_{\mu\mu} = \frac{1 + iq_{\mu\mu}}{1 - iq_{\mu\mu}} + \frac{2i\beta_{\mu}^2}{\mathcal{E} - E - i\sum\beta_{\lambda}\gamma_{\lambda}},$$

where

$$(6c) \quad \beta_{\mu} = \frac{\gamma_{\mu}}{1 - iq_{\mu\mu}}.$$

The absolute square of the expression $6a$, if multiplied by π/k_{μ}^2 , gives the cross section for the reaction $\mu \rightarrow \nu$, and the absolute square of $(1 - S_{\mu\mu})$, if multiplied by π/k_{μ}^2 , gives the scattering cross section for the particle μ . In the former case, one obtains the usual formula. The partial width for the emission of particle ν is:

$$(7) \quad \Gamma_{\nu} = 2|\beta_{\nu}|^2 = \frac{2\gamma_{\nu}^2}{1 + q_{\nu\nu}^2} \\ = \frac{2\gamma_{0\nu}^2}{(G_{\nu} - G'_{\nu} r_{\nu\nu})^2 + (F_{\nu} - F'_{\nu} r_{\nu\nu})^2}.$$

The expression for the scattering cross section is, on the other hand,

$$(7a) \quad \sigma_{\mu\mu} = \frac{\pi}{k_{\mu}^2} \frac{1}{1 + q_{\mu\mu}^2} \times \\ \times \frac{[2q_{\mu\mu}(\mathcal{E}' - E) + \Gamma_{\mu}]^2 + q_{\mu\mu}^2(\Gamma - \Gamma_{\mu})^2}{(\mathcal{E}' - E)^2 + \frac{1}{4}\Gamma^2}.$$

In this expression, \mathcal{E}' differs from the \mathcal{E} given in Eq. 5c by a level shift $\Delta = \sum \gamma_{\lambda}^2 q_{\lambda\lambda} / (1 + q_{\lambda\lambda}^2)$ which is usually unimportant; Γ is the sum of the partial widths Γ_{ν} . If one neglects all q , expression 7a goes over into the analogue of the reaction cross section, that is, it neglects what is called the potential scattering. If only one channel is open, $\Gamma = \Gamma_{\mu}$, and the second term in the numerator vanishes. The corresponding expression was given, independently, in several papers. In the general case, Eq. 7a was given by Brockhouse, except that he writes $q_{\mu\mu}^2 \Gamma^2$ for the second term in the numerator. This is permissible in the case he considers (slow neutron scattering and hence $\Gamma_{\mu} \ll \Gamma$). The expression 7a for the scattering already shows that the corresponding cross section cannot become zero as long as there are other channels open, that is, as long as $\Gamma - \Gamma_{\mu} \neq 0$.

It is somewhat perturbing that all these formulas are so complicated. In particular, the q and γ in Eq. 7a are yet to be expressed by means of Eqs. 5a to 5c in terms of the energy-independent r , γ_0 . This is a trivial matter if the F , G , etc., are energy independent. In this case the q and γ will be also energy independent. This will be the situation if

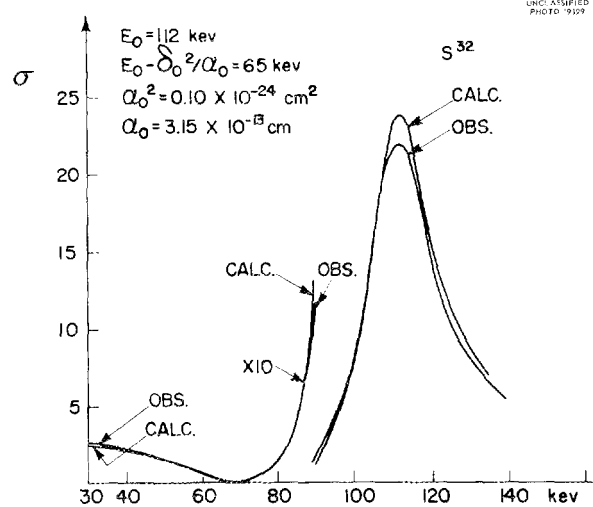
the energy region in which the formulas are to be applied is small as compared with the total energy. The most important case in which this does not apply is that of slow neutrons. Then $F = \text{const.} \times k^{-1/2} \sin kr$, $G = \text{const.} \times k^{-1/2} \cos kr$, and the corresponding q , given by Eq. 6, is proportional to k while γ is proportional to $k^{1/2}$. This also means that the argument given above for the form of Eq. 1a being independent of the internal region's boundary does not apply. However, this remains true also in this case. It is also perturbing that the computations which lead from Eq. 1a to the cross sections are so lengthy, even in the simplest case of a diagonal $r_{\lambda\mu}$.

The great drawback of the approximation 1a with diagonal r (that is, $r_{\lambda\mu} = r_{\lambda\lambda} \delta_{\lambda\mu}$), which we are now considering, and from which the preceding expressions for the cross sections follow, is that it is more difficult to justify a priori than the more general assumption that r is an arbitrary (symmetric) energy-independent matrix. A necessary condition for the diagonal nature of r is that the contribution of the resonance closest to E_0 be negligible. This contribution will be, in general, of the same order of magnitude as the contribution of the resonance at E_0 midway between two lines. Hence, the contribution of the resonance closest to E_0 will give a negligible contribution to the off-diagonal elements of r if the reaction cross section due to the resonance at E_0 , as calculated with the usual resonance formula, is negligible midway between two lines. Whether or not this is the case depends on the size of the cross section which one is willing to consider to be negligible.

Even if the contribution of the resonance closest to E is negligible in Eq. 1, the aggregate effect of all distant resonances may be appreciable. However, there is in this regard an important difference between the diagonal elements of r and the non-diagonal elements: the contribution of all the high-energy resonances has the same (positive) sign for the diagonal elements, but can be positive as well as negative for the non-diagonal elements. This was recognized already by R. G. Thomas and is the most reasonable justification of the approximation 1a with a diagonal $r_{\lambda\mu} = r_{\lambda\lambda} \delta_{\lambda\mu}$. In addition, this is the simplest approximation for Eq. 1 the form of which is independent of the choice of the internal region's boundary in the sense indicated.

The randomness of the signs of the $\gamma_{s\lambda}$ corresponds, physically, to the absence of direct interaction processes, such as stripping. These would be described, in the language of the derivative-matrix theory, in a very cumbersome way, as resulting from the combined effect of high-energy resonances. They do not have resonance behavior, and indeed the nondiagonal nature of r entails a nondiagonal nature of q , that is, an appreciable reaction cross section also between resonances.

The diagram for the scattering cross section of S^{32} (Slide 1) is an illustration of the validity of the approximation 1a. Since there is only one channel



Slide 1. Comparison of the Experimental and the Theoretical Total Cross Section of Sulfur.

free in this case, r is naturally diagonal. The cross section is given theoretically by the well-known expression:

$$(8) \quad \sigma(E) = \frac{4\pi[(a-r)(E-E_0) + \gamma_0^2]^2}{(E-E_0)^2 + k^2[(a-r)(E-E_0) + \gamma_0^2]^2}$$

It represents the measurements quite well. The point which I wish to make is, however, the following. In Eq. 8, a is the radius of the boundary of the internal region, that is, the radius of the point at which Eq. 1 compares the value and derivative of the wave function; r is the constant in Eq. 1a. Its indices are omitted since there is only one channel open. In the expression for the cross section (Eq. 8), only the difference $a - r$

occurs: this expression is independent of the radius of the channel, since the increase of r with channel radius just compensates the increase of a . On the other hand, γ is in this case ($ka \ll 1$) practically independent of a . The expression $a - r$, which occurs in Eq. 8, is not the radius but the difference between the nuclear radius and the contribution of all the other levels. It is true that the number of constants in Eq. 8 is not very small: E_0 , γ_0^2 , $a - r$. Essentially, the E_0 in Eq. 8 is the energy of maximum cross section, the γ_0^2 is fixed by the width at half maximum, and $a - r$ is fixed by the position at which the cross section dips to zero. The rest of the curve fits very nicely. In particular, the cross section fits even at the lowest energy remarkably well.

Recently the scattering of absorbing resonances has been measured by Tittman and Sheer and by Brockhouse. This is given, theoretically, by Eq. 7a. Since, in the case of neutrons, $q_{\mu\mu}$ and $\Gamma_{\mu} = 2\gamma_{\mu}^2$ are both proportional to k , this can be written, if one omits terms which are proportional to k ,

$$(8a) \quad \sigma_{sc}(E) = \frac{4\pi[(a-r)(E-E_0) + \gamma_{0\mu}^2]^2 + (a-r)^2 \Gamma^2}{(E-E_0)^2 + \frac{1}{4}\Gamma^2}$$

As was mentioned before, this is Brockhouse' formula. The agreement with the experimental results is again so good that one cannot see the difference between the experimental points and the theoretical curve (Slide 2). Again, the significance of the agreement is somewhat limited by the fact that the theoretical expression 8a contains several parameters. Two of these were known before from the measurement of the absorption cross section.

D. J. HUGHES: In the actual case that you computed, how do a and r compare in order of magnitude, and is either one about the same as the nuclear radius?

E. P. WIGNER: In the case of sulfur, you see that a and r have no separate significance whatever. I can choose a virtually anywhere, and $(a - r)$ is not equal to the nuclear radius, but it is considerably smaller in the case of S^{32} . This is undoubtedly due to the fact that there happen to be more resonances at higher energies than 120 kev than at lower energies which contribute positively to r . As a result, $a - r$ is not much more than half of the nuclear radius. The case of cadmium is

different: $a - r$ is very nearly equal to the nuclear radius.

One thing to be noticed is that if, in addition to scattering, there is absorption or some other reaction, then the scattering cross section can no longer go to zero. In the numerator of expression 8a there is an added term of the form

$$(a - r)^2 (\Gamma - 2k\gamma_{0\mu}^2) ,$$

where Γ is the total width.

In the case of cadmium, for which a comparison was made, the quantity $-2k\gamma_{0\mu}^2$ was left out from the original formula. This cannot be correct, because this term must be zero for pure scattering ($\Gamma = 2k\gamma_{0\mu}^2$). In cadmium this is not important, because the neutron width is much smaller than the total width, so that $\Gamma - 2k\gamma_{0\mu}^2 \approx \Gamma$; in general the $-2k\gamma_{0\mu}^2$ must be present. It would seem that with the accuracy now available it should be possible to distinguish the effect of this second term in the U^{238} resonances, for example.

The next thing to be considered is the analysis, not of the resonances, but of the region between resonances. Between resonances, as far as I know, there is only one very nice and beautiful measurement by Bollinger *et al.* The agreement in this case is also very good. There is not too much to be said about that. I am sure you have seen the comparison and theory either by Bollinger *et al.* or by Krotkov, and they show essentially the same thing (Slides 3 and 4).

We have learned today that in many cases it is possible to measure not only the total absorption but the absorption into a definite channel. This is done by measuring the emission of a particle or gamma ray in the course of the reaction, rather than the attenuation of the incident beam. This makes it possible to observe something which Dr. Hughes has often commented upon: namely, the interference of different resonances with each other between the two resonances and this is quite an amusing thing.

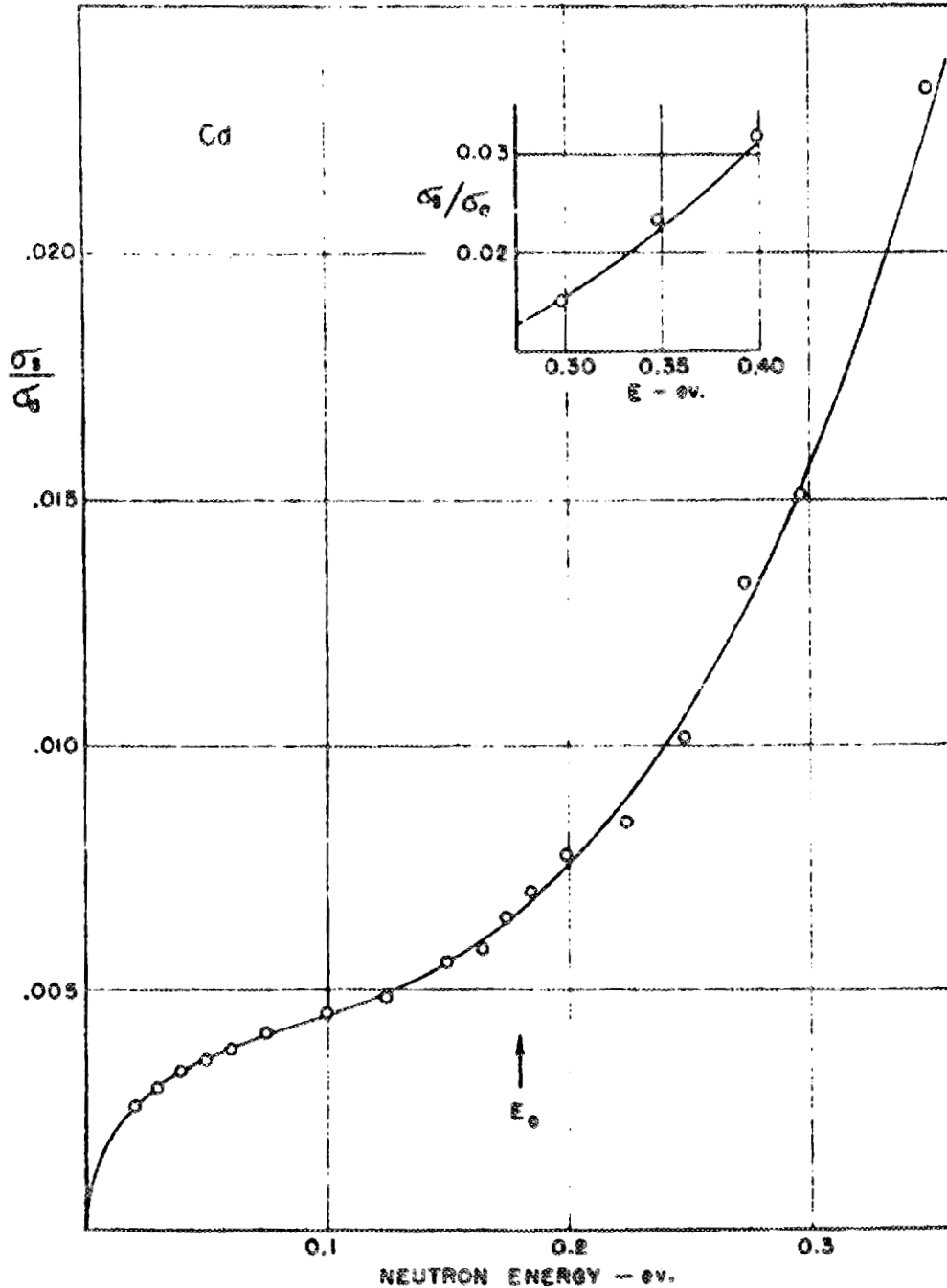
In the case of elastic scattering, $\lambda = \mu$, in the expression $\sum \gamma_{s\lambda} \gamma_{s\mu} / (E_s - E)$ of Eq. 1 all the numerators are positive, and thus the sum has the appearance illustrated in Slide 5. On the other hand, for a particular kind of absorption, for $\lambda \neq \mu$, the numerators $\gamma_{s\lambda} \gamma_{s\mu}$ may be positive or negative, and so the numerators may have different signs at two successive resonances. In this case, the

curve has the appearance illustrated in Slide 6. If $\gamma_{s\lambda}\gamma_{s\mu}$ has the same sign at two adjacent resonances, the curve is very similar to Slide 5. In this case there is a cancellation of terms, and the absorption cross section drops to a very small value, of the order Γ^4/D^4 . On the other hand, between two resonances for which $\gamma_{s\lambda}\gamma_{s\mu}$ have opposite

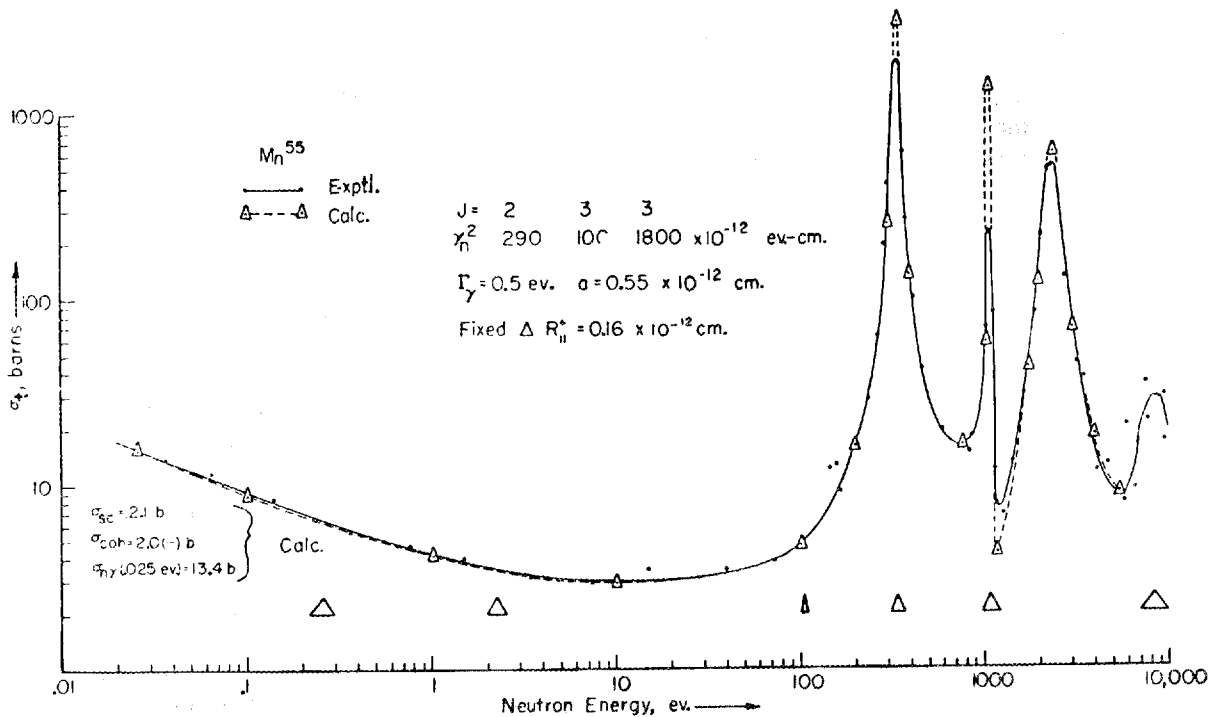
signs there is no cancellation, and one obtains a much larger cross section, $\sim\Gamma^2/D^2$, between resonances. This has been pointed out already by T. Teichman.

This suggests an interesting distinction between successive levels with respect to absorption which does not exist with respect to scattering. It is an

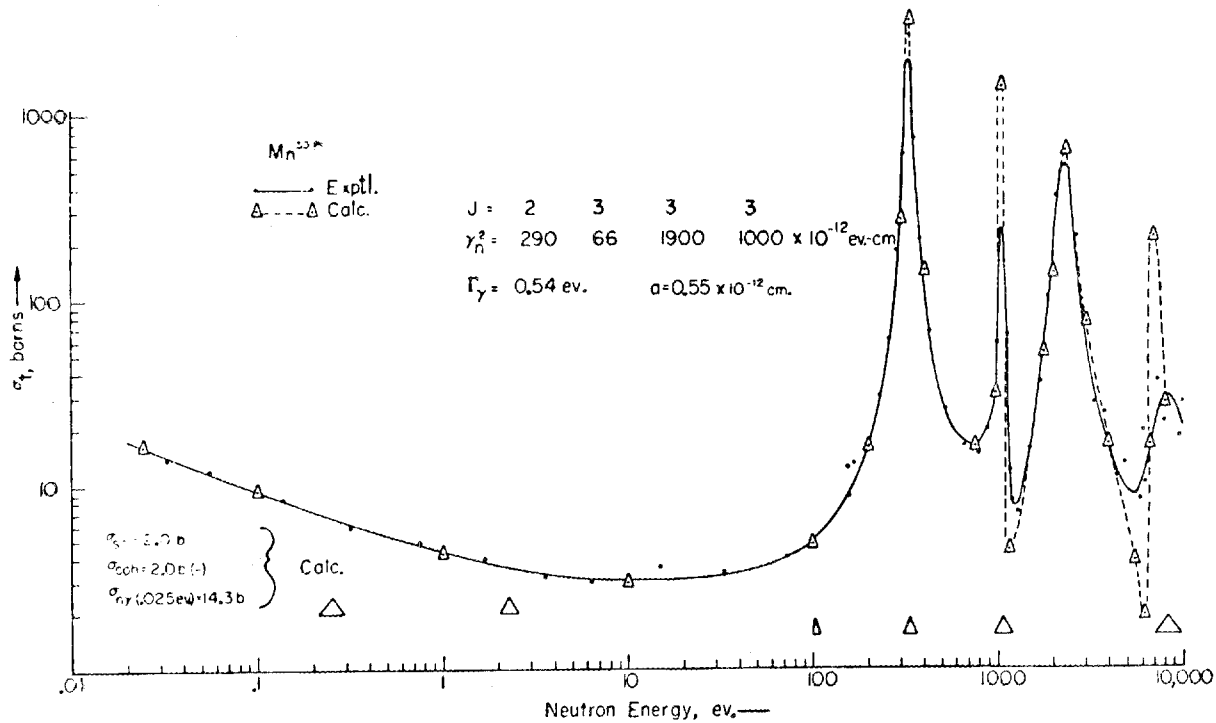
UNCLASSIFIED
PHOTO 19201



Slide 2. The Ratio σ_s/σ_a for Cadmium as a Function of Neutron Energy.



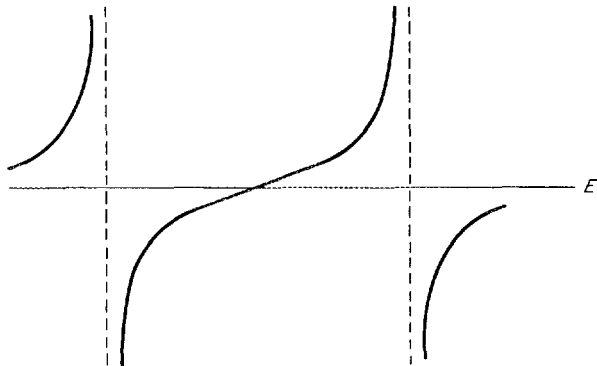
Slide 3. Comparison of the Experimental and a Three-Level Theoretical Total Cross Section of Manganese.



Slide 4. Comparison of the Experimental and a Four-Level Theoretical Total Cross Section of Manganese.

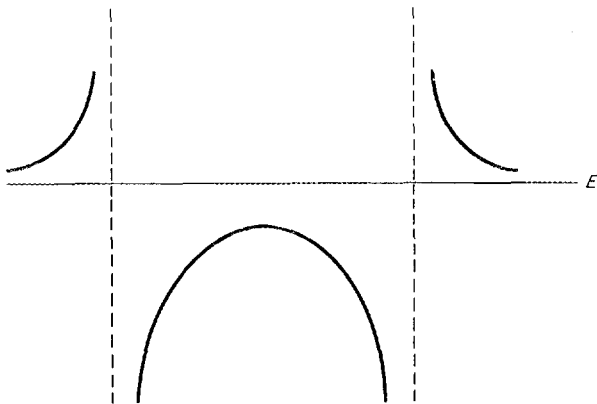
effect which may be worth while to observe. According to what we believe (and this now brings us to the less formal part of the comparison between experiment and theory), the number of cases in which the minimum is deep and the number of cases in which the minimum is not deep should be about equal.

UNCLASSIFIED
ORNL-LR-DWG 20544



Slide 5. $\sum_s \frac{\gamma_{s\lambda} \gamma_{s\mu}}{E_s - E}$ vs E Between Two Adjacent Resonances When the Signs of the γ 's Are the Same for the Two Resonances, As in Elastic Scattering.

UNCLASSIFIED
ORNL-LR-DWG 20544A



Slide 6. $\sum_s \frac{\gamma_{s\lambda} \gamma_{s\mu}}{E_s - E}$ vs E Between Two Adjacent Resonances When the Signs of the γ 's Are Different for the Two Resonances, As Is Possible for Capture or Fission.

What I have covered so far are the very formal parts of the theory, and I think they are the parts of the theory with which everybody would agree. They are based on fundamental concepts of quantum mechanics, and experimentally, at least in the nonfissionable elements, I don't know of any serious contradiction. In the case of the fissionable elements, as Dr. Hughes told us, the situation is much less favorable. He proposed explanations for this, and quite likely the explanations which he gave are the correct ones.

The rather consistently high values of a appear to me the most puzzling feature. As long as we treat all channels in the same way, it will remain difficult to understand that some channels – the fission channels – carry between resonances a greater fraction of all particles than at resonances. In fact, the ratios of the reaction cross sections at the resonances are equal to the ratios of the partial widths, which are given by Eq. 7, and, if one assumes complete randomness of the signs of the $\gamma_{s\lambda}$, exactly the same expression describes the ratio of the reaction cross sections *between* resonances. It is possible, of course, to assume that the signs of the γ are not random, for instance that the signs of the γ which correspond to fission alternate. At the low-energy resonances this would be a very artificial assumption. The existence of a direct process leading to fission – in other words, a nondiagonal $r_{\lambda\mu}$ in Eq. 1a – may appear less artificial. A consequence of this assumption would be that the minimum of the fission-to-capture ratio would not coincide exactly with the center of the resonance line: the interference between resonance and direct processes would lead to a shift similar to the shift in the maxima of the scattering and capture cross sections with respect to each other. We have heard about indications of such a shift.

Unfortunately, in the case of fission the ratio of the level width to the level spacing is much higher than in the nonfissionable case. This makes the interference effect of successive levels, to which Dr. Hughes has already alluded, much more complicated, and we begin to reach the situation where Eq. 1 is so general that it can describe almost every experimental situation. In other words, although Eq. 1 may still be correct, it begins to become useless. A formula can become valueless for two reasons: that it is invalid, or that it does not tell us anything. I am afraid the latter case applies here.

I come now to the next point of the comparison of experiment and theory, which is much less formal. The value of an expression such as Eq. 1 lies to a large degree in the fact that one can estimate the density of the resonance levels and the reduced widths reasonably well, and that one can make approximations taking into account only one term, replacing the rest with a constant, and similar approximations. It is, therefore, very important to know the statistics of the level densities and the statistics of the reduced widths. The statistics of the reduced width, often alluded to already today, have been experimentally ascertained by Hughes and Harvey and their collaborators, and then theoretically interpreted by Scott and by Porter and Thomas.

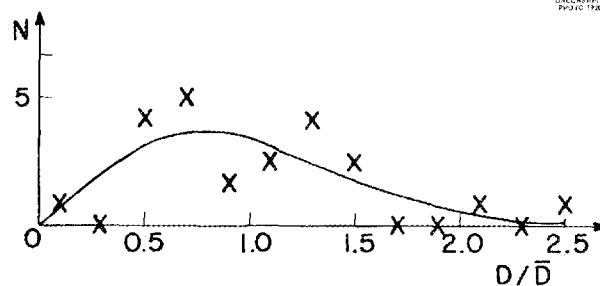
All of us theoreticians should feel a little embarrassed. We know the theoretical interpretation of the reduced width γ : it is the value of a wave function at the boundary, and we should have been able to guess what the distribution of such a quantity is. However, none of us were courageous enough to do that. Although we knew that the $\gamma_{s\lambda}$ were just as likely to be positive as negative, none of us dared even to think that their distribution is simply Gaussian, which is virtually the simplest distribution in which the positive and the negative values have the same weight. We all thought that the distribution has two maxima, one at positive γ , the other at the opposite negative value. Perhaps I am now too courageous when I try to guess the distribution of the distances between successive levels. I should re-emphasize that levels that have different J values are not connected at all with each other. They are entirely independent. So far experimental data are available only on even-even elements, and Dr. Hughes has projected a curve showing the probability of a spacing as a function of the spacing itself. The data with which I am familiar (Slide 7) come from Th^{232} and U^{238} . Many more data will become available as we shall learn more and more to distinguish levels, that is, to ascertain their J values.

Theoretically the situation is quite simple if one attacks it in a simple-minded fashion. The question is simply what are the distances of the characteristic values of a symmetric matrix with random coefficients? We know that the chance that two such energy levels coincide is infinitely unlikely. We can consider a two-dimensional matrix,

$$\begin{vmatrix} a_{11} & a_{12} \\ a_{21} & a_{22} \end{vmatrix},$$

in which case the distance between the two levels is $\sqrt{(a_{11} - a_{22})^2 + 4a_{12}^2}$. This distance can be zero only if $a_{11} = a_{22}$ and $a_{12} = 0$. The difference between the two energy values is the distance of a point from the origin, the two coordinates of which are $a_{11} - a_{22}$ and a_{12} . The probability that this distance be S is, for small values of S , always proportional to S itself, because the volume element of the plane in polar coordinates contains the radius as a factor.

Now Dr. Hughes, and several speakers before him, mentioned that one would expect an exponential distribution for the probability of a certain spacing as a function of the spacing. The reasoning which leads to this expectation is as follows. If we have a level at a certain point, then the probability of finding another level a distance S from it is independent of S and given by ρdS , where ρ is the mean level density. Therefore, the probability for finding the next adjacent level at distance S , in dS , is $e^{-\rho S} \rho dS$. I think that this is the basis for expecting an exponential distribution of the level spacing. However, the argument is erroneous, because the probability that there shall be a level at a distance S from a given level is not independent of this distance; for small values of S it is proportional to S . If this same law is assumed for large S also, the probability of finding the next level at a distance S becomes proportional to SdS . Hence this simplest assumption will give the probability $\frac{1}{2}\pi\rho^2 e^{-(1/4)\pi\rho^2 S^2} SdS$ for a spacing between S and $S + dS$.



Slide 7. Distribution of Level Spacings.

It must be admitted that Dr. Hughes' curve did not look very much like this expression. Perhaps the assumption that the probability is proportional to S also for large S is incorrect.

Weisskopf's formula for the level density has been discussed recently, particularly carefully, by T. D. Newton at Chalk River. As is well known, Weisskopf's formula gives the level density as function of the excitation energy. The question naturally comes up, from what level do we calculate the excitation energy? Originally, this was thought to be the lowest energy level, but Bethe and Hurwitz pointed out that one obtains more satisfactory results if one replaces the normal state by some fiducial state. This fiducial state eliminates the even-odd and magic-number fluctuations. If it coincides with the normal state for odd- A nuclei, it lies an amount δ above it for even-even nuclei, where δ is the pairing energy. It lies at $-\delta$ for odd-odd nuclei. The interpretation of Bethe and Hurwitz has been accepted also by Newton in his very careful study.

It seems to me, nevertheless, that the experimental data do not entirely support this interpretation. I am referring in particular to the level-density determinations at the excitation provided by the addition of a slow neutron, that is, to the level density measured in slow-neutron experiments. The excitation energies calculated on the bases of the original and the modified assumption are summarized below for even-even, even-odd, odd-even, and odd-odd target nuclei (the second adjective refers to the neutron number). The quantity B is expected to have the same value for all four types of nuclei. According to the original formulation, the level density should run parallel to the binding energy, that is, the second column.

Type of Target Nucleus	Binding Energy	Fiducial Level	Excitation Energy (Bethe and Hurwitz)	Level Density (Experimental)
e-e	$B - \delta$	0	s	s
e-o	$B + \delta$	δ	n	i
o-e	$B - \delta$	$-\delta$	n	l
o-o	$B + \delta$	0	l	?

According to the more recent interpretation, it should run parallel to the difference between the second and third columns, the third column giving

the position of the fiducial level in the product nucleus. The product nucleus is e-o, e-e, o-o, and o-e for the four successive rows. The excitation energy should be, according to the more modern interpretation, small, normal, or large, as indicated in the fourth column.

Experimentally, the level density is lowest for even-even nuclei, and this is in agreement with both interpretations. It is largest for the o-e class, which is, of course, strongly at variance with the original interpretation, but in agreement with the ideas of Bethe and Hurwitz. It is, however, distinctly lower for the even-odd than for the odd-even class, which is in agreement with neither interpretation. The level densities for odd-odd target nuclei are not available.

The picture is very different if one compares magic or magic ± 1 with average nuclei. The comparison will not be given in detail, but it should be remarked that this comparison bears out the original interpretation of the quantity which appears in Weisskopf's formula as the excitation energy of the product nucleus.

It was my intention to comment more in detail on the giant-resonance interpretation of the cloudy-crystal-ball model. It is perturbing that this interpretation has not been, so far, more successful, and that one hardly can have the impression that the experimental information strongly supports the giant-resonance model. This is quite perturbing, because, as far as I know, nobody has proposed any other interpretation of the cloudy-crystal-ball model, and certainly the idea that neutrons are "absorbed" is not something that has a very direct relation with the usual concepts that we use in quantum-mechanical theory.

H. FESHBACH: I just want to see if I can get you to tell us something more. In particular, you made the comment earlier today that you would show us there should be no correlation between the width and level-spacing fluctuations, and that you would talk about this later. This is an appropriate time.

E. P. WIGNER: The giant-resonance interpretation considers, as a first approximation, an individual-particle picture in which there are very few levels of nonzero width, but these are very wide. When interaction is taken into account, then the very wide level will, so to speak, distribute its width among all the many other nearby levels. How it distributes it will depend on accidental facts and accidental things. One level

will receive much, another little, and so on. The thing that one can be quite sure of is that, if you have originally a width of 100, all the nearby levels together will have a total width of 100. This will be distributed, however, with large fluctuations, since the original level throws out its width at random.

A. M. LANE: I should like to ask if you think the distribution of the level spacing is a correlated distribution or a noncorrelated one. I think I am using the right term here. The correlation that I have in mind is the following: If you are given two levels, 1 and 2, is the spacing between 2 and 3 affected by the spacing between 1 and 2, or are these both chosen out of the set of samples corresponding to the distribution that you get at random? Are they both chosen at random, or is there a correlation between adjacent spacings?

E. P. WIGNER: There is one in the only case in which the mathematicians have calculated a formula. Let me give that formula. The mathematicians have considered the case of a real symmetric N -dimensional matrix in which every matrix element has a Gaussian distribution. Then the probability for the characteristic values $\lambda_1, \lambda_2, \dots, \lambda_N$ is:

$$P(\lambda_1, \lambda_2, \dots, \lambda_N) = e^{-(\lambda_1^2 + \lambda_2^2 + \dots + \lambda_N^2)} |(\lambda_2 - \lambda_1)(\lambda_3 - \lambda_1) \dots (\lambda_N - \lambda_{N-1})| .$$

The product contains all $N(N-1)/2$ differences between the λ . To calculate the probability of a spacing of two adjacent levels requires an integration over all the other levels, with the space between the two considered levels excluded from the region of integration, and as far as I know this has not been done. But it is pretty evident, I believe, that there are further correlations in this case at least, and I would think that is general.

E. GUTH: May I ask what the reference for this is?

E. P. WIGNER: This is called the Wishart distribution.

APPENDIX

This Appendix will contain the calculation of the expression for the matrices F, F', G, G', R , and

$$(A1) \quad Q = (F - F'R)(G'R - G)^{-1} ,$$

under the following assumptions:

(a) The matrices F, F', G, G' are symmetric and commute with each other; furthermore,

$$(A2) \quad F'G - FG' = cI$$

is a constant matrix which commutes with every other matrix, in particular with R .

(b) The matrix R is symmetric (equal to its transpose). In the text, $c = 1$. However, if F, F' are replaced by I, I' and G, G' are replaced by $-E, -E'$, the resulting expression becomes the collision matrix if

$$(A3) \quad \begin{aligned} I &= E^* = G - iF , \\ I' &= E'^* = G' - iF' . \end{aligned}$$

In this case,

$$(A2a) \quad I'E - IE' = 2iI ,$$

so that the following calculation permits one to obtain not only Q but also the collision matrix.

(c) The last assumption is:

$$(A4) \quad R = r + a\gamma_0 \times \gamma_0 ,$$

where r is a symmetric matrix, γ_0 a vector, and a a

number. The elements of the matrix $\gamma_0 \times \gamma_0$ are the products $\gamma_{0\lambda}\gamma_{0\mu}$ of the components of the vector γ_0 .

There are four simple rules of calculation with projection operators of the form $\gamma_0 \times \gamma_0$:

$$(A5) \quad \begin{aligned} r(\gamma_0 \times \gamma_0) &= r\gamma_0 \times \gamma_0 , \\ (\gamma_0 \times \gamma_0)r &= \gamma_0 \times r\gamma_0 , \\ (\gamma_0 \times \gamma_0)(\gamma \times \gamma) &= (\gamma_0 \cdot \gamma)(\gamma_0 \times \gamma) , \\ (\gamma_0 \times \alpha) + (\gamma_0 \times \beta) &= \gamma_0 \times (\alpha + \beta) . \end{aligned}$$

In these equations, $r\gamma_0$ is the vector obtained by applying the matrix r to γ_0 . The second equation assumes that r is symmetric (otherwise its transpose appears on the right side). The product $(\gamma_0 \cdot \gamma)$ is the scalar product of the vectors γ_0 and γ . The rules A5 can be verified by direct calculation.

Let us verify first that Q is symmetric. This statement is independent of the assumption (c) except for the symmetric nature of R . The condition of symmetry is that Q be equal to its transpose. Since all matrices in the expression A1 for Q are symmetric, this amounts to:

(A6)

$$(F - F'R)(G'R - G)^{-1} = (RG' - G)^{-1}(F - RF')$$

If this expression is multiplied with $RG' - G$ on the left, $G'R - G$ on the right, one obtains:

(A6a)

$$(RG' - G)(F - F'R) = (F - RF')(G'R - G)$$

or

$$(A6b) \quad R(G'F - F'G) = (FG' - GF')R$$

which is an identity because of Eq. A2.

We now proceed to calculate Q , using the form A4. We set

$$(A7) \quad Q = q + by \times \gamma$$

so that Eq. A1 is equivalent to:

$$(A8) \quad (q + by \times \gamma)(G'r + aG'\gamma_0 \times \gamma_0 - G) = F - F'r - aF'\gamma_0 \times \gamma_0$$

By means of the rules A5, this gives:

$$(A8a) \quad qG'r + a(qG'\gamma_0 \times \gamma_0) - qG + b(\gamma \times rG'\gamma) + ab(\gamma \cdot G'\gamma_0)(\gamma \times \gamma_0) - b(\gamma \times G\gamma) = F - F'r - a(F'\gamma_0 \times \gamma_0)$$

Equating the matrices which are not \times products gives:

$$(A9) \quad q = (F - F'r)(G'r - G)^{-1}$$

and Eq. A8 goes over into:

$$(A10) \quad a[qG'\gamma_0 + b(\gamma \cdot G'\gamma_0)\gamma + F'\gamma_0] \times \gamma_0 = by \times (-rG'\gamma + G\gamma)$$

This equation can be correct only if the vectors after the \times are, apart from a constant, equal. We set, in fact:

$$(A9a) \quad \gamma_0 = (G - rG')\gamma$$

Equation A10, and hence also Eq. A8, will then be satisfied if the vectors to the left of the \times on both sides are also equal. This equality must be essentially a consequence of Eqs. A9 and A9a, since only the number b remains at our disposal. The equation in question reads, if Eq. A9a is used to express γ_0 :

$$(A11) \quad [a(qG' + F')(G - rG') + ab(\gamma \cdot G'\gamma_0)]\gamma = by$$

This equation will be valid if the matrix equation:

$$(A11a) \quad a(qG' + F')(G - rG') = b[1 - a(\gamma \cdot G'\gamma_0)]1$$

holds. It will be possible to satisfy this with a suitable choice of b if the matrix on the left side is a multiple of the unit matrix. This, however, is a consequence of Eq. A9 and the fact that the F , G , etc., commute:

$$\begin{aligned} & (qG' + F')(G - rG') \\ &= (F - F'r)(G'r - G)^{-1} G(G - rG') + F'G - F'rG' \\ &= (F - F'r)(G'r - G)^{-1} (G - G'r)G' + F'G - F'rG' \\ &= -(F - F'r)G' + F'G - F'rG' = F'G - FG' = c1 \end{aligned}$$

The last step is a consequence of Eq. A2. As a result, Eq. A11a and all previous equations will be satisfied for:

(A9b)

$$b = \frac{ac}{1 - a(\gamma \cdot G'\gamma_0)} = \frac{ac}{1 - a[(G - rG')^{-1}\gamma_0 \cdot G'\gamma_0]}$$

Equations A9 are equivalent to Eqs. 5 of the text, except that $c = 1$ in that case.

NUCLEON DENSITIES IN A DIFFUSE-BOUNDARY INDEPENDENT-PARTICLE MODEL

A. E. S. Green
Florida State University

A. E. S. GREEN: We have been laboring with a particular type of diffuse-boundary model for some time. It is a model chosen because we can handle the wave functions analytically. Dr. Kuick Lee, Mr. R. J. Berkley, and I have finally worked out the wave functions and the total densities of the protons and neutrons in typical spherical nuclei. These may have some relevance to some of the earlier discussions at this conference.

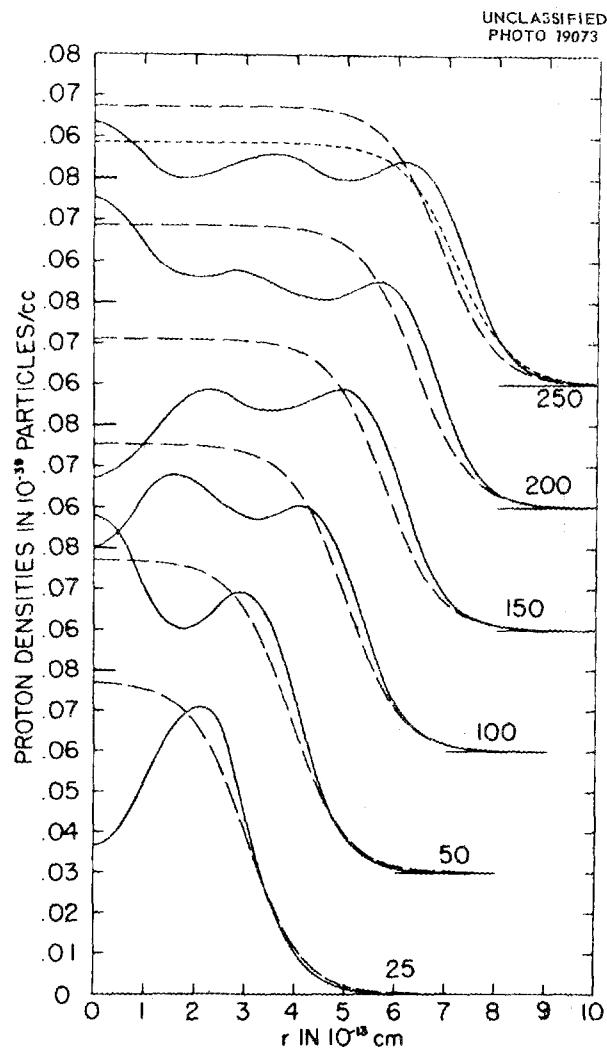
The wells chosen are 40 Mev deep and have an exponential decay constant of 1 fermi. That would be equivalent to a 0.9 to 0.1 distance of about 2.2 fermis. The inner uniform region has a radius $1.32A^{1/3} - 0.8$. This particular adjustment of the neutron well was chosen in an effort to get the last neutron bound from about 10 to 6 Mev as one increases the mass number, and also to ensure that the 3s neutron resonance occurs at mass number $A = 55$ and the 4s resonance at $A = 170$. We have worked with this simplified panoramic well in the hope of getting a broad picture of nuclear densities. I might say that we have compared this with a well used by Beyster, Walt, and Salmi in a study based purely on neutron-scattering data. The wells are found to be quite compatible in most respects.

We let the protons see the neutron well, the coulomb repulsion of the other protons, and in addition a potential anomaly, an extra attraction that is needed to hold the protons at approximately their proper binding energy. All the proton densities have then been calculated in six nuclei, and these are shown on Slide 1.

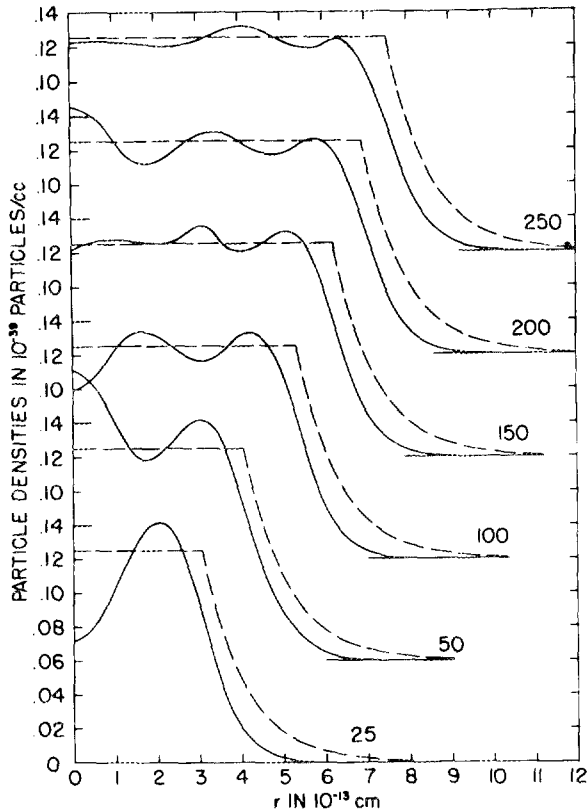
These are the sums of the proton densities in all the individually occupied states in nuclei with mass number 25, 50, 100, 150, 200, and 250. The proton numbers are chosen appropriately to give a beta-stable nucleus. The dotted curves represent the proton densities interpolated from the Stanford experiment. It should be apparent that the theoretically and experimentally inferred densities build up in a remarkably similar manner in all gross aspects. While in some instances the agreement looks pretty bad, particularly in the central densities, it would take only a relatively small adjustment in the radius, about 2 or 3%, to greatly improve these agreements. Thus the predicted curves

would be difficult to discriminate against on the basis of the Stanford experiments.

On Slide 2 the total neutron and proton densities are summed up for these six cases, and are compared with the form function used for the potentials. We see here that our potential radius is significantly larger in each case. Furthermore, the densities definitely have a fine structure. Let us



Slide 1. Proton Density Distributions for Six Different Nuclei.



Slide 2. Particle Density Distributions for Six Different Nuclei.

consider what would be expected if you were to pursue a self-consistent-field calculation in the following way. Let us start with our potential function, and then find a density function by getting all the individual particle densities. Then let us take a direct connection between density and potential:

$$(1) \quad \nabla^2 V - a_{\pi}^{-2} V = 4\pi g \rho(r),$$

which is a mesonic generalization of Poisson's equation. If from the density curve we derive a potential, that potential would definitely have a fine structure which varies from case to case. Thus in a self-consistent-field calculation you would expect local irregularities, local departures from any results predicted from a smooth family of potentials.

I have calculated the differences between the potential radii and the density-squared radii if you

assume Eq. 1 as the connection between density and potential. I might say that it appears indirectly from the work of Talman that if one followed this connection completely the nucleus would collapse. If, however, you assumed that this connection is good in so far as surface considerations are concerned, you are led to expect:

$$(2) \quad \langle r^2 \rangle_V - \langle r^2 \rangle_d = 6a_{\pi}^2.$$

Well, we have a set of total density curves that we get as a result of this phenomenological model. We cannot say that these densities agree with the experiment, but we can say that the proton densities do agree pretty well. We also have a set of potential curves which seem good from the standpoint of particle binding energy and neutron scattering. We have taken those curves and numerically determined the density radii and the potential radii. We have found that the differences are indeed of the same order of magnitude as expected from Eq. 2. In detail, the differences are somewhat smaller in light nuclei, but in heavy nuclei they approach the number 11.9. I think a good direction to look in further work with self-consistent-field calculations would be to find a modification of Eq. 1 which would give us, instead of Eq. 2, predictions of differences more in agreement with our phenomenological potentials and densities.

E. P. WIGNER: It is necessary, in addition to this equation which you have, to write another equation giving the density in terms of the potential. What did you use for that?

A. E. S. GREEN: We solved Schroedinger's equation, and got the wave functions for every state. Then we filled up the states, obtaining all the individual densities and finally the sums of the individual particle densities.

E. P. WIGNER: I thought you did that for this original potential.

A. E. S. GREEN: Yes.

E. P. WIGNER: When you calculated this one with what you called Talman's equation, what did you do then?

A. E. S. GREEN: We didn't complete the cycle. We started out with a potential, or a family of potentials, and we got the densities from Schroedinger's equation. All we really show is that the family of potentials is in reasonable conformity with the experiments which measured the potentials, and that the densities which we got, and

particularly the proton densities, are in reasonable conformity with the density measurements. So we really haven't used this explicitly to complete the self-consistent-field calculation.

E. P. WIGNER: What is that second equation?

A. E. S. GREEN: This equation is based on an arbitrary potential function, for essentially I can derive Eq. 2 from Eq. 1 directly.

H. FESHBACH: Is that independent of the form of V ?

A. E. S. GREEN: It is independent of the form of V as long as it dies out fast enough at infinity. The derivation involves some simple manipulations including integrations by parts.

E. GUTH: What is the difficulty of trying to complete your Schroedinger's equation?

A. E. S. GREEN: We would need a general code for solving Schroedinger's equation. After we get a density and from it a potential, we would have to solve Schroedinger's equation again. I think, however, from the work of Talman one knows what is going to happen. The nucleus will probably shrink and in successive steps collapse.

E. P. WIGNER: It is true, too, that after a couple of cycles the two agree quite well, and do give a width of this intermediate region (or what you call the region where the density isn't full, that twilight region), which is about as long as the real one, which was quite surprising, because most of us expected it to be much larger.

A. E. S. GREEN: So you have to introduce something that is going to stop that collapse, and we are working on doing something of this sort.

SESSION II

ELASTIC AND INELASTIC NEUTRON SCATTERING

INELASTIC SCATTERING OF FAST NEUTRONS IN RHODIUM AND NIOBIUM

M. A. Rothman
Bartol Research Foundation

M. A. ROTHMAN: At the Bartol Foundation we have been interested in the use of gamma rays from inelastic neutron scattering to determine the position of energy levels of medium-weight nuclei. Accurate determination of both the gamma-ray energies and the thresholds for excitation of these gamma rays should give an unambiguous location of these levels. Two elements which we have studied are rhodium and niobium. Both Rh^{103} and Nb^{93} are of 100% isotopic abundance.

The level scheme of rhodium up to 640 keV has been determined recently at the Bartol Foundation by using radioactive isotopes which decay to Rh^{103} . In the case of niobium, no levels have been known except the metastable state at 29 keV with a half life of 3.65 years. The scattering samples were in the form of thin squares. The rhodium weighed 55 g; the niobium weighed 127 g.

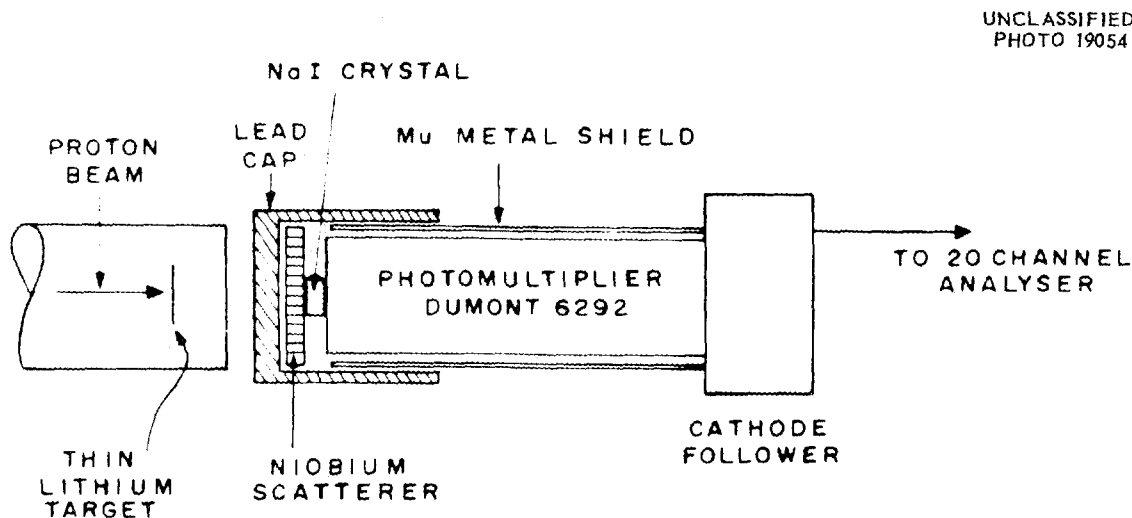
To obtain the greatest yield of gamma rays, we investigated the method suggested recently by Guernsey and Wattenberg of MIT. The setup is shown in Slide 1. This shows the business end of the Van de Graaff generator. Neutrons are produced in the thin lithium target. The NaI crystal is directly in the neutron beam and is made very small to minimize background due to neutron scattering

and capture in the iodine. Gamma-ray spectra are taken with the scatterer inside the lead cap, right up against the crystal can. Background is taken with the scatterer outside the lead cap. We have found that we can work with gamma-ray energies up to 1 MeV by choosing the size of the crystal appropriate to the energy range we are interested in. For rhodium, we used a crystal 3 mm thick. For niobium, a 1-cm crystal was used.

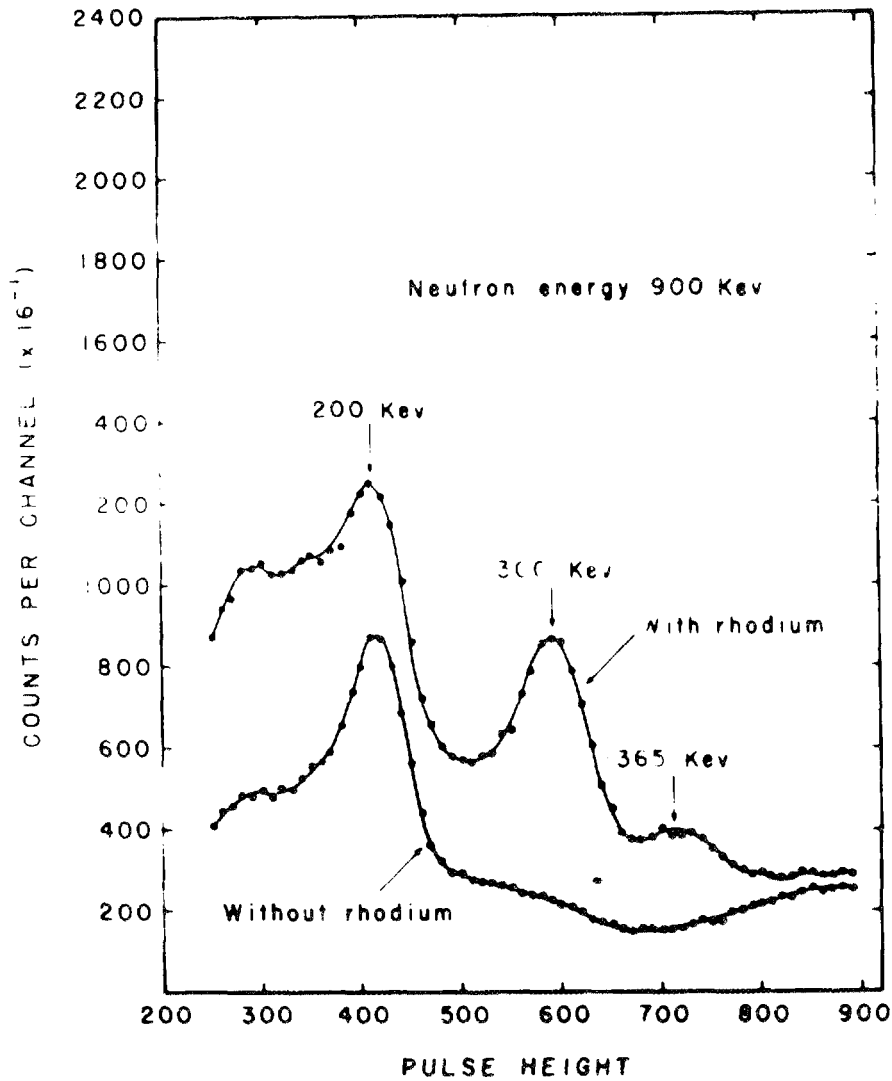
Slide 2 shows a typical pair of spectra using the rhodium. The 200-keV peak is from neutron scattering in iodine. The 300- and 365-keV peaks are from the rhodium.

Slide 3 shows the subtracted spectrum. Slide 4 shows the excitation curves for the two gamma rays. The threshold for the 300-keV gamma ray is quite close to 300 keV. The threshold for the 365-keV gamma ray seems high, but the peak was not well resolved, and this could not be considered a good threshold determination.

Slide 5 shows the level scheme as determined by Saraf from the decay of Ru^{103} and Pd^{103} . This shows levels at 300 keV and 365 keV. Using the spins assigned in this scheme, we made a theoretical calculation of the neutron scattering cross section, using a square potential of 42-MeV depth and 0.2



Slide 1. Apparatus for Inelastic Neutron Scattering Experiment.



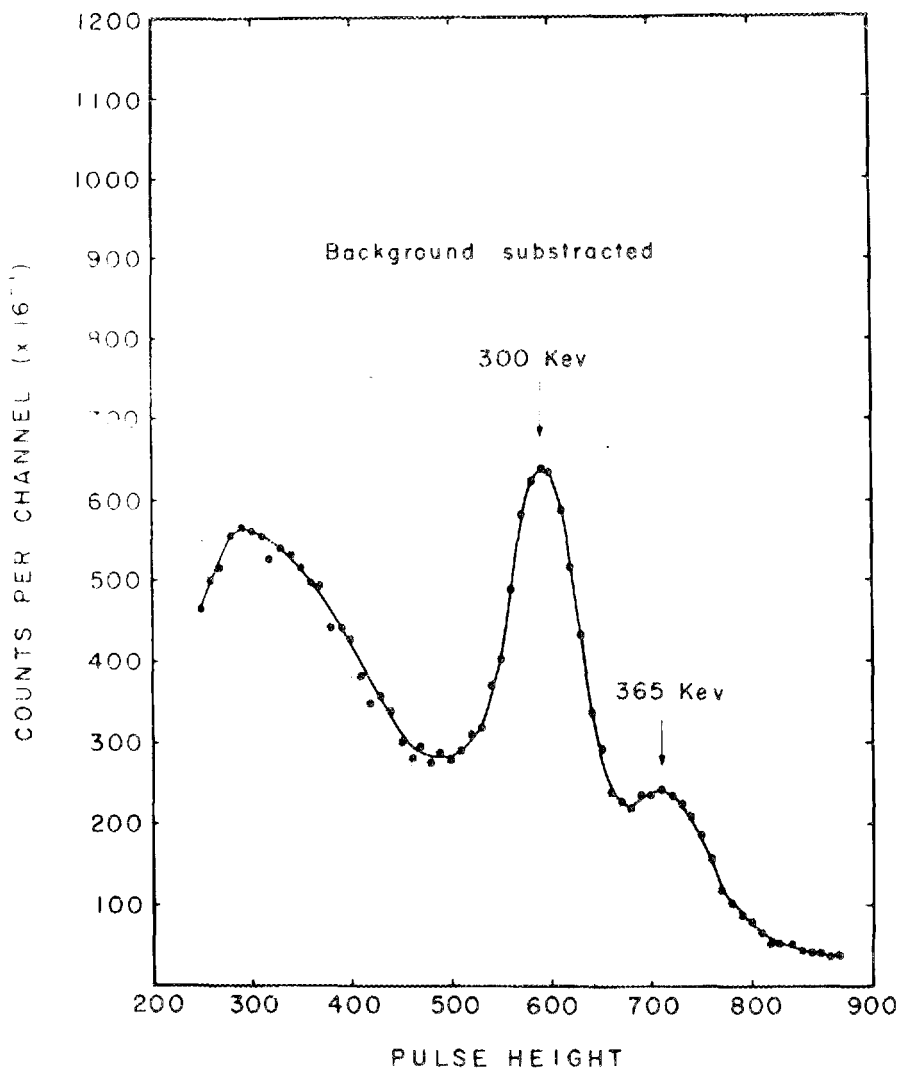
Slide 2. Pulse-Height Spectrum of Gamma Rays from Inelastic Neutron Scattering in Rhodium.

imaginary fraction. The shapes of the experimental and calculated curves do not agree very well. The experimental curves rise much more steeply than the theoretical curves. However, the ratio of the cross sections for the two gamma rays agrees well with the calculated ratio. This would be most sensitive to the spin assignment.

Slide 6 shows the spectrum obtained from niobium. This shows two gamma rays, whose energies have been more recently determined as 736 ± 8 and 957

± 10 kev. Slide 7 shows the excitation curves for the two gamma rays. The thresholds have been re-determined since preparation of these slides, using thinner targets, with the following results:

Threshold energy (kev)	772 ± 8	987 ± 10
Level energy (kev)	764 ± 8	977 ± 10
Gamma-ray energy (kev)	736 ± 8	957 ± 10
Difference (kev)	28 ± 11	20 ± 14



Slide 3. Pulse-Height Spectrum of Gamma Rays from Inelastic Neutron Scattering in Rhodium. Background subtracted.

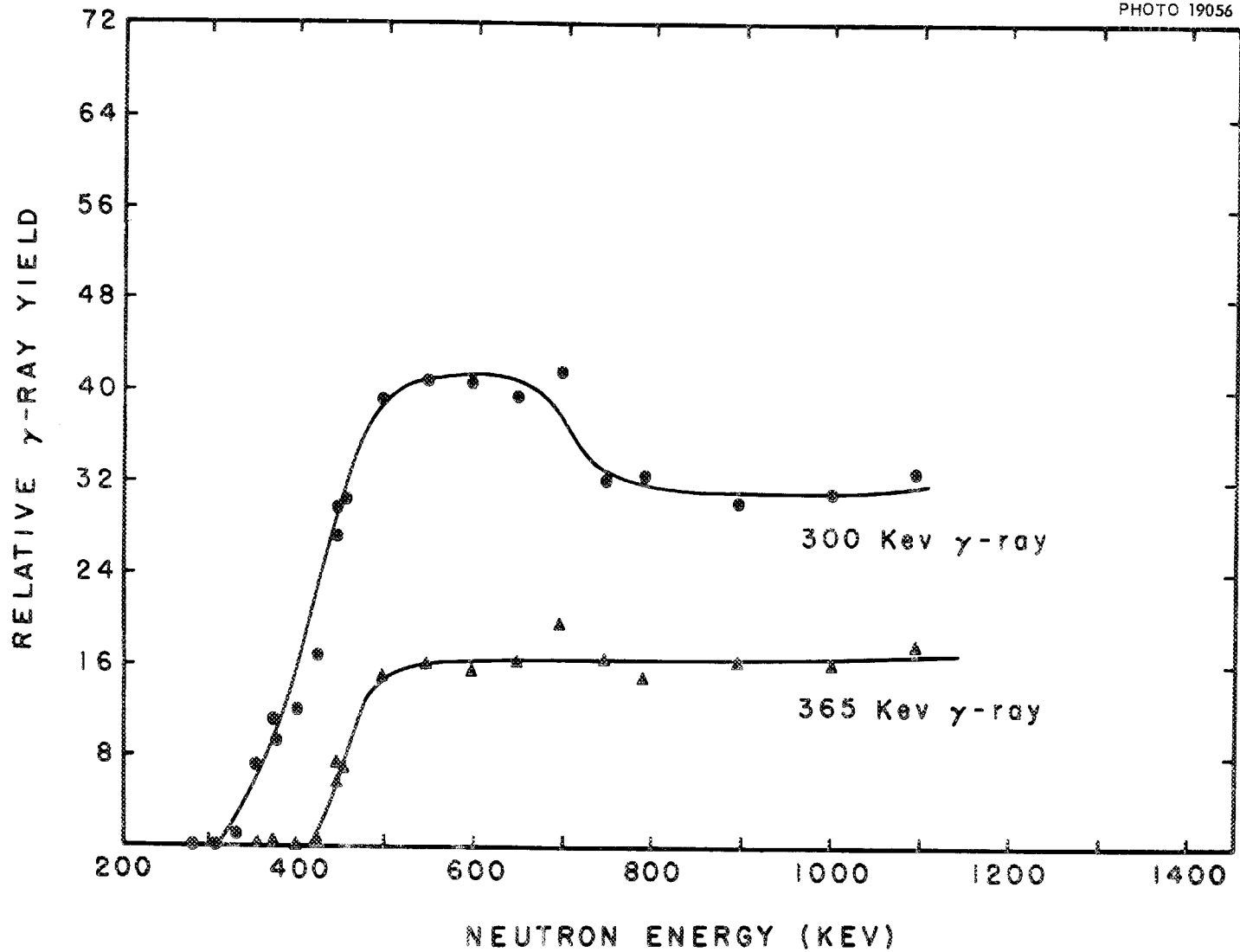
The level energy is calculated by means of the equation:

$$\text{Level energy} = -Q = \text{Threshold energy} \times \left(1 - \frac{1}{A + 1}\right).$$

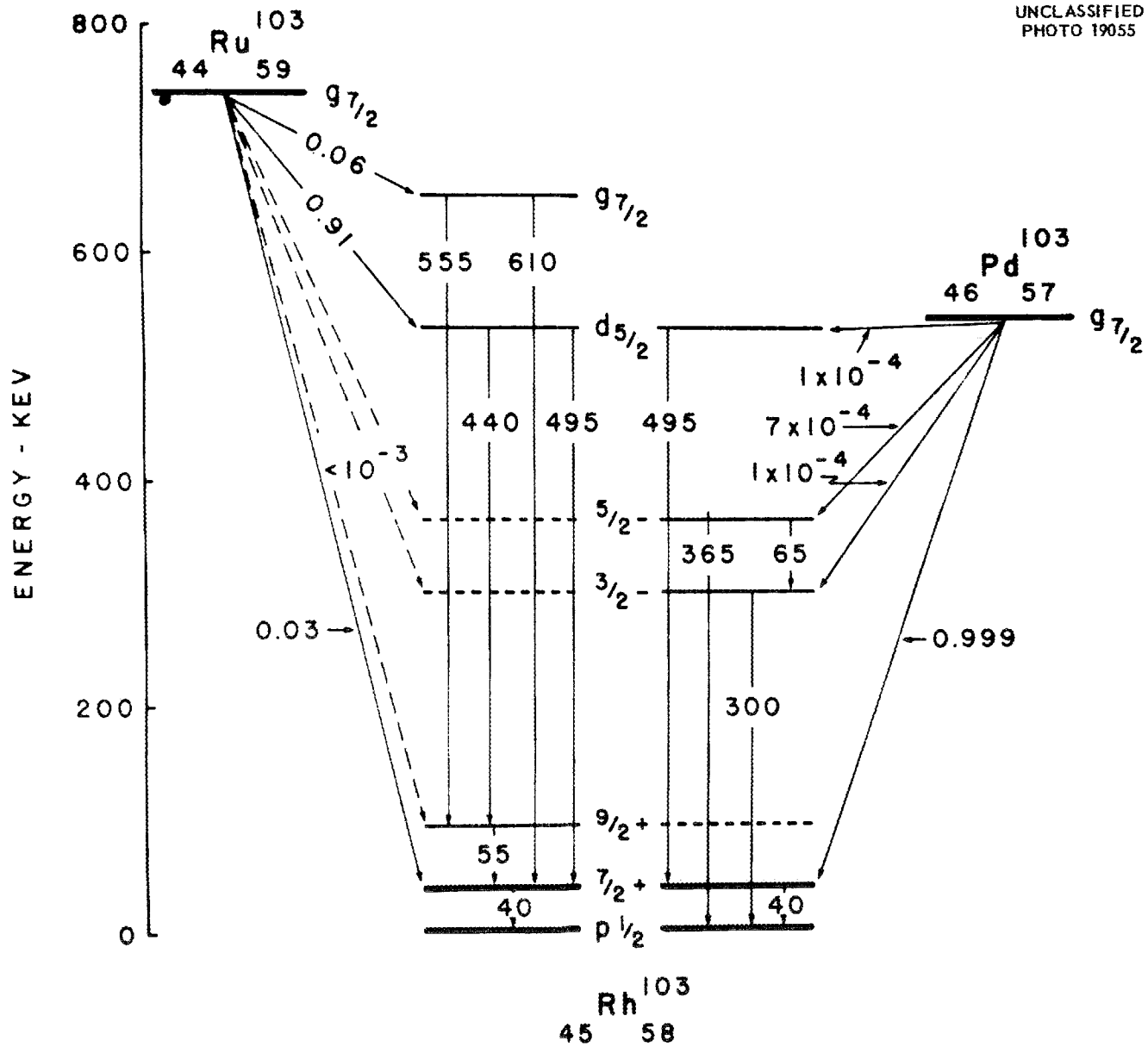
These results indicate that the gamma rays observed are the result of transitions to the 29-kev metastable state rather than to the ground state.

The cross section for production of these gamma rays has been measured by comparison with the known cross section for iron. The cross section for the first gamma ray goes up to a maximum of about 1 barn.

The magnitude of this cross section, together with the known spins of the ground and metastable states, fairly well defines what the spins of the higher states must be. The ground state is known



Slide 4. Excitation Functions for Gamma Rays from Inelastic Neutron Scattering in Rhodium.



Slide 5. Energy-Level Scheme of Rh^{103} from the Decay of Ru^{103} and Pd^{103} .

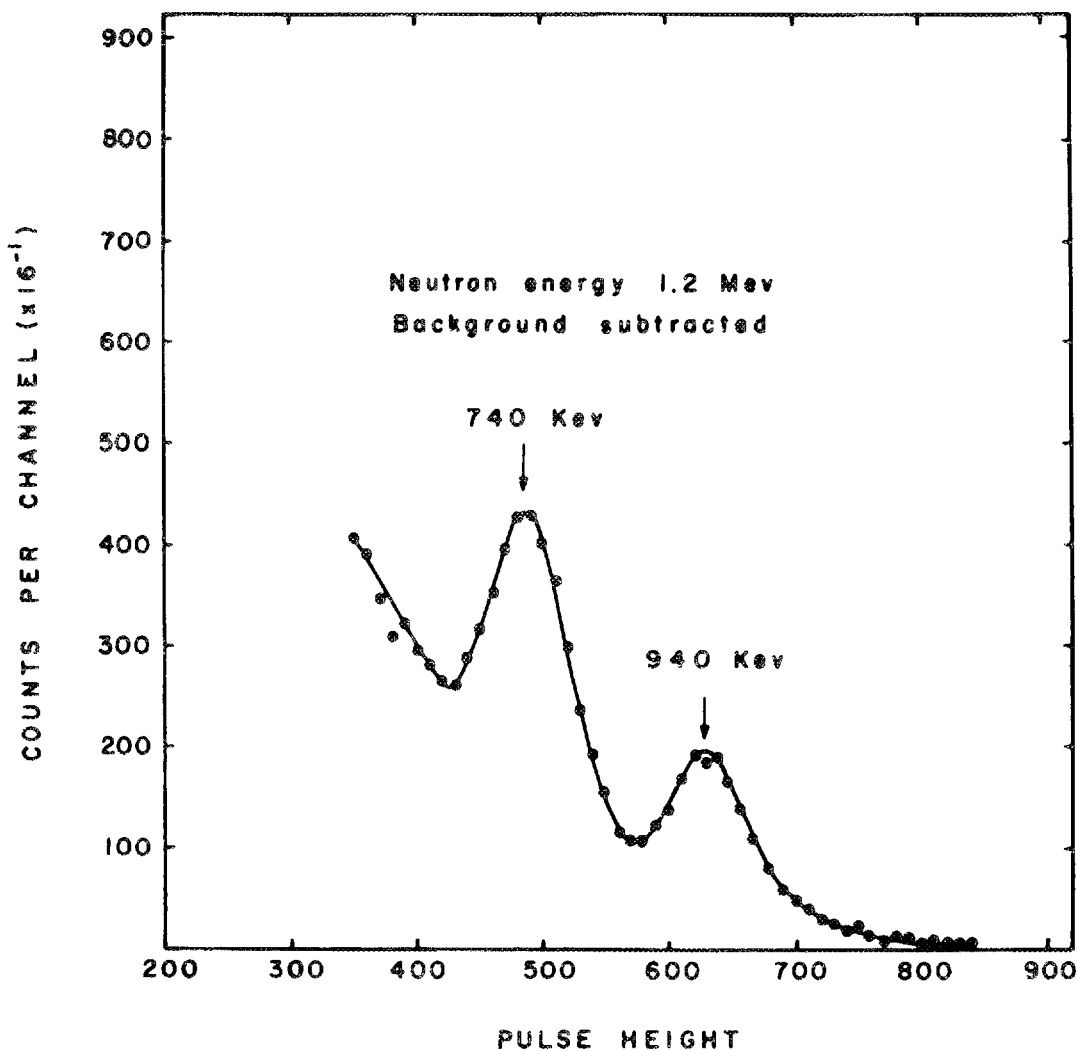
to have a spin of $\frac{3}{2}^+$, while the metastable state has a spin of $\frac{1}{2}^-$. If the transition from the higher state to the metastable state is preferred to the ground-state transition, then the higher state can have a spin no greater than $\frac{5}{2}^-$. This gives an electric-quadrupole transition to the metastable state and a magnetic-quadrupole transition to the ground state.

At the same time, the slope of the excitation curve requires that the spin of the excited state be no farther away from the ground state than 2 angular momentum units. A theoretical calculation of the cross section using a spin of $\frac{5}{2}^-$ for the

764-kev state gives a curve whose height is about $\frac{1}{6}$ of the measured excitation curve in the region within 100 kev of the threshold. Changing the parameters of the potential well does not alter this ratio by more than a factor of two. However, changing the spin of the excited state to $\frac{3}{2}$ produces at least a factor of ten reduction in the calculated cross section, so that we conclude the correct spin must be at least $\frac{5}{2}$.

Since we have already said that the spin can be no greater than $\frac{5}{2}^-$, this must be the most probable value for the spin and parity of the 764-kev state. Since the 977-kev level has approximately the same

UNCLASSIFIED
PHOTO 19049



Slide 6. Pulse-Height Spectrum of Gamma Rays from Inelastic Neutron Scattering in Niobium.

cross section, we conclude that it has the same spin value.

The measured cross section is still high compared to theory, so that the situation with regard to this is still ambiguous.

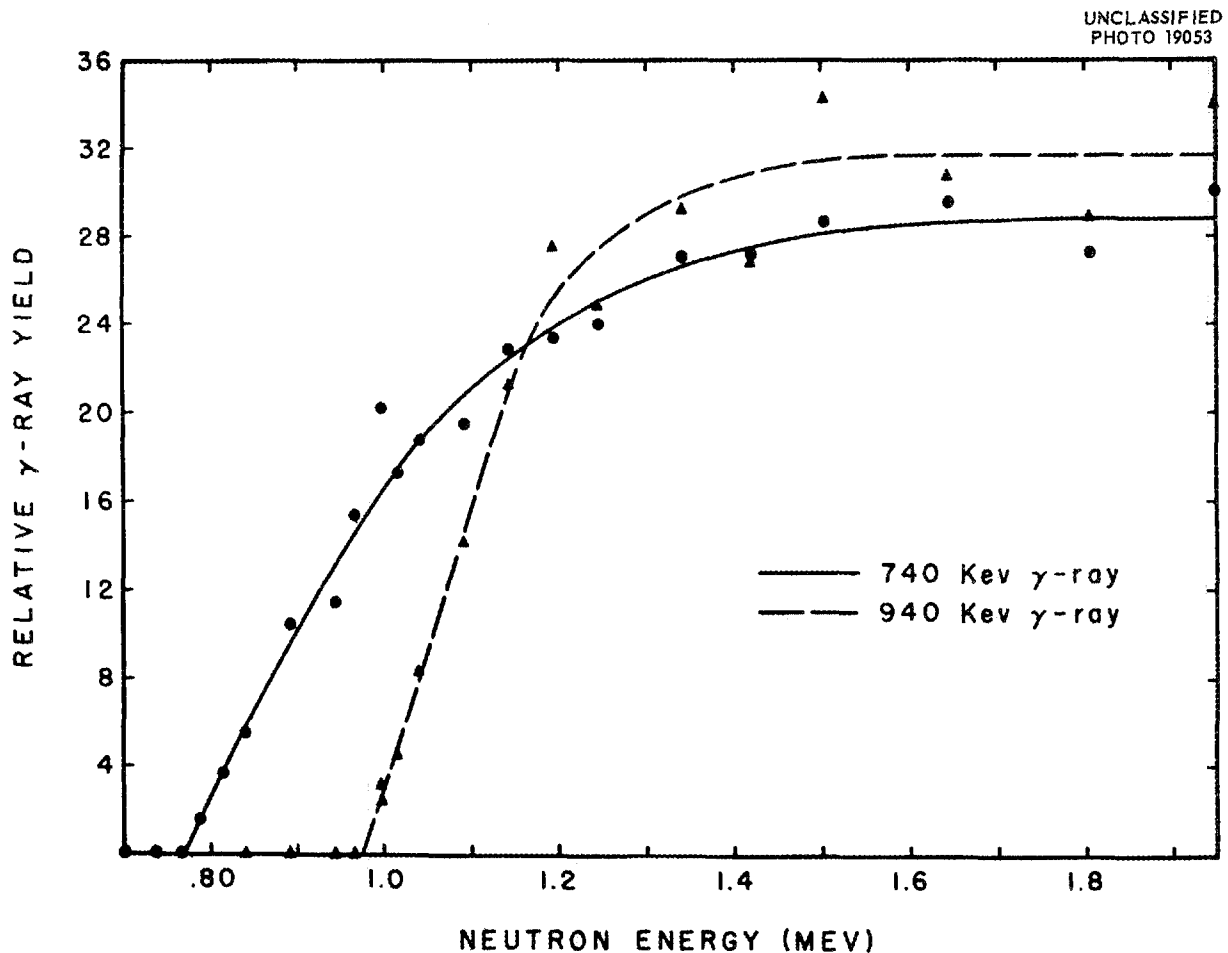
R. B. DAY: Is the low-energy state too highly converted for you to see gamma rays from it?

M. A. ROTHMAN: It is very highly converted, yes.

E. BRETSCHER: Did you not measure exactly how the excitation rises beyond threshold?

M. A. ROTHMAN: Yes, we have tried to get points as close together as our resolution would allow. The slope of the experimental curve appears to rise five or six times faster than the curve calculated on the basis of the $\frac{5}{2}^-$ spin.

H. FESHBACH: I have a comment to make about the application of the cloudy crystal ball. The cloudy crystal ball with the square well does not give the proper inelastic cross section, as we stated in the original publication. To those people who would like to make calculations on this, I would recommend using an incorrect model, the old black nucleus model. That always gives the right answers.



Slide 7. Excitation Functions for Gamma Rays from Inelastic Neutron Scattering in Niobium.

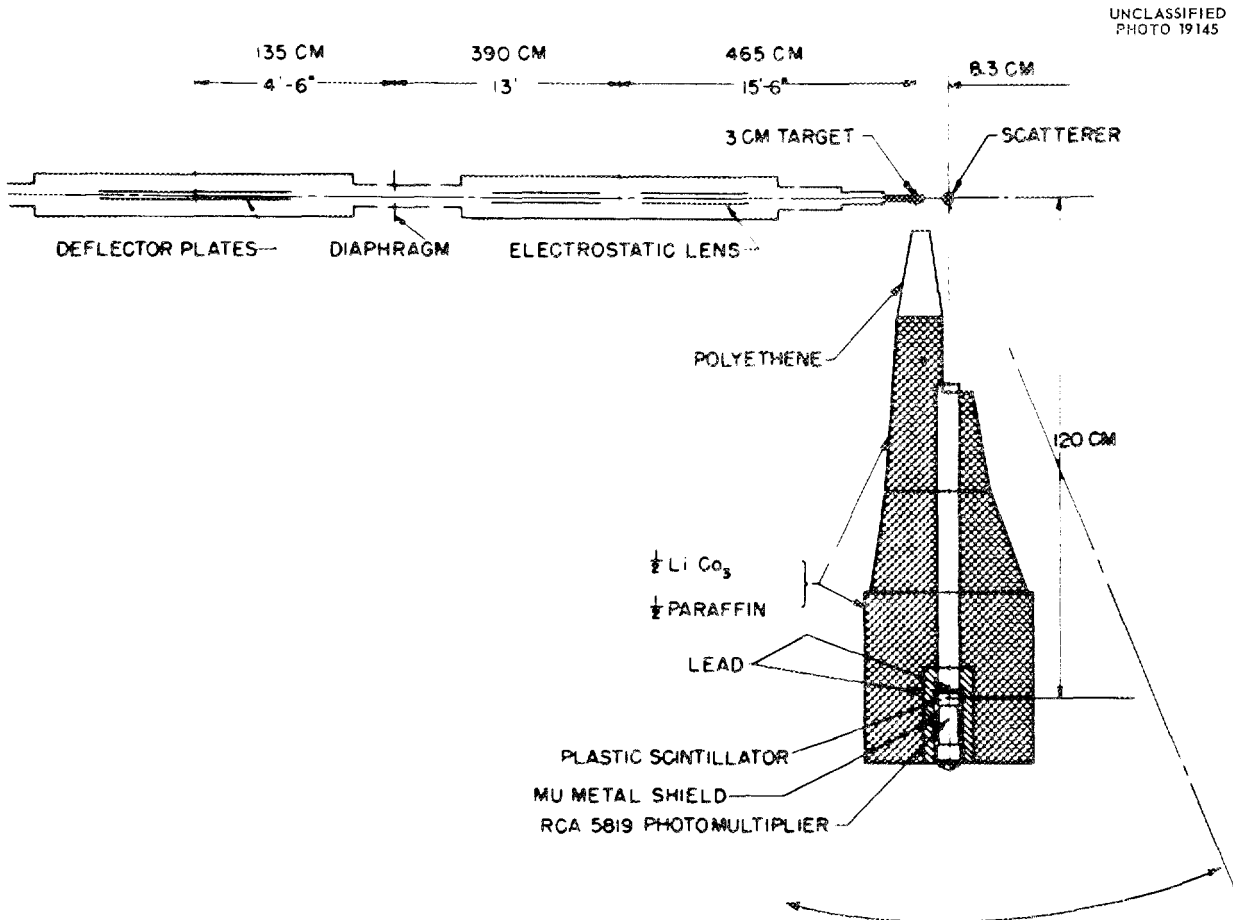
INELASTIC SCATTERING FROM TANTALUM, TUNGSTEN, AND GOLD

J. S. Levin and L. Cranberg
Los Alamos Scientific Laboratory

L. CRANBERG: The technique of measuring inelastic neutron scattering by time-of-flight is straightforward. One makes monoenergetic neutrons with an accelerator in bursts of a few millimicroseconds' duration several million times a second. These neutrons are then scattered, and one stands off at a distance between 1 and 2 m and observes the spectrum of arrival times of the neutrons in a proton recoil detector.

Slide 1 shows the general features of the experimental arrangement. The pulsing of the charged-particle beam is accomplished by applying a sweep voltage to a pair of electrostatic deflector plates

at an appropriate frequency, so that the beam is stopped on the diaphragm except for an interval of a few millimicroseconds twice per r-f cycle. Neutrons are then made in the target by one of two reactions. For lower-energy neutrons we use the reaction $T(p,n)He^3$. This is for neutrons of energy of a couple of Mev. For neutrons having higher energies, 5 or 6 Mev, we use the $D(d,n)He^3$ reaction. Neutrons are produced in the gas target shown here. We use the neutrons in the forward direction, since the yield is high there. The neutrons are scattered and observed in a detector, which is a plastic scintillator.



Slide 1. Pulsing Equipment, Detector, and Shielding for Millimicrosecond Neutron Time-of-Flight Spectrometry.

The detector has to be carefully shielded from the direct flux from the target, because that flux is several hundred times greater than the flux from the scatterer, which one is interested in detecting. This whole apparatus is mounted on a turntable which pivots about the scatterer, so that one can measure the scattered neutrons as a function of angle.

Our earliest studies with this system were devoted to the inelastically scattered neutrons which are associated with the excitation of single levels in the residual nucleus. These give well-resolved neutron groups. We have previously made a report on this. I should like to describe today some of the results which we obtained recently on heavy elements. By "heavy" I mean elements like gold, tantalum, and tungsten.

For these nuclides, because of the high level density and our finite resolution, we do not resolve neutron groups in the spectrum of inelastically scattered neutrons, but we see essentially a continuum. The interest that these spectra have is that they allow a test of the predictions of nuclear evaporation models. The predictions are that the inelastically scattered neutrons will be isotropic and that their energy distribution will be Maxwellian with characteristic nuclear temperatures.

Anticipating that one does get a Maxwellian distribution, one then envisages a program which would aim at elaborating the systematics of the dependence of nuclear temperature on scatterer mass and neutron energy. This is, indeed, a very ambitious program, on which we have made only a very modest beginning with the preliminary results on which I want to report now.

Our first observations have been on tantalum, tungsten, and gold, for each of three neutron energies and for each of three angles. The energies we used were 2.5, 3.4, and 6.3 Mev. The ensemble of three elements at each of three angles and each of three energies gives a family of 27 curves.

MEMBER: What angles were they?

L. CRANBERG: Thirty, 90, and 150 deg. Incidentally, I have all nine curves for gold with me. If anyone is interested in seeing them, I shall be glad to show them privately. I shall show slides only of the three curves at 90 deg for gold.

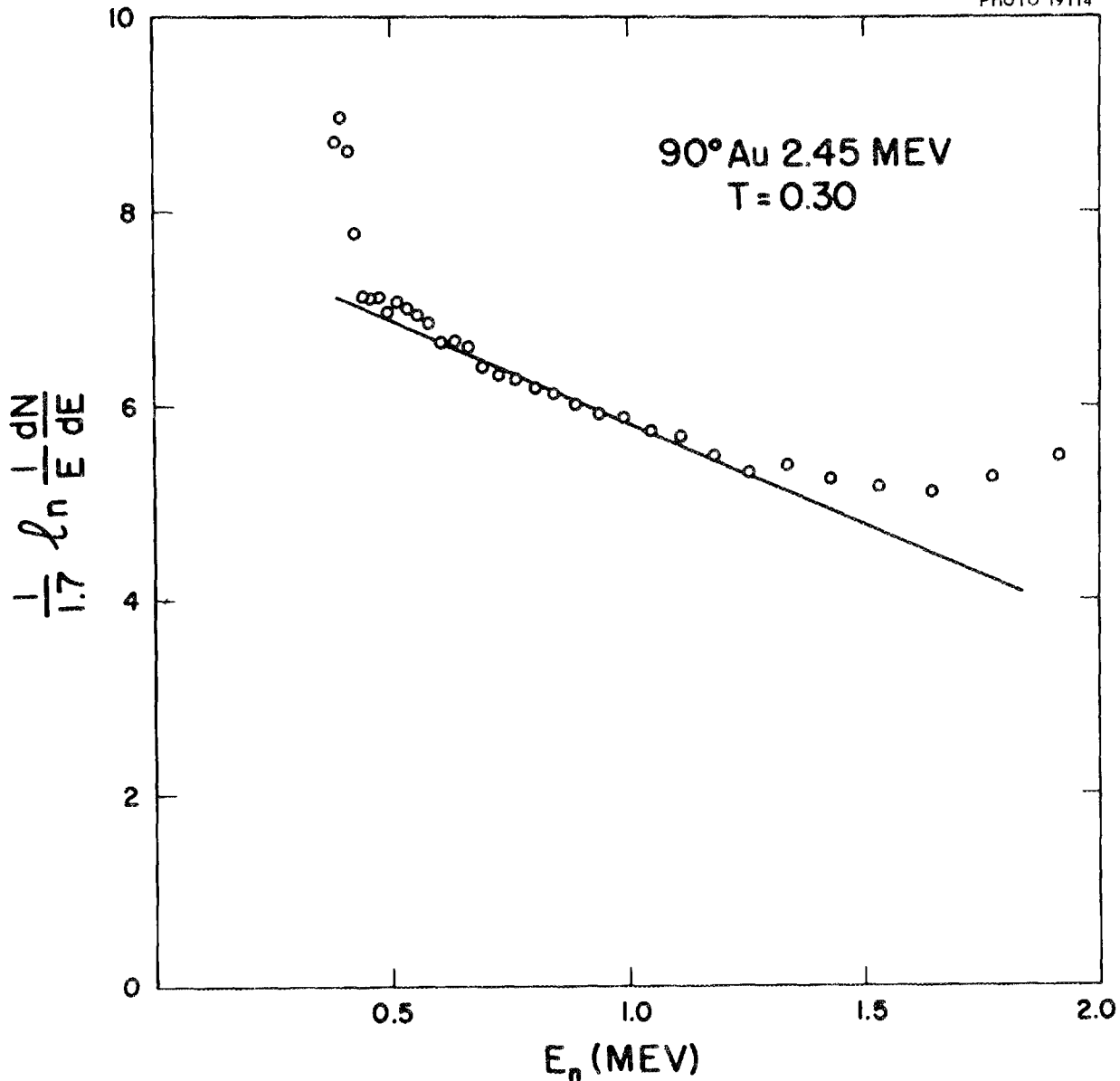
First let me say what the results were on the angular distributions. Within experimental error,

which is statistical and between 5 and 10%, we observed isotropy. This simple statement has to be qualified. At the time these measurements were made, we were not able to see neutrons having energies less than 400 or 500 kev. On the other hand, our resolution puts an upper limit on the energy of neutrons which can be resolved from elastic scattering. Thus the statement that the neutrons are isotropically scattered applies to those which lose about 1 Mev or 2 Mev and have at least 400 kev left. The number of inelastically scattered neutrons in the region corresponding to a small energy loss is very small. Those with large loss are more numerous. It is estimated that in these measurements one can see about 50% of the inelastically scattered neutrons in the least favorable case of low bombarding energy.

Now with regard to the energy distribution of these inelastically scattered neutrons, the question is whether or not the distribution is Maxwellian. Slide 2 shows the result on gold for a primary-neutron energy of 2.45 Mev. The data are plotted in such a way as to give a straight line if they conform to a Maxwellian distribution. The high points to the left are just the gamma rays from the next duty cycle and are to be ignored. We have tried to fit the intermediate range of neutrons with a straight line corresponding to a nuclear temperature of about 0.3 Mev. The discrepancy from a Maxwellian fit is real at 2.45 Mev, particularly for neutrons which have lost little energy. These neutrons correspond to the excitation of the very lowest-lying states of the target nucleus. This is perhaps not surprising.

Slide 3 shows the spectrum for 3.4-Mev neutrons and again 90-deg scattering angle. The straight line corresponds to a temperature of 0.45 Mev. Obviously, the agreement is considerably better. Since this slide was made, these high-energy points have been dropped in the process of making the correction for the tailing of the elastic peak.

Slide 4 shows the results at the highest energy, 6.34 Mev. Again to the left we have the gamma ray from the succeeding cycle, and the fit to the temperature 0.65 Mev is reasonably good as long as the neutrons have lost a couple of Mev of energy.



Slide 2. Energy Spectrum of 2.45-Mev Neutrons Inelastically Scattered at 90 Deg in Gold.

Table 1 shows a summary of the temperatures obtained at each of these three energies for the three elements. In the case of the lowest energy, the fit for gold, as you saw, is quite poor, and it is not much better in the case of tantalum and tungsten. So one might say that we only have a basis for saying something about the temperature systematics for the two higher energies. The one point on silver represents just a single run

at the highest energy at 90 deg. The theory with which these results invite comparison is based on the degenerate-gas model of the nucleus as given by Weisskopf and others, which predicts that these temperatures should go as the square root of the excitation energy. In the case of gold this prediction does describe the picture fairly well, but not so well in the case of tantalum and tungsten.

For silver the temperature should be higher than for the heavier nuclides, and it is not. But not much weight can be attached to this single datum point yet.

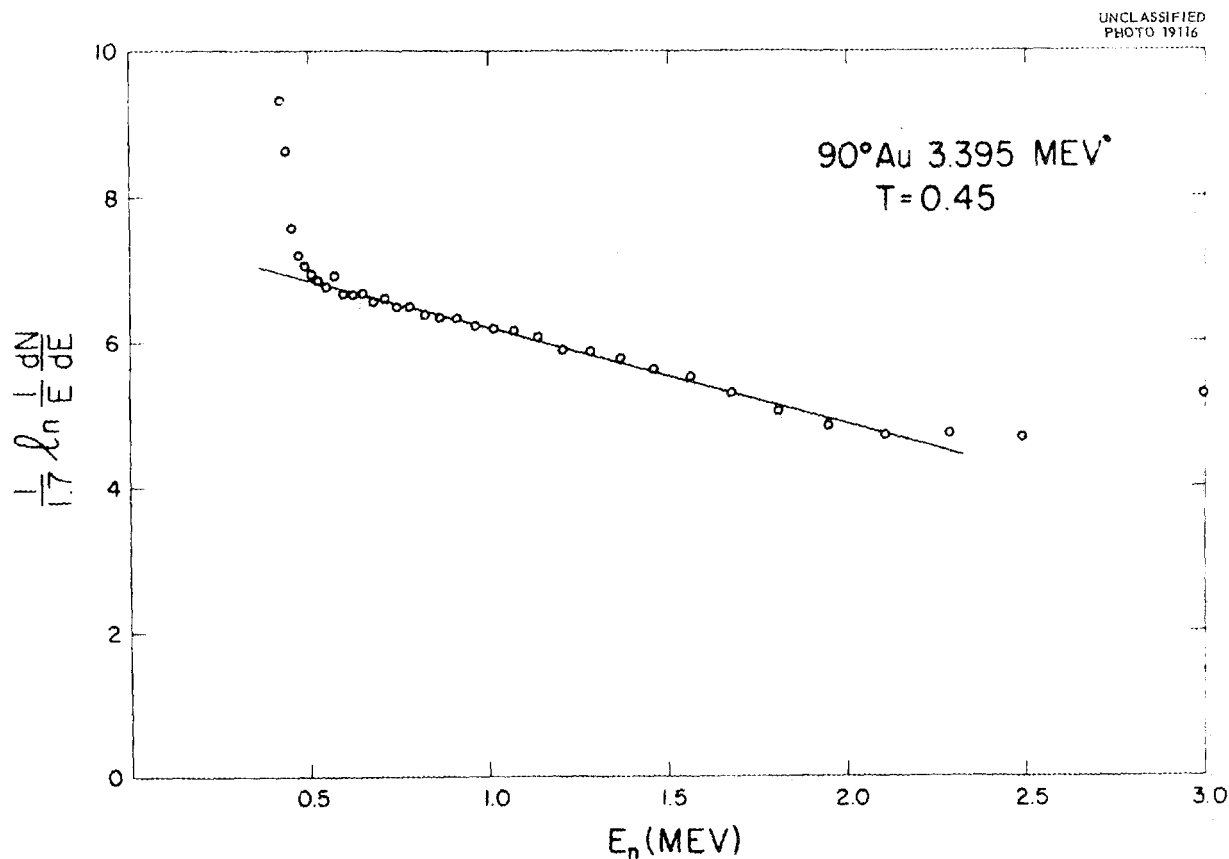
Our plans for the future are to continue these measurements and to extend them to a wider range of mass numbers and neutron energy. There is

Table 1. Nuclear Temperature from Inelastic Neutron Scattering

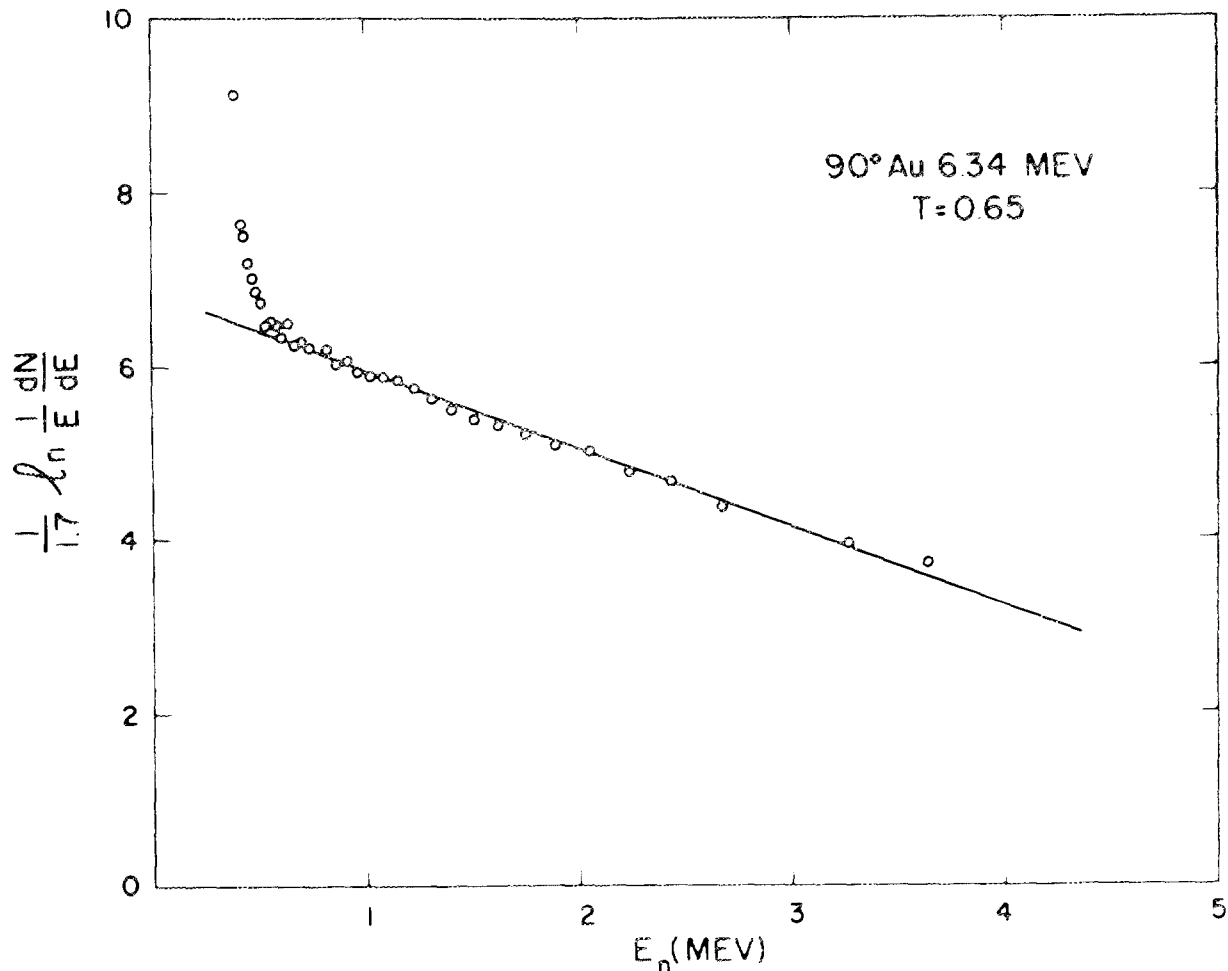
Primary-Neutron Energy (Mev)	Nuclear Temperature (Mev)			
	Gold	Tantalum	Tungsten	Silver
2.45	0.30	0.32	0.36	
3.40	0.45	0.39	0.36	
6.34	0.65	0.50	0.44	0.59

much that we can do so far as mass number is concerned, but not so much that we can do so far as energy is concerned. The underlying reason for the energy limitation is a point worth bringing to the attention of the experimenters here. To obtain higher-energy neutrons we have to use the $D(d,n)He^3$ reaction at higher deuteron energies, and we have found, contrary to earlier reports, that the deuteron breaks up at the appropriate threshold. Thus, when one tries to make 8-Mev neutrons, this breakup reaction begins to give severe competition to the reaction $D(d,n)He^3$, and, since the breakup is a three-body process, there is present a continuum of low-energy neutrons which makes it very difficult to do inelastic-scattering work.

H. GOLDSTEIN: I should like to make an observation about the spectrum which you observed at the lowest incident-neutron energy, 2.5 Mev, with its discrepancy from the Maxwellian. There



Slide 3. Energy Spectrum of 3.395-Mev Neutrons Inelastically Scattered at 90 Deg in Gold.



Slide 4. Energy Spectrum of 6.34-Mev Neutrons Inelastically Scattered at 90 Deg in Gold.

is by now a fairly old *Ansatz* of Weisskopf's suggesting, empirically, that the low-excitation portion of the level-density formula might be corrected by saying that the level density, at low excitation energies, does not rise exponentially as one would expect, but is relatively constant up to an energy which depends upon the particular nucleus involved. The effect of this *Ansatz* is to give just this kind of deviation which you have observed, this increase toward the low excitation-energy (high neutron-energy) end.

P. A. EGELSTAFF: I noticed in the table you just showed that at the 6.35-Mev incident energy the temperature decreased in the order of gold, tantalum, and tungsten. This seems to be possibly a significant decrease. I should like to ask you,

first, whether you think that decrease is significant, and whether you would like to comment on the difference in temperature between the tantalum and tungsten results, remembering that both are just about an equal number of nucleons.

L. CRANBERG: No, I am afraid I have no comment to make. I feel that the picture as we have developed it thus far is too fragmentary for me to make any kind of significant comment about it.

P. A. EGELSTAFF: Do you feel that this difference is really significant?

L. CRANBERG: We assign an uncertainty of about 10% to these temperatures, and the difference between 0.4 and 0.5 is not definitely outside our uncertainty.

H. H. LANDON: I wanted to ask what is the lowest energy group that you might see in tantalum; that is, how close to the elastic peak could you go at the energies at which you worked?

L. CRANBERG: The limits are given right here. That is, the neutron has to lose 1 Mev at the two lower energies and 2 Mev at the highest energy. In other words, we are not seeing neutrons corresponding to excitation of the first 1 to 2 Mev in the residual nucleus. These limits increase monotonically with the primary-neutron energy and could be greatly reduced by sufficiently reducing the primary-neutron energy. (Note added 1/17/57: We can resolve the 45-kev level in U^{238} at 550 kev primary-neutron energy.)

H. GOLDSTEIN: What about the temperatures which Graves and Rosen got at 14 Mev?

L. CRANBERG: I am glad you raised that question because it focuses on another problem in developing the systematics of these neutron spectra - namely, the competition with inelastic scattering that arises when one is above the threshold for the $(n,2n)$ process. The threshold of the $(n,2n)$ process in most nuclei is at about

9 Mev. I think only recently have sphere multiplication type measurements been made at 14 Mev which indicate the importance of this $(n,2n)$ process. The indications now are that the yield of neutrons from $(n,2n)$ is comparable to the yield from (n,n') at 14 Mev. To unravel the spectra due to each process is difficult. This job is under way with some theoretical help, and I believe that Graves and Rosen hope to be able to infer something about the spectra due to each of the two processes.

H. FESHBACH: With respect to that last issue, I would imagine that if the $(n,2n)$ reaction was not properly taken into account the Graves and Rosen temperatures should be lower than yours. Is that the case?

L. CRANBERG: They are not lower; they are comparable to ours or higher.

H. FESHBACH: Not relative to the square root of the energy?

L. CRANBERG: Extrapolated on a square root basis, their results are lower, as you suggest they should be. Another thing that is in agreement is that they have observed isotropy for all but a small fraction of the neutrons.

GAMMA RAYS FROM INELASTIC SCATTERING BY Zr^{94} AND Pt^{194}

R. B. Day

Los Alamos Scientific Laboratory

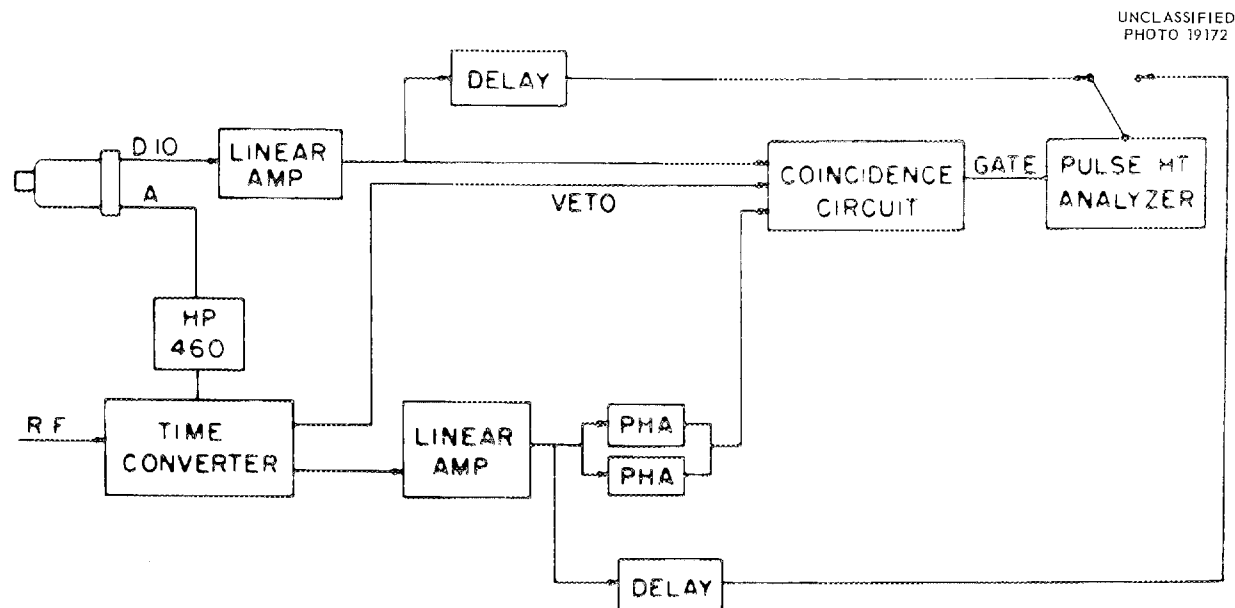
R. B. DAY: The techniques that have been used in the past for studying gamma rays from neutron inelastic scattering have suffered from a serious defect, namely, the background produced by neutrons scattered into the NaI detector. In general there is no really satisfactory way of determining this background, although at neutron energies below 4.5 Mev substitution of a carbon scatterer gives an approximate shape to the background pulse-height distribution. To eliminate the difficulties associated with this background, we have developed a new technique which is based on a suggestion of Cranberg's that time-of-flight be used to distinguish between gamma rays from inelastic scattering and the background produced by neutrons scattered into the detector.

The experimental arrangement utilizes a pulsed source of monoenergetic neutrons produced by deflecting a proton beam across a slit to obtain short pulses of protons and then allowing these to enter a tritium gas target. A scattering sample is placed at 0 deg about 4 cm from the neutron source, and the gamma-ray detector is 15 cm from the scatterer at 90 deg to the beam. A tungsten

shield between the source and detector helps in reducing the background produced by neutrons arriving directly from the target. Since the time of flight of a 1-Mev neutron over a 15-cm path is 10 μsec , the distance between the scatterer and detector is sufficient for one to distinguish between gamma rays and neutrons by means of their velocity.

To study the time resolution of the system, we moved the detector to 0 deg and observed the time distributions obtained for gamma rays from proton inelastic scattering when suitable targets were substituted for the tritium gas. At a gamma-ray energy of 0.5 Mev, the time resolution (full width at half maximum) was somewhat under 2 μsec . However, this became progressively worse at lower energies, and for gold K x rays the resolution was only 6 μsec .

The block diagram of the electronics is shown in Slide 1. The time-to-pulse-height converter is similar to the one described by Weber *et al.* except for a veto circuit that was added to eliminate the difficulties that occur when a stop pulse occurs at the same time as a signal pulse. With the



Slide 1. Block Diagram of Electronic Equipment for Studies of Gamma Rays from Neutron Inelastic Scattering.

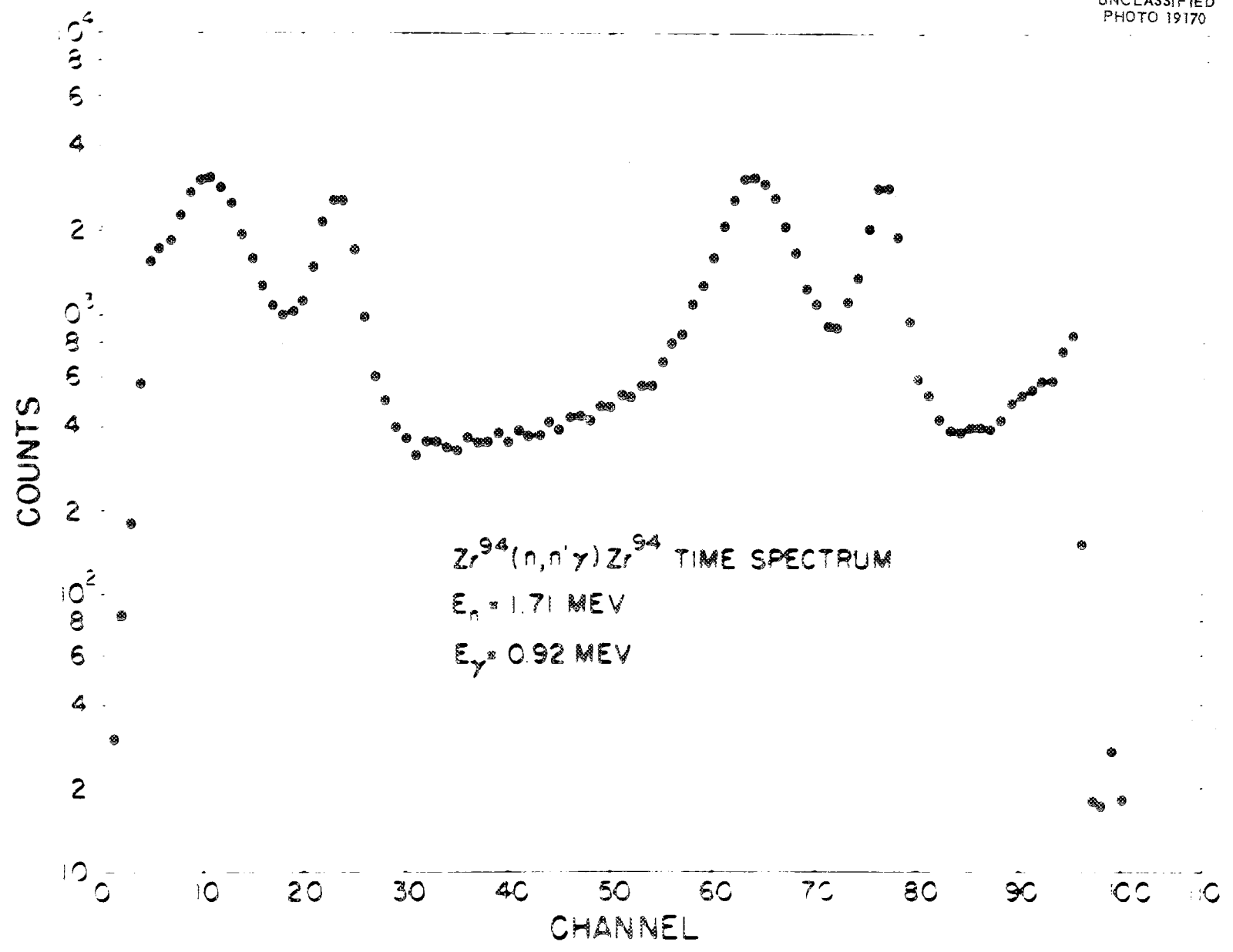
equipment shown here, one can measure either the pulse-height spectrum in coincidence with part of the time spectrum or vice versa.

A typical time spectrum is shown in Slide 2. The sharp peaks at channels 22 and 78 result from the arrival at the detector of 0.92-Mev gamma rays produced by inelastic scattering in a sample of Zr^{94} . The broader peaks at channels 10 and 63 result from the interaction of scattered neutrons with the NaI crystal. If one now adjusts two single-channel analyzers to cover the gamma-ray peaks shown in Slide 2 and gates the pulse-height analyzer with them, one obtains the pulse-height distribution shown in Slide 3. The solid circles here show the spectrum obtained with the Zr^{94} scatterer in place, while the open squares show the distribution with the scatterer removed. From the good agreement of the two curves above 90 v, it is evident that this method is a good way of taking the background into account.

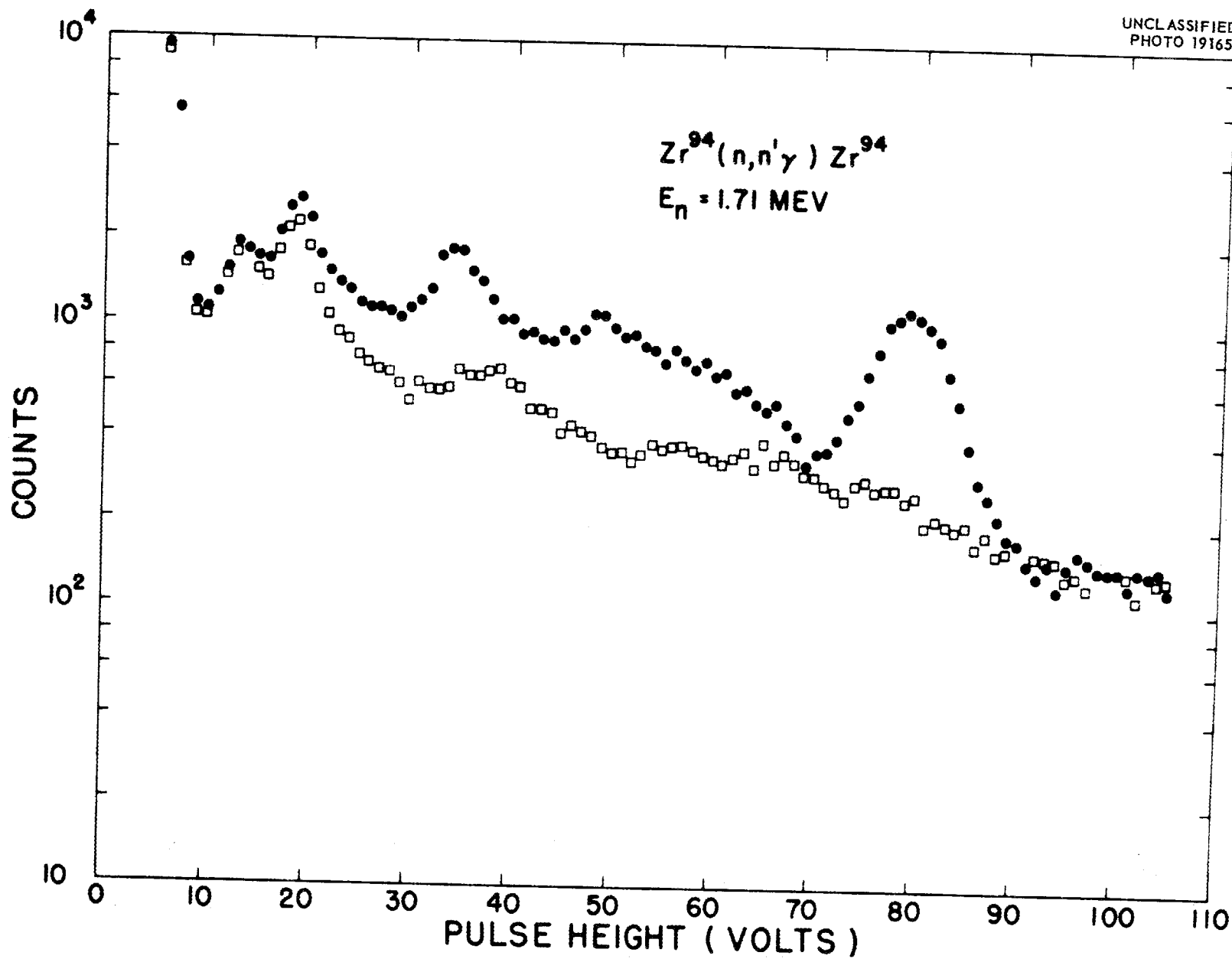
Slide 4 shows the pulse-height spectrum obtained in the same manner for Pt^{194} . The peak at 55 v is the photopeak of a 0.62-Mev gamma ray from the second excited state of Pt^{194} , while the broad peak at 35 v results from two gamma rays - a

0.29-Mev transition from the second to the first excited state and a 0.33-Mev transition from the first excited state.

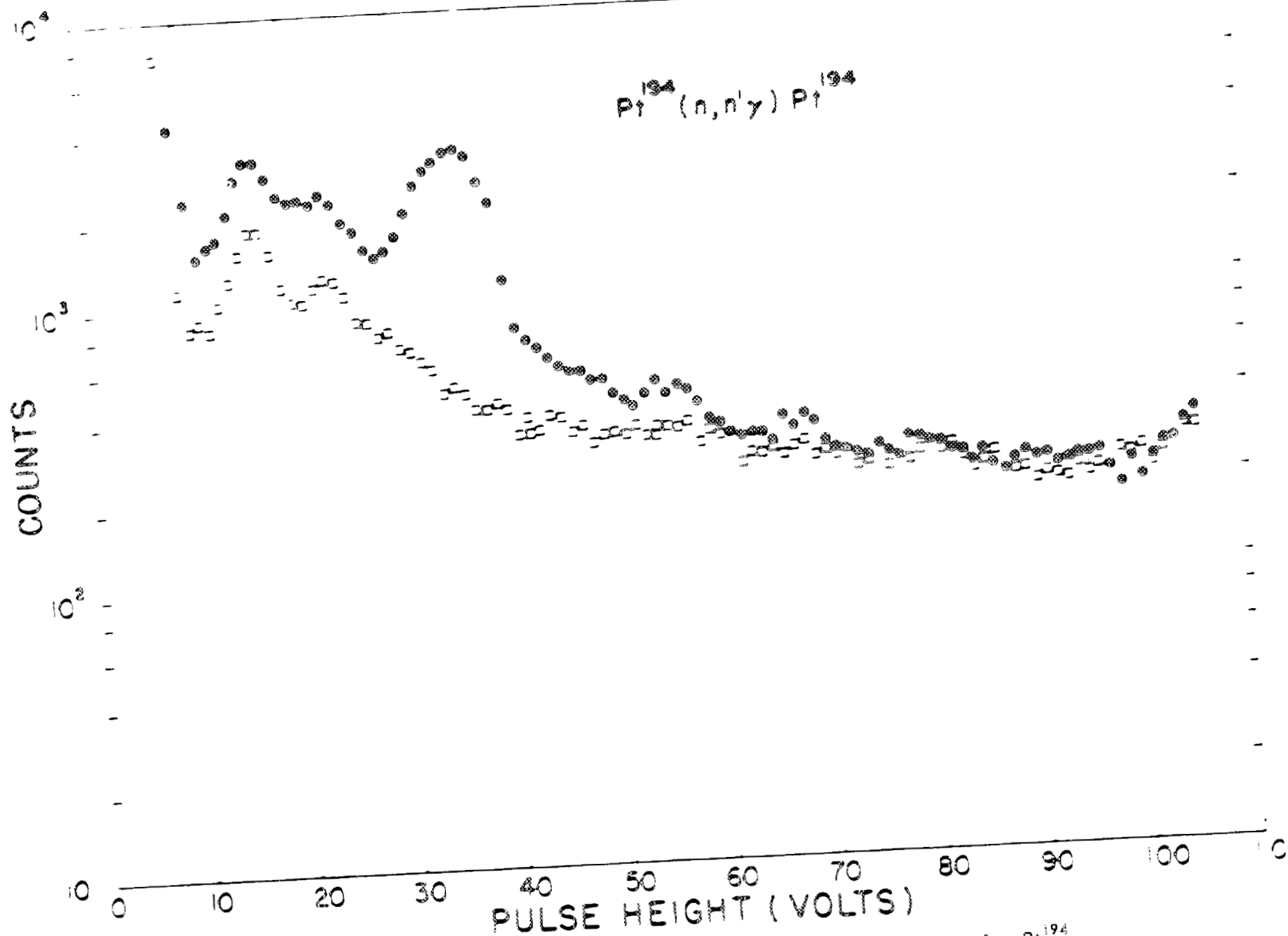
Although it has not been possible to eliminate the neutron-induced background completely, a large improvement in the signal-to-background ratio has been made. This ratio is at least an order of magnitude better than was previously the case, the amount of improvement depending on the neutron energy. Furthermore, the sensitivity of measurements has been increased to the point where one can now obtain satisfactory data with scattering samples of a few grams, whereas it was formerly possible to observe only the strongest gamma rays from such small samples. To date, the technique has been used mainly to investigate the level schemes of separated isotopes, and absolute cross sections for $(n, n'\gamma)$ reactions have not been measured. However, it should also be possible to obtain the cross sections. The easiest way to do this would be to compare the gamma-ray yield with that from a line whose cross section is known and then to make a correction for the variation of detector sensitivity with energy.



Slide 2. Time Spectrum from Bombardment of Zirconium by 1.71-Mev Neutrons.



Slide 3. Pulse-Height Spectrum of Gamma Rays from Inelastic Scattering of 1.71-Mev Neutrons from Zr^{94} .



Slide 4. Pulse-Height Spectrum of Gamma Rays from Inelastic Scattering of 1.71-Mev Neutrons from Pt^{194} .

TIME-OF-FLIGHT NEUTRON SCATTERING WITH THE BROOKHAVEN NATIONAL LABORATORY SMALL CYCLOTRON

C. O. Muehlhause
Brookhaven National Laboratory

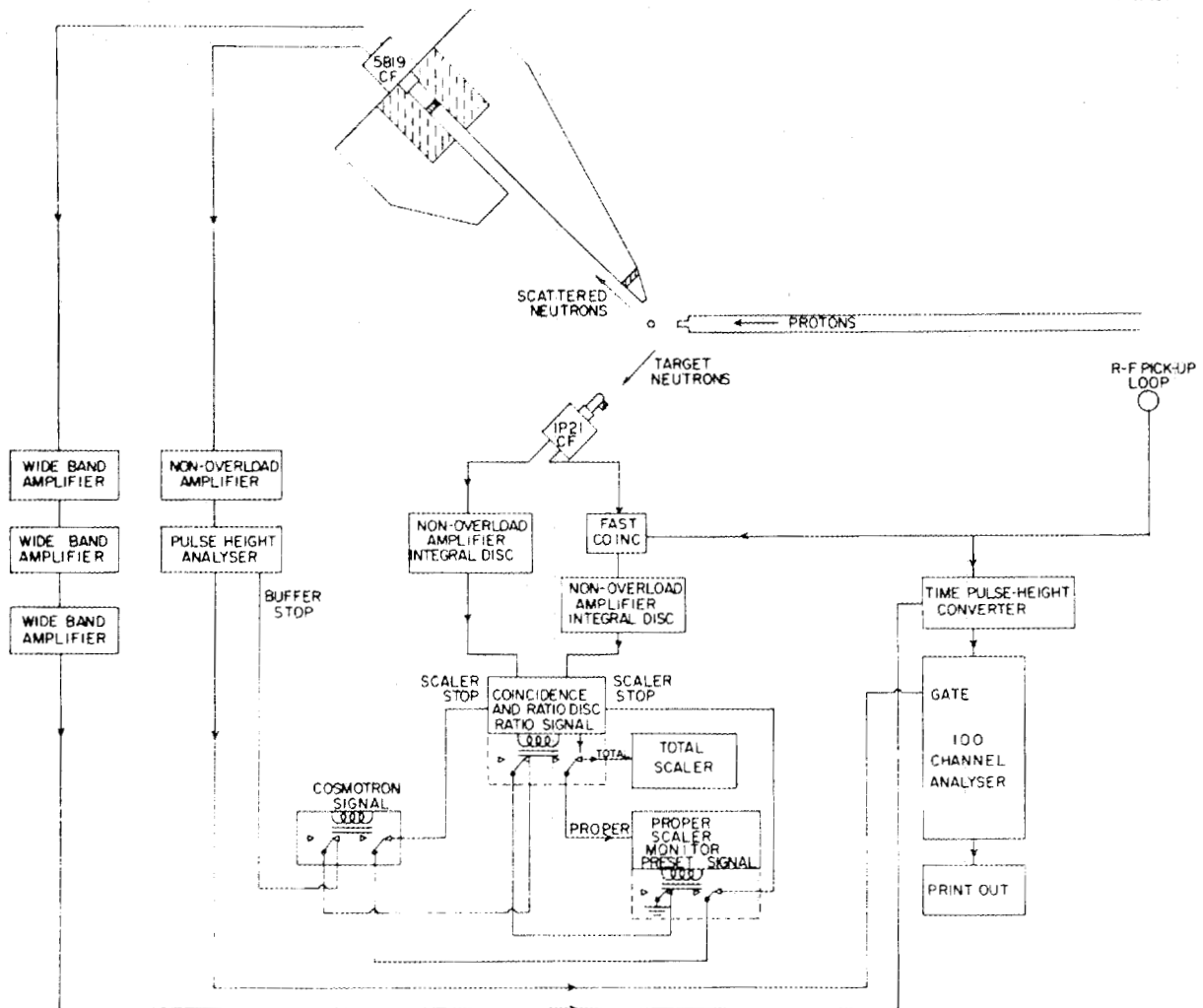
C. O. MUEHLHAUSE: This will be a report on two technical improvements in the inelastic-neutron-scattering work at the BNL small cyclotron.

Our machine produces about 2.8-Mev protons at 50- μ sec intervals in 2- μ sec bunches. This is accomplished by taking advantage of the phase bunching in fixed-frequency cyclotron operation. Neutron bunches of about 2.0 Mev are produced in

the forward direction by using a zirconium-tritium target.

Slide 1 illustrates the first of the technical improvements I wish to discuss. Shown here is a monitoring system which the author believes is most appropriate for a system operating with a pulsed beam. The monitor operates as follows: A plastic scintillator receives about 10^5 events per

UNCLASSIFIED
PHOTO 19183



Slide 1. Block Diagram of Time-of-Flight Equipment and Monitoring System at the BNL 18-Inch Cyclotron.

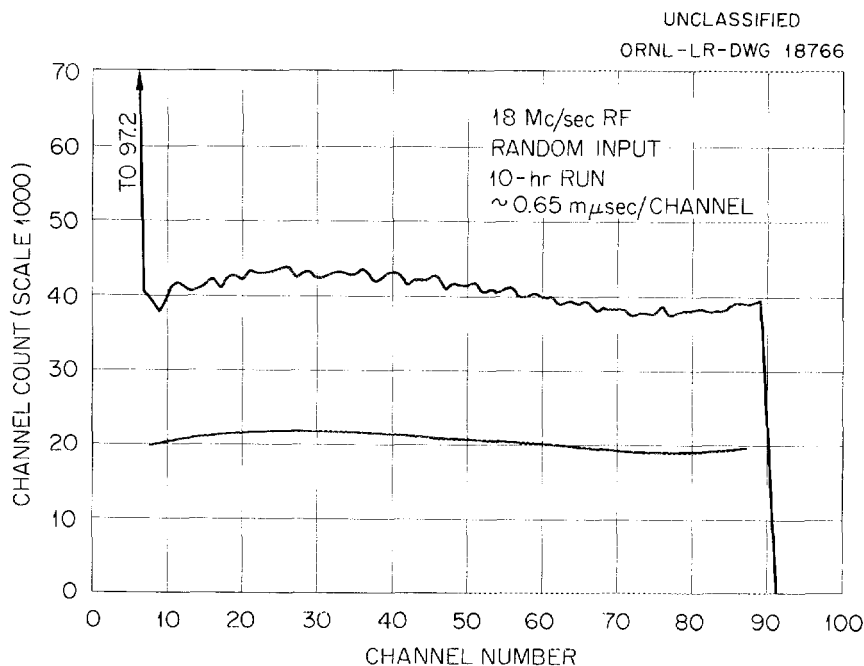
second, which are divided into two electronic legs. One (phase-insensitive) simply amplifies and passes the pulses through an integral discriminator. The other (phase-sensitive) requires a delayed coincidence with respect to the rf. The delay is set for maximum intensity, and the time channel is made about 2 μsec wide. This requirement results in an output from this leg of about 3×10^4 counts/sec. The principal function of the remaining monitor electronics is to measure the ratio of the two counting rates described and to reject data from the detector system if this ratio deviates from its normal value (30%) by 1 or 2%.

The counting-rate ratio referred to is measured by allowing the phase-insensitive rate to generate 100 v in an integrating circuit. At the same time the phase-sensitive rate is generating a voltage in another integrating circuit. When the phase-insensitive integrator reaches 100 v, the phase-sensitive integrator is stopped, and its voltage (normally 30 v) activates a voltmeter. The voltmeter indicates the ratio by reading the 30 v on a 100-v scale. Two contacts are placed close to and on either side of the indicating pointer of the voltmeter. If this potential differs sufficiently from 30 v, a contact to a relay is made which blanks out the data to the 100-channel recorder. Under these conditions the ratio is tested every 0.1 sec.

The ratio referred to will change as a result of either a change in proton energy or a change in proton phase relative to the rf. The monitor thus rejects transients in the generator which occur in 0.1 sec or longer, and the 100-channel recorder accumulates only proper data.

The second technical improvement which I wish to discuss has to do with a new time-to-pulse-height converter circuit. This was developed by R. Chase of BNL and operates as follows: A tank circuit tuned to a frequency which is 1% different from the rf is placed in the plate of a fast-acting tube. A detector pulse cuts the tube off and rings the tank circuit for 5 or 10 μsec . The tank frequency is made to beat against the rf of the machine in a proper mixing circuit to generate a beat note of 200-kc frequency. In this system phase angles are preserved, so that the passage of the beat note through null is an expanded time measure of the original time delay between the rf and the detector pulse. Having thus expanded the millimicrosecond interval to the microsecond scale, it is an easy matter to convert time into pulse height by a variety of means.

Slide 2 shows the performance of this circuit to a random source. The author believes it to be superior to all other such results. Only 2% of the total time (out of 50 μsec) is lost, and the distribution appears very flat.



Slide 2. Response of the Ringing-Circuit Time-to-Pulse-Height Converter to a Random Source.

BACK-ANGLE ELASTIC SCATTERING WITH 14-Mev NEUTRONS

C. Wong J. D. Anderson C. C. Gardner M. P. Nakada
University of California Radiation Laboratory,
Livermore

M. P. NAKADA: S. Fernbach and F. Bjorklund have been making optical-model calculations on the angular distributions of the elastic scattering of neutrons at 7 and 14 Mev. By using the following potential,

$$U_0/[1 + \exp(R - R_0)/a] + iV_0 \exp[-(R - R_0)^2/b^2],$$

where

$$\begin{aligned} U_0 &= 44 \text{ Mev,} \\ R_0 &= 1.27A^{1/3} \text{ fermis,} \\ a &= 0.65 \text{ fermi,} \\ V_0 &= 9.5 \text{ Mev,} \\ b &= 0.98 \text{ fermi,} \end{aligned}$$

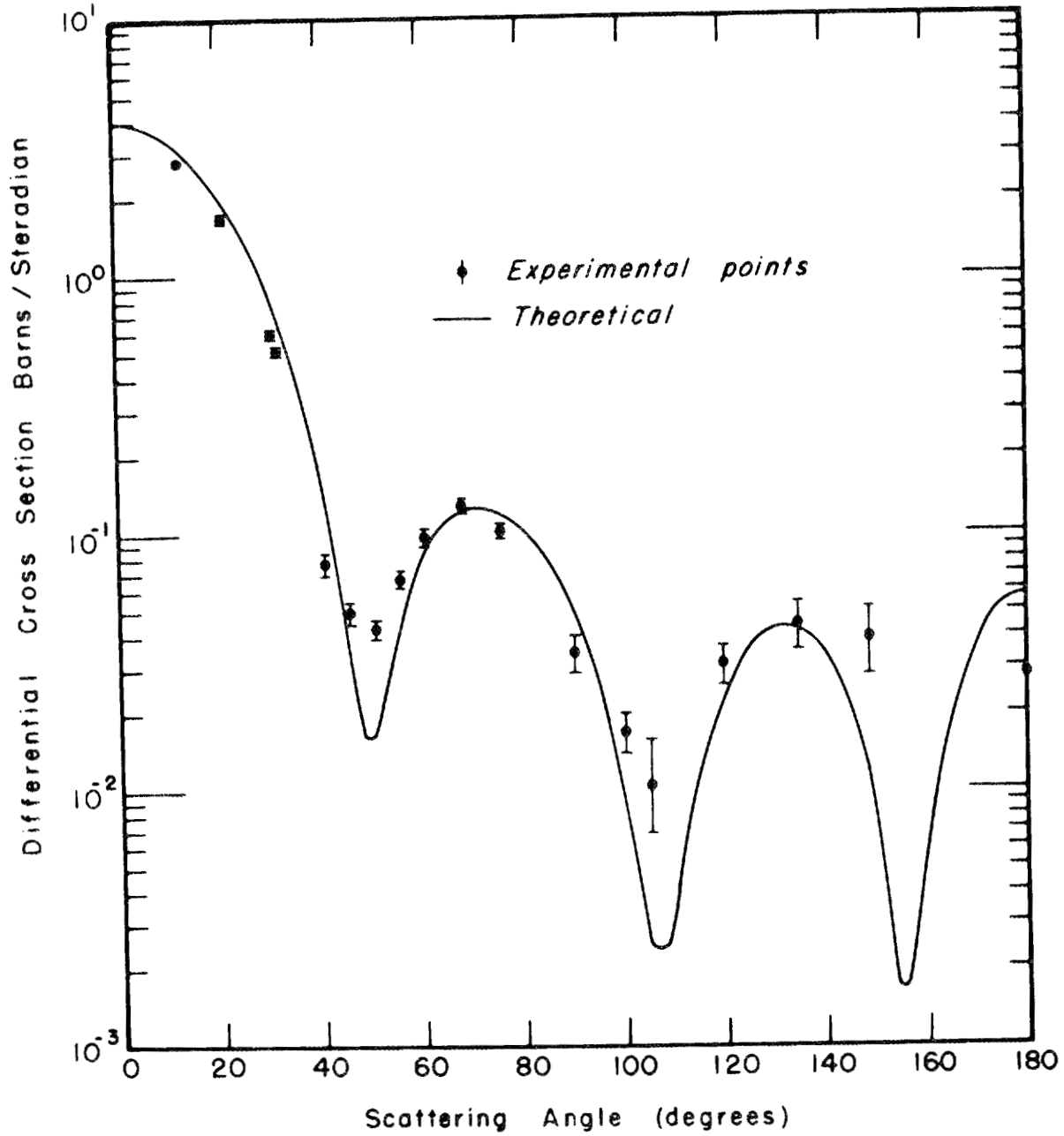
they have had considerable success at fitting existing experimental results at 7 and 14 Mev, as can be seen in Slides 1 and 2 (experimental points at 7 Mev by Walt and Beyster, LASL; those at 15 Mev by W. Cross, Chalk River). The interesting thing about their calculations is that, although they have added an additional parameter to the potential, they were able to fit all the data with no further changes in these parameters. This is in contrast to difficulties that they and others have had in trying to make fits with the Saxon-type potential, where many changes in parameters are necessary. In addition, they calculated total and nonelastic cross sections for neutrons from 6 to 50 Mev with the same potential and parameters, and found good agreement. One observation that they made was that, although different potentials fit forward-angle results at 14 Mev equally well, there were large variations in the predictions for back-angle scattering, where no experimental results existed. Further, the Bjorklund-Fernbach potential predicted rather large dips in the cross section (e.g., the dip near 155 deg for iron).

We undertook this experiment to see if we could clear the picture by getting results at back angles. In particular, we were interested in seeing if the predicted dip at 155 deg in iron really existed.

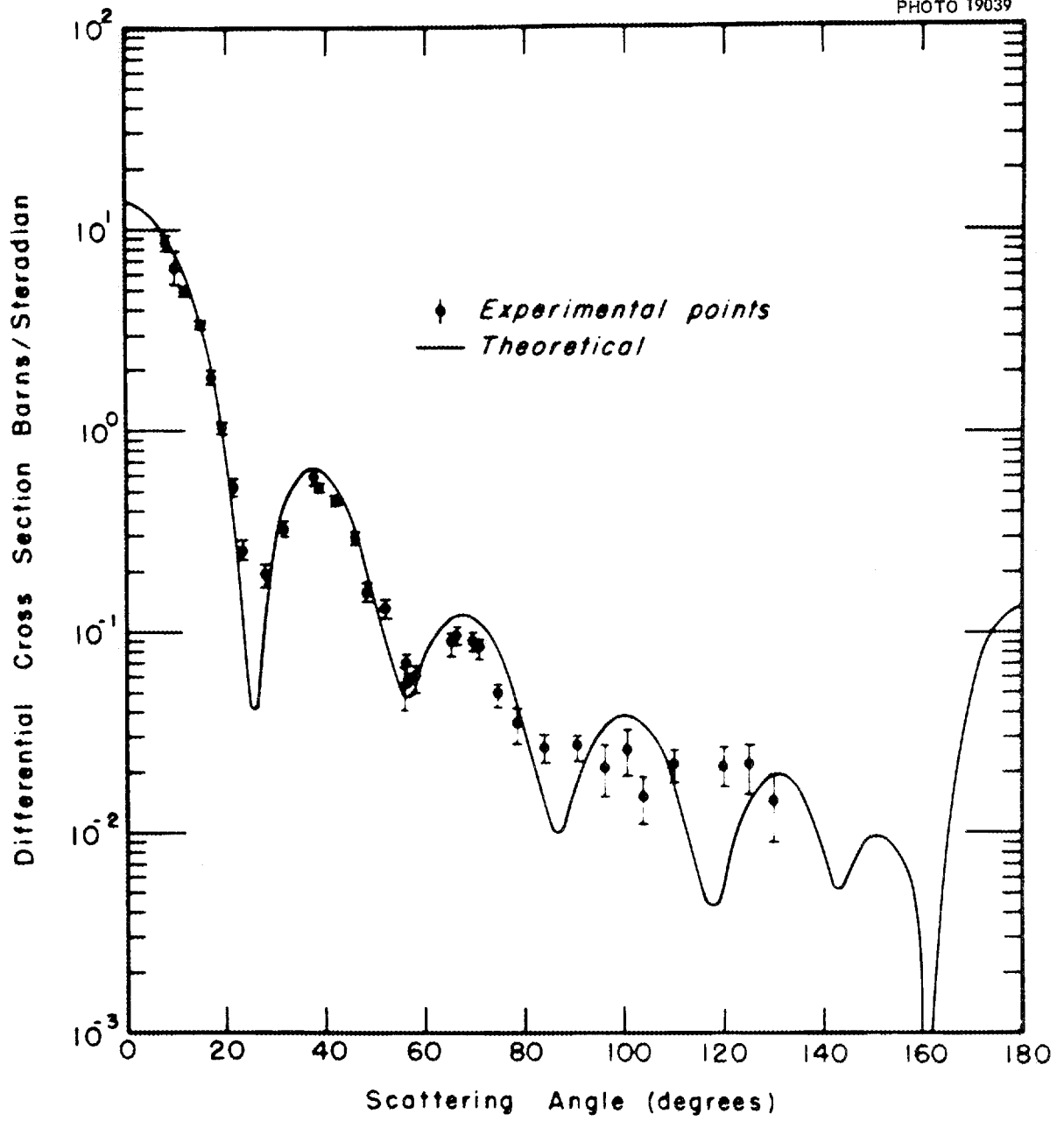
High background and low counting rates are two difficulties encountered in this experiment. The pulsed and bunched beam that has been developed at Livermore and the ring geometry gave us enough counting rate. The high background was eliminated by means of the time separating the signal from the background. Slide 3 shows the geometry used. The 2-m-dia ring was centered on the tritium target at 90 deg to the deuteron-beam direction. A plastic detector was moved along the beam line to change angles. A 30-cm copper attenuator was placed between the target and the detector; by minimizing the length of this we were able to get to 160 deg.

Time-of-flight techniques similar to those described here by Cranberg, but with 11.5- and 12-Mev biases on the slow channel of the detector, were used to select the elastic neutrons. Slide 4 shows typical experimental results. Time after production of neutrons increases to the left; each channel is 1.5 μ sec wide. The early large peak is due to neutrons that traverse the copper or are scattered at small angles in air. The next peak is due to gamma rays produced by neutrons in the iron ring. The third peak is due to the elastically scattered neutrons. The crosses are background. The cross-section results are shown on Slide 5. The points from 130 to 160 deg were obtained by the above method; the angular resolution is ± 2 deg. The points from 30 to 140 deg were obtained as a by-product of time-of-flight inelastic measurements at Livermore by the same group. The points from 0 to 60 deg are due to Elliot at NRL.

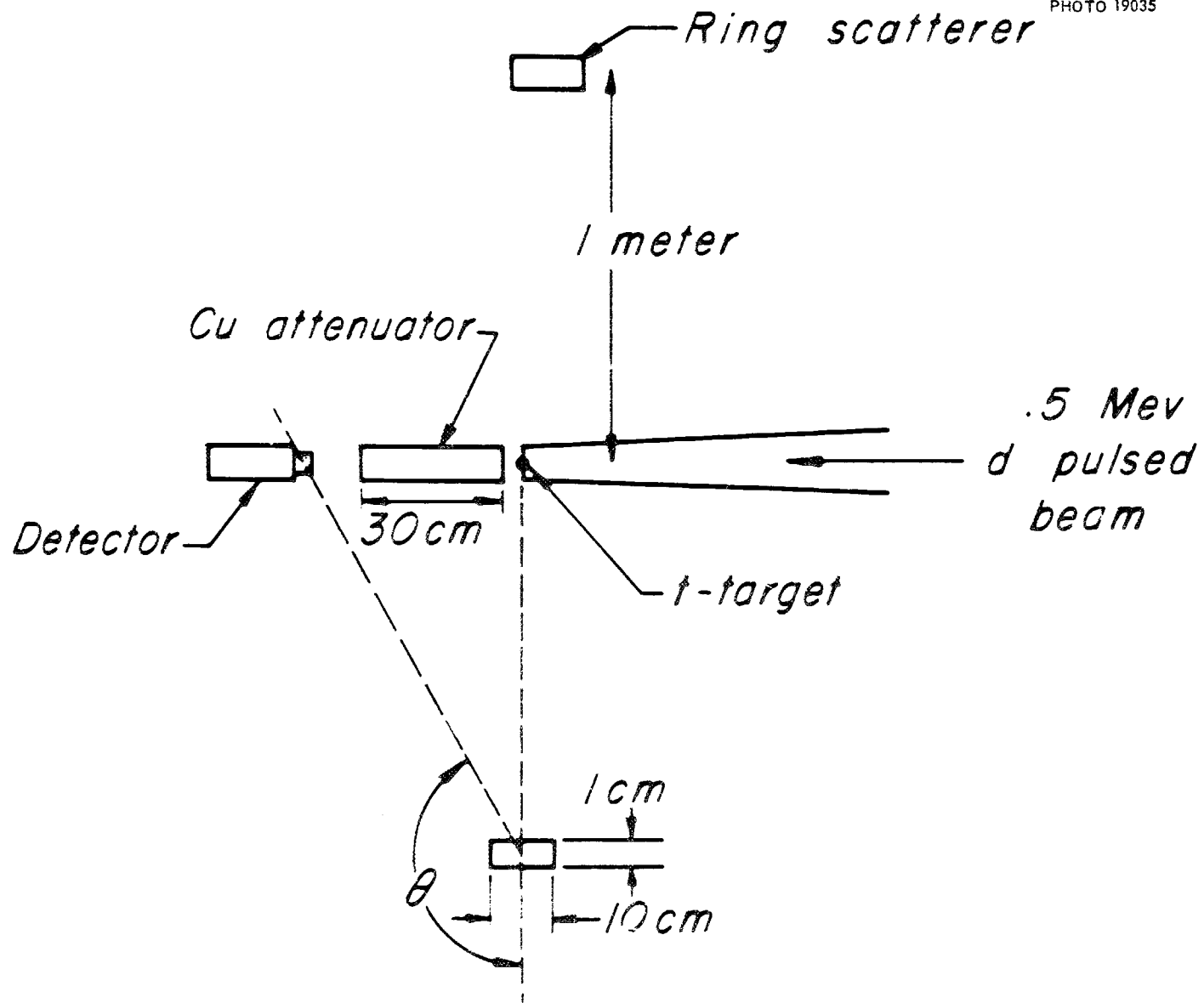
We did not see the predicted dip at 155 deg. However, further calculations by Bjorklund and Fernbach using a Thomas spin-orbit term in addition to their potential have given much better agreement.



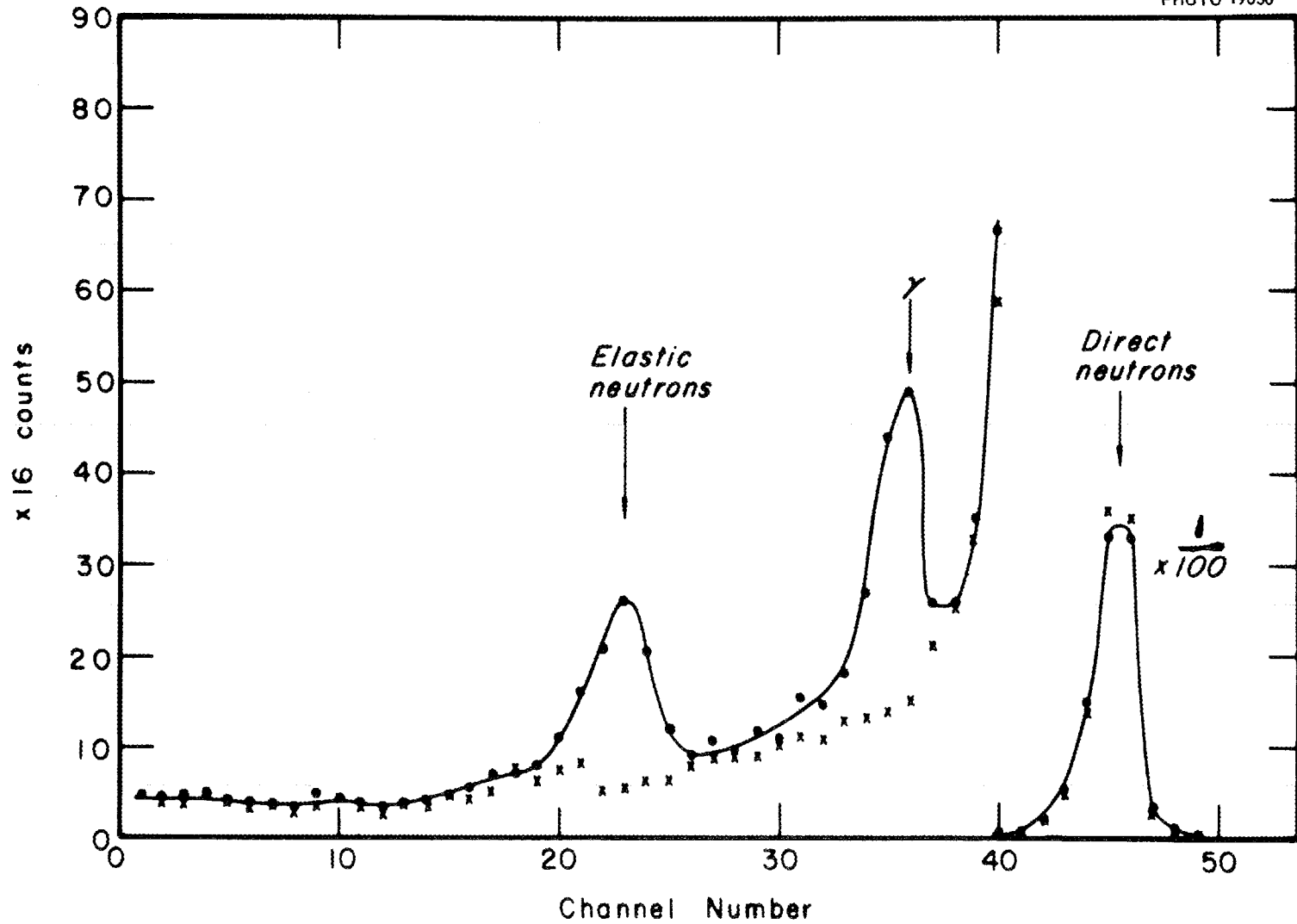
Slide 1. Elastic Scattering of 7-Mev Neutrons by Zirconium.



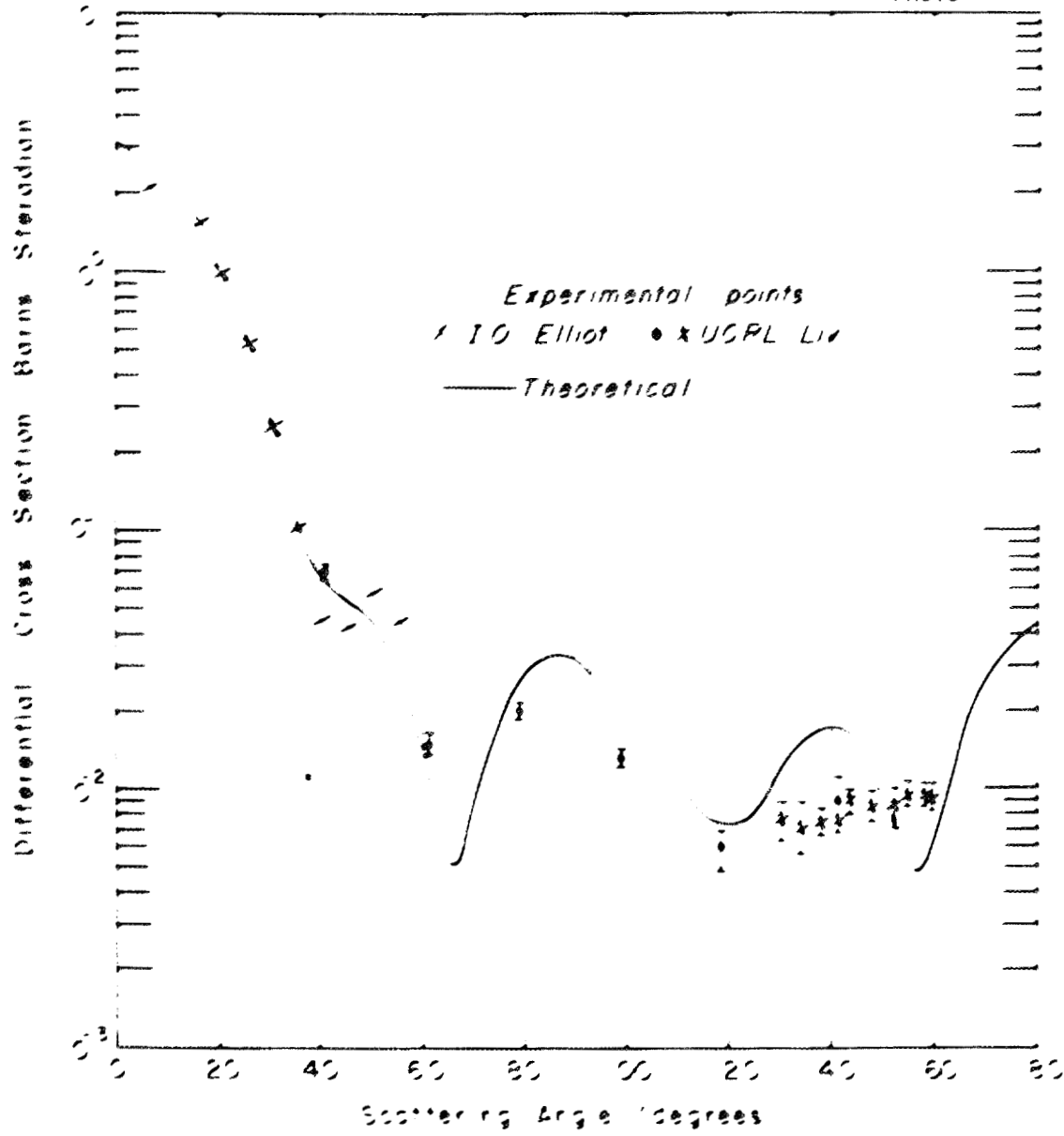
Slide 2. Elastic Scattering of 15-Mev Neutrons by Bismuth.



Slide 3. Time-of-Flight Equipment for Studying Back-Angle Elastic Scattering of 14-MeV Neutrons.



Slide 4. Typical Time Spectrum of 14-Mev Neutrons Scattered by Iron.



Slide 5. Elastic Scattering of 14-Mev Neutrons by Iron.

ELASTIC AND INELASTIC SCATTERING OF FAST NEUTRONS

R. V. Smith
Westinghouse Research Laboratory

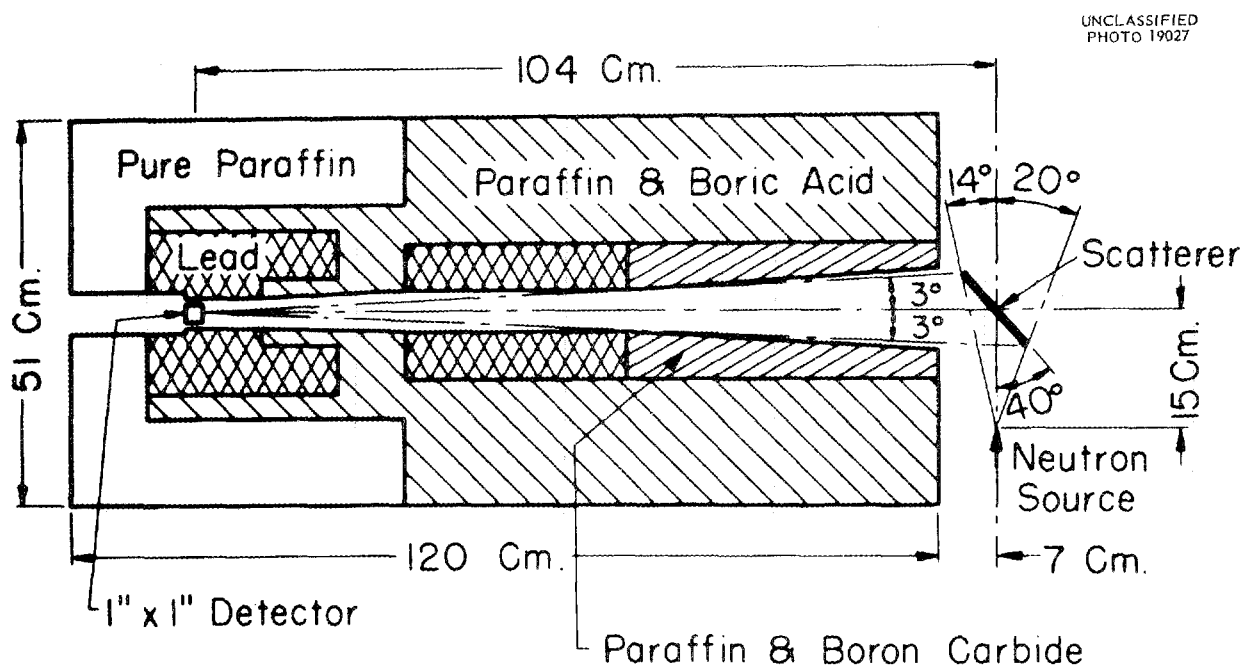
R. V. SMITH: The first part of this report will deal with the apparatus used at Westinghouse for neutron inelastic scattering from a primary energy of 4.3 Mev, while the second part will contain a summary of results obtained and a comparison with similar data obtained elsewhere.

Slide 1 shows the geometry used. The deuteron beam from the Westinghouse electrostatic generator is chopped into 1- to 1.5- μ sec pulses every 80 μ sec, producing bursts of neutrons from a deuterium gas target. At the scatterer position in the forward direction, these primary neutrons have an energy of 4.3 ± 0.1 Mev. To detect scattered neutrons, a plastic scintillation detector is placed inside a rather large and cumbersome collimator at 90 deg and 1 m from the scatterer.

Slide 2, illustrating the timing arrangement, has very few boxes containing great quantities of

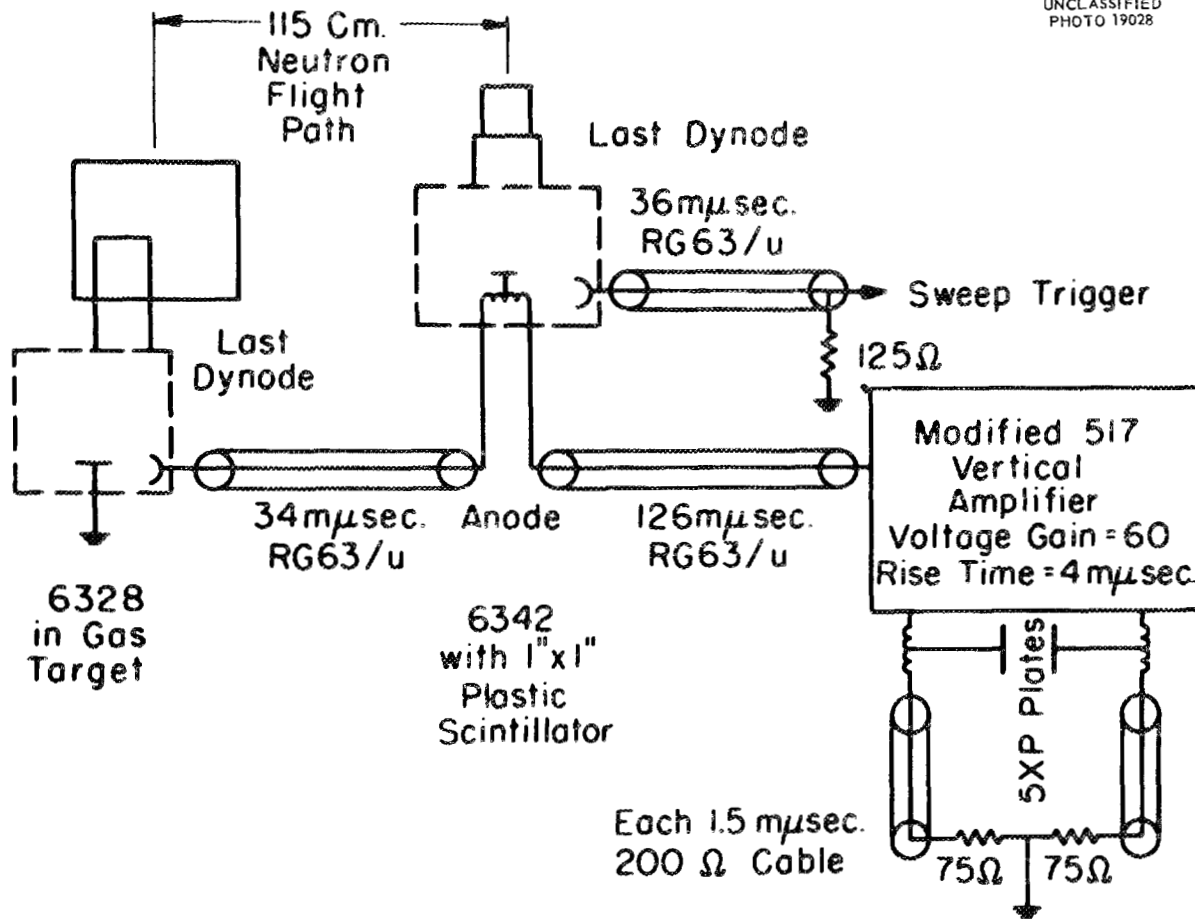
electronics. The start pulse, rather than coming from the r-f deflection voltage, is taken from a 6328 photomultiplier placed inside the deuterium gas target. The resultant positive "starter" pulse is inserted into a single signal cable together with a negative pulse from the neutron detector. The two pulses are amplified by a single distributed amplifier, displayed on a cathode-ray tube, and photographed continuously with a moving-film camera. This recording system can measure the time difference between the two photomultiplier pulses with a resolution width at half maximum of 0.8 μ sec, as checked by various methods over periods of time exceeding one year.

Slide 3 shows a typical result for zirconium. The number of traces observed is plotted against flight time from scatterer to detector. The space between 20 and 30 μ sec corresponds to overlapping of the



**Geometry #4, scattering angle $79^\circ - 107^\circ$,
scatterer 13.5 cm. x 9.0 cm. ellipse.**

Slide 1. Geometry of Scattering Apparatus.



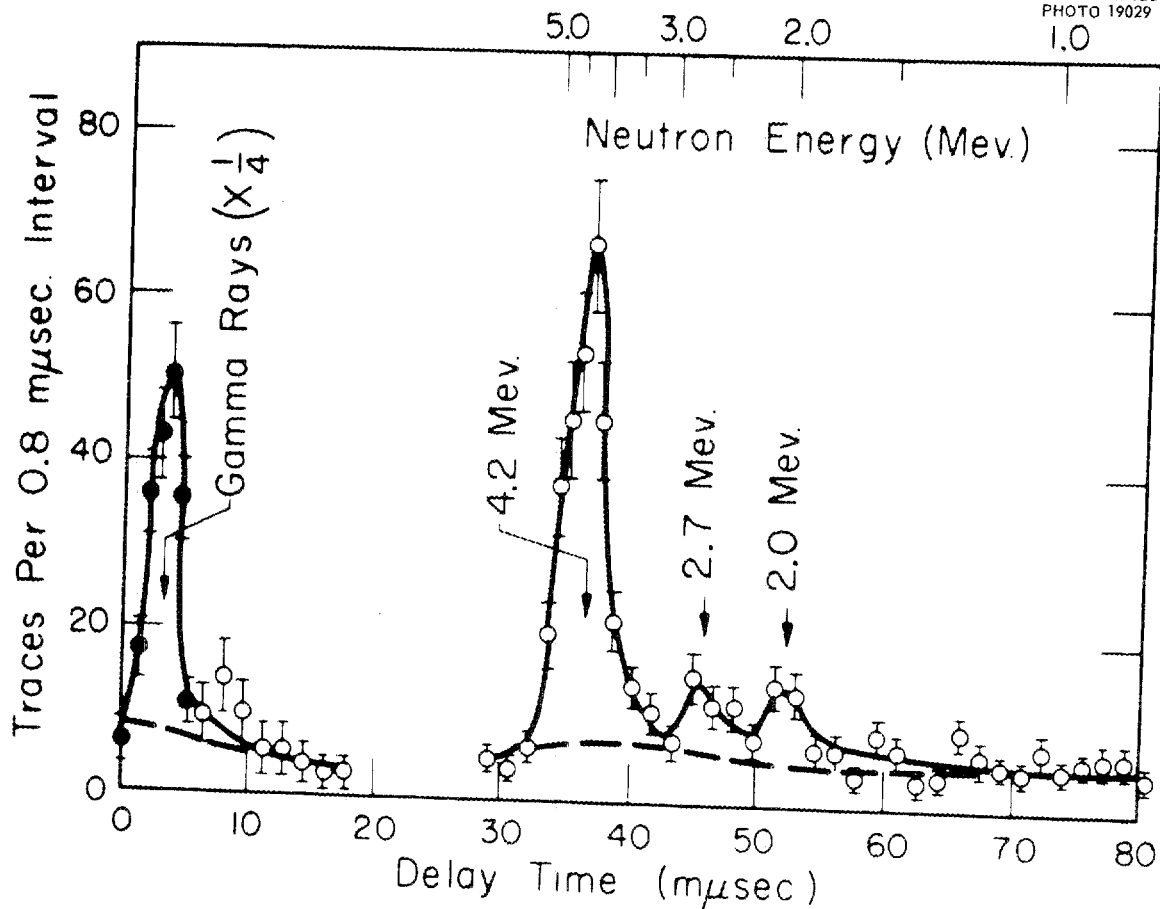
Slide 2. Typical Cabling Diagram.

two pulses and, by choice of cable lengths, has been placed in an uninteresting region. The spectrum shows an elastic and two inelastic neutron groups in addition to the strong peak due to de-excitation gamma rays. The observed resolution in the elastic peak is $3.5 \mu\text{sec}$, and that in the gamma-ray peak somewhat better.

The dashed background curve is almost time independent and can come from air and room scattering, collimator penetration, or from about 99% of the deuteron beam which is accelerated but never used. The latter predominates in these experiments, but air scattering seems to be not far below. The over-all background is large enough so that any significant decrease of signal level in the interest of resolution would make the inelastic groups indistinguishable.

Slide 4 is a similar plot for carbon, which is known to have no levels in this energy region. The lack of both inelastic neutron groups and de-excitation gamma rays is taken as evidence that none of the groups observed for other elements is instrumental.

Table 1 is a compilation of factors comprising the over-all time resolution for scattered-neutron energies of 2 and 4 Mev. The first five factors can be reduced only by a reduction of intensity which is more than linear in many cases. It is possible to rearrange the various factors, but intensity and ratio to background place a lower limit on their combination. The contribution due to the photomultipliers has been reduced to $2 \mu\text{sec}$ by using only a 1-in.-dia scintillator on the 2-in.-dia 6342 photocathode.



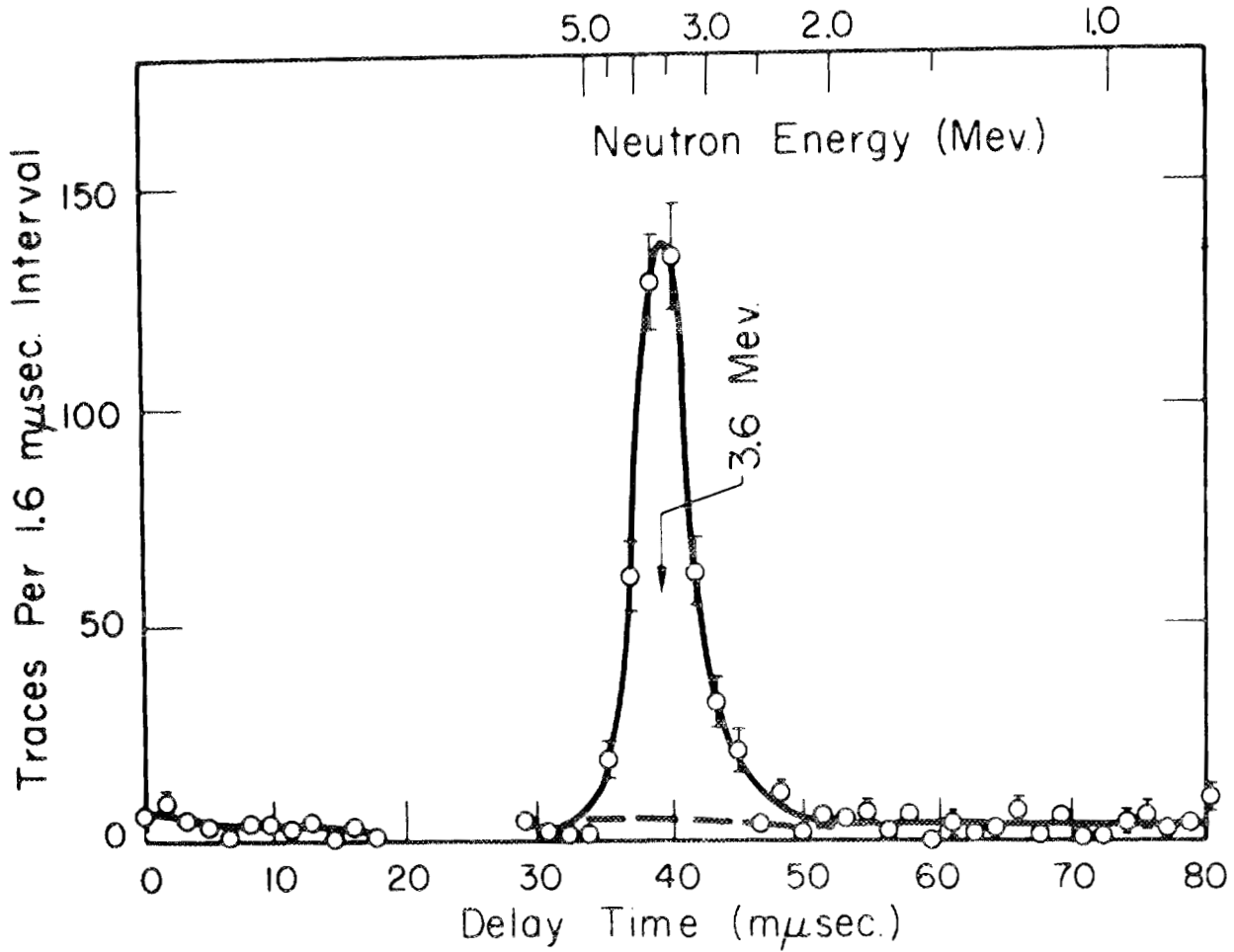
Geometry no. 4; solid curve: zirconium scatterer 1123 traces; dashed curve: no scatterer 1036 traces normalized to same neutron flux.

Slide 3. Spectrum from Zirconium Scatterer.

Table 2 is a compilation of results and a comparison with other work. The second column, labelled "2.5 Mev," is the time-of-flight work of Cranberg at Los Alamos; the third column, entitled "Photoplate," contains data obtained at 4.4 Mev by Weddell at Westinghouse using nuclear emulsions; and the last column is a combination of the gamma-ray results of Day at Los Alamos, Griffith at Westinghouse, and Scherrer, Faust, and Allison at the Naval Research Laboratory.

The over-all conclusion to be reached from these data is that there are many levels to be observed at 4 Mev, and there are many cross sections and many angles. In short, there is much work to be done; this is only an indication of the possibilities at higher energies.

L. CRANBERG: I should like to make this brief remark. In some respects I think Dr. Smith's presentation sounded a little pessimistic. I think that our own work on the heavier elements, since



Geometry no. 4; solid curve: carbon scatterer
624 traces; dashed curve: no scatterer 1036
traces normalized to same neutron flux.

Slide 4. Spectrum from Carbon Scatterer

our interest is in the heavier elements, indicates that there is also much to be done with relatively poor energy resolution.

In connection with the question of improving the method, in particular of compromising the resolution and intensity problems, I should like to mention the advent of a technical development which should be interesting to people in this field who have just had a chance to explore it a little, and that is the C 7170 RCA photomultiplier. This photomultiplier, which apparently is available only in handmade units for experimental purposes, has a 5-in. photocathode and a very special electron-optical focusing system which assures uniformity of collection of photoelectrons from the photocathode within 2 μsec , and our preliminary tests on this tube confirm the manufacturer's claims for it.

Table 1. Contributions to Time Resolution

Source	Time Spread ($m\mu\text{sec}$)	
	Scattered-Neutron Energy	
	4 Mev	2 Mev
Beam Pulse	1.0	1.0
Source Energy Spread	0.9	3.2
Path in Source	1.2	1.2
Path in Scatterer	0.5	1.0
Path in Detector	0.9	1.3
Photomultiplier Spread	2.0	2.0
Recording	0.8	0.8
Total	3.0	5.5

Table 2. Level Energies (Mev)

Element	Present	2.5 Mev	Photoplate	Gamma Rays
Al	—	—	0.9	0.85
	1.0	1.03	—	1.02
	2.3		2.1	2.24
	3.0		2.8	3.10
Cr	1.4	1.49	1.4	1.43
	2.5		2.3	
	2.9		2.9	
Fe	0.9	0.86	0.8	0.85
	2.2		2.0	2.07
	2.7		2.6	2.58
	3.0		3.0	2.90
Co	1.2	1.20	1.2	1.15
	—	1.51	—	1.49
	1.8	1.75	—	1.7
	—		—	2.5
Ni	1.4	1.4	1.4	1.33-1.49
	2.2		2.2	2.16
	2.7		2.6	2.66
	3.2		—	—
Zr	—	0.94	—	0.92
	1.5	—	—	1.5
	2.2		2.2	2.20
	2.8 (?)		2.8 (?)	—
Pb	—	0.84	—	0.80
	—	1.44	—	1.34
	1.7	1.74	—	1.73
Bi	—		2.6	2.66
	0.9 (?)	0.93	0.9	0.92
	1.8	1.65	—	1.62
	—	—	2.60	

COMMENTS ON NEUTRON SCATTERING

H. Feshbach

Massachusetts Institute of Technology

H. FESHBACH: I would like to discuss tonight what sorts of things about the interaction of neutrons with nuclei we may expect to learn from the experiments and analyses reported today and what the future trends might be. I shall restrict the discussion to the average total cross section and the average inelastic cross section, where by "average" we mean that many levels in the compound nucleus contribute to the process. The cross sections no longer show a fine structure, only what we have termed a gross structure.

From the average total cross section and the associated angular distributions, certain parameters describing the neutron-nucleus potential have been elicited. The parameters describing the interaction include V_0 , the depth of the real part of the potential; ζV_0 , the depth of the imaginary part; the nuclear radius, R ; and the diffuseness of the edge, a . Finally, in many calculations, the relative radial distribution of the imaginary and real parts of the potential has been modified. For example, several groups have put the absorption at the nuclear surface when higher-energy neutron data (e.g., ~ 14 Mev) are being examined.

Now, one has to be rather careful not to exaggerate the significance of these results. Just to indicate what I mean, let me mention a few of the possible phenomena which have been omitted in all these analyses. First, all the above parameters are expected to vary with the velocity of the neutrons. Secondly, a particular type of velocity-dependent potential, the spin-orbit force, is known to be present from polarization experiments. Third, there is a possibility of forces which depend on the spin of the nucleus and the spin of the neutron, that is, spin-spin forces. Fourth, many of the nuclei are not spheres but spheroids, and we know from the calculations of Margolis and Troubetzkoy that at low energies this gives rise to important effects, and we may expect that this will not be restricted to the low-energy domain only. Finally, we may expect fluctuations from element to element.

We see that we have many effects here. At the very best, only the average of the usual parameters, V_0 , ζV_0 , etc., over many elements is meaningful. Deviations in a particular element from a best fit

with these parameters might be a measure of the omitted effects. Ideally, of course, it would be best if a theory of nuclear structure would provide the form, if not the parameters, of the potential. This is, however, not as yet available.

The "average" theory, as given by these parameters, does not suffice to predict either the inelastic neutron cross section or the related compound elastic cross section. To this, one must add still another set of assumptions, which go under the name of "statistical" model. You are all familiar with the model so that I will refrain from describing it. It suffices to say that, once the approximation is made, completely definite results are obtainable for inelastic cross sections for both the total inelastic cross section and the angular distribution. For example, it asserts that the angular distribution is symmetric about 90 deg and that at sufficiently high incident-neutron energy the low-energy emergent neutrons are isotropic. The experiments of Cranberg and Levin bear directly on this result and show that it holds very well indeed. Another prediction, which is still to be verified, is that these emergent neutrons will be unpolarized.

However, at the higher energies, where it first was discovered, it was found that another sort of thing was happening, in which the incident neutron, instead of interacting with the target nucleus as a whole, interacted essentially with a nucleon in a nucleus. By this I mean that the neutron comes in, and as it goes through, it sees the nucleus as a whole, but every once in a while it gets very close to another nucleon, and then there is a direct interaction between the two. In this we have several things. The so-called surface interaction is probably the most important thing, particularly at higher energies. Then there is the possibility that it might happen inside the nucleus, which is more possible at the lower energies where the nucleus is less opaque. Finally, there, of course, are other collective things, like the rotational excitation. All of these are grouped together in the direct interaction.

I feel that one of the more important tasks of the immediate future is the discovery of a unified description of the direct interaction and the

compound-nuclear process. This might look somewhat as follows. The wave function for the system, neutron plus nucleus, is of the form:

$$\Psi = \sum C_p \psi_p ,$$

where ψ_p is a wave function describing a particular possible reaction, that is, asymptotically ψ_p breaks up into the wave function for the residual nucleus and for the emergent nucleon (or possibly nucleons). We obtain the "statistical" hypothesis if we assert that the phases of the coefficients C_p are random. On the other hand, we obtain direct interaction processes if the phases are perfectly correlated. The actual truth might very well lie somewhere in between, or might possibly vary continuously from random correlation of the phases to perfect correlation as we change the energy, the level or group of levels being examined, etc. The apparatus required to describe this picture and its application to experimental results still needs working out, but it seems to me that, as time goes on, we shall find ourselves looking for the law describing the correlation in the phases.

In this context, it should be remarked that the statistical assumption, like Christianity, has never been really tried, so that the first task is to see what the statistical assumption tells us. Here we need to compute not only averages but fluctuations away from the averages. It is conceivable that some of the effects that have been interpreted as coming from direct interaction might just be fluctuations, which one can now predict from the Porter-Thomas

results. For example, fluctuations will give rise to deviation from symmetry about 90 deg in the angular distribution; they will give rise to fluctuations in the total inelastic cross section, particularly in the neighborhood of the threshold; polarization may fluctuate away from zero; etc.

In this connection, it is interesting to note that in the past even the averages have been calculated incorrectly. For example, the average value over a distribution in level widths of

$$\frac{\Gamma_i \Gamma_j}{\Sigma \Gamma_\alpha}$$

is not

$$\frac{\langle \Gamma_i \rangle \langle \Gamma_j \rangle}{\langle \Sigma \Gamma_\alpha \rangle} .$$

The correction factor to the last can indeed be considerable, going to 1 only when the number of outgoing channels is very large. For example, if there are N outgoing channels, each with the same average width, then from the Porter-Thomas distribution:

$$\left\langle \frac{\Gamma_i \Gamma_j}{\Sigma \Gamma_\alpha} \right\rangle = \frac{\langle \Gamma_i \rangle \langle \Gamma_j \rangle}{\langle \Sigma \Gamma_\alpha \rangle} \frac{1}{1 + \frac{2}{N}} .$$

SESSION III

**EXPERIMENTAL AND THEORETICAL LOW- AND INTERMEDIATE-ENERGY
NEUTRON PHYSICS**

WIDTHS AND SPACINGS OF NUCLEAR RESONANCE LEVELS

A. M. Lane

Atomic Energy Research Establishment, Harwell

1. INTRODUCTION

This paper is concerned with the characteristic distributions of level spacings, D , neutron widths, Γ_n , radiation widths, Γ_γ , and fission widths, Γ_F , of nuclear resonance levels. The next three sections will deal with the mean values of these quantities, that is, the first moments of their distributions:

$$\bar{x} = \int_0^\infty x p(x) dx .$$

The "frequency function" of a given quantity x will be written $p(x)$, so that $p(x) dx$ is the probability of finding a value in the range $(x, x + dx)$. The corresponding "distribution function,"

$$\int_0^x p(x') dx' ,$$

will be written $P(x)$.

The last three sections will be concerned with other features of the distributions, especially the second moment:

$$\overline{(x^2)} = \int_0^\infty x^2 p(x) dx ,$$

which is related to the variance by the definition of variance:

$$\text{Var } x = \overline{(x - \bar{x})^2} = \overline{(x^2)} - (\bar{x})^2 .$$

Although there is perhaps little of profound theoretical interest in the study of distribution laws of widths and spacings, it is exceedingly important to know what these distributions are. For instance, on the practical level, the temperature coefficient of reactivity of fast reactors due to Doppler broadening is determined by the distributions.¹ On the more academic level, in cosmology, the dependence of fast capture cross sections on the distribution of Γ_n affects the production rate of Cf²⁵⁴ (which is a vital isotope in the new theory² of certain galactic phenomena).

¹G. Goertzel, *Proc. Intern. Conf. Peaceful Uses Atomic Energy, Geneva, 1955* 5, 472 (Pub. 1956); A. M. Lane, J. E. Lynn, and J. S. Story, *An Estimation of the Doppler Effect in Fast Neutron Reactors*, AERE-T/M-137 (July 1956).

²G. R. Burbidge *et al.*, *Phys. Rev.* 103, 1145 (1956).

2. THEORETICAL VIEWS ON MEAN VALUES

2.1. Level Spacings

Newton³ has recently revised the earlier work of Bethe,⁴ of Bloch,⁵ and of Lang and Le Couteur⁶ on the problem of predicting mean level spacings as a function of nuclear excitation energy, E^* , and mass number, A . The object of this revision was to try to take account of shell effects in order to explain the well-known anomalies in level spacings near closed shells (e.g., in Pb²⁰⁷ at $E \sim 7$ Mev, the value of D is $\sim 10^3$ or so above normal). Newton agrees with the form of the expressions given by the previous authors, that is, something essentially of the type:

$$\bar{D} = D_0 e^{(aE^*)^{1/2}} ,$$

where D_0 and a do not depend on E^* but do depend on A .

Bethe and Hurwitz⁷ suggested some years ago that the excitation energy E^* in this formula ought to be measured not from the ground state but rather from some other "base line" such as is provided by the semiempirical mass formula. They expressed the hope that this simple adjustment would take account of shell effects (and perhaps other effects as well). The basis of this idea is the observation that the shell structure of the nucleus causes the position of the nuclear ground state to fluctuate anomalously with A , so that this state is unsuitable as a base line for measuring statistical properties of the whole nucleus. If the ground-state binding were the *only* thing affected by shell structure, the Bethe-Hurwitz suggestion would be very reasonable. However, Newton has found that, in applications, the simple adjustment of E^* does not give agreement with experiment (although the effects are in the right direction). Furthermore he contends that

³T. D. Newton, *Can. J. Phys.* 34, 804 (1956).

⁴H. A. Bethe, *Revs. Mod. Phys.* 9, 69 (1937).

⁵C. Bloch, *Phys. Rev.* 93, 1094 (1954).

⁶J. M. B. Lang and K. J. Le Couteur, *Proc. Phys. Soc. (London)* 67A, 586 (1954).

⁷H. Hurwitz, Jr., and H. A. Bethe, *Phys. Rev.* 81, 898 (1951).

this is because not only E^* but also the constant a is affected by shell structure. In particular, near major closed shells the value of a will be smaller than normal. This results from the fact that a is a measure of the density of single nucleon states above the highest occupied state. For very large systems (which have been assumed in previous evaluations of a) this density varies smoothly and monotonically with A . For finite systems, however, the density has minima at major shell closures.

As far as the J dependence of \overline{D} is concerned (J being the spin), Newton predicts, like the previous authors, that:

$$\overline{D(J)} \sim (2J + 1)^{-1} \exp \left[\frac{(J + \frac{1}{2})^2}{2\sigma^2} \right].$$

The value of the "cutoff," $J_{\text{crit.}} \sim (2\sigma^2)^{1/2}$, has been estimated by various authors. According to Lang and Le Couteur, it is about 6 or 7 for $A \sim 240$.

2.2. Neutron Widths

Predictions about the mean values of neutron widths, $\overline{\Gamma}_n$, are obtained by combining the above predictions of \overline{D} with predictions about the so-called "strength function," $\overline{\Gamma}_n/\overline{D}$. These latter predictions come from various theories of nuclear reactions, such as the "strong absorption" theory⁸ and the "cloudy-crystal-ball" theory.⁹

The extent to which $\overline{\Gamma}_n/\overline{D}$ depends on J is not specified by the present theories without further assumptions. However, one can confidently say that such a dependence is expected to be mild and to be conditioned by the nuclear spin-orbit force. (For example, consider target spin $l = 0$ and orbital angular momentum l . The compound states have spins $J = l \pm \frac{1}{2}$. The single-particle states of angular momentum l will be split by a spin-orbit force into two states with $J = l \pm \frac{1}{2}$, so that, at a given energy, states of the two spins have somewhat different values of $\overline{\Gamma}_n/\overline{D}$.)

2.3. Fission Widths

The theory of fission width is, in the first instance, a simple classical one due to Bohr and

Wheeler¹⁰ and makes the prediction:

$$\frac{\overline{\Gamma}_F}{\overline{D}} = \frac{N}{2\pi},$$

where N is the number of "open" fission channels. This relation is a consequence of the fact that the configuration of nucleons finds itself in all allowed configurations once every period $\tau \sim 2\pi\hbar/\overline{D}$. Included in these configurations are the N fission-saddle-point configurations, so: $\tau_F \sim 2\pi\hbar/N\overline{D}$. Using the relation $\tau_F = \hbar/\overline{\Gamma}_F$, the above expression for $\overline{\Gamma}_F/\overline{D}$ follows.

Before applying the formula for $\overline{\Gamma}_F/\overline{D}$, one must note that, because of quantum-mechanical barrier penetration, N is not really an integer equal to the number of "open" channels. Rather it is $\sum_c P_c$, where the sum is over all channels, c , and P_c is the penetration factor for channel c . (N.B. For an energy just at the top of the fission potential barrier, $P_c \sim \frac{1}{2}$. The factor P_c only approaches unity at energies several Mev higher.)

$\overline{\Gamma}_F/\overline{D}$ is predicted to depend on J , because the effective number of open fission channels $N (= \sum_c P_c)$ depends on J , especially for energies near the fission threshold.¹¹ This threshold will, in general, be associated with just one channel and J value, and so, for a certain energy interval above the threshold, states of one J value have appreciable fission widths while other states have not.

2.4. Radiation Widths

There has been no serious attempt to make absolute predictions of the value of $\overline{\Gamma}_\gamma$ as a function of E^* and A . However, Brink¹² has tried to predict the value of $\overline{\Gamma}_\gamma$ for any given nucleus by relating it to the photonuclear absorption cross section, σ_γ , for that nucleus. As is well known, this cross section, when plotted against gamma-ray energy (which equals E^*), has the form of a resonance peak of width ~ 4 Mev centered at values of E varying from ~ 20 Mev in light nuclei to ~ 12 Mev in heavy ones. If E1 excitation is assumed to

⁸H. Feshbach, D. C. Peaslee, and V. F. Weisskopf, *Phys. Rev.* **71**, 145 (1947).

⁹H. Feshbach, C. E. Porter, and V. F. Weisskopf, *Phys. Rev.* **96**, 448 (1954).

¹⁰N. Bohr and J. A. Wheeler, *Phys. Rev.* **56**, 426 (1939).

¹¹A. Bohr, *Proc. Intern. Conf. Peaceful Uses Atomic Energy, Geneva, 1955* **2**, 151 (Pub. 1956).

¹²D. M. Brink (Thesis, Oxford University, 1955).

be the predominant mechanism for gamma-ray absorption, the cross section $\sigma_\gamma(E^*)$ is proportional to

$$\frac{\overline{\Gamma_{\gamma p}(0; E^*)}}{\overline{D(E^*)}}$$

where $\overline{\Gamma_{\gamma p}(0; E^*)}$ is the mean partial radiation width for $E1$ transitions between the ground state and the various excited states near energy E^* .

To predict the total radiation width $\Gamma_\gamma(E^*)$ of resonance levels at E^* , one must add all the partial widths $\Gamma_{\gamma p}(E^*; E')$ to all the lower states E' . The particular width to the ground state can be found from $\sigma_\gamma(E^*)$ as just described, but the other widths can only be found after making some assumptions. Brink assumes that the plot of mean-square $E1$ matrix elements taken between any excited state at E' and all other states is just the same as for the ground state ($E' = 0$) except that it is displaced upwards by amount E' . With this assumption, the total radiation width can be evaluated from:

$$\begin{aligned} \Gamma_\gamma(E^*) &= \sum_p \Gamma_{\gamma p}(E^*; E') \\ &= \int_0^{E^*} \left[\frac{\Gamma_{\gamma p}(E^*; E')}{\overline{D(E^*)}} \right] \left[\frac{\overline{D(E^*)}}{\overline{D(E')}} \right] dE' \end{aligned}$$

provided that some level spacing $\overline{D(E')}$ is specified.

In practice there are two main sources of uncertainty in carrying out this evaluation. The first is the specification of $\overline{D(E')}$. The second arises from the fact that $\sigma_\gamma(E^*)$ is not known in the region from $E^* = 0$ to $E^* \sim B$, the neutron binding energy. Thus one must take the curve of $\sigma_\gamma(E^*)$ observed for higher energies and extrapolate it to the lower range. (Brink does this with the aid of the classical formula for $E1$ absorption by a liquid drop.)

Brink has also produced a theory of the J dependence of $\overline{\Gamma_\gamma}$. This theory is based on some assumptions. Unfortunately, it seems difficult to justify these assumptions. The vital hypothesis of this theory for our purposes is that:

$$\frac{\overline{\Gamma_{\gamma p}(E^*J; E'J')}}{\overline{D(E^*J)}}$$

is independent of J and J' . This hypothesis immediately enables one to deduce the J dependence of

$\overline{\Gamma_\gamma}$ provided that the J dependence of $\overline{D(E^*J)}$ is given. One can easily check the following results:

1. If $\overline{D(J)} \propto (2J + 1)^{-1}$, $\overline{\Gamma_\gamma}$ is the same for all J .
2. If $\overline{D(J)}$ is independent of J , $\overline{\Gamma_\gamma}$ is the same for all J except for J equal to $\frac{1}{2}$ and 0 , when $\overline{\Gamma_\gamma}$ equals $\frac{2}{3}$ and $\frac{1}{3}$ of the value for other J .

We will not enter here into a discussion that Brink gives of the justification of the above hypothesis. However, there are two remarks on the hypothesis itself:

1. The analogous hypothesis for neutron widths is that the strength function is independent of J and J' , where J' is to be interpreted as channel spin. As we have seen, this is not strictly true for neutrons.

2. Using the fact that the width for a transition $J \rightarrow J'$ is related to the width for the inverse transition $J' \rightarrow J$ by the factor $(2J + 1)/(2J' + 1)$, one finds on applying the hypothesis in the limit $E' \rightarrow E^*$ that it implies: $\overline{D(J)} \propto (2J + 1)^{-1}$. If this were true, it would mean that it is inconsistent to hypothesize any other dependence of $\overline{D(J)}$ on J after using the hypothesis. In order to avoid this difficulty (which would invalidate Brink's conclusions for the case: $\overline{D(J)}$ independent of J) one must assume that the hypothesis cannot be applied in the limit $E' \rightarrow E^*$. Such an assumption has no evident basis.

3. INFORMATION ON MEAN VALUES FROM RESONANCES LEVELS; COMPARISON WITH THEORY

This topic has been discussed in many papers, both published and contributed at this conference. Therefore the following will be the briefest outline of the present situation.

3.1. Level Spacings

Newton³ has compared his theoretical formula for mean level spacings with observation and concludes that there is always agreement to within a factor of three. This appears extremely good. It must, however, be borne in mind that there is some arbitrariness in choosing the effective values of a that take account of shell effects. This certainly makes the fitting easier, but Newton's results are impressive nevertheless.

In his comparison, Newton has not considered level spacing as a function of spin J , but only of excitation energy and mass number. The reason is that there are still almost no data on the J values of resonance levels.

3.2. Neutron Widths

The theory makes predictions about the values of the ratio $\overline{\Gamma}_n^0/D$. As is well known, the large number of experimental values of $\overline{\Gamma}_n^0/D$ for different nuclei are all of the order of 10^{-4} (where $\overline{\Gamma}_n^0$ is normalized to 1 ev), and this agrees with the expected theoretical magnitude. As far as the detailed values and variations of $\overline{\Gamma}_n^0/D$ with A are concerned, the cloudy-crystal-ball model of Feshbach, Porter, and Weisskopf⁹ seems to describe the main features (such as the peaks at $A \sim 55$ and ~ 160 in a plot of $\overline{\Gamma}_n^0/D$ against A). On the other hand, the finer features (such as the depth of the minimum at $A \sim 90$) are not well fitted by the model. However, there are various refinements that are being built into the model that may bring about more complete agreement. For instance, (1) the potential-well shape may be varied from the square shape, (2) the nuclear shape may be varied from the spherical shape.

3.3. Fission Widths

The only nuclei where experimental values of $\overline{\Gamma}_F/D$ are established are U^{235} , for which $\overline{\Gamma}_F = 50 \pm 15$ mev (milli-electron volts), and Pu^{239} , for which $\overline{\Gamma}_F = 46 \pm 12$ mev. The theoretical values for $\overline{\Gamma}_F/D$, namely, $(\sum_c P_c)/2\pi$, cannot be predicted, unfortunately, because of lack of independent knowledge of the fission thresholds and of the penetration factors, P_c . We will see in Section 6.3 that the factors P_c are determined to some extent by the observed distribution laws of fission widths. Nevertheless,¹³ in the absence of actual knowledge of the fission thresholds, there always seems to be sufficient freedom in choosing the P_c to enable one to fit the observed mean values. Of course, the fact that the observed levels are composed of two sets of levels with different J values and different fission characteristics should be taken into account. This provides even more freedom in the fitting.

3.4. Radiation Widths

Values of mean total radiation widths of levels have been established in a number of nuclei. The values appear to have a systematic dependence on mass number, falling from $\overline{\Gamma}_\gamma \sim 150$ mev at $A \sim 100$ to $\overline{\Gamma}_\gamma \sim 30$ mev at $A \sim 240$. Brink's

¹³J. A. Wheeler, this conference.

theory¹² fits the general trend of these numbers with A but overestimates them by a factor of about three. Considering the uncertainties in the theory, this agreement is more than could be expected.

As far as the J dependence of $\overline{\Gamma}_\gamma$ is concerned, experimentally there appears to be none. In particular, there is the observation that levels of spin $J = 0$ and 1 have about the same width. According to Brink's theory, this has implications for the J dependence of the level density and decides in favor of " $D(J) \propto (2J + 1)^{-1}$ " as opposed to " $D(J)$ independent of J ." However, as mentioned in Section 2.4, there are certain objections to the theory that must be removed before one can apply it with full confidence.

4. OTHER METHODS FOR OBTAINING INFORMATION ON MEAN VALUES

Although the measurement of individual resonances is evidently the most direct method for deriving mean values, there are other methods that also yield information on these values. I will briefly mention three such methods.

4.1. Measurement of Average Total Cross Sections in the keV Region

The exact theoretical expression for the total s -wave average cross section is (assuming for simplicity that $l = 0$ for the target nucleus):

$$\overline{\sigma}_{\text{tot}} = \frac{4\pi}{k^2} \left\{ \frac{\rho x (1 + \rho x \cos^2 \rho) + (\rho y \cos \rho - \sin \rho)^2}{(1 + \rho x)^2 + (\rho y)^2} \right\},$$

where ρx stands for $\overline{\pi \Gamma}_n^0/2D$ and ρy represents the deviation of the interresonance (background) phase δ from the hard-sphere phase $\delta = -\rho$. To be more precise, ρy is such that:

$$\delta = -\rho + \tan^{-1}(\rho y).$$

In practice, at low energies, where $\rho \ll 1$, we can approximate the above expression by the first few terms in a series development in powers of ρ :

$$\overline{\sigma}_{\text{tot}} = \frac{4\pi}{k^2} \left\{ \rho x + \rho^2 [(y - 1)^2 - x^2] + \dots \right\}.$$

If this series is cut at the term in ρ^2 , then we have an expression for $\overline{\sigma}_{\text{tot}}$ as a function of energy:

$$\overline{\sigma}_{\text{tot}} = \frac{A}{(E)^{1/2}} + B,$$

where

$$A = \frac{4ax}{(2M/b^2)^{1/2}},$$

$$B = 4\pi a^2[(y-1)^2 - x^2].$$

Clearly, the slope A of the plot of $\overline{\sigma_{\text{tot}}}$ against $E^{-1/2}$ gives a value for x . The value of the intercept B can then be made to yield a value for y . Special attention should be given to the form of B , because Feshbach, Porter, and Weisskopf⁹ quote a formula for $\overline{\sigma_{\text{tot}}}$ with the term x^2 absent (their slope is the same as the above A , but their intercept is $4\pi(a - a')^2$, where $a' = ay$). Lynn¹⁴ has examined with numerical examples the consequences of ignoring the term x^2 on the extracted value of y and has found them to be often quite serious. Clearly the omission of the x^2 term is more serious near $A \sim 55$ and ~ 160 than near $A \sim 120$ and ~ 240 , because the value of x is larger in the former cases.⁹ Most of the experimental plots of $\overline{\sigma_{\text{tot}}}$ against $E^{-1/2}$ that have been reported are such that the intercept B is very uncertain (although the slope A is usually well determined). Therefore the correction is not of much practical importance at present, but it may be of future importance.

Lynn¹⁴ has also examined the effects of p -wave contributions to $\overline{\sigma_{\text{tot}}}$ and has found that they become significant when the higher terms (in p^3 , etc.) of the s -wave contribution become significant.

4.2. Measurement of Transmission as a Function of Target Thickness in the keV Region¹⁵

For neutrons of some range of energies that includes many resonances, one can write the transmission $T = e^{-Nt\overline{\sigma_{\text{tot}}}}$ of a sample of thickness t and N nuclei per square centimeter as:

$$T = T_0(1 + \alpha),$$

where T_0 is the usual transmission factor $T_0 = e^{-Nt\overline{\sigma_{\text{tot}}}}$, and α is a correction term:

$$\alpha = e^{-Nt(\overline{\sigma_{\text{tot}}} - \overline{\sigma_{\text{tot}}})} - 1.$$

Provided that the exponent is usually small, we can expand the exponential to the term in second

¹⁴A. M. Lane and J. E. Lynn, to be published as AERE report.

¹⁵R. G. Thomas, *Phys. Rev.* 98, 77 (1955).

order; then

$$\alpha = \frac{(Nt)^2}{2!} \text{Var } \overline{\sigma_{\text{tot}}} + \text{higher terms}.$$

Thomas¹⁶ has shown that, for s -waves, the following relation holds:

$$\text{Var } \overline{\sigma_{\text{tot}}} = \frac{2\pi}{k^2} \overline{\sigma_{\text{ce}}},$$

where σ_{ce} is the compound elastic cross section of Feshbach, Porter, and Weisskopf. If elastic scattering is the only possible process (no capture or inelastic scattering), then $\overline{\sigma_{\text{ce}}}$ equals $\overline{\sigma_{\text{c}}}$, the cross section for compound-nucleus formation. At low energies:

$$\overline{\sigma_{\text{c}}} = \frac{2\pi^2}{k^2} \frac{\overline{\Gamma_n}}{D} + \text{higher terms}.$$

Thus we have:

$$\alpha \sim \frac{2(Nt)^2}{k^4} \pi^3 \frac{\overline{\Gamma_n}}{D},$$

so that, in principle, a measurement of α can be made to yield a value of $\overline{\Gamma_n/D}$. However, the applicability of this method is evidently limited. The energies used must be such that capture, inelastic scattering, and p -wave effects are unimportant. Furthermore, no Doppler broadening is allowed.

4.3. Measurement of Average Capture Cross Sections in the $E > 1$ keV Region

For s -waves on an $l = 0$ target, the average capture cross section in the absence of inelastic scattering is:

$$\overline{\sigma_{n\gamma}} = \frac{2\pi^2}{k^2} \frac{1}{D} \frac{\overline{\Gamma_n \Gamma_\gamma}}{\overline{\Gamma_n + \Gamma_\gamma}} S(\overline{\Gamma_n/\Gamma_\gamma}),$$

where the last factor, S , is usually of order unity and takes into account the effect of fluctuations in Γ_n on the averaging. Clearly, from this formula, measurement of $\overline{\sigma_{n\gamma}}$ will give a relation between \overline{D} , $\overline{\Gamma_n}$, and $\overline{\Gamma_\gamma}$.

¹⁶R. G. Thomas, unpublished.

At higher energies up to ~ 1 Mev, the capture cross section is a sum of contributions from the various partial waves.¹⁷ At these higher energies, the neutron width dominates the radiation width. This means that Γ_n cancels itself in the above equation, with the result that $\overline{\sigma_{n\gamma}}$ gives a value for $\overline{\Gamma_\gamma/D}$. Lane and Lynn¹⁷ have fitted the observed capture cross sections in Th²³² and U²³⁸ and find that the value they obtain for $\overline{\Gamma_\gamma/D}$ agrees well with the directly observed value from thermal resonances. (N.B. One must be careful to take proper account of inelastic neutron competition in this type of work.)

5. THEORETICAL VIEWS ON DISTRIBUTION LAWS

5.1. General Observations

Porter and Thomas¹⁸ have formulated a theory of the distribution laws for neutron, radiation, and fission widths. The essential starting point for the consideration of all three types of width is the same, namely, the assumption that the values of individual nuclear matrix elements have a Gaussian (normal) distribution centered on the value zero, that is, they have the frequency function:

$$p(x) dx = \frac{2}{\sqrt{\pi}} e^{-x^2/\pi \overline{|x|}^2} \frac{dx}{\overline{|x|}},$$

where $\overline{|x|}$ is the mean value of $|x|$. Now, if we have ν sets of quantities $(x_1) \dots (x_\nu)$, each one of which has the same frequency function (with the same mean value), then it can be shown that the frequency function for the quantity $X = x_1^2 + x_2^2 + \dots + x_\nu^2$ is:

$$p_\nu(X) dX = \frac{\nu/2}{\Gamma(\nu/2)} (\alpha X)^{(\nu/2)-1} e^{-\alpha X} \frac{dX}{\overline{X}},$$

with $\alpha = (\nu/2)\overline{X}$. This distribution for X is called "the chi-square distribution with ν degrees of freedom." Particular examples are:

$$\nu = 1: \frac{1}{2(\pi)^{1/2}} \frac{e^{-X/2\overline{X}}}{(X/2\overline{X})^{1/2}} \frac{dX}{\overline{X}};$$

$$\nu = 2: e^{-X/\overline{X}} \frac{dX}{\overline{X}};$$

$$\nu = 3: \frac{3}{(\pi)^{1/2}} \left(\frac{3X}{2\overline{X}}\right)^{1/2} e^{-(3X/2\overline{X})} \frac{dX}{\overline{X}};$$

$$\nu = 4: 2 \left(\frac{2X}{\overline{X}}\right) e^{-2X/\overline{X}} \frac{dX}{\overline{X}}.$$

Since observed widths are made up of sums of squares of matrix elements, it is clear that this chi-square family of distributions is especially convenient as a framework for discussion of the distribution laws of observed widths. In general, however, we do not expect distributions to coincide with members of the chi-square family, because the mean values of various matrix elements contributing to a width may differ (see, e.g., the case of fission below).

Before discussing the predictions for the various types of width, we note that $p_\nu(X) dX$ has the property that: $\text{Var } X = (2/\nu) \overline{X}^2$. Clearly $\text{Var } X \rightarrow 0$ as $\nu \rightarrow \infty$, as is expected.

5.2. The Level Spacings

The only suggestion (with any theoretical foundation) on the distribution law of level spacings has been made by Wigner.¹⁹ Although, in principle, the problem for deducing the law is well defined, it is difficult to solve such a problem because of mathematical difficulties. The problem can be stated thus: On the independent-particle model with no interparticle forces, the positions of states are expected to be distributed at random. In the presence of forces, however, states are expected to repel each other to some extent. To estimate the repulsion, one must estimate the distribution of differences in eigenvalues of a large matrix with randomly spaced diagonal elements in the presence of nondiagonal elements with a normal distribution (and random signs). Wigner expects that the solution to this problem has the form:

$$p(D) dD = 2b(bD) e^{-(bD)^2} dD,$$

where $b = \pi^{1/2}/2\overline{D}$. The variance of this distribution is:

$$\text{Var } D = \left(\frac{4}{\pi} - 1\right) \overline{D}^2 \approx 0.27 \overline{D}^2.$$

¹⁷A. M. Lane and J. E. Lynn, *Proc. Phys. Soc.* (London), to be published.

¹⁸C. E. Porter and R. G. Thomas, *Phys. Rev.* **104**, 483 (1956).

¹⁹E. P. Wigner, this conference.

5.3. Neutron Widths

The neutron width for a given channel (i.e., given residual state, l value, and channel spin) is simply the square of a matrix element (the so-called "reduced width amplitude"). Therefore we expect neutron widths to be distributed as:

$$p_1(X) dX = \frac{1}{2\pi^{1/2}} \left(\frac{X}{2\bar{X}} \right)^{-1/2} e^{-(X/2\bar{X})} \frac{dX}{\bar{X}},$$

the "Porter-Thomas distribution."¹⁸ The distribution law for neutron widths summed over channel spin in cases where there are two channel spins will be:

$$p_2(X) dX = e^{-X/\bar{X}} \frac{dX}{\bar{X}},$$

assuming the mean widths to be the same for the two channel spins. For s -wave neutrons, of course, each width corresponds to a single channel spin, so one predicts a " $\nu = 1$ type distribution" for the widths of s -wave neutron resonances of given J value.

5.4. Fission Widths

As discussed in Section 2.3, one expects the total fission width of a resonance to be composed of a sum of partial fission widths, one for each fission channel: $\Gamma_F = \sum \Gamma_{Fc}$. Thus one expects the appropriate distribution law for the observed total widths to be that of a sum of quantities each one of which has a $\nu = 1$ type distribution. This distribution law will not be exactly a member of the chi-square family, in general, because the mean values $\bar{\Gamma}_{Fc}$ of the various partial widths are different¹³ (each is proportional to the penetration factor, P_c , for the appropriate channel). Nevertheless it is instructive to make best fits to the data in terms of the chi-square family. The optimal value of ν (which need not be integral) is then referred to as the "effective number of open fission channels."

5.5. Radiation Widths

As in the case of fission widths, the problem here is to specify the distribution law for a quantity Γ_γ which is the sum of a number of quantities, the partial widths $\Gamma_{\gamma p}$, each one of which has a $\nu = 1$ type distribution. The mean values of the various partial widths are different (each is pro-

portional to the phase-space factor E_γ^3), and so the resulting distribution will not be a "pure" member of the chi-square family. A decided simplification arises in the case of Γ_γ (as opposed to the case of Γ_F) as a result of the very large number of partial widths $\Gamma_{\gamma p}$ that contribute to Γ_γ . The number is so large that one can safely use asymptotic considerations,¹⁸ which predict that the Γ_γ will have a normal distribution with mean value $\bar{\Gamma}_\gamma = \sum_p \bar{\Gamma}_{\gamma p}$. If we assume for the moment that all partial widths are independent, the variance will be:

$$\text{Var } \Gamma_\gamma = \sum_p \text{Var } \Gamma_{\gamma p}.$$

Assuming that each partial width has a $\nu = 1$ type distribution then gives:

$$\frac{\text{Var } \Gamma_\gamma}{(\bar{\Gamma}_\gamma)^2} = \frac{2 \sum_p (\bar{\Gamma}_{\gamma p})^2}{(\sum_p \bar{\Gamma}_{\gamma p})^2}.$$

It is possible to make a numerical estimate of this last quantity if one assumes a definite level-spacing law. Assuming a law of the form $D(E^*) \sim e^{-E^*/T}$, Porter and Thomas find:

$$\frac{\text{Var } \Gamma_\gamma}{(\bar{\Gamma}_\gamma)^2} = \frac{2}{n} (1 - e^{-\alpha}) \frac{\gamma(7, \alpha)}{\gamma(4, \alpha)},$$

where γ is the incomplete gamma function; $\alpha = B/T$, where B is the neutron binding energy; and n is the total number of partial widths. If, as Porter and Thomas suggest, the various partial widths are not all independent, the above analysis is unchanged except that n is to be interpreted as the effective number of independent widths.

6. INFORMATION ON DISTRIBUTION LAWS FROM RESONANCE LEVELS; COMPARISON WITH THEORY

6.1. General Remarks on Practical Difficulties

All the remarks in this section are based on the paper by Porter and Thomas, where a more adequate account can be found. In principle, all that has to be done is to measure a large number of widths in any given nucleus and then plot a histogram to discover the distribution law. The practical snags with this program are the following:¹⁸

1. In many cases targets are not monoisotopic, so that a mixture of at least two sets of widths is measured.

2. For cases with target spin $I \neq 0$, a mixture is measured of two sets of widths corresponding to the two sequences of resonance levels with $J = I \pm \frac{1}{2}$.

3. Each extracted width has a certain error on it due to experimental resolution and perhaps to some effects of level interference, etc.

4. There is a bias in the samples of widths, because the experiments tend to miss the very small ones.

5. Even if difficulties 1 to 4 are removed (i.e., one measures a single set of widths exactly), the number of widths is always limited (usually < 20), so that the experimental distribution is correspondingly indeterminate.

For definiteness, let us discuss these difficulties with reference to neutron widths:

1. The mean neutron widths in various isotopes will differ, in general, reflecting the difference in level spacings and binding energies (since $\overline{\Gamma_n}/D$ should be the same for all isotopes). This is unfortunate, because it leads to distortion in the distribution of widths. Therefore, one must discard such mixed samples unless one is sure that the mean values are the same.

2. When spins J of resonances are not measured, really only the combination $(2J + 1) \Gamma_n(J)$ is measured at each resonance. If it is assumed that $\Gamma_n(J) \propto D(J)$ and that $D(J) \propto (2J + 1)^{-1}$, then the mean value of $(2J + 1) \Gamma_n(J)$ is the same for both sequences, so that the observed distribution is not distorted.

3. The presence of errors in an observed set of widths evidently leads to uncertainty in the experimental distribution law. The precise amount of the uncertainty can be estimated either by numerical means (by selecting various samples allowed by the errors and examining the change in distribution) or analytically as described by Porter and Thomas.

5. Forgetting about difficulty 4 for the moment, let us suppose that we want to find the correct ν value for a set of observed widths. If the set is limited, it is impossible to determine the correct value. The best that one can do is to determine the "most likely" value and a corresponding range of "reasonable" values of ν . There is a standard method for doing this. If the set of widths is

$\Gamma_1 \dots \Gamma_\mu$, one considers the so-called "likelihood function":

$$L(\nu) = \prod_{i=1}^{\mu} p_\nu(\Gamma_i) .$$

One can remove the limitation that ν is integral and regard L as a continuous function of ν . The form of $L(\nu)$ is normally a peak centered at some value $\nu = \nu_0$ with width $\Delta\nu$. The "most likely" value of ν is ν_0 , and $\nu_0 \pm \Delta\nu$ is the range of "reasonable" values.

4. Having described the likelihood-function method, the means of taking account of difficulty 4 can be specified. This is simply done by always replacing $p_\nu(\Gamma_i)$ by the product $E(\Gamma_i) p_\nu(\Gamma_i)$, where $E(\Gamma_i)$ is the "efficiency function," defined as the probability that a level of width Γ_i will be observed.

6.2. Neutron Widths

If one considers sets of widths in various elements separately, the above method gives very poor estimates of ν , because of the fewness of the number of widths in individual elements (usually the number is less than ten and often is only two or three). Therefore one tries to combine sets of widths from various isotopes. Evidently one cannot just add all sets together, because each set has its own special mean value. There are two ways in which to proceed:

1. *The Porter-Thomas Method*,¹⁸ which emphasizes the few nuclei with large sets (> 5). This method implies dividing each width by its sample average and then combining all sets. This introduces an error (and uncertainty in the best ν value) arising from the fact that the sample average may depart from the true mean. However, this uncertainty can be estimated, and it turns out to be small if the sets used are restricted to those > 5 or so. Proceeding in this way, Porter and Thomas analyze 148 values and conclude that the best ν value is 1.02, with a range of reasonable values of ± 0.065 . This is in excellent agreement with the expected result, $\nu = 1$.

2. *The Lynn Method*,¹⁴ which emphasizes the large number of nuclei with small sets (< 5). A disadvantage of the Porter-Thomas method is that it cannot make full use of the large number of widths that occur in such small sets that no reliable sample average can be established. Lynn

has suggested that one can use this type of data by combining widths in pairs in each nucleus and forming quantities

$$X = \frac{2(\Gamma_1^2 + \Gamma_2^2)}{(\Gamma_1 + \Gamma_2)^2}$$

One can now apply the likelihood-function analysis to the set of X from all nuclei (N.B. The values of X are restricted to the range $1 \leq X \leq 2$). Lynn has applied this method and has found results in agreement with the Porter-Thomas method but with a larger uncertainty ($\nu = 1.5 \pm 0.5$) due to taking a sample of only 60 widths.

6.3. Fission Widths

Porter and Thomas apply the likelihood-function analysis to 15 fission widths in U^{235} and find: $\nu = 2.3 \pm 1.1$. Unfortunately, the data do not distinguish levels of the two J values, and so, if the two distributions of fission widths are different, this value of ν represents a rather involved average value from the two sequences. Wheeler¹³ has suggested a certain combination of independent fission channels that, in the case of U^{235} , will simultaneously fit the observed distribution law and the mean fission width. Farley has measured 25 fission widths in Pu^{239} and concludes that $\nu = 2$ is a good fit, but he has not made a proper statistical analysis.

6.4. Radiation Widths

There are not many nuclei where more than one or two radiation widths have been measured. Two exceptional cases are Ta^{181} and U^{238} , where six widths are quoted. These have been analyzed by Porter and Thomas.¹⁸ In the case of Ta^{181} the errors on the six values are such that all the values overlap so that no satisfactory analysis can be made. The set of values for U^{238} is better, and Porter and Thomas conclude that the effective number of independent channels, n , lies in the range $50 < n < 300$. They find that this can be stated with "95% confidence." The effective number of channels is considerably less than the total number of levels between the ground state and the excited state corresponding to the neutron binding plus kinetic energy.

6.5. Level Spacings

Quite large samples of spacings are available in some nuclei, but, in spite of this, there is serious uncertainty in the distribution law. This is due to three main causes:

1. A very small level spacing between two resonances implies that the two resonances may not be resolved separately, and so small spacings are missed.

2. Very weak levels are missed. This biases the sample towards higher values in a twofold manner, because it implies that two small spacings are counted as one larger one.

3. Often spacings of more than one sequence of levels are involved (due to a mixture of isotopes or of J values). If, however, one can estimate the ratio of the mean values for the various sequences, there is no real problem here. For instance, consider the case of an odd target nucleus, which will give two sequences of resonance levels ($J = I \pm \frac{1}{2}$). Quite generally, if one has two independent sequences of events with spacing frequency functions $p_1(D)$ and $p_2(D)$, the frequency function of the superposed sequence is:¹⁴

$$p(D) = \frac{1}{D_1 D_2} \left[p_1(D) \int_0^\infty y p_2(y+D) dy + p_2(D) \int_0^\infty y p_1(y+D) dy + 2 \int_0^\infty p_1(y+D) dy \int_0^\infty p_2(y+D) dy \right]$$

If the two sequences are independent, it is clear that the superposed sequence will be such that there is appreciable probability of finding small spacings, although this may not be true of the separate sequences. This implies that more small spacings are predicted in an odd nucleus than in an even one. To mention examples: Clearly the superposition of two random $\nu = 2$ sequences with equal means leads to a resulting random sequence. The superposition of two $\nu = 4$ sequences with equal means leads to a resulting frequency function with only a small dip at zero spacing (instead of the zero values of the separate frequency functions). Proper comparison of the distributions observed with even and odd target nuclei should give a

useful guide as to the extent to which small spacings are missed experimentally.

The present general situation is that most analyses agree that there is a mild repulsion between observed levels which can be roughly represented by $\nu = 4$ or $\nu = 6$ type distributions or a distribution of the type suggested by Wigner.¹⁹ The fact that these different distributions give equally good accounts of the data demonstrates that there is room for considerable improvement in the data.

7. OTHER METHODS FOR OBTAINING INFORMATION ON DISTRIBUTION LAWS

Just as with the mean values, there are other methods for obtaining information on distribution laws, apart from direct measurement of resonances. Two of these are derived, in fact, from methods already mentioned in connection with mean values in Section 4.

7.1. Measurement of Average Capture Cross Sections

In Section 4.3, it was assumed that one knew the distribution law for Γ_n . This meant that the S factor in the formula for $\overline{\sigma_{n\gamma}}$ can be evaluated as a function of $\overline{\Gamma_n}/\overline{\Gamma_\gamma}$, with the result that the measured $\overline{\sigma_{n\gamma}}$ gives a relation between $\overline{\Gamma_n}$, $\overline{\Gamma_\gamma}$, and \overline{D} . Clearly one can reverse the argument. By assuming values of $\overline{\Gamma_n}$, $\overline{\Gamma_\gamma}$, and \overline{D} taken from resonance data, the values of $\overline{\sigma_{n\gamma}}$ will indicate the nature of the distribution of Γ_n (under the assumption that Γ_γ is constant). By an extension of the same ideas, mean fission cross sections in the key region can be made to yield information on the distributions of Γ_n and Γ_F .

7.2. Measurement of Transmission as a Function of Sample Thickness¹⁵

As indicated in Section 4.2, this kind of measurement gives a value of $\overline{\sigma_{ce}}$. If the incident energy is low enough for Γ_γ and Γ_n to be comparable, it is not correct to equate $\overline{\sigma_{ce}}$ to $\overline{\sigma_c}$, as was done in Section 4.2. Instead, $\overline{\sigma_{ce}}$ depends on the distribution of Γ_n through the evaluation of

$$\left(\frac{\overline{\Gamma_n^2}}{\overline{\Gamma_n} + \overline{\Gamma_\gamma}} \right).$$

7.3. Measurement of Fluctuations in the key Region

This method has considerably more interest and promise than the previous two. It is based on the

observation by Egelstaff²⁰ that reproducible variations occur in total (and fission) cross sections in the energy region where the resolution width may span several resonances. Evidently these variations are due to the fluctuations in level spacing and neutron (and fission) widths, so that it should be possible to extract useful information from the variations concerning the distribution laws for D , Γ_n , and Γ_F . The best way to proceed seems to be to divide the energy range of measurement into equal intervals W which must be such that $W > \Delta$, where Δ is the largest experimental resolution width. (It follows that, on the average, there are several levels in each interval W .) One can now integrate²¹ the cross section in each interval W and construct a distribution function for the integrated cross sections $\int_W \sigma dE$. Now one must solve the theoretical problem of predicting the distribution of $\int_W \sigma dE$ for various assumed distributions of spacings and widths. Stripped of its physical content, the problem can be expressed in a purely mathematical way as follows: Given a sequence of events with frequency function $p_D(D)$ for the spacings; also given that a "score," s , is associated with each event, and a frequency function $p_s(s)$ for the scores; what is the frequency function $p(S, W)$ for finding a total score S in an interval W ? The solution to this problem¹⁴ is that

$$P(S, W) = \int_0^S p(S', W) dS'$$

is the Laplace transform with respect to u and v of the function:

$$\frac{1}{uv^2\overline{D}} \left\{ \frac{v\overline{D}[1 - Y(u)\Phi(v)] - [1 - Y(u)][1 - \Phi(v)]}{1 - Y(u)\Phi(v)} \right\},$$

where $\Phi(v)$ and $Y(u)$ are the Laplace transforms of p_D and p_s , respectively. Using the fact that the Laplace transform of $p_\nu(x)$ is $(\alpha + 1)^{-\nu/2}$, where $\alpha = \overline{x}\nu/\nu$, one can straightforwardly compute $p(S, W)$ for various chi-square distributions for p_D and p_s .

Often it is unnecessary to go through the labor of evaluating $p(S, W)$ in this way. This will be so if W is chosen large enough so that many levels fall inside W on the average (say $W > 10\overline{D}$). In

²⁰P. A. Egelstaff, this conference.

²¹In the case of total cross sections, one must subtract the potential-scattering cross section.

this case, one can use asymptotic considerations.¹⁴ The function $p(S, W)$ is expected to become Gaussian centered about the mean value $\bar{S} = (W/\bar{D})\bar{s}$ and with the variance:

$$\frac{\text{Var } S}{(\bar{S})^2} = \frac{1}{W/\bar{D}} \left[\frac{\text{Var } s}{(\bar{s})^2} + \frac{\text{Var } D}{(\bar{D})^2} \right].$$

If the scores and spacings are characterized by

chi-square distributions with $\nu = \nu_s, \nu_D$, this becomes:

$$\frac{\text{Var } S}{(\bar{S})^2} = \frac{1}{W/\bar{D}} \left(\frac{2}{\nu_s} + \frac{2}{\nu_D} \right).$$

Egelstaff²⁰ has applied these considerations to the analysis of fluctuations observed in both fission and total cross sections.

FLUCTUATIONS IN AVERAGE NEUTRON CROSS SECTIONS

P. A. Egelstaff

Atomic Energy Research Establishment, Harwell

P. A. EGELSTAFF: In the work I am going to review, we consider the region between 500 ev and something like 10 kev and plot the total cross section as a function of time of flight. The intercept with the cross-section axis is related to the nuclear radius in a slightly complicated fashion, and the slope of the best line through the points is proportional to Γ_n^0/D .

In any experimental observations of this type you notice that the points fluctuate quite widely about the best line. It is usually clear that this fluctuation is away outside of the counting statistics and that there is some information on resonance levels held in it. I want to consider how to get at this information. At the present time we have to combine this new information with that from individual resonance analysis to get the complete results that we want. But, one advantage is that one can consider very large samples of resonances, and another is that there is a unique analytical solution to this problem.

We will write the product of total cross section minus the intercept on the cross-section axis times (time of flight)⁻¹ as the quantity σ . The average value of σ in the energy range W we call $\langle\sigma\rangle_W$. Each $\langle\sigma\rangle_W$ represents a sample. We are going to discuss the distribution of those samples. (Note: In finding the values of σ a variety of corrections and precautions must be taken which we do not have space to deal with here. Further, the distribution of $\langle\sigma\rangle_W$ has to be corrected for the fluctuations due to counting statistics.)

The relation between the distribution of $\langle\sigma\rangle_W$ and the distributions in Γ_n and D was shown by Lane to be:

$$(1) \quad \frac{\text{Var } \langle\sigma\rangle_W}{\langle\sigma\rangle_\infty^2} = \frac{\langle D \rangle}{W} \left[\frac{\text{Var } \Gamma_n}{\langle \Gamma_n \rangle^2} + \frac{\text{Var } D}{\langle D \rangle^2} \right].$$

This formula is valid only if you have such a large number of levels in the interval W that the distribution of $\langle\sigma\rangle_W$ is a Gaussian distribution. Experimentally this is found to be true.

Equation 1 applies only to the case where you have a zero-spin target. For nonzero spin we assume that the level density is proportional to

$(2J + 1)^{-1}$. In this case Eq. 1 holds both for target nuclei of zero spin and for target nuclei of nonzero spin. For other relationships it would not hold. Thus by using this method you have an indirect, but very simple, technique of checking the relationship between spin and level spacing. For the rest of my talk I will assume that Eq. 1 is valid for all target nuclei. If you have a mixture of isotopes, it is necessary to use a suitably weighted average level spacing. If a_i is the abundance of the i th isotope, then the weighted average is $\sum_i a_i^2 D_i$.

Table 1 shows the various elements we have studied in the total cross section: plutonium, platinum, and a series of rare-earth elements. The major isotopes are listed in column 2. The spins are listed in column 3. The value of the average spacing as observed for the whole element is in column 4, and the weighted value of the level spacing is written in column 5. In order to obtain this number you have to make quite an arbitrary assumption. I have assumed that all even-odd isotopes in the same element have the same value of D and that all even-even isotopes have five times that value of D . This gives you some idea of the factor involved.

The last column shows the value of:

$$(2) \quad E = \frac{\text{Var } \langle\sigma\rangle_W}{\langle\sigma\rangle_\infty^2} \cdot \frac{W}{\langle D \rangle}.$$

The errors, on the whole, are large, about 50%, because at the present moment we have not sufficiently good data to get accurate values. If we use Professor Wigner's distribution for D and the Porter-Thomas distribution for Γ_n in Eq. 1, we find $E = 2.27$. This number should be the same for all target nuclei. It represents the shape of the various distributions. So the numbers in column 6 of Table 1 should all be the same and should average 2.27. Within the errors they are perhaps just about the same. The average is 1.7. I don't feel that this is significantly different from the theoretical predictions.

Now I should like to go on to the fission cross section of U²³⁵. The fission cross section is

Table 1. Total-Cross-Section Results

Element	Major Isotopes	Spin	Assumed Value of $\langle D \rangle$ for Element (ev)	Calculated Value of $\sum_i a_i^2 D_i$ (ev)	Value of E
Pu	239	$\frac{1}{2}$	1.8		1.6 ± 0.8
Pt	194	0	15	29	1.5 ± 0.8
	195	$\frac{1}{2}$			
	196	0			
	198	0			
Ta	181	$\frac{1}{2}$	4		3.5 ± 2
Yb	171	$\frac{1}{2}$	3	7	1.5 ± 0.8
	172	0			
	173	$\frac{5}{2}$			
	174	0			
	176	0			
Dy	161	0	1.5	3	2.5 ± 1.5
	162				
	163				
	164				
Gd	155	$\frac{3}{2}$	2	4.5	0.8 ± 0.4
	156	0			
	157	$\frac{3}{2}$			
	158	0			
	160	0			
Eu	151	$\frac{5}{2}$	0.5		1.0 ± 0.4
	153	$\frac{5}{2}$			
Sm	147	0	1.8	3.8	1.9 ± 0.9
	148				
	149				
	150				
	152				
	154				
Pr	141	$\frac{5}{2}$	80		~ 1

proportional to $\Gamma_n/D = \Gamma_F/\Gamma$, so that we must add the quantity

$$(3) \quad \frac{\langle D \rangle}{W} \cdot \frac{\text{Var}(\Gamma_F/\Gamma)}{(\Gamma_F/\Gamma)^2}$$

to the right-hand side of Eq. 1. This assumes that the ratio of fission to total widths is the same for both spin states.

In the case of the U^{235} I have used the data obtained by Gaertner and Yeater at KAPL. These are extremely detailed and good data. I have determined the product

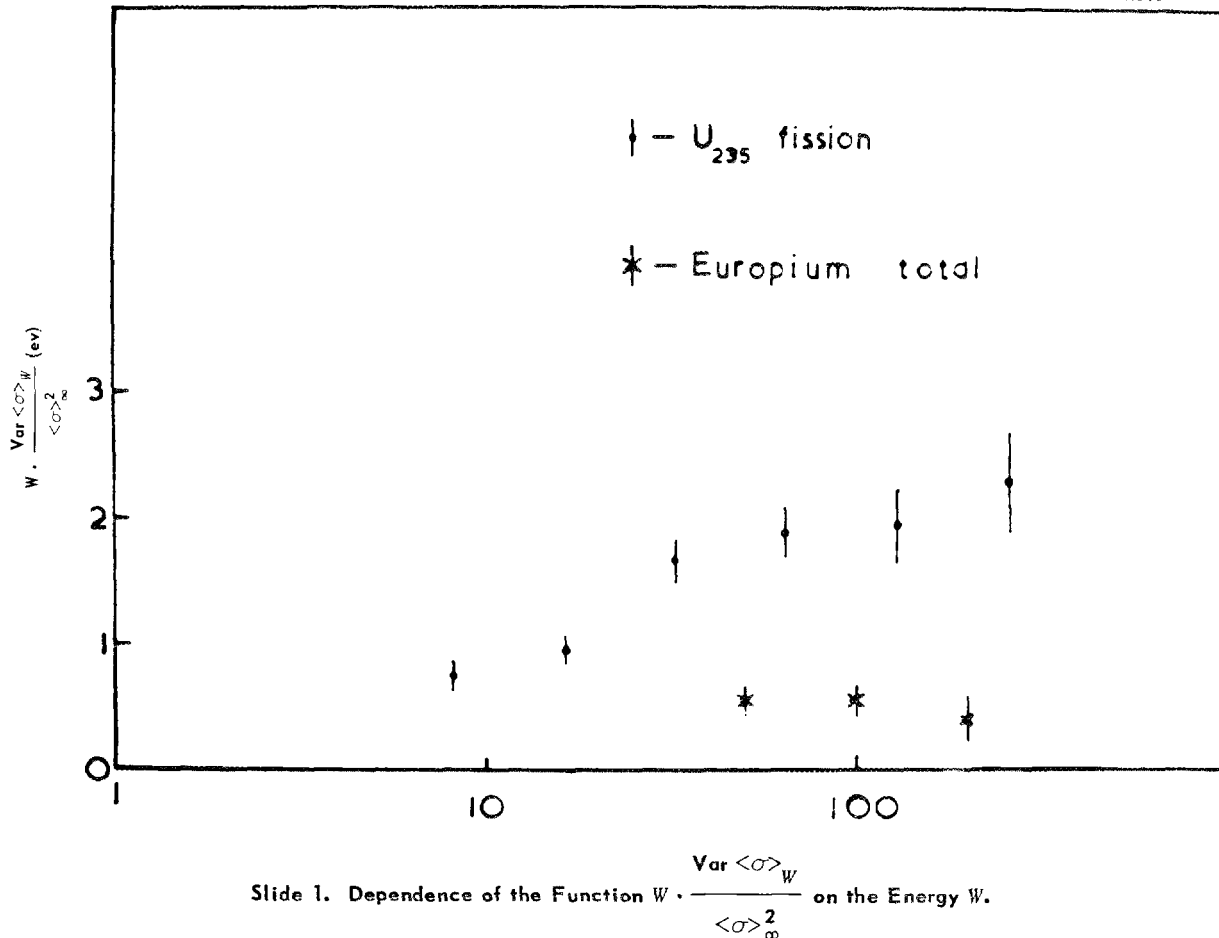
$$\frac{\text{Var} \langle \sigma \rangle_W}{\langle \sigma \rangle_\infty^2} \cdot W$$

for about five different values of W . The result is shown in Slide 1.

The quantity plotted should be constant. As you will see, it is not. This is at present the big puzzle in this work. For comparison, we have shown also on Slide 1 the total-cross-section data in the case of europium. There are three values of $(\text{Var} \langle \sigma \rangle_W / \langle \sigma \rangle_\infty^2) \cdot W$ for three values of W , and you can see they fall on a straight line. One point of interest is perhaps that the theoretical value for the product is obtained for $W > 100$ ev. The values for $W < 100$ ev are lower than one would theoretically think at the present time.

I want to suggest that we should consider for a moment whether the result shown in Slide 1 represents some new feature in slow-neutron cross-section data, perhaps only for the fission nuclei, which has not hitherto been obtained. It might, for example, represent an increase of fluctuation with increasing neutron energy, because for the larger values of W we include a wider range of results.

UNCLASSIFIED
PHOTO 19153



However, it does not appear that this is the whole answer.

The alternative, which perhaps from the point of view of these data is more reasonable, is that on top of the fluctuation which one should have there is a long-range fluctuation. This might be due to some type of correlation between Γ_n and D . If that interpretation is correct, we should then find that we get one value for small W increasing to a final constant value for large W . That is consistent with the data of Slide 1, although the errors are very large.

H. H. LANDON: May I ask again whether the Doppler effect has been taken into account explicitly? For the cases where the total width is dominated by the neutron width, the Doppler effect is not so large. Thus the large resonances are not affected much by the Doppler width, whereas the smaller and narrower ones are being broadened.

P. A. EGELSTAFF: No, this effect has not been taken into account explicitly. I don't think it affects the argument used here, particularly for U^{235} , where you have a very small neutron width. The argument used is that the area of a resonance for the thin-sample case is independent of Doppler width.

H. FESHBACH: I just wonder how sensitive all of these calculations are to the assumption of compound-nucleus formation, let's say, as compared with some of the things going by direct interaction.

P. A. EGELSTAFF: I don't really know how to answer the question in detail. I would only like to point out that one is not really assuming anything about any particular nuclear model here. One is merely saying that we have a lot of resonances with a certain distribution, and Eq. 1 follows straightaway from that statement.

C. O. MUEHLHAUSE: I am thinking a little along the line that Herman Feshbach is thinking, perhaps. At the higher energies, would it be interesting to compare the fluctuation phenomenon of the cross section, let's say of the total cross section, with just the inelastic cross section? For example, where the energy is greatest, would it not mean, then, that the fluctuation in the inelastic part would gradually wash out as the process went over to a direct interaction?

P. A. EGELSTAFF: Well, I think this is possible. My point is that at the present state we have considered only the situation at low energies.

As far as I know there aren't experimental data on fluctuations at higher energies that make it worth while doing such work.

A. M. LANE: I would just like to ask about the spin dependence of the fission widths in U^{235} . In your treatment you have assumed that the mean ratios of fission to total widths for the two sequences are the same. If the mean fission width is different for the two spin sequences, the ratios will be different. Thus in principle you have a method for seeing what is the mean fission width.

P. A. EGELSTAFF: Yes, that is a good point. If we could get over this difficulty about the dependence of the variation of $\langle\sigma\rangle_W$ on W , then we could use that method.

E. P. WIGNER: The way I understood your theory, it assumes only that the quantities which you plotted are statistically independent.

P. A. EGELSTAFF: Yes.

E. P. WIGNER: Now really, as far as I can understand, no other assumption enters significantly. In view of the difficulty which you encountered, one does wonder, however, whether this assumption of statistical independence is valid. I am reminded, in this connection, of the question as to whether the variations of successive level distances are statistically independent, and they are probably not. One wonders, then, could the paradox which you find be explained by that second term on the right-hand side of Eq. 1, or is it too large for that?

P. A. EGELSTAFF: I think it is too large for that. I mean, the value of the second term is small compared to the first. However, some types of correlation may fit the data.

I might mention another thing, that even with the smallest value of W for U^{235} , if you assume that $\langle D \rangle$ is 0.65 ev from the Brookhaven measurements, then there are something like 12 levels included in each sample. For the higher values, many hundreds of levels are included. Thus a correlation must exist over a range larger than 12 levels, and peter out for much larger ranges.

E. P. WIGNER: Then the conclusion, if one takes your data at face value, is that the Γ_n 's are not statistically independent.

P. A. EGELSTAFF: Yes, unless there is something rather odd about the fission process, so that you do have something else going on.

H. FESHBACH: Is the remark correct that the method gives you constant results for the case of

europium, and it therefore seems to work for europium but not for U^{235} ?

P. A. EGELSTAFF: Yes. But if in U^{235} I had only gotten a few points, I would probably have said we had a constant. It is only because I got a big range of points that the effect shows up. In europium we are able to get three points, and you can see that you could draw a line through the points with a little slope. So, when we say that it works for europium, it ought to be slightly qualified, perhaps.

C. E. MANDEVILLE: Aren't those europium values rather unreasonable, or are they that uncertain?

P. A. EGELSTAFF: That is a point. As I pointed out, the actual numbers I listed in the last column of Table I do jump about a bit. The errors are large, but the europium value is 1.0 ± 0.4 . Just taking it at its face value, that number does seem unreasonably small, I agree, and it suggests that the distributions are not as wide as hitherto assumed.

I think there is a very great deal more to be done on this type of work.

DISCUSSION ON CROSS-SECTION MEASUREMENTS IN THE kev REGION

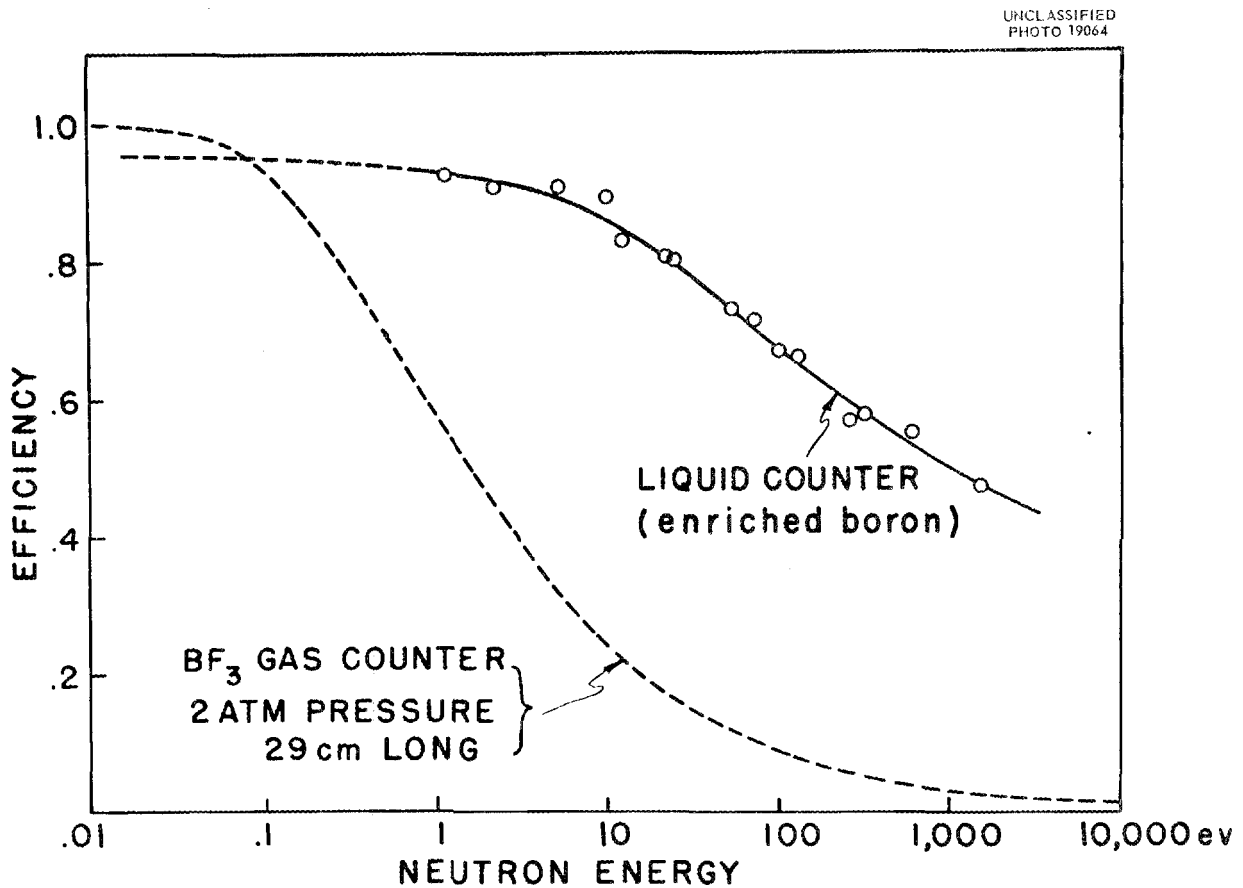
R. E. COTÉ (Argonne National Laboratory): The usefulness of the fast chopper is confined to the lower part of the kilovolt region, so I will talk about that part below 100 kev. The reason for this is that the resolution width increases as $E^{3/2}$. We can compete with Van de Graaff work over most of the region below 25 kev.

During the last five years, however, the resolution of choppers has improved, I think by a rather large factor, from about 1 $\mu\text{sec}/\text{m}$ to about 0.04 $\mu\text{sec}/\text{m}$; shortly 0.01 $\mu\text{sec}/\text{m}$ will be available. Besides resolution, there have been two problems which have further limited the usefulness of the existing choppers in the kilovolt region.

One of these is concerned with the structure of rotors, the other is a detection problem. Some of the materials which have the required strength

properties have neutron resonances which introduce structure into the open beam shape in the kilovolt region, thus making it difficult to interpret the structure due to the sample. More recent designs do not have this disadvantage, however.

The detection problem is this: BF_3 counters have been used extensively by the chopper groups. The efficiency of these counters is about 1% at 10 kev, while being nearly 100% at 1 ev. At Argonne we have used a liquid scintillation detector, developed by Muehlhause and Thomas, which has an efficiency of about 30% at 10 kev (Slide 1). It has been convenient for us to work in the kilovolt region, while this has not been the case for other groups. A glance at BNL-325 shows that about four-fifths of the data in the kilovolt region produced by choppers were taken at Argonne.



Slide 1. Comparison of the Efficiencies of Liquid and Gas Counters.

This has been due largely to this detection advantage.

Along with improvements in time-of-flight systems came improved techniques aimed at obtaining resonance parameters, so that major emphasis lay on work in the low electron-volt region, where this analysis could be applied, and the kilovolt region was left largely alone. The resolution available at present still does not permit one to obtain resonance parameters for many resonances in the kev region. The resonances in manganese and sodium are just about the only ones. However, the resolution of choppers has improved enough so that one can see much structure in such elements as arsenic and scandium, where just a few years ago their cross sections were represented by straight lines in the kilovolt region.

Interest in the "cloudy-crystal-ball" model of the nucleus led to studies of the variation of the "strength function," Γ_n^0/D , with mass. The Brookhaven fast-chopper group compiled data which showed that one of the predicted maxima did exist. At Argonne we studied the elements which lay in the mass region in which another maximum was predicted. This meant that elements of mass near 50 had to be studied. The levels of such nuclei are widely spaced, so that most of the resonance structure lies in the kilovolt region. It is for this reason that one block of kev-region data obtained by choppers is for elements in this mass region.

The other mass region in which choppers have contributed is that of the very heavy nuclei, such as uranium and plutonium. Data obtained on these elements are of the type discussed this morning, in which one observes only fluctuations in cross section due to the statistical distributions of level spacings and widths. Since, as we heard yesterday, there exist difficulties in the interpretation of some things in the electron-volt region, a bit of attention has been turned to the kilovolt region for this kind of work. Values of the strength function have been obtained from kilovolt-region data for these heavy elements.

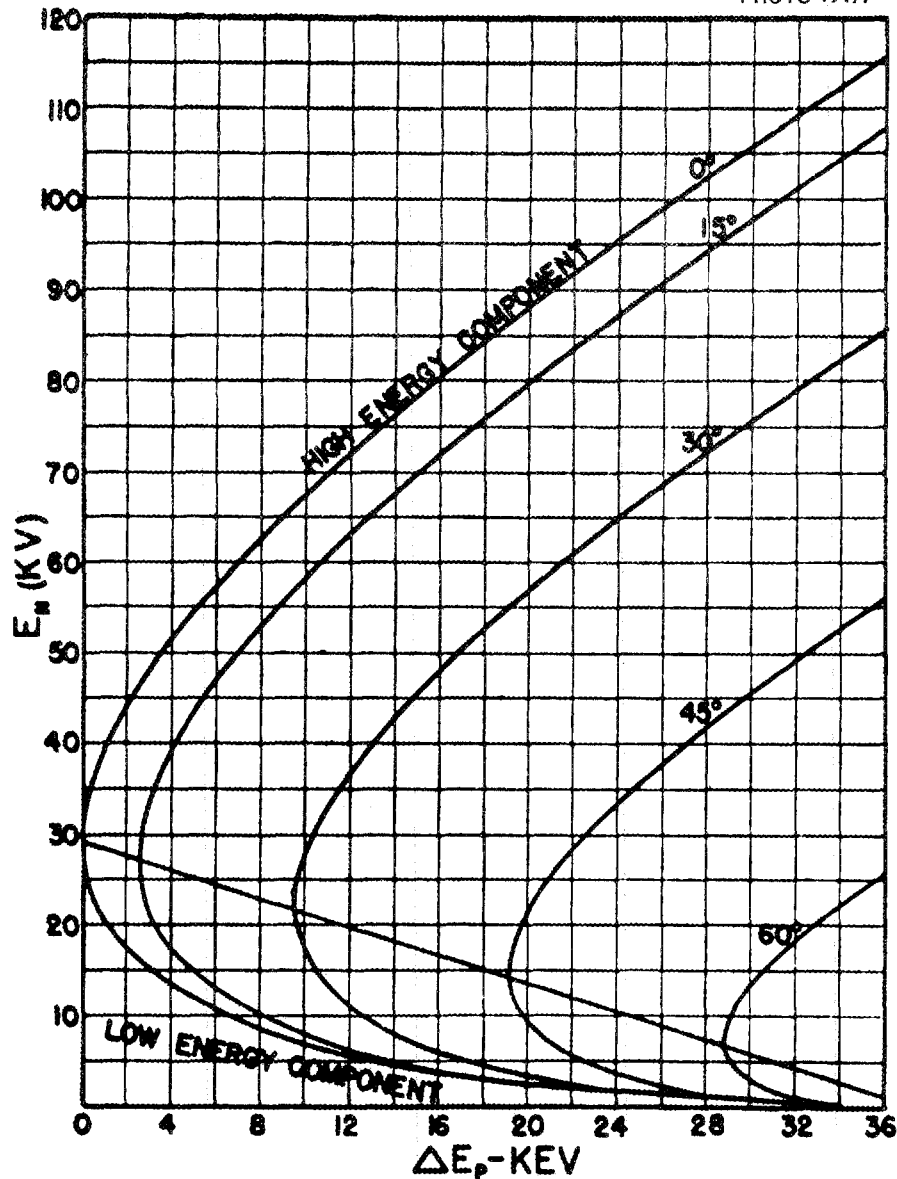
Due to the fact that samples as small as 5 mg may be used with choppers, isotopic identification of kilovolt resonances has been made in several elements through the use of separated isotopes. In addition, otherwise unresolved spectra can be resolved through the use of the separated isotopes, in some instances. The kilovolt-region resonance structure of chromium is an example of this.

So far I have referred only to total-cross-section work. The only partial-cross-section measurements that have been made are those on the fission cross section. At Argonne we have measured the fission cross section of Pu^{239} up to about 35 kev. These data were taken with poorer resolution than total-cross-section data because of intensity problems.

W. W. HAVENS, JR. (Columbia University): The self-detection technique we presently use at Nevis is only applicable to the measurement of resonances and cannot be used to measure average cross sections in the kilovolt region. The data on U^{238} and tantalum which I showed yesterday illustrate how this method can be applied to the kev region. Tantalum has an average level spacing of 4.8 ev and U^{238} an average level spacing of 18 ev. These data show that we can clearly resolve levels 1.3 ev apart at 225 ev and less than 10 ev apart at 600 ev. This gives an experimental resolution of about $0.01 \mu\text{sec}/\text{m}$. Thus at 1 kev we should be able to resolve levels separated by 10 ev, and at 10 kev we should be able to resolve levels separated by 300 ev. It should be possible to improve the resolution by a factor of ten, which would mean the resolution of levels separated by 3 ev at 1 kev and by 100 ev at 10 kev. Other methods seem to be better above 10 kev. We intend to study the resonance structure of all the elements available up to an energy where levels are just separable. The maximum energy studied will, of course, depend on the level spacing of the element.

J. H. GIBBONS (Oak Ridge National Laboratory): As you may know, we are using a pulsed-Van de Graaff millimicrosecond time-of-flight technique, involving a very short flight path and high repetition rate. For cross-section measurements in the kev region, we use the lithium (p,n) reaction near threshold, in which two neutron energy bands are produced. The lower energy band of neutrons is employed without moderation as the primary source of neutrons for transmission studies by time-of-flight in the conventional sense. In a moment I will show what our resolution is in millimicroseconds per meter now, and perhaps later on we can indicate some hopes for the future.

The first slide shows the well-known lithium (p,n) reaction as a function of energy above threshold. One can see that for a given proton energy there are two neutron energy groups.

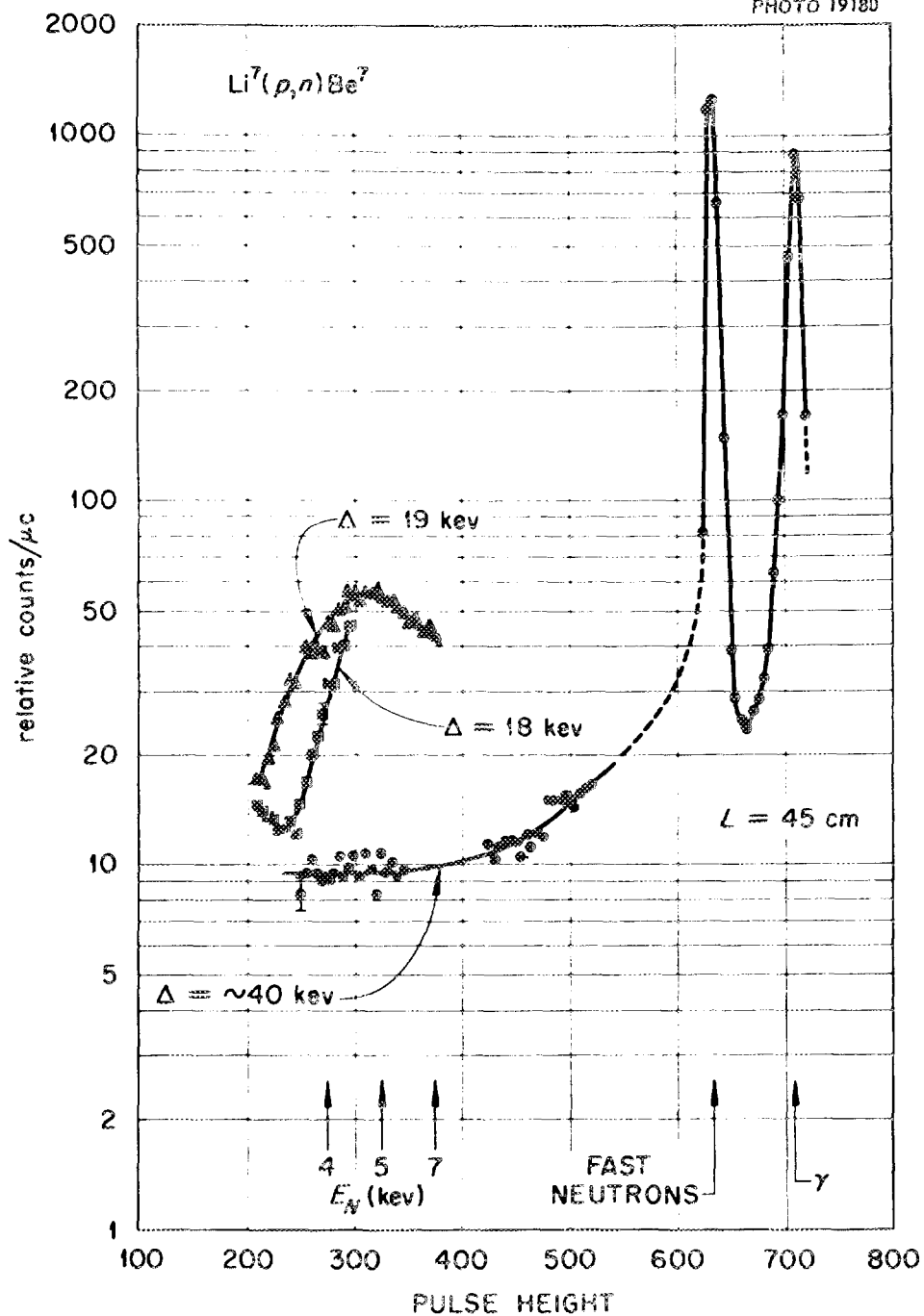


Slide 1. Neutron Energies from a Thin Lithium Target as a Function of the Difference Between the Bombarding Energy and the Threshold Energy for Various Angles of Emission in the Laboratory.

We have measured on a very modest program, coincident with development work, a few total cross sections to see what we might be able to do in the range from 5 to 30 kev.

Slide 2 illustrates how one runs into a new problem of Van de Graaff control. For instance, this is the spectrum found above the 90-deg threshold, where the low-energy neutron groups have disappeared and we simply see the high-energy groups.

This affords a very nice way of finding out what magnitude of background is present. One lowers the proton energy to give neutrons of the desired energy range. For instance, if we want neutrons at about 5 kev, we go to about 19 kev above threshold. However, a shift of 1 kev of proton energy at 1.9 Mev will change the spectrum by a large amount. Thus we have to use an in-out type of measurement, where we rotate in to out about every 2 min in order



Slide 2. Spectrum of Neutrons from Li⁷(p,n)Be⁷ at 18, 19, and 40 keV Above Threshold. Pulse Height Corresponds to Time of Flight.

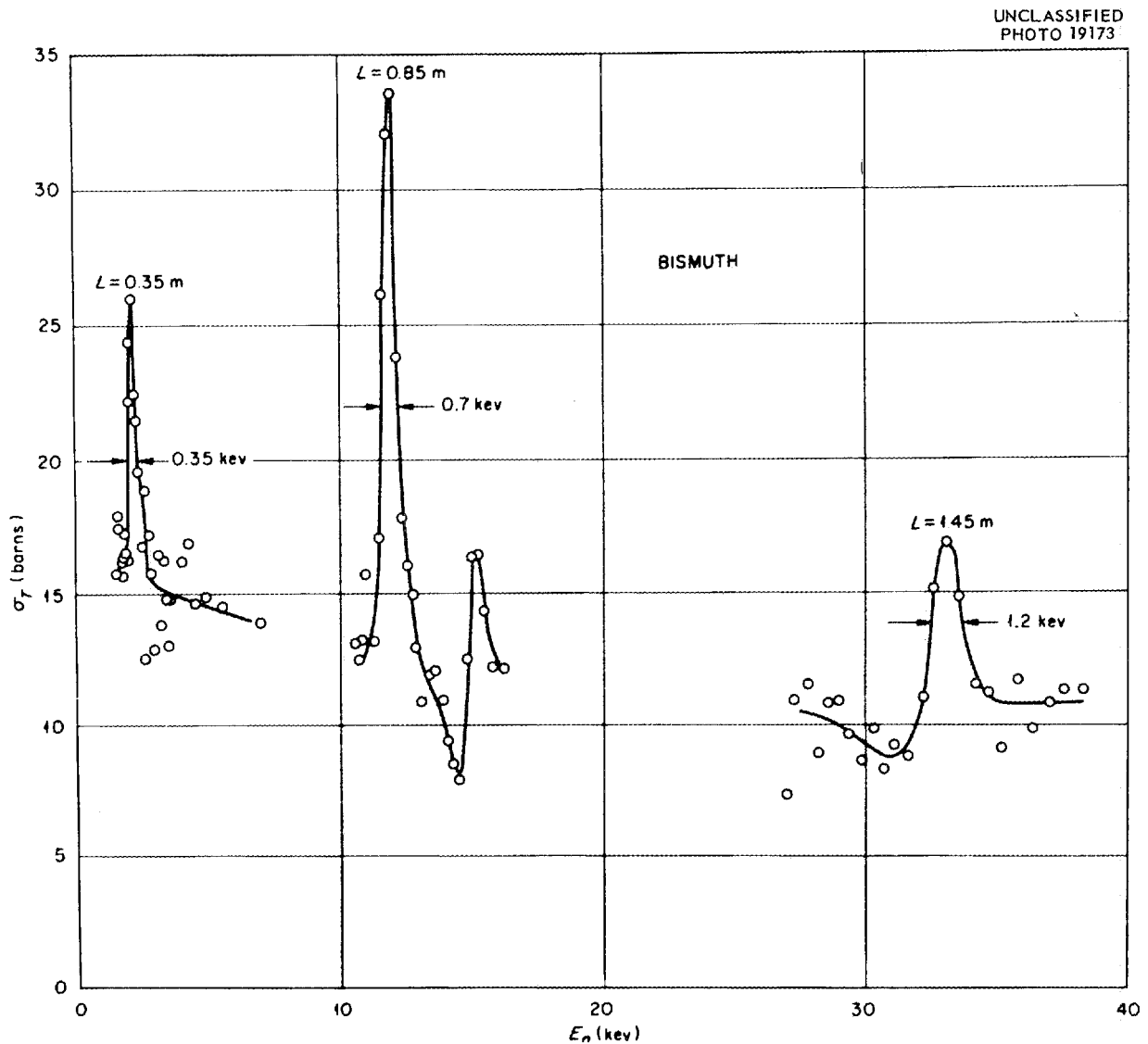
to cancel any slowly changing spectrum shifts due to any one of several causes.

Slide 3 shows the bismuth cross section we measured about a year ago to see how we compared with Henry Newson's work at Duke. There is good agreement up to 35 keV. The resolution at low energies, as evidenced by the resonance at 2 keV, was improved considerably over the Duke work.

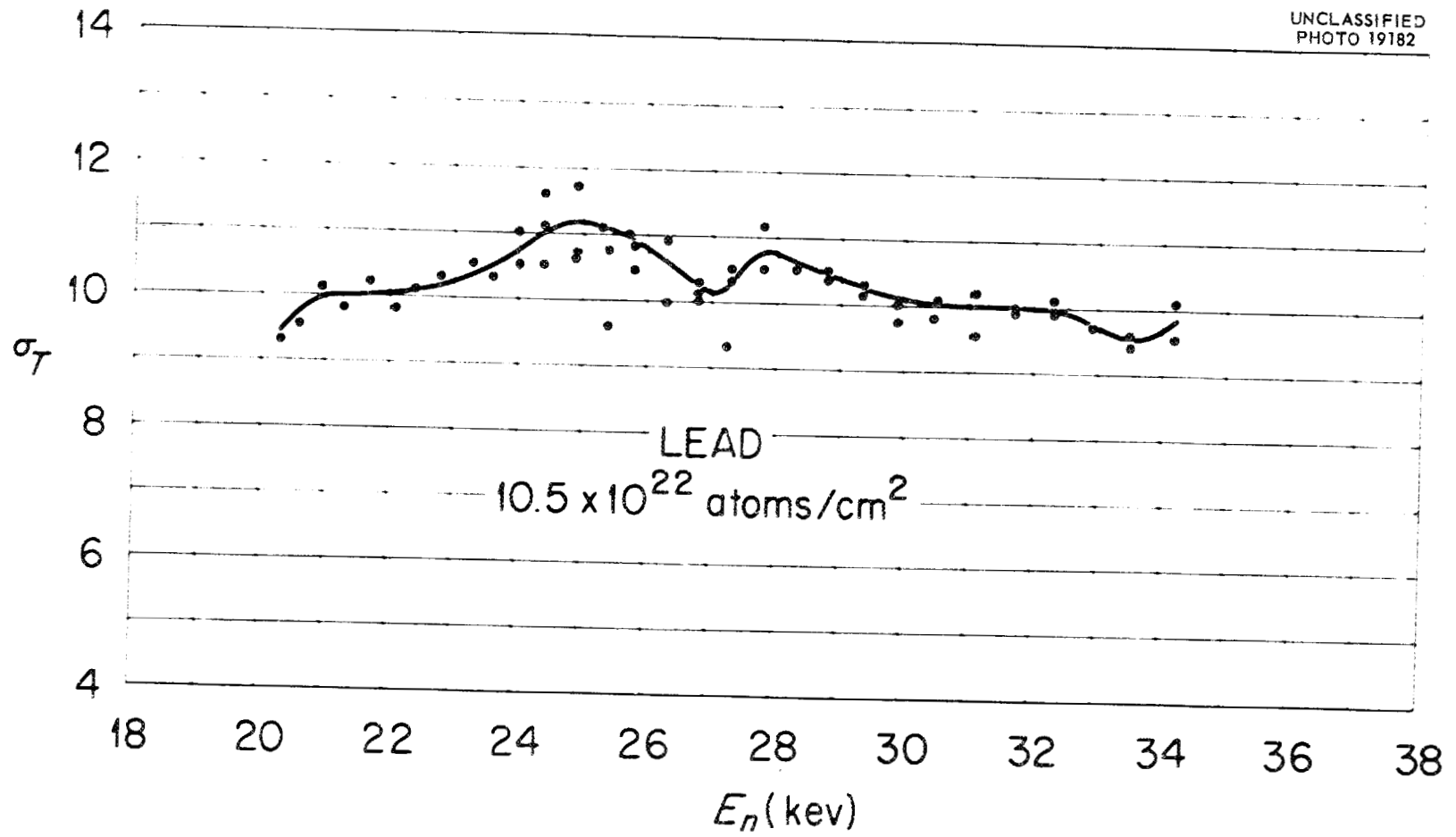
Slide 4 is a look at lead. The Advisory Committee wanted us to take a look at this because at Duke were seen what appeared to be small variations in the cross section in the low kilovolt range.

The sample was quite thick, as you see, and, indeed, there do appear to be some very funny variations in the cross section. Our having better resolution didn't seem to do much to the widths of these variations.

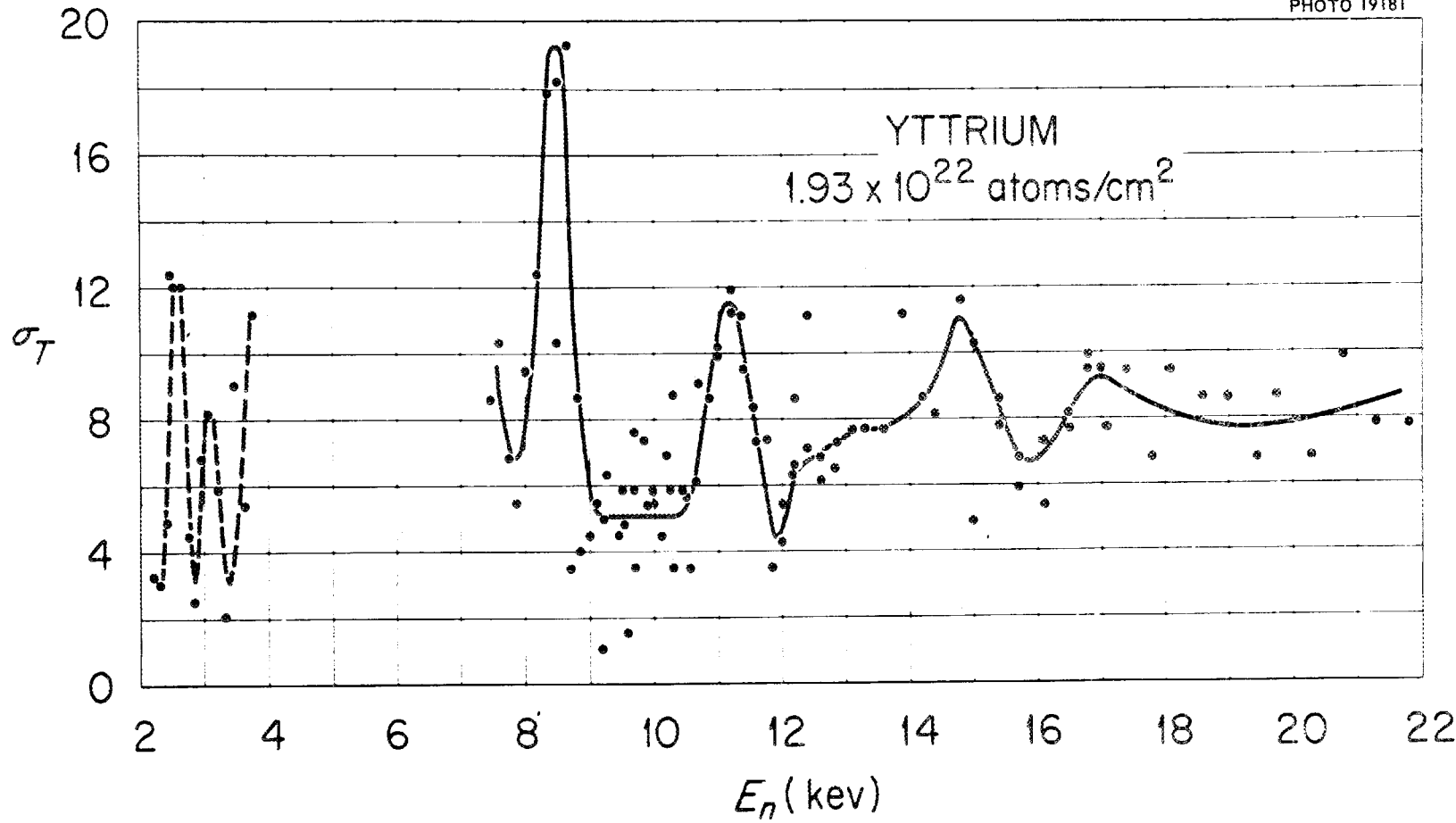
Slide 5 looks like somebody took a shotgun and fired at the page. This was due to some instrumental difficulty. Note that the yttrium sample was quite thin. The low-energy points are preliminary data which were taken with very poor statistics and thus are dotted. We did a rough area analysis of the 8.5-keV resonance, and the



Slide 3. Total Neutron Cross Section of Bismuth as a Function of Energy.



Slide 4. Total Neutron Cross Section of Lead as a Function of Energy.



Slide 5. Total Neutron Cross Section of Yttrium as a Function of Energy.

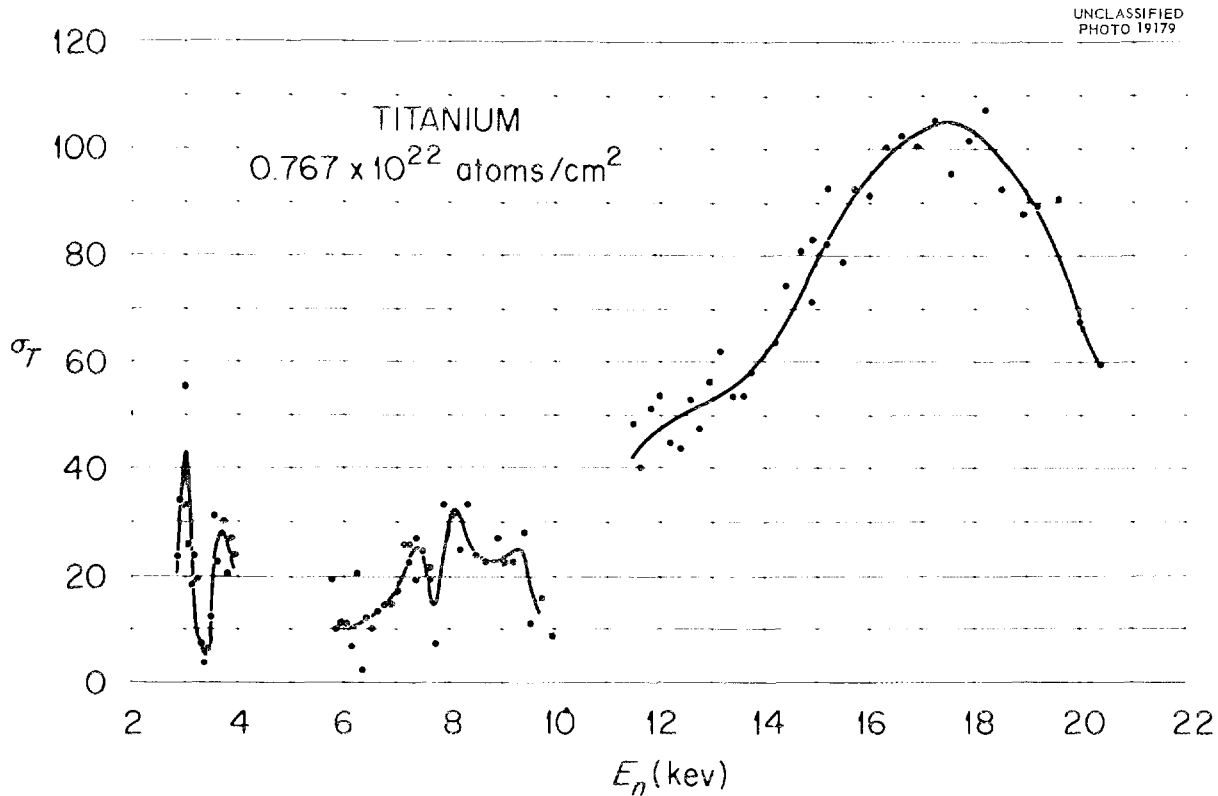
$\sigma_0 \Gamma^2$ is about 7×10^5 barns \times ev², which means it has a total width on the order of 100 ev for $g = \frac{1}{2}$ or 50 ev for $g = \frac{3}{4}$. The resonance at 11.2 kev has a width of the order of 70 ev. The 11.2-kev peak is probably $J = 0$.

Slide 6 is the total cross section of natural titanium. The doublet at 3.0 and 3.7 kev has been observed by both the Argonne fast-chopper and Langsdorf groups. Their data, I believe, show a double-hump maximum with a small dip between. It appears as though we have resolved, or rather separated, the levels to where we get back to potential scattering between the two. The variations between 6 and 10 kev appear to be riding on the tail of a very large resonance at 17.5 kev, and are due in all probability to the minor isotopes. The principal isotope, Ti⁴⁸, obviously causes the 17.5-kev resonance. The observed width of this

unusually wide resonance is 7 kev. The peak observed cross section, corrected for isotopic concentration and potential scattering, is about 130 barns, or about 90% of the theoretical value. The reduced width of 52 ev is 1% of the single-particle width.

The peak at 3 kev must also be due to Ti⁴⁸, since if it were due to Ti⁴⁶ our resolution would have to be considerably better than obtainable at present. Assuming it is due to Ti⁴⁸, its width is of the order of 20 ev. Titanium obviously needs study with separated isotopes.

Slide 7 is the cross section of selenium from about 4 to about 9 kev. Previously only one broad maximum had been observed in this region. It now appears that the maximum is composed of at least five individual resonances. The peaks at 4.25 and

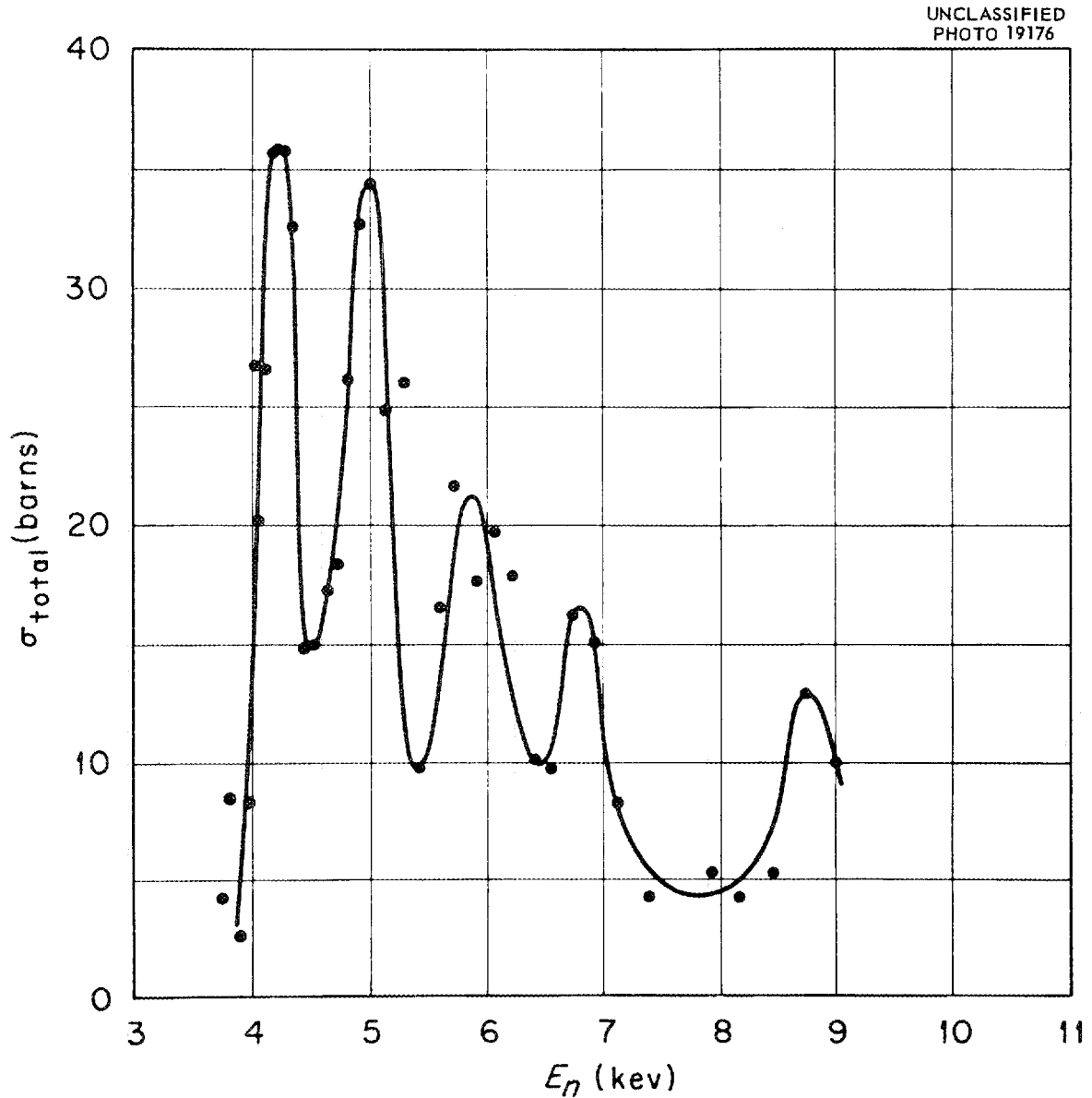


Slide 6. Total Neutron Cross Section of Titanium as a Function of Energy.

4.95 kev both have total widths of about 35 ev. Again, however, work with separated isotopes is badly needed.

A final word about future plans is in order. We could conceivably try to consider what could be achieved by the method just described if a Van de Graaff were to be developed exclusively for this

application. Such considerations would involve going back to the ion source itself, and we have no idea of such a pursuit. However, with our present Van de Graaff we are achieving 15 $\mu\text{sec}/\text{m}$ at 5 kev, and 10 $\mu\text{sec}/\text{m}$ seems just around the corner. Anything much better than this seems unlikely with present equipment.



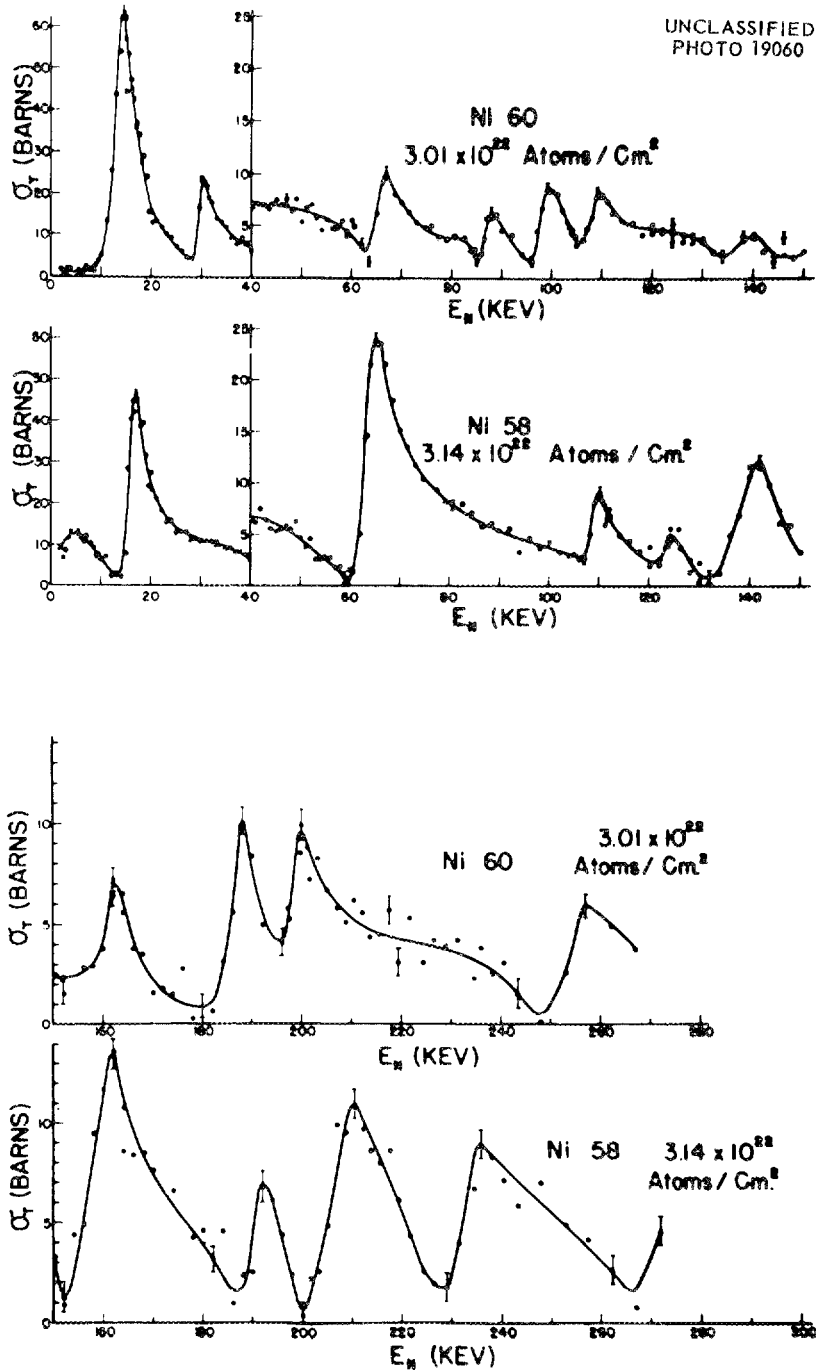
Slide 7. Total Neutron Cross Section of Selenium as a Function of Energy.

H. W. NEWSON (Duke University): I appreciate the concession which allows the unclean to mix with the clean, and I will review very briefly what one can do and what the limitations are of the Van de Graaff method of resolving resonances.

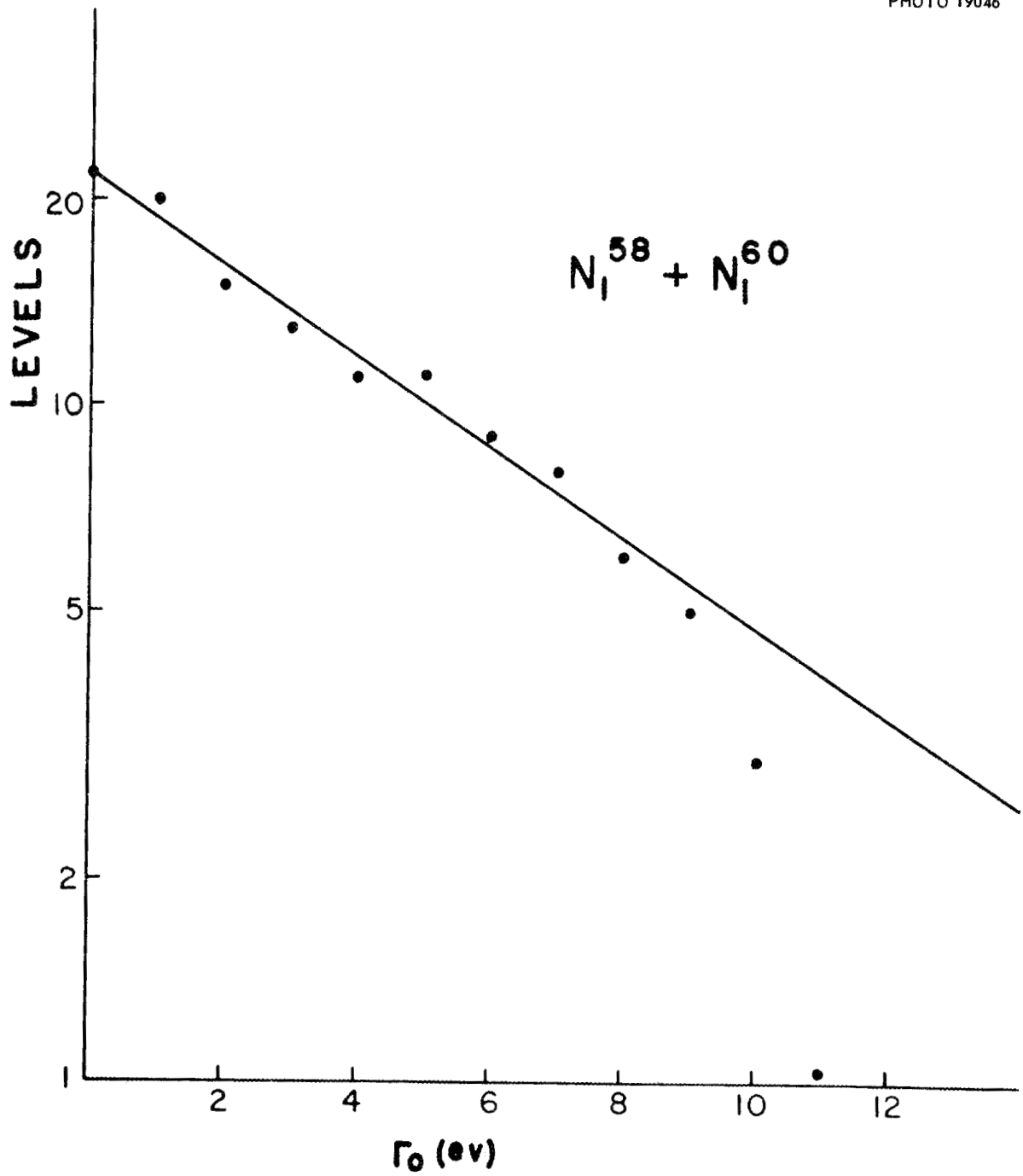
Slide 1 represents the kind of spectrum with which we have been most successful. The average spacing of these resonances is about 25 keV. Most

of them show the asymmetry of a typical *s* resonance. In Slide 2 we have plotted the number of nickel levels above a certain reduced width. One sees a roughly exponential behavior, as is to be expected from the low-energy work.

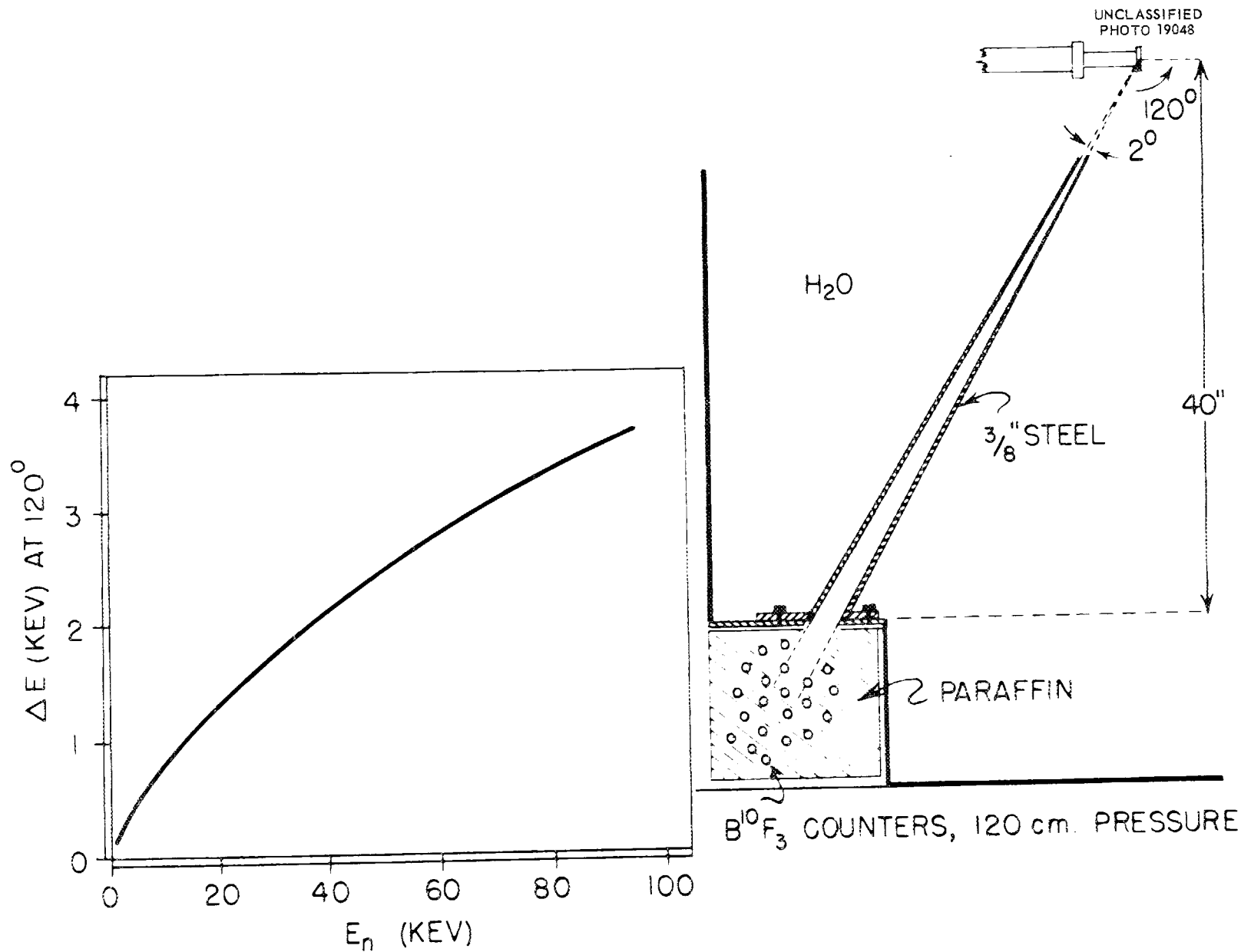
Slide 3 is just a schematic sketch of our apparatus. The proton beam impinges on a lithium target and produces neutrons through the $\text{Li}(p,n)$



Slide 1. Total Neutron Cross Section of Nickel as a Function of Energy.



Slide 2. Frequency of Widths Greater Than Γ_0 as a Function of Γ_0 .



Slide 3. Apparatus and Energy Resolution of the Original Duke University Neutron Spectrometer.

reaction. We count the neutrons through the 120-deg collimator with an efficiency of $\sim 50\%$. At the left of Slide 3 is approximately the neutron-energy spread which we get. This energy curve is calculated from the angular acceptance of the 120-deg collimator. Compared to time-of-flight devices, this is a very favorable curve as far as the flatness goes. Our energy spread increases at about $E^{1/2}$ rather than $E^{3/2}$. The line of our present development, which is well under way now, is to flatten this curve out further.

I will not now attempt to describe our newest apparatus other than to say it is essentially the same idea as our older equipment except that we are going to an angle of 150 deg instead of 120 deg (of the neutron with respect to the proton) and that we can vary the acceptance angle of the collimator.

In Slide 4 I have plotted what we think we can do with this new 150-deg equipment; the energy spread of the neutron beam (Δ) is plotted as a function of neutron energy for various temperatures and thicknesses (D) of lithium targets. (For comparison the corresponding spread for our apparatus at 0 deg is also plotted.) We have no plans as yet for cooling the lithium target; these lower curves are just there for advertising. I feel that the $D = 300$ ev curve is most practical. This curve roughly corresponds near 5 keV to the best chopper work, and we have a flat curve for resolution as compared to an extremely steep chopper curve. In fact the chopper energy spread is such a steep function of neutron energy that I would make a modest wager that, as far as resolving separate resonances goes, the favorable point for our method is above 10 keV and the favorable point for choppers is below.

Now if I may have a minute or two more I should like to show you a little unclean physics.

Slide 5 is the capture cross section of U^{238} , which was not measured with any of the collimating devices that I showed you. It was obtained from a straight bombardment method. The dotted line is the component of the capture cross section calculated from the Brookhaven parameters. You see, within the experimental error the lower energy points are pure s . What we do then is extend this curve and subtract it from the measured curve, and then the difference for most of this region is entirely due to the p wave. (A small d -wave correction, the lower right curve, was also subtracted off.) What we find is that Γ_γ/D for the p wave is equal to roughly a factor of two times Γ_γ/D for

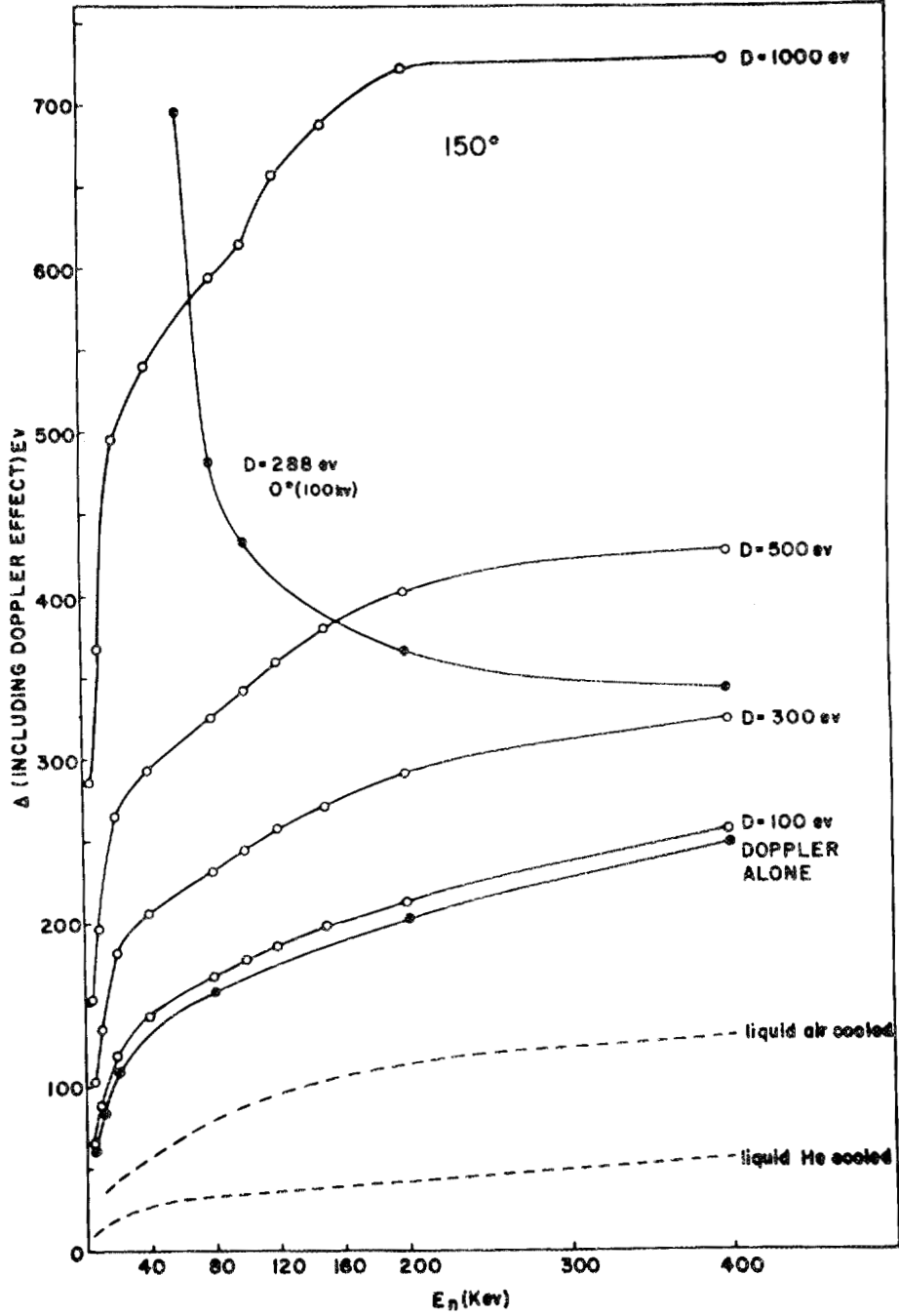
the s wave. That factor is not at all accurate, for several obvious reasons, but there does not seem any possibility that this number can be 1, and it is a fairly straightforward separation of the two components.

Slide 6 is a plot of Γ_n^0/D of the elements around iron, determined from total cross section measurements from 1 to 100 keV. The maximum seems to be about 4.5. If we average our results just for 30 keV we get higher values of Γ_n^0/D , similar to the results reported yesterday below 20 keV. We think that means that there simply are not enough resonances below 20 keV to give a decent statistical sample. This agrees with the observation of total cross sections.

R. B. DAY: How do you overcome the problem of neutron intensity fluctuations in the kilovolt region in order to get fission and capture cross sections?

H. W. NEWSON: I won't waste any time on this. The work I showed you was based on using a McKibben counter and hoping it was flat. I am glad that Dick Taschek isn't here, because there is much argument about a good way to fix this up. What we have done, which was based pretty much on what we had on hand, is the following: We placed a pair of BF_3 counters at 90 deg to the $Li(p,n)$ proton beam and placed a McKibben counter on the opposite side of the lithium target and also at 90 deg to the beam axis. Then we divided the counting rates of the two counters, divided by the velocity, and we got a flat curve up to 100 keV, meaning that, to the extent the McKibben counter is flat, $Li(p,n)$ has a $1/v$ cross section. Now there is probably some compensation of errors here. Probably neither is true, but probably both are true within 10 or 20 per cent. The next step is to use a hydrogenous counter of the Harwell type and compare these two cross sections at 100 keV. We have already used a 25-keV Sb-Be source to measure the cross section at 25 keV. This is a procedure that everybody seems to favor. Taschek thinks that lithium would be more accurate in the long run than boron for essentially the same procedure. My own feeling is that He^3 is the way to do this, that it is a good counter gas and does not have the disadvantage of using Sb-Be or the disadvantages of using solid lithium.

I think that, within the accuracy which I discussed, these data are all right, but to get down, say, to 2 or 3 per cent accuracy more work has to be done on standardizing.

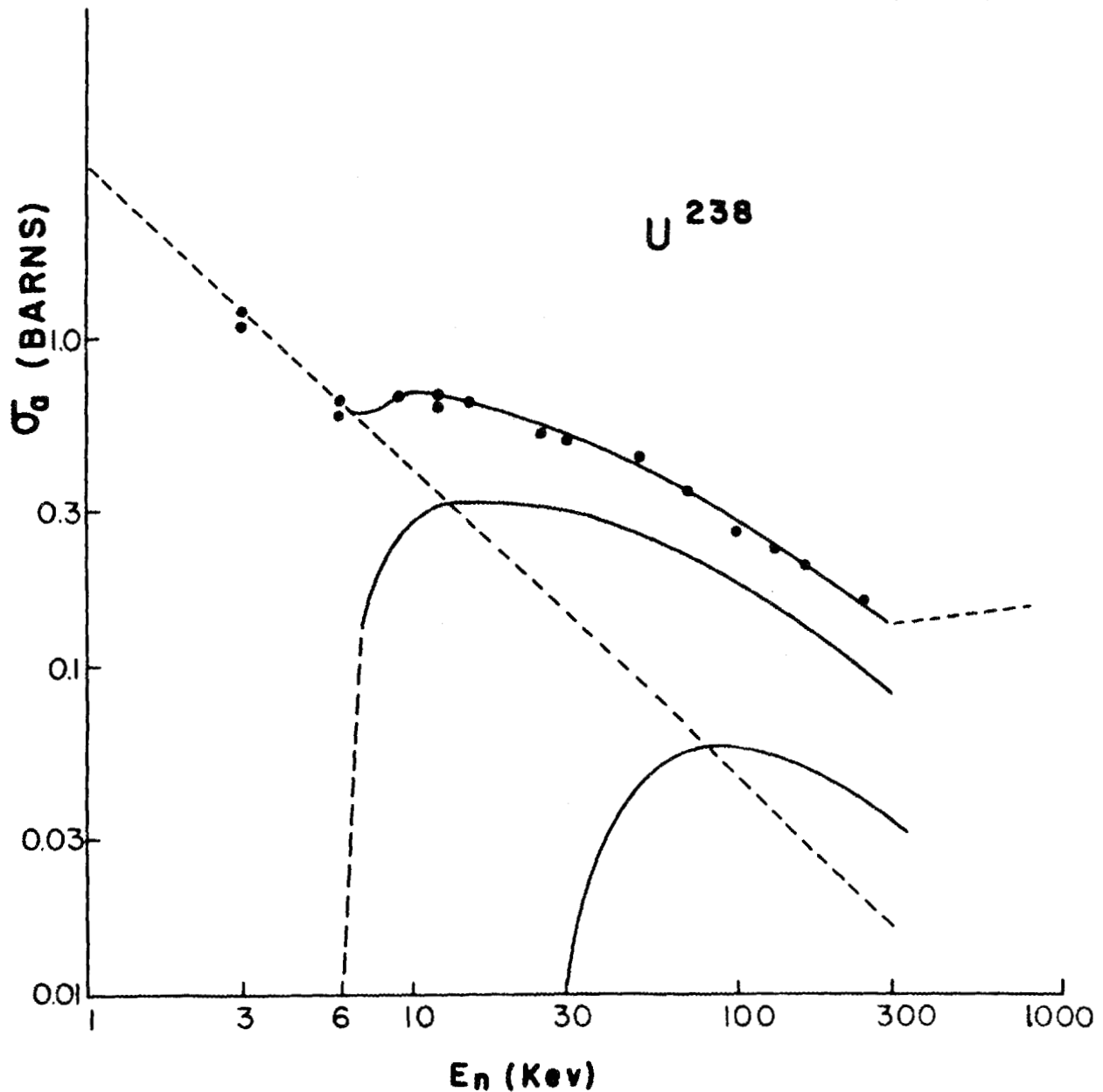


Slide 4. Energy Definition of Kilovolt Neutrons as Used in the Measurement of Neutron Total Cross Sections at Duke University.

L. A. TURNER: Picking up Henry Newson's figure, I will venture a couple of dirty remarks having to do with the Van de Graaff situation. I realize that their relevance may be dubious in view of the wonderful advantages that Cranberg has told us about. Nevertheless I am all wound up to say this, so I have to say it.

The business of exploring the whole energy region at high resolution with a Van de Graaff machine is tedious business, as anybody who has tried it knows. Perhaps that is now obviated, but at any rate I just merely want to mention some work that Langsdorf and his collaborators have done at Argonne, whereby they were able to take a

UNCLASSIFIED
PHOTO 19061

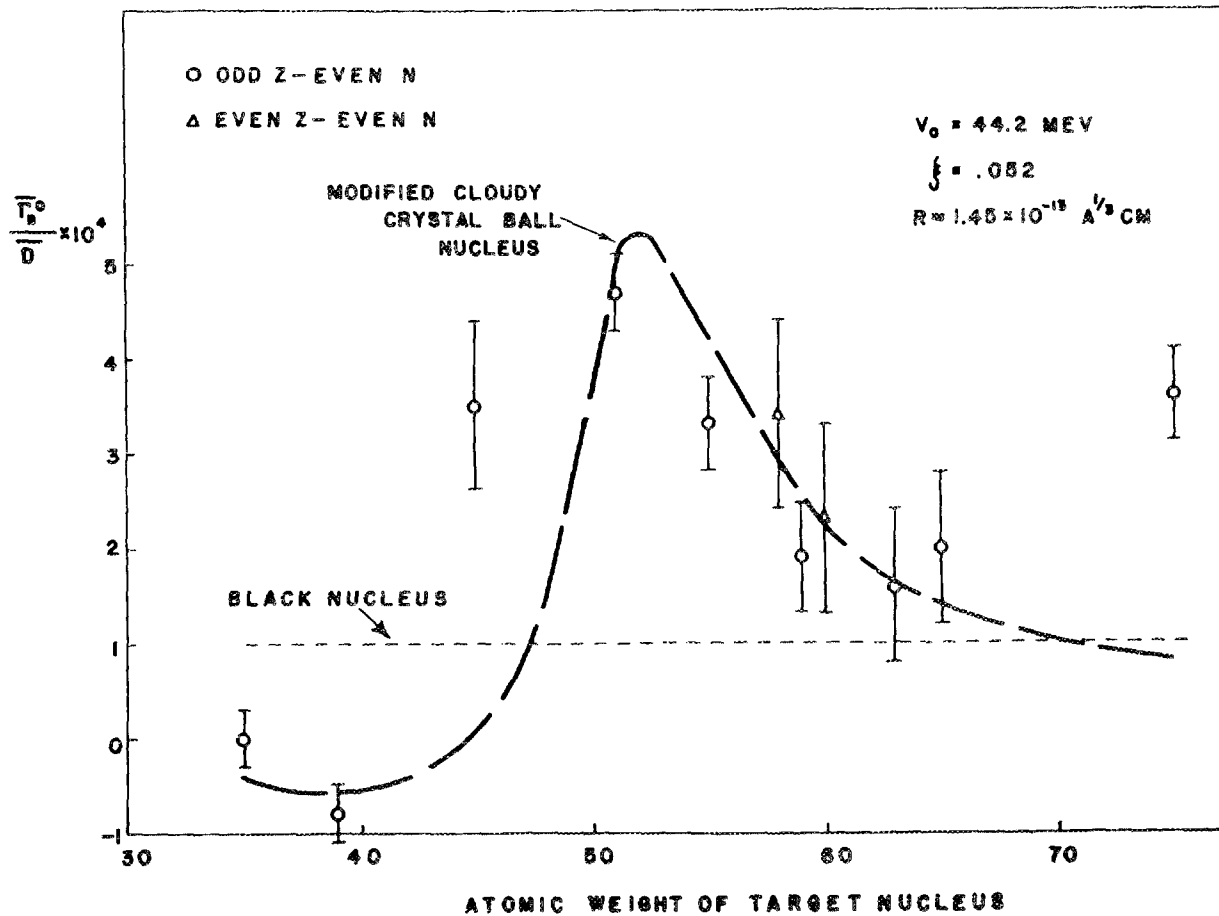


Slide 5. Capture Cross Section of U²³⁸.

rather quick survey look at some of these things in order to discover whether there was anything really to find out by going to as high resolutions as has been done with the self-detector. The detectors of neutrons that Langsdorf and his collaborators customarily use are scattering detectors. If the scatterer is a substance like carbon, which is a flat scatterer or an impartial scatterer, you get one set of results for the cross section. If, on the other hand, you use the same material for scattering as you do for taking the neutrons out

of the beam, then you may get higher values if the resonances are, indeed, separated for infinite resolution. If, on the other hand, they are so wide and so numerous and so messed up by the Doppler effect and one thing or another, there will be no difference. The difference, then, between what you get in self-detection and in flat detection gives you a very quick and dirty criterion for deciding whether there is anything worth looking at in detail.

UNCLASSIFIED
PHOTO 19062



Slide 6. Experimentally Determined Strength Functions Compared to the Prediction of the Complex Square-Well Potential Model.

THE OAK RIDGE NATIONAL LABORATORY FAST-CHOPPER PROGRAM

R. C. Block
Oak Ridge National Laboratory

R. C. BLOCK: I will give a very brief outline of the Oak Ridge chopper program. We have decided to make high-resolution total and partial cross-section measurements, that is, scattering, capture, and fission, over the energy range from 15 ev to 10 kev. In order to do these measurements successfully we have decided to build two separate choppers, and this means actually two separate rotors, housings, and everything else that goes with it.

Our first chopper, which we call the M1, will be a vertical-suspension rotor similar to the Brookhaven rotor, and we are shooting for a resolution of about $0.04 \mu\text{sec}/\text{m}$. The rotor will be machined in two halves out of age-hardened "K" Monel. It will consist of eight arms with 15 parallel slits per arm. The slits will each be 0.030 in. wide by 1 in. high. The rotor will be spun at 12,000 rpm, producing about $2\text{-}\mu\text{sec}$ -wide bursts. We will go to a 45-m flight path for this chopper and will employ a 256-channel magnetic-core time-of-flight analyzer with channel widths variable from 0.5 to $8 \mu\text{sec}$. A bank of 100 BF_3 counters of the MTR type, but filled to a pressure of 120 cm Hg, has been ordered for use as a detector.

This rotor, as I have said, is a parallel-slit-design rotor. This will produce intense, well-collimated

bursts of neutrons at our flight path of 45 m. We will wind up with a beam about 4 in. wide; therefore, we can do scattering experiments by placing our sample at the end of the flight path and placing our detectors alongside it. We expect to get rather good counting rates. We expect to achieve a counting rate at 1 kev of about 4000 counts per channel per hour in a $\frac{1}{2}\text{-}\mu\text{sec}$ channel at the LITR pile and a counting rate of about 27,000 counts per hour in a $\frac{1}{2}\text{-}\mu\text{sec}$ channel at the new ORR pile.

I want to just sketch what we hope to accomplish with this chopper. I said a resolution of $0.04 \mu\text{sec}/\text{m}$. This means that at 100 ev we will get a resolution of approximately 1.1 ev wide, at 1 kev we expect a resolution of 34.9 ev wide, and at 10 kev we expect a resolution of 1100 ev, which is overlapping Henry Newson's work at about 10 kev.

I will now describe briefly the M2 chopper, which is going to be in operation about a year from now. This chopper will have a resolution of $10 \text{ m}\mu\text{sec}/\text{m}$, and it will be installed at the ORR with a 180-m flight path. We are going to have an 18-in.-dia rotor producing about $1.2\text{-}\mu\text{sec}$ -wide bursts, and we expect a counting rate of about 120 counts per $\frac{1}{2}\text{-}\mu\text{sec}$ channel per hour at this resolution. We are having built right now a 2048-channel time analyzer to do this work.

ISOLATION OF CYCLOTRON BEAM BUNCHES FOR NEUTRON SPECTROSCOPY

J. E. Draper

Brookhaven National Laboratory¹

J. E. DRAPER: I should like to discuss a method of obtaining millimicrosecond pulses at a sufficiently low repetition rate that the resolution is not limited by the flight path. This was proposed at the New York meeting in January 1956. It was then decided to test the feasibility of this method with a minimum of equipment.

The method is to isolate one of the phase-bunched 22-Mev-deuteron beam bunches in the 60-in. cyclotron. First the arc is pulsed, as has been done in lower-energy-neutron work. Slide 1 shows the target burst with individual beam bunches at one r-f period separation.

Slide 2 shows the path of the beam at deflection radius. A single bunch is isolated by putting a pulse on the conventional deflector of the cyclotron.

Slide 3 is a block diagram showing how the deflector is pulsed in synchronism with the rf after a delay suitable for the bunches to reach deflector radius. The deflector pulse is now 15 kev by 50 μsec (the r-f period being 90 μsec) so that only one bunch is extracted.

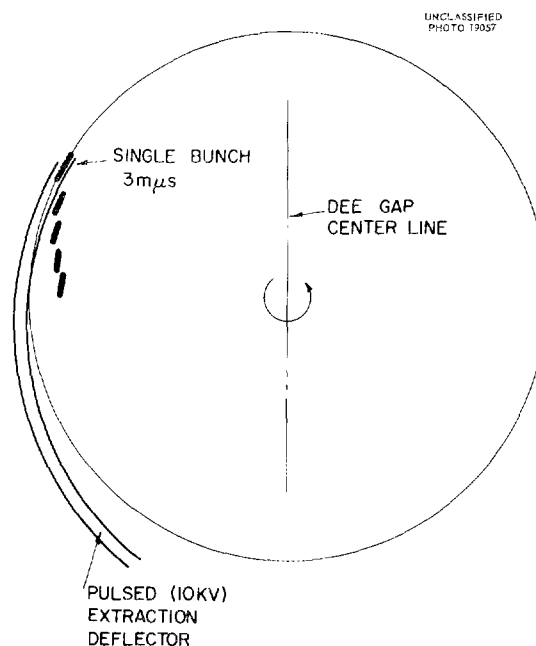
Although the deflector is large and of high capacitance, it is on the end of a coaxial line formed by the concentric dee stem and deflector stem and of about 70-ohm impedance.

Individual bunches have been isolated which are less than 5 μsec long. Each bunch is about 10 ma of 22-Mev deuterons, and the repetition rate (as now limited by the power supply of the deflector pulser) is 400 cps.

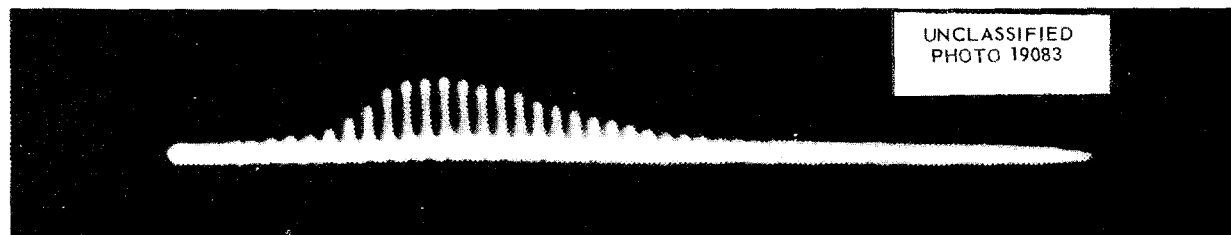
Slide 4 shows the counting rate plotted against flight time for gammas and for neutrons in a 2.7- to 25-Mev range. The gamma spike is clean and

symmetrical. The counting rate with a 1.5-in. plastic scintillator at 12.5 m is one pulse somewhere on this figure for every five cycles. That is just about as high a counting rate as the analyzer can accept, anyway.

The completeness of isolation of one bunch is here demonstrated — especially by the depth of the valley between gammas and neutrons (which would otherwise have contained the next beam burst).



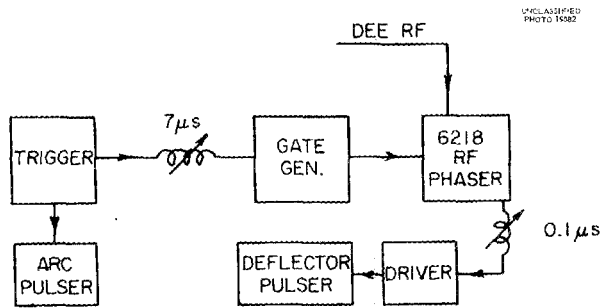
Slide 2. Radial Extraction of One Bunch.



Slide 1. Oscilloscope Trace of a Single Burst from the 60-Inch Cyclotron, Showing the Individual Beam Bunches.

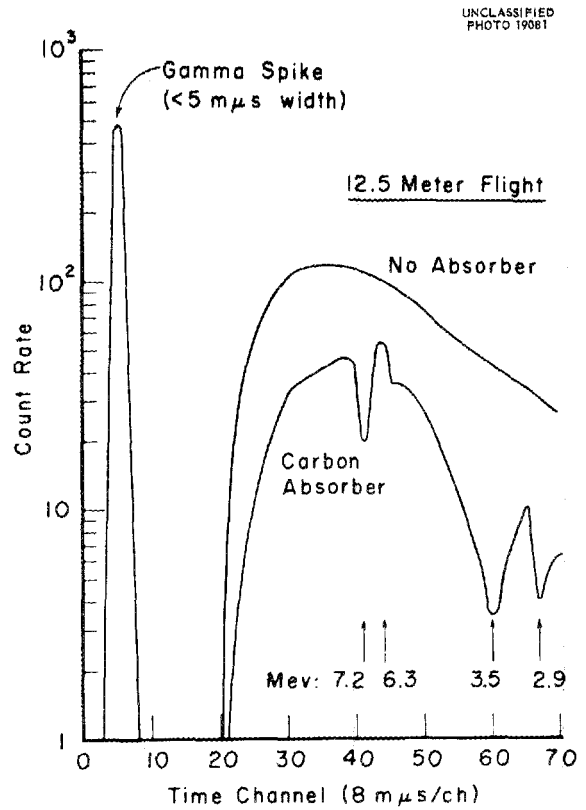
Several days have been devoted to the investigation of this method for kev-neutron spectroscopy. A paraffin moderator was placed at the target, which affects the resolution by adding a flight-path uncertainty of about ± 1 cm. The detector was a 2-cm slab of B^{10} viewed by a shielded 3×4 cm NaI crystal placed 10 cm from the center of the 6.5-cm-dia collimated neutron beam. The flight path was 440 cm. Pulses were accepted only from the 478-kev photopeak from B^{10} .

The resonances in fluorine at 50 and 100 kev were detected in a LiF absorber with a count rate of 0.5 count per minute per kev channel. However, there are strong background peaks of gammas at the cyclotron r-f repetition rate from beam bunches striking the internal structure of the cyclotron. Attempts to shield out this background have been unsuccessful because of the small space available between cyclotron tank and target. The above



Slide 3. Block Diagram of Deflector Pulsing Synchronizing Circuit.

Mev-neutron work indicates that, if most of the present beam could be piped to a target several feet from the cyclotron, this background could be substantially reduced. However, the strong divergence of the cyclotron beam is not favorable for efficient piping.



Slide 4. Counting Rate vs Time of Flight for Gamma Rays and Neutrons in the Energy Range from 2.7 to 25 Mev.

NEW SYSTEM FOR FAST-NEUTRON CROSS-SECTION MEASUREMENTS

L. Cranberg
W. P. Aiello

R. K. Beauchamp
H. J. Lang

J. S. Levin
J. E. Midgley

Los Alamos Scientific Laboratory

L. CRANBERG: I shall describe a system for measurement of total cross sections for fast neutrons at high resolution and high counting rate. "Fast" neutron means above 50 kev, "high resolution" about 1 kev or better, and "high counting rate" is in the neighborhood of 100 counts/sec. The basic features are familiar - that is, the detector is a proton-recoil device, and a lithium target whose thickness is 1 kev or less is used as a source of monoenergetic neutrons by the reaction $\text{Li}^7(p,n)\text{Be}^7$.

The distinctive features of the system are three. First, for the detector we use a thick hydrogenous scintillator at an extremely low bias, so that the system has a sensitivity as a function of neutron energy which is flat over a wide range, with an efficiency of about 50% in the flat region.

The second distinctive feature is the use of pulsed-beam time-of-flight technique to surmount the difficulties that arise from the use of a thick scintillator. The reason the thick scintillator has not been used in the past for this kind of work is that it is sensitive to the gamma rays and to "wrong" energy neutrons which are produced in the reaction $\text{Li}^7(p,n)\text{Be}^{7*}$. By gating the detection system at the right time, one only sees those events which arrive at the detector at the time which is appropriate for a neutron of the correct energy.

The third distinctive feature of the system is the use of a technique we call "energy modulation," which enables one to obtain 100 energy datum points simultaneously, in effect, for a single energy setting of the accelerator. This is accomplished in the following way. The lithium target is insulated for high voltage, and a sweep voltage of 50 kev peak-to-peak is applied to it at 10 cps. We then have a "black box" into which we put a sample of the sweep voltage and the signals from the neutron detector. Signals from the neutron detector are converted to pulses whose heights are proportional to the instantaneous sweep voltage, so that out of the black box we get a pulse-height spectrum which is representative of the counting rate as a function of instantaneous

neutron energy. This spectrum can be presented on a 100-channel analyzer, and so we effectively get data at 100 points simultaneously, corresponding to a 50-kev energy interval, with a single energy setting of the accelerator. The procedure for taking data with this system is to run "sample in," "sample out," till adequate statistics are obtained on the data in each channel. The sample transmission is obtained by dividing one spectrum by the other, channel by channel. Thus the procedure resembles that for a chopper, with concomitant advantages.

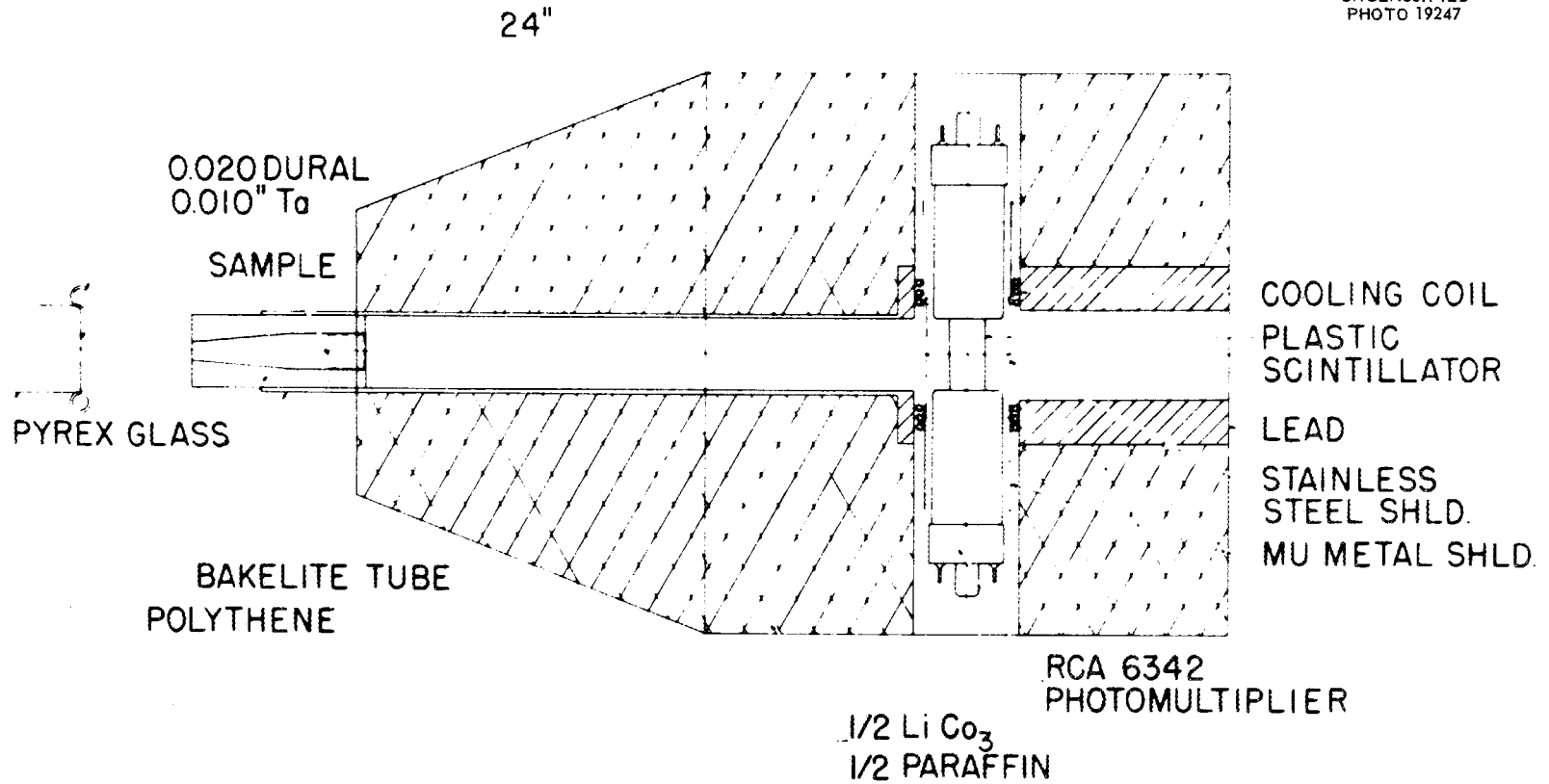
Slide 1 shows the geometry of the system. The flight path, 24 in., is necessary in order to separate the low-energy neutron group when the main neutron group is at 1.5 Mev.

The scintillator is viewed by two photomultipliers operated in coincidence to reduce the effect of photomultiplier noise. Also the detector is cooled to reduce the noise. This detector is flat down to 80 kev, and it has about 5% efficiency at 30-kev neutron energy. At the high-energy end, it starts to taper off above 1 Mev. The "cone-in" background is in the neighborhood of 1.5% of the "sample out" count at 585 kev neutron energy.

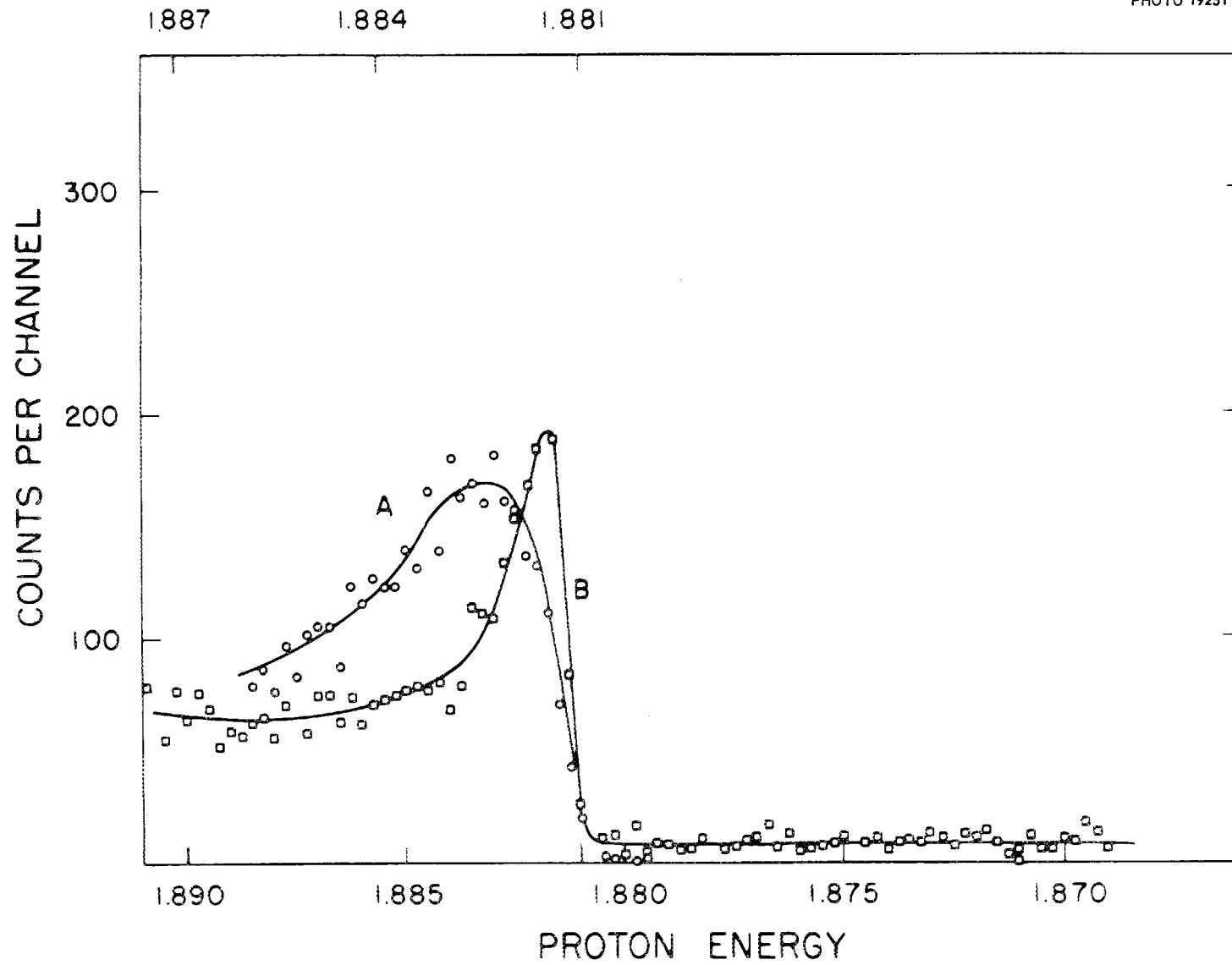
Slide 2 shows the effective resolution of the system by the rise in yield from a very thin lithium target. This is one of the simplest applications of the sweep principle. One curve, *A*, was taken with the 50-kev sweep, and the other curve, *B*, was taken with a 10-kev sweep. The latter corresponds to 150 ev per channel. We estimate that the stability of the machine and the target thickness amount to about $1\frac{1}{4}$ kev.

The first results are for the well-known resonance at 585 kev in sulfur (plotted in Slide 3), and this has been compared with careful work done by Peterson, Bockelman, and Barschall. We obtain the same peak cross section as they did and the same width, but this measurement required only about $\frac{1}{500}$ the time required for the earlier measurement, reckoned per datum point. The whole 50-kev interval with the statistics shown required about $\frac{1}{2}$ hr, but it could have been done more rapidly if

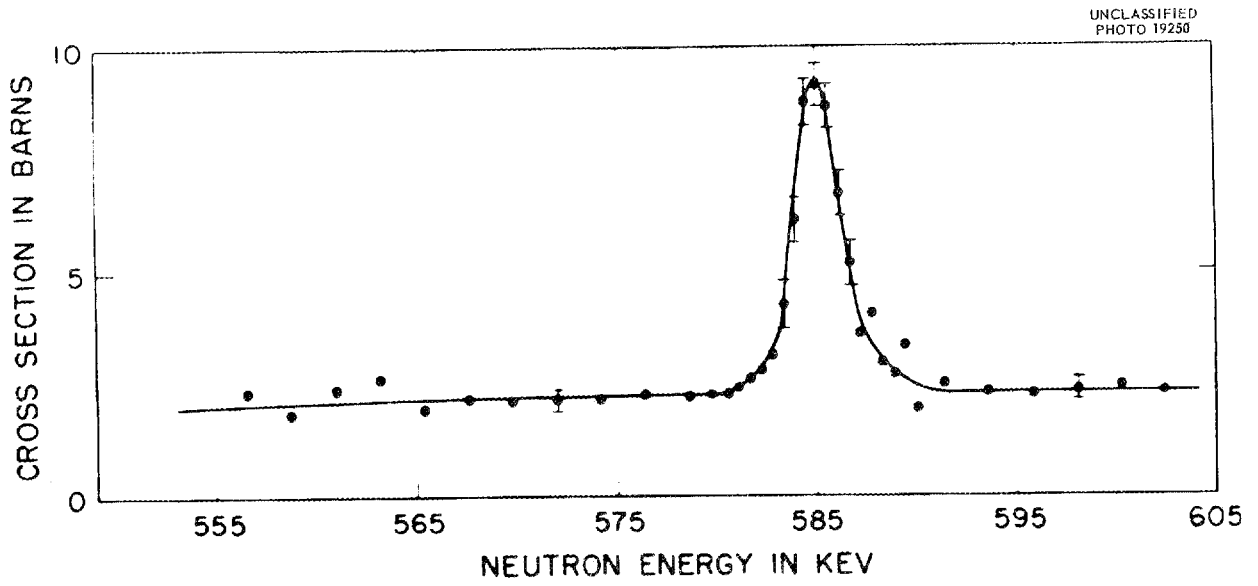
UNCLASSIFIED
PHOTO 19247



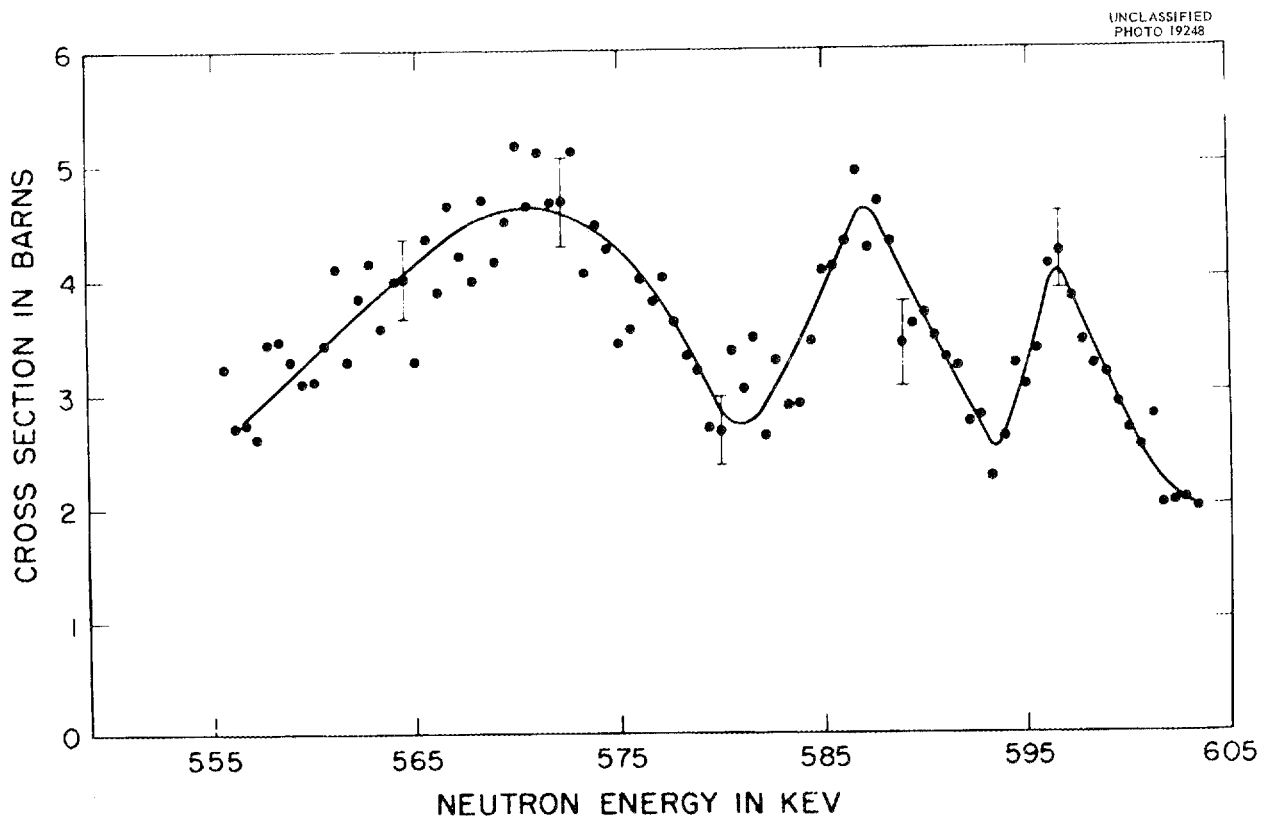
Slide 1. Detector and Shielding for Neutron Time-of-Flight Transmission Measurements.



Slide 2. Yield of Neutrons from a Thin Lithium Target in the Neighborhood of the $\text{Li}^7(p,n)$ Threshold.



Slide 3. Total Cross Section of Sulfur.



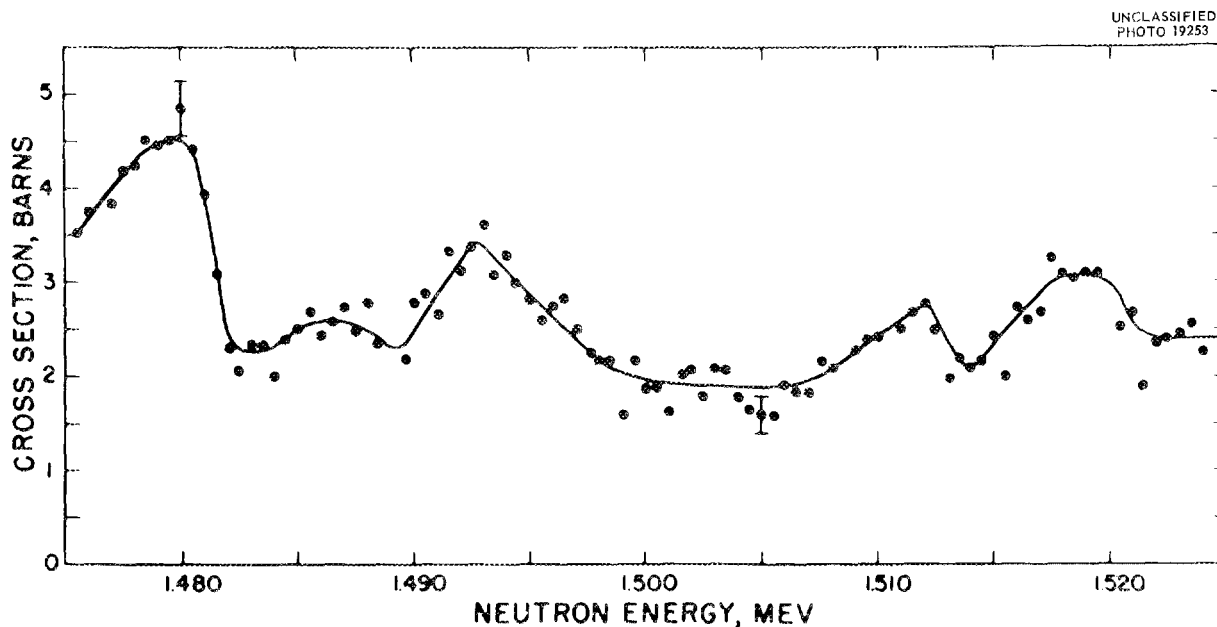
Slide 4. Total Cross Section of Aluminum.

the sweep amplitude had been reduced so that only the region of the resonance had been covered,

Slide 4 shows aluminum, run for 10 min. The smooth curve represents the results of three 10-min runs for a center energy of 585 kev. The broad resonance has been reported previously. Two additional ones are shown here.

Slide 5 is the result for iron at 1.5 Mev. The interest in iron was motivated by our scattering

work, and the result is pertinent to the question of the applicability of the Hauser-Feshbach theory of inelastic scattering to iron at 1.5 Mev. The large fluctuations in total cross section apparent here are consistent with the fluctuations we observe in angular distributions of inelastic scattering and suggest we are not satisfying the statistical assumption of the Hauser-Feshbach theory for iron at 1.5 Mev neutron energy.



Slide 5. Total Cross Section of Iron.

HARWELL SUPERCHOPPER

P. A. Egelstaff

Atomic Energy Research Establishment, Harwell

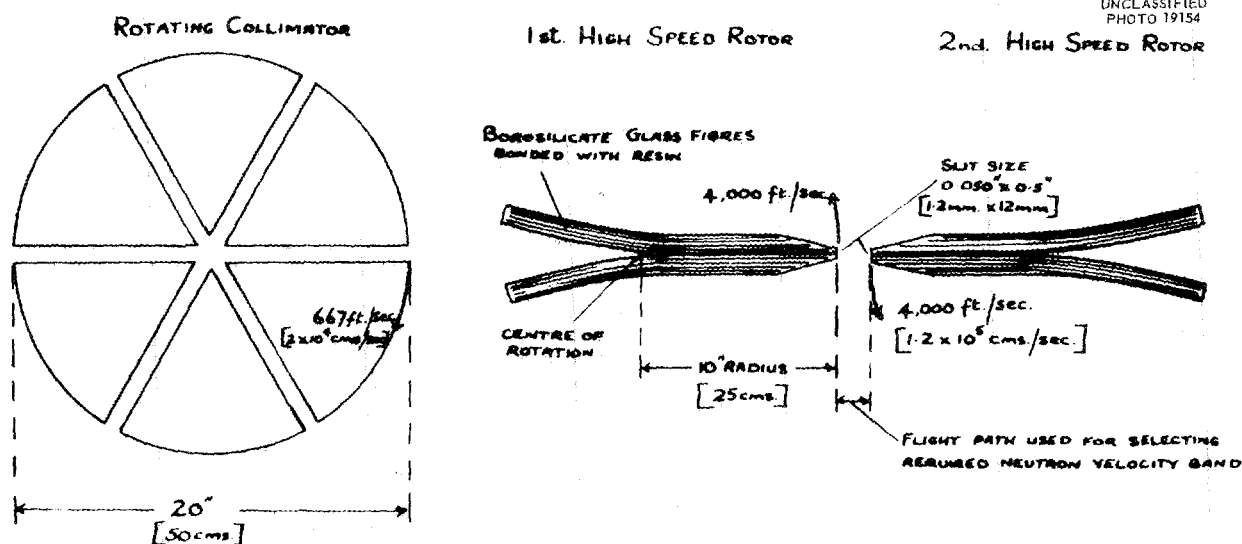
P. A. EGELSTAFF: I will omit such things as the size of the flight path, the details of the detector, the electronics, and so on, and tell you about the chopper apparatus only.

Slide 1 shows the principle. In this instrument we divide up the functions of a chopper. We have a rotating collimator which is a big, heavy disk with wide channels in it, and it rotates relatively slowly. From it you get wide pulses of neutrons. Then we have two high-speed rotors which take a very short pulse out of the wide one. We are trying to make use of the fact that if you use glass fiber longitudinally you can make a material with a much greater strength-weight ratio than high-strength steel. But it is strong only in the longitudinal direction, so we must use a rotor of the shape shown. We also assume that eventually we can phase two rotors together and so get a factor of two in chopping speed. In addition we should have the great advantage of doing some velocity selec-

tion in the gap between the rotors, thereby taking out that part of the neutron spectrum we want to study.

Slide 2 is a photograph of the actual high-speed rotor we have built. It is somewhat different from that shown in Slide 1, since that was drawn a year ago. The main structure is made of glass fiber, with the fibers running longitudinally. The wing across the center is made of steel and is added to give dynamic balance. The rotor ought to run at 48,000 rpm. We have done strength tests on the material to show that that speed is very feasible. It has not yet been tested at full speed.

Phasing tests on two rotors have been carried out up to 24,000 rpm. At this speed the short-period jitter between them is less than 2 minutes of arc. The resolution for the complete spectrometer will be initially 20 $\mu\text{sec}/\text{m}$, and then we hope to go down to 2.5 with the full development.



NOTES.

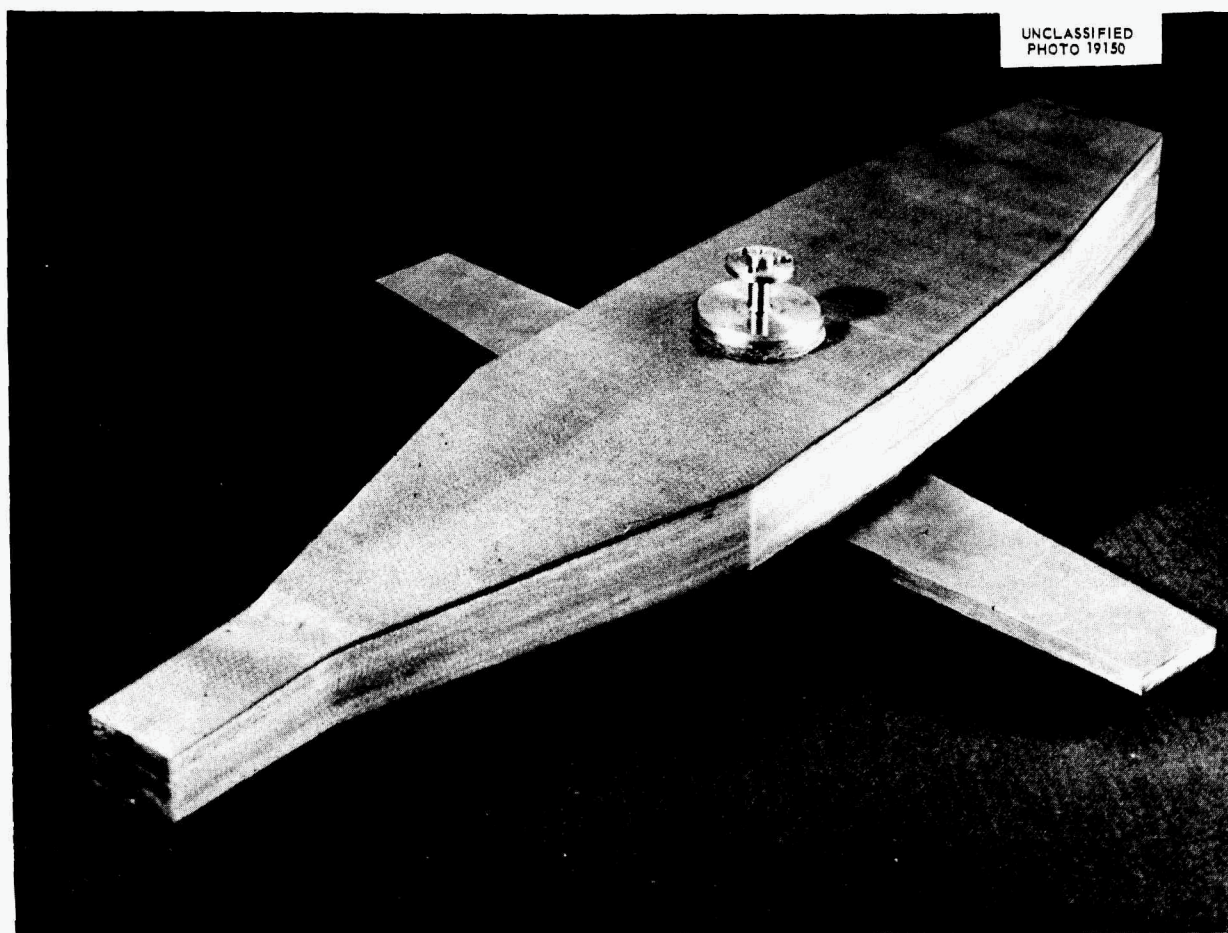
1. THE PRESENT ROTORS (1.2mm SLIT WIDTH) PROVIDE A 0.5 μsec NEUTRON PULSE, LATER ROTORS WILL BE DESIGNED FOR SHORTER PULSES DOWN TO 0.1 μsec .
2. THE WEIGHT OF ONE HIGH SPEED ROTOR IS APPROX. 3 lbs. [1.4 kg.]
3. THE ROTATING COLLIMATOR OR A HIGH SPEED ROTOR TAKEN ALONE WILL PASS NEUTRONS FROM 0.5 eV to ∞ .

Slide 1. Plan View of Superchopper.

Now I would like to discuss the philosophy of resonance measurements. In my opinion, the methods applied at the present time to the analysis of cross-section curves have gone as far as they permit one to go. They have come up against the difficulty of putting the proper level statistics into the analysis. Thus I think that one should use methods which start from the concept of a cross section averaged over several resonances; for example, the fluctuation method. When the mathematics of such methods is properly worked out, we shall be able to consider the limiting case of a cross section averaged over a little bit of

several resonances. This problem is the stumbling block at present. At the same time one should work with very great detail on a few isolated resonances to try to understand precise facts about resonance shape.

One of our future aims with the superchopper, probably about a year away at the present stage, is to use $2\frac{1}{2}$ - μ sec resolution at 1 ev. If you do that, you will get 1000 points in an energy span of 0.2 ev. From this we hope to obtain resonance parameters of rather good precision. Then we will be able to see whether these parameters predict the correct cross section away from the resonance.



Slide 2. Harwell High-Speed Glass-Fiber Rotor.

SESSION IV

EXPERIMENTAL AND THEORETICAL FISSION PHYSICS

ANOMALIES AND REGULARITIES IN FISSION

J. A. Wheeler
Princeton University

L. A. TURNER: It is a pleasure to have John Wheeler here to tell us about the latest anomalies and regularities in fission. John has been leading us by the hand down the way of wisdom with respect to fission for so long I can't quite remember when it began, but it was practically when fission was first heard of.

Without further ado, John Wheeler.

J. A. WHEELER: Three topics present themselves with special insistence: the question of level widths in fission, the question of channel analysis of the fission processes, and the question of the asymmetry of nuclear fission. Behind all of these and the analysis of them stands the circumstance that the fission process is perhaps more clearly a collective phenomenon than any other process of nuclear physics. It is evident when one has to deal with a split-up into two fragments of comparable size that one is dealing with something that is by no stretch of the imagination a single-particle process.

The justification for thinking that the incoming particle has formed a compound nucleus is essentially this: the time for a nuclear vibration of the order of 5×10^{-21} sec is so very long compared to the time of the order of 0.3×10^{-21} sec for a nucleon to cross the nucleus. This means that the particles have time to adjust themselves to the configuration of the slowly changing shape of the nucleus as it leads to fission.

I don't need to go into the well-known four principal ways by which the nucleus can be induced to undergo fission: by bombardment with neutrons or charged particles, by absorption of electromagnetic radiation, or by sitting in the ground state as in the case of spontaneous fission.

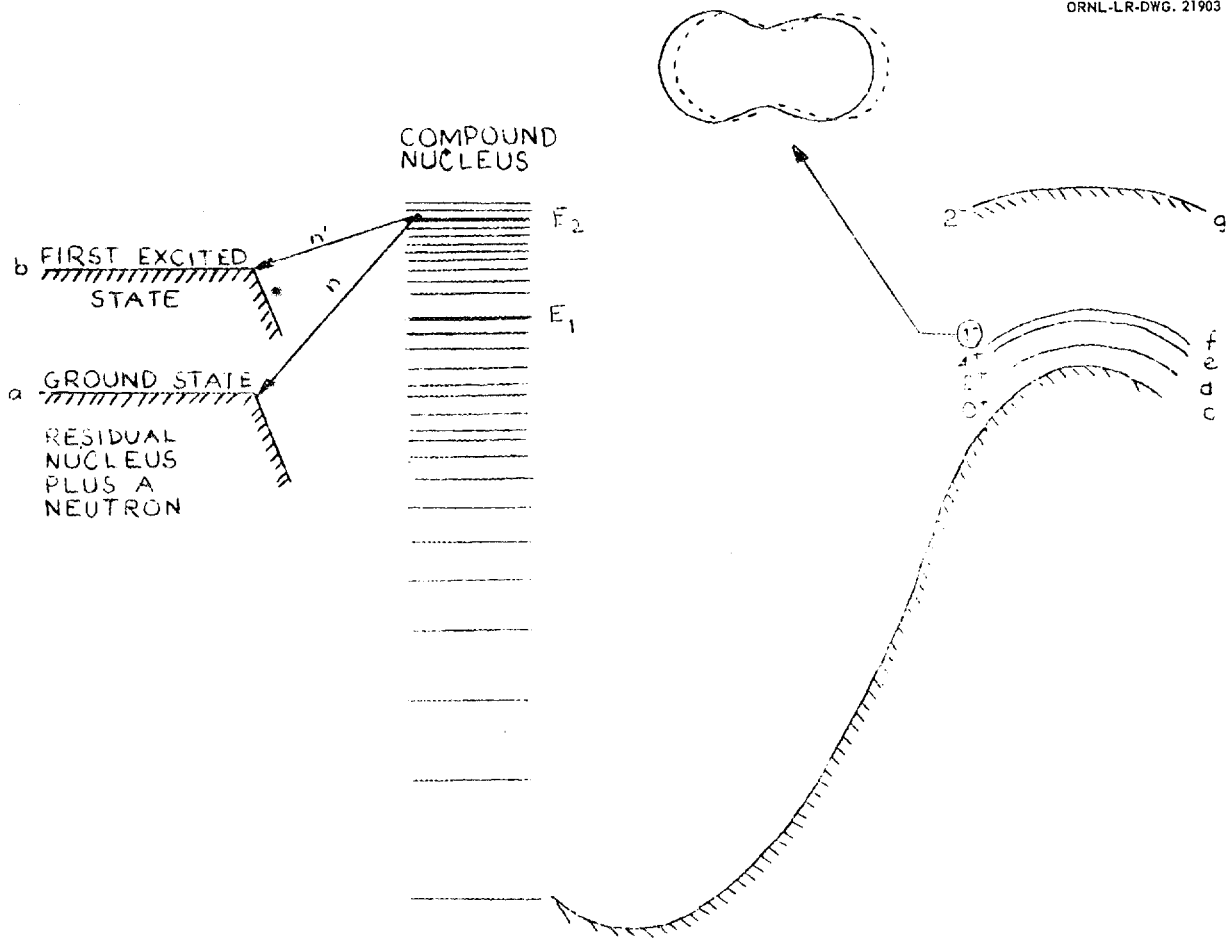
Let us consider the energy levels of the compound nucleus (center) compared to the barriers for neutron emission (at left) and fission (at right), as shown in Slide 1. When the compound nucleus is in the state of energy E_1 , neutron emission is possible only to the ground state of the residual nucleus, a . When the compound nucleus is more highly excited, to the state E_2 , two channels are open for neutron emission, leaving the residual nucleus either in the ground state, a , or in the first excited state, b . The probability for this neutron

emission process varies with energy as illustrated in Slide 2. The diagram drawn here (Slide 1) has to be considered to apply to levels of the compound nucleus of one well-determined spin and parity. For a different spin and parity, the energy-level pattern will differ for the compound nucleus but will remain unchanged for the residual nucleus.

In addition to neutron emission, we know that there is competition from de-excitation by gamma-ray emission to lower levels and finally from the process of the greatest interest here now, passage over a fission barrier leading to fission. There is a fairly well-defined division between two ideas – one of passage over the barrier, which we might call the key step in the process of fission, and then later on in the game an actual splitting into two parts, that we might give the name of scission.

The curve at the right, for fission barrier as a function of the deformation coordinate, α , applies to the case where the compound nucleus is even-even and has the character 0^+ . For fission the probability does not cut off sharply when the excitation of the compound nucleus drops below the barrier height. Instead it is 0.5 at the top of the barrier and approaches zero exponentially in the manner of a typical barrier penetration process when the energy is substantially below the barrier height, E_F . The curve of energy as a function of deformation indicated by c in the diagram corresponds to the ground state of the "intrinsic" or characteristically nucleonic state of motion of the system. Without changing this intrinsic state of motion, one can excite collective states of rotation of the system which put it into a level with angular momentum 2^+ , or 4^+ , or 6^+ , etc.

Also with a small additional expenditure of energy one can excite the lowest mode of pear-shaped deformation (inset at top of Slide) to its first vibrational state. The nuclear fluid, if one wants to use simplified terms, sloshes back and forth, and the oscillatory motion is no longer in its lowest state but in its first excited state; this gives rise to the odd parity that we have here. In this odd parity state the vibrational wave function is antisymmetric with respect to a rotation of the system by 180 deg. Consequently the rotation state must also be antisymmetric, and the system

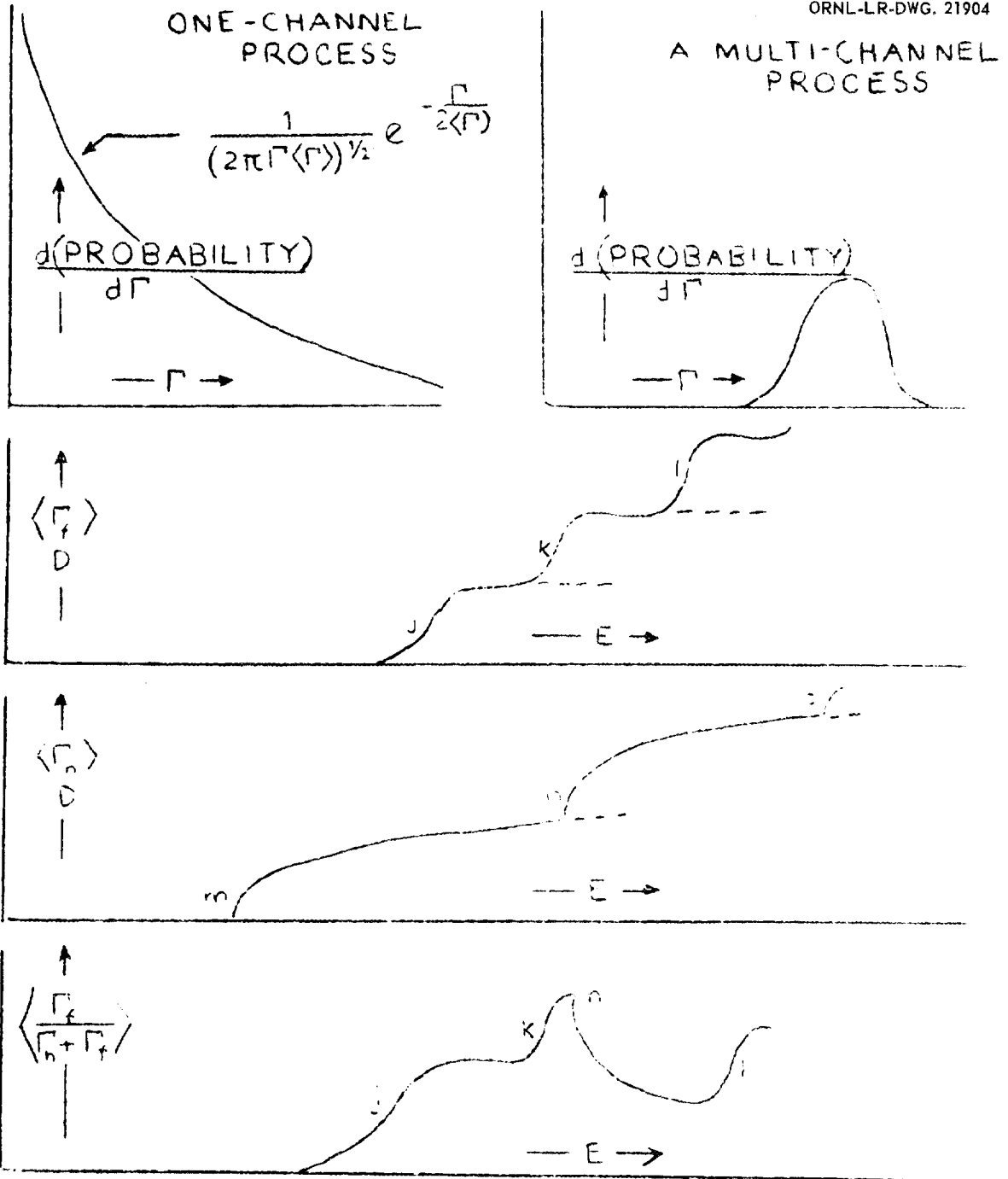


Slide 1. Energy Level Diagram for a Fissile Nuclide.

is restricted to the rotational states 1^- , 3^- , etc. The corresponding potential barriers against fission, indicated in the diagram by the letters d , e , f , really ought not to appear on a diagram that purports to describe fission of a compound nucleus in the 0^+ state. However, the appropriate barrier (a few tens of kev above 0^+) does govern the rate of fission when the compound nucleus is prepared instead in one of the states of character 1^- , or in one of the states 2^+ , or 3^- , or 4^+ , etc. When instead the compound nucleus is prepared in an incompatible state, such as 2^- , on which one can again build a whole family of rotational levels, fission is impossible via the lowest "fission" channel. However, the transition-state nucleus can exist also in one or another excited intrinsic state, characterized by a higher energy and generally altered angular momentum of the specifically

nucleonic state of motion. The diagram illustrates at g the fission barrier associated with an intrinsic excitation of the character 2^- (perhaps ~ 1 or 2 Mev above 0^+).

The state of the compound nucleus that is formed under slow-neutron bombardment will have a spin which can have one of two values. If we take the assignment of the spin of $\frac{7}{2}^-$ for U^{235} , then, of course, it is clear that from this we could build up a spin of either 3^- or 4^- for the compound nucleus. Let's consider the case, then, where the compound nucleus is formed in the 3^- state. Then out of this whole picture that appears to the right of Slide 1 most is to be thrown away. Only that part of the picture to the right is relevant which bears the designation 3^- . Actually nothing bears such a designation here. The 3^- state will sit just slightly higher than the 1^- state, and it is this



Slide 2. Probability Distribution for One-Channel and Multichannel Processes. The lower three curves show variations of $\frac{\langle\Gamma_f\rangle}{D}$, $\frac{\langle\Gamma_n\rangle}{D}$, and $\left\langle\frac{\Gamma_f}{\Gamma_n + \Gamma_f}\right\rangle$ vs E .

barrier which has to be surmounted, then, to lead to fission. But this is a relatively low barrier.

If, on the other hand, the compound nucleus is formed in the 4^- state, then this barrier for the 3^- state is quite irrelevant to the question of fission, and the barrier which in this case must be surmounted is a barrier which is built from the 2^- state by adding on the appropriate amount of rotational energy. The 4^- barrier may be 1 or 2 Mev higher, for instance, depending upon the circumstances.

From this it therefore follows that one might very well offhand expect rather different fission to take place for the compound nucleus in the one or the other spin state, and one of our problems will be to see what we can say about the experimental situation.

As regards the channel-analysis point of view, we think of the gamma-ray process as occurring by way of a great many different alternative channels, the sum of which gives rise to the total probability of gamma-ray emission observed in typical neutron-capture processes. Those resonances, as we know, are typically fairly symmetrical. On the other hand, fission resonances, as we will hear, are often asymmetrical.

We can see some light in the understanding of this effect if we consider that a typical one-channel process should be given by a cross section which is the square of the sum of terms – the typical term having an amplitude factor which is slowly dependent upon energy, a resonance denominator, and a width term – coming to something of this form, where we have a collection of terms of this kind which has to be squared:

$$(1) \quad \sigma \sim \left| \frac{A_j e^{i\delta_j}}{E - E_j + i\Gamma/2} + \dots \right|^2 .$$

We may even have several such squares which have to be added together, if there are different spin states which contribute to the cross section which are incoherently related to each other. The important point is that one really has to add amplitudes of the separate levels, rather than intensities; so for a single-channel process one will be led to expect a curve for cross section as a function of energy which will be quite unsymmetrical in character.

However, if we talk not of the cross section for a single gamma-ray-emission process or for emission by way of a single fission channel but of a process such as gamma-ray emission altogether, where we add up the contribution of a great many such terms, then we expect the phases that come into these several terms to have a random relationship to each other (at least this is not an unreasonable expectation); and, when we add a long column of such terms together, then we do expect to get out of that a curve for the total cross section for radiative capture which will show the familiar symmetrical resonance. But we recognize that this symmetry is a consequence, then, of the great number of channels which we deal with and that there is no reason we should expect such a symmetry for a single-channel process such as the process of fission is. This is one important point that we should therefore think of in raising the question whether the observed asymmetries are really anomalous in effect. The argument presented here is that these asymmetries are not to be considered as anomalies.

As Dr. Lane has already discussed also, there is another consequence of the difference between a many-channel process and a one-channel process. In the one-channel process the probability of a given level width follows a curve like that shown in Slide 2. In a many-channel process the probability for this, that, or the other width, expressed as a function of the total width rather than the partial width for a given gamma ray, follows a curve of the shape shown in Slide 2 with a distribution which is much narrower percentagewise than the total width.

Now we have to discuss a little the distinction that is going to be very important between two quite different concepts of channel number. One is the concept that we have talked about, that comes from the statistical composition of probabilities due to several competing processes. The other is the N that comes into this formula for the fission width:

$$(2) \quad \frac{\langle \Gamma_F \rangle}{D} = \frac{N}{2\pi} .$$

A simple statistical analysis says that the fission width is related to the level spacing on the average (not for any individual level, but for the average of several fission levels) by a formula of this

kind, where N is the number of channels which are accessible, that is, the number of channels over which one can pass.

I won't try to give the derivation of this formula here, except to give a qualitative idea of what is going on behind the scene in the derivation. The idea is essentially that the compound nucleus is a complicated system. It represents points of that system moving around in many-dimensional configuration space, in a tortuous path determined by the energy surface in the many-dimensional configuration space. In that space there is a mountain pass which can be surmounted if the particle is clever enough and intelligent enough at the representative points to pass over those several points and go over in the direction of fission. The likelihood that this can happen depends upon the accessible region in this transition-state region. The accessible space in the transition-state region is, of course, zero if the energy is just exactly equal to the energy of the saddle point and rises as the energy increases above the saddle point.

Quantum-mechanically, that result appears this way: One counts the number of independent channels which are accessible — how many different barriers of this kind all have the same given spin, whatever the spin happens to be of the compound nucleus — how many barriers there are of that same spin for which the compound-state energy is sufficient to cross the barrier. That, then, is this quantity N .

Now, that quantity is really not going to make a sharp jump as the excitation energy of a compound system is increased. Instead of making a sharp jump, as one expects from classical arguments, it will instead rise with a penetration-factor curve. There is, after all, a certain finite probability of penetrating through the potential barrier, and this barrier-penetration formula is given by the expression

$$(3) \quad N = \frac{1}{1 + \exp [2\pi(E_F - E)/\hbar\omega]} ,$$

where this formula is really a little different from what one is accustomed to for barrier penetration. Ordinarily one sees e to the minus something or other for the barrier factor, and there is a factor that depends on how sharply the barrier is curved.

In Eq. 3, ω is a measure of barrier thickness (ω represents the circular frequency that would be

associated with collective vibrations of the compound nucleus about the transition point if the sign of the deformation potential were reversed). Any simple estimate that one makes of the fission barrier indicates a curvature near the top of the barrier very similar to that at the bottom of the barrier. What evidence one has indirectly suggests an energy of oscillation in this barrier, at the bottom, of $\frac{1}{2}$ to 1 Mev, and therefore a similar characteristic energy near the top, so that one knows within perhaps a factor of two the coefficient that enters into this penetration factor. So this, Eq. 3, is what the quantity N looks like according to a quantum analysis. The justification again holds in a similar way as each successive channel becomes available (see Slide 2, $\langle \Gamma_F \rangle / D$ vs E).

The probability of neutron emission, of course, shows no such barrier penetration. In this case the neutron width increases as the first power of the velocity of the escaping neutron, as indicated in Slide 2, $\langle \Gamma_n \rangle / D$ vs E .

One expects, then, the cross section for fission, which is governed by the competition between these effects, to go as $\Gamma_F / (\Gamma_F + \Gamma_n + \Gamma_\gamma)$. The average cross section for fission by neutrons one expects to go like this. One has to average after the quotient is formed, but the averages after the formation of the quotients are not very different from what one would calculate from the averages directly. So we can see from the qualitative behavior, just by looking at these two curves themselves without regard to the fluctuations, that a more precise analysis has to be considered.

There is no fission for energies below region j (Slide 2, lowest graph). Due to a barrier penetration, the probability rises exponentially with increasing energy, and it levels off. Then at k a new channel comes in. This new fission channel comes in, and fission probability again goes up. But then at n a neutron channel comes in that gives an unfavorable competition. This unfavorable competition knocks the curve down again, and then we go on up again as a new fission channel comes in at l .

This is the type of effect that one could have foreseen, perhaps, in the early days of fission theory, but no one was at that time prepared to take seriously the detailed consequences of this formula, least of all these definite jumps and these effects of individual resonances. One treated this previously always on a smeared-out

basis, and now one has come to learn from the results right here at Oak Ridge on U^{234} and U^{236} by Lamphere and Greene that there are really these wiggles in the cross section (Slide 3), and it appears reasonable to interpret them in this way. For instance, one of the drops in the case of U^{238} fission is a drop at the energy corresponding to the first excited state of the U^{238} nucleus. Well, so much for this channel analysis of fission as applied in qualitative terms.

To talk a little more about how things go, it is evident from this picture that the cross section for fission does not go really to zero anywhere, and that if one now looks more carefully at the structure here, getting out a magnifying glass, one will see, of course, individual neutron resonances, and some of these neutron resonances will show fission widths of appreciable size. Unfortunately, very little has been done yet to study fission widths of levels well below the fission barrier. I think this will be quite instructive in telling one about the nature of the fission barrier as more work is done on this point.

Leonard, at Hanford, has shown that the previously well-known capture level at 1.06 eV in Pu^{240} also shows some fission. The probability of fission is so small that one can say that the fission width of that level is of the order of magnitude of 10^{-5} eV. He will give us more details. If one puts this into the penetration formula, one finds a penetration probability which is quite low, much lower than one would expect from the distance below the top of the barrier. This, then, is an anomaly, and we don't understand the reason for the anomaly, that is, why this is so very low. I won't give the details of calculating how far below the barrier we are, and we are somewhat uncertain, but not uncertain enough, I think, to make this great discrepancy.

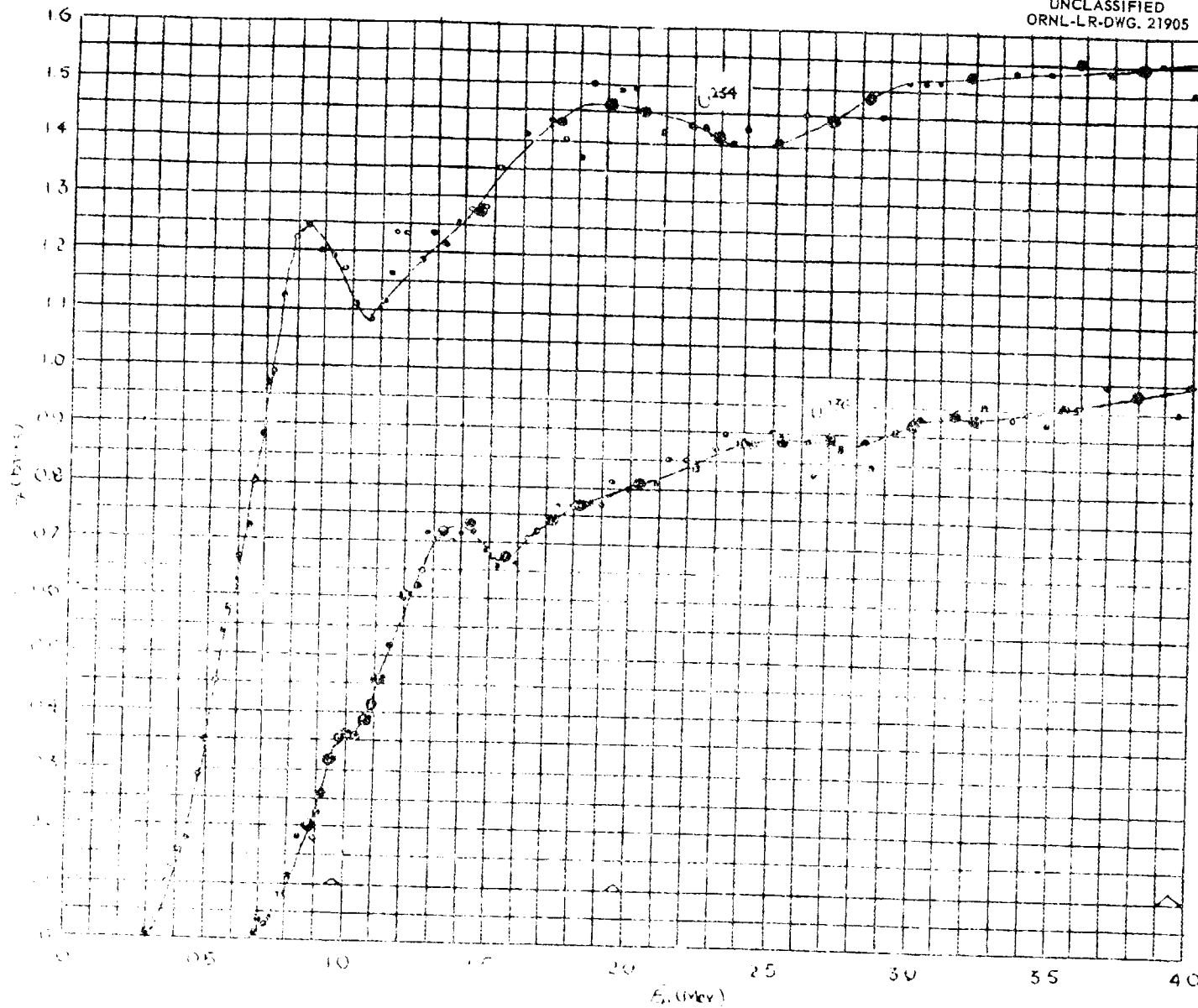
There are at least two ways to account for this discrepancy:

1. This level might belong to a spin state for which one is really well below the top of the barrier. The barrier of Pu^{241} which is surmounted on the way to fission could correspond, for example, to a spin of $\frac{5}{2}$. The Pu^{241} which is originally formed has, of course, spin $\frac{1}{2}$. Perhaps I can put it this way, then: There is this barrier, which is easy to surmount with the energy achieved by neutron addition. Other barriers belong to other nuclear states considerably higher in energy; for

example, a barrier here with a spin of $\frac{1}{2}$, which is very unfavorably situated to lead to fission. One has then an enormously low probability for crossing the barrier, but the increase of neutron energy as one goes up introduces partial waves of higher angular momentum, and therefore one quickly comes to a point where he does have available a spin of $\frac{5}{2}$, and he can easily go over the barrier with substantial probability. This is one way that one could account for this low figure.

2. The other way one could account for it is in terms of statistical fluctuation, in terms of a picture like this, that there is a reasonable probability of very low widths. Let me not take a great deal of time to discuss such issues.

One of the most interesting points is the question about the levels, however, of U^{235} . The question raises itself, how does it come about that the levels of U^{235} show the widths which they do? Let me state the problem in the following terms: U^{235} has a number of levels which have been studied in detail with regard to fission widths (actually 15). One might expect, from the simple picture, that there would be a very different behavior for a 3^- state, formed with the spins combined in one direction, and for a 4^- state, formed when the spins combine in the other direction. One might, therefore, have expected from this simple picture that the two sets of levels of the nucleus U^{235} would fall into two distinct classes, one of which would show a high fission probability, going over the barrier readily, and the other a low fission probability, having to go through the barrier. The fact that this division into two well-defined groups is not seen can be explained in several ways, none of which are entirely satisfactory. Sailor has suggested that all the 15 levels, or practically all of them, might have the same spin, but C. Bloch's statistical analysis of nuclear levels with respect to their spin argues for a comparable number of levels of spin 3 and spin 4, in contradiction to this picture. Of course, it is true that the Bloch analysis counts up the total number of levels of spin 3 regardless of their parity, and the total number of levels of spin 4 regardless of their parity, whereas in point of fact we are concerned with particular parities, but there is no evident reason why the frequencies of even and odd parity should be particularly different.



Slide 3. Fission Cross Section vs Energy for ^{234}U and ^{236}U , from Measurements of R. W. Lamphere and R. E. Greene, *Phys. Rev.* 100, 763 (1955).

Of course, one way to test this explanation is to find a way to determine the spins of these states, and I should like to say just a word, after a moment, about a way to get at this from the asymmetry of fission, or about a possible way to get at it. If I take very much longer on this, I will run out of time to discuss that point; therefore, let me just skip over details here and conclude by saying that one explanation that seems to me quite possible for the situation in the U^{235} case is this: One of these barriers is well below the energy achieved by thermal-neutron fission, and the other is only slightly above it. In fact, there is a group of levels of a characteristic nucleonic state (and not necessarily one characteristic nucleonic state) which contributes to this probability. Now we have two quite different factors to reconcile. One is the absolute width of the levels. From the absolute width we can judge the number of channels. The effective number of channels, as judged from the absolute average width, comes out to be about one-third of a channel. That is point 1.

Point 2 is that from a study of the statistical distribution of widths one can say that the statistically effective number of channels is somewhere of the order of magnitude of two. These numbers are not contradictory at all. They refer really to two quite different concepts. One refers to the question of statistical variance, and the other refers to the absolute number. It turns out that if one says there are three levels which contribute each one about a quarter of a channel's worth to N and one level which contributes about three-quarters of a channel's worth to N , one has a number of contributions coming in which are sufficient, when one goes through the statistical analysis, to reconcile both of these numbers, that is, one gets a variance number effective of the order of 1.5, which seems to be consistent with what one observes.

Now let me just skip over a great many other points and come last to this point of asymmetry of fission. In the mass distribution, the drop at symmetric fission to a factor of $\frac{1}{600}$ of the peak is familiar. Yet, if we have a nucleus which passes over the fission barrier of this 1^- type, we will expect really quite a different kind of a result. For a nucleus in the first excited state of this asymmetric mode of vibration, as for a mechanical oscillator whose first excited state has a wave function which has a node exactly at the middle point, there is exactly zero probability for being in

the state of zero disturbance. In other words, there should be exactly zero probability for complete symmetry of this system with respect to the two sides if it passes over this kind of a barrier. That means, in other words, that the likelihood of symmetric fission, in that case, instead of being 1 in 600, should go to zero.

This means that if one can look at the probability of symmetric fission for various levels, there is a possibility that those levels which correspond to fission over a barrier of this kind will show zero probability of symmetric fission, whereas those levels which correspond to passage over the other kind of barrier will show the usual probability of symmetric fission. If one can develop a technique for the study of the likelihood of symmetric fission, therefore, there is a chance that one might then be able to assign spins to these nuclear states. Then let me just add that I hope that Dr. Bollinger will talk and also Dr. Landon will say a word about the thoughts they have on how one might observe this symmetry effect.

I won't try to say anything about the interpretations of the photofission experiments. They are very interesting in this respect, but the ideas which one needs for analyzing those kinds of experiments, I think, have been presented, and it would only be an application of those ideas, and not a development of new ideas. Instead let me talk a little about the distribution of kinetic energies in the process of fission.

Let's say that for simplicity we will talk about passage over the barrier in a 0^+ state (see Slide 1). That barrier goes down to where finally scission occurs, and then the nucleus is coasting down, with two separated fragments moving apart from each other, after this point of scission. There will, of course, be a great many other potential barriers which will come in here and different possible excited states, because, after all, we are dropping down by an amount which may be 10 or 20 Mev here, and so there is room for lots of other states of the same spin and parity, and we will have an exceedingly great number of them at these higher excitations.

Now the issue presents itself: Does the nucleus coast down to this lowest curve and remain on this lowest curve, or does it pass across to another curve? To put it another way: Is the passage from the point of fission to the point of scission a smooth passage, or is the nuclear fluid sticky? It is a remarkable circumstance about the behavior of

individual particles in nuclei that the situation lies almost exactly midway between the two conceivable extremes: (a) the particle moving completely through the nuclear interior, so that the idea of an average potential could be fully justified, and (b) the opposite idea of the particle moving such a short distance through the nuclear fluid that the nucleus should be compared instead to a liquid drop.

The question raises itself, what about the damping time for a vibration of the nuclear oscillation? Is that damping time very short or very long compared to the time of an oscillation, or of the same order of time as an oscillation? We just don't know what ball park we are in. If the nucleus, however, is completely free, then we would expect always to observe the same kinetic energy for the separating fission fragments. This we certainly do not see. We see instead widespread kinetic energies. We can interpret that by saying that the nucleus is a sticky fluid, that when we pass to any one of these curves there is a statistical distribution among them, and that the likelihood of any given energy is governed by the familiar statistical arguments. Since there is 20 Mev available here, this 20 Mev won't all go into kinetic energy; far from it. Something of the order of 1 or 2 Mev is all that will go into kinetic energy of separation, and the rest will go into energy of excitation.

If one can learn more about this question, one may have a chance to learn a good deal about the stickiness of the nuclear fluid. This is very important with respect to the question of the mass distribution of the fission fragments as they separate. But I won't try to discuss any of the ramifications of that question, since it would lead us a little away from our main subject.

E. GUTH: I would like to ask what form of $\langle \Gamma_F \rangle / D$ is equal to $N/2\pi$. We discussed that this morning, but there seems to be a language difficulty. I wonder if you would elucidate on what the critical significance is.

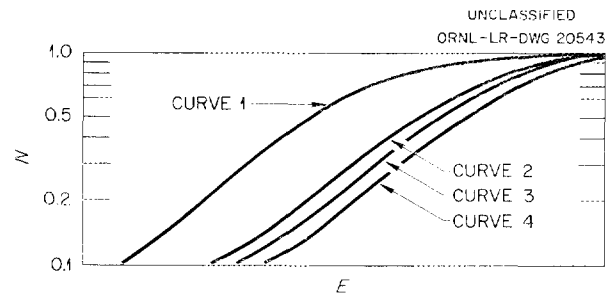
J. A. WHEELER: The question is about the difficulty of applying the formula $\langle \Gamma_F \rangle / D = N/2\pi$. The difficulty, as I have already mentioned, is only an apparent difficulty. It is a difficulty of the sort that, from the observations for U^{235} , N comes out to be of the order of 0.35, and from the statistical spread in level widths, the fact that level widths vary the way they do, one arrives at a statistical number of channels of the order of 1.5.

The only trouble that has arisen in the past is that people have been identifying these two numbers as being the same number. The point, however, is the following: The channel number is a function of neutron energy. Consider the channel number, N , plotted as a function of energy for one channel. If one has a second channel of only slightly different energy, he gets a similar curve, but slightly displaced, and similarly for a third channel of slightly different energy. Now the total value of N is given by the sum of the three capital N values associated with that energy.

Now what about ν ? ν is a number whose determination is governed by the fluctuations here. It depends on how many separate, independent contributions you have, and nothing at all on their abscissas.

H. PALEVSKY: On this same subject, in U^{235} do you think the situation is that we are above the threshold for one of the spin states? That is, if you are definitely above threshold, doesn't N , then, have to be at least 1?

J. A. WHEELER: Let me draw the following sketch (see Slide 4). For the channel that is easily crossed, I will draw a curve for N as a function of energy like this (curve 1). So I will say



Slide 4. Number of Channels vs Energy.

that N for that channel which is easily crossed is 0.7. That would correspond to the parity variety that is easily surmounted. For the variety that is not easily surmounted, I will draw a curve like this for one intrinsic state (curve 2), another intrinsic state slightly different in energy (curve 3), and a third intrinsic state slightly different in energy (curve 4). Each of those states contributes an N value which is of the order of magnitude of 0.25. This is 0.35 (curve 2), 0.25 (curve 3), 0.15 (curve 4), giving an average of 0.25, and this (curve 1) is 0.7. I shall assume that we have ten

levels of this variety (curves 2, 3, 4) and five levels of this variety (curve 1). You have to make some assumptions, and as a typical illustration I have assumed this. This leads to a result for N of about 0.4, as compared to the experimental 0.35, and it leads to a value of ν , the fluctuation effective value, of 1.5, as compared to the experimental value of around 2.

A. M. LANE: This one (curve 4) is not exactly above the barrier for any particular energy that is on that diagram.

J. A. WHEELER: The barrier is really the half-way point, where you have exactly a 50% chance. This is the quantum-mechanical formula. One does not see this in the book, but if one really does it right this is what one gets.

P. A. EGELSTAFF: If the situation is as shown in your drawing, we are a bit below the barrier for curves 2, 3, and 4, and only a little ways above it for curve 1, so wouldn't you expect the average fission width to increase with energy if you go from thermal up to 1 Mev?

J. A. WHEELER: That is correct in so far as the fission width is concerned. That is what one would expect from this, and whether this could be reconciled with the experimental cross section would depend, of course, upon neutron capture.

P. A. EGELSTAFF: That is what I am wondering. This means the value of α has to show some steady decrease from thermal to 1 Mev.

J. A. WHEELER: That would appear reasonable, wouldn't it?

P. A. EGELSTAFF: And you could more or less predict that change with your result.

J. A. WHEELER: How much is the experimental change?

P. A. EGELSTAFF: Well, I cannot really give it offhand. I would have to look at figures. As I remember it, there isn't much change.

H. GOLDSTEIN: Alpha is $\frac{1}{2}$ at 1 kev and $\frac{1}{10}$ at about 1 Mev.

H. PALEVSKY: I don't think you want α . You want the average fission width.

P. A. EGELSTAFF: The point I was getting at is, there is a variation here. If you do your arithmetic properly, you correlate your effect here, and you decide whether you are at the right barrier.

J. A. WHEELER: That is a very good point. It seems to be qualitatively in the right direction.

P. A. EGELSTAFF: Yes, I am not quite sure that it predicts quite as smooth a curve as you have drawn there. It more or less depends on your value of the barrier.

J. A. WHEELER: It is of the order of $\frac{1}{2}$ to 1 Mev.

P. A. EGELSTAFF: Then some fitting has to be done.

J. A. WHEELER: I think it would be very worth while to follow this up and check it out.

A. M. LANE: I think that is in the right direction to change α , but is there not another factor to be taken into account? That is, at 1 Mev you have other higher-partial waves, and for those you may be well above several fission barriers, and so α may drop off on that account alone.

J. A. WHEELER: Absolutely correct.

PROBLEMS AND PROGRESS IN MEASURING CROSS SECTIONS OF FISSIONABLE NUCLEI

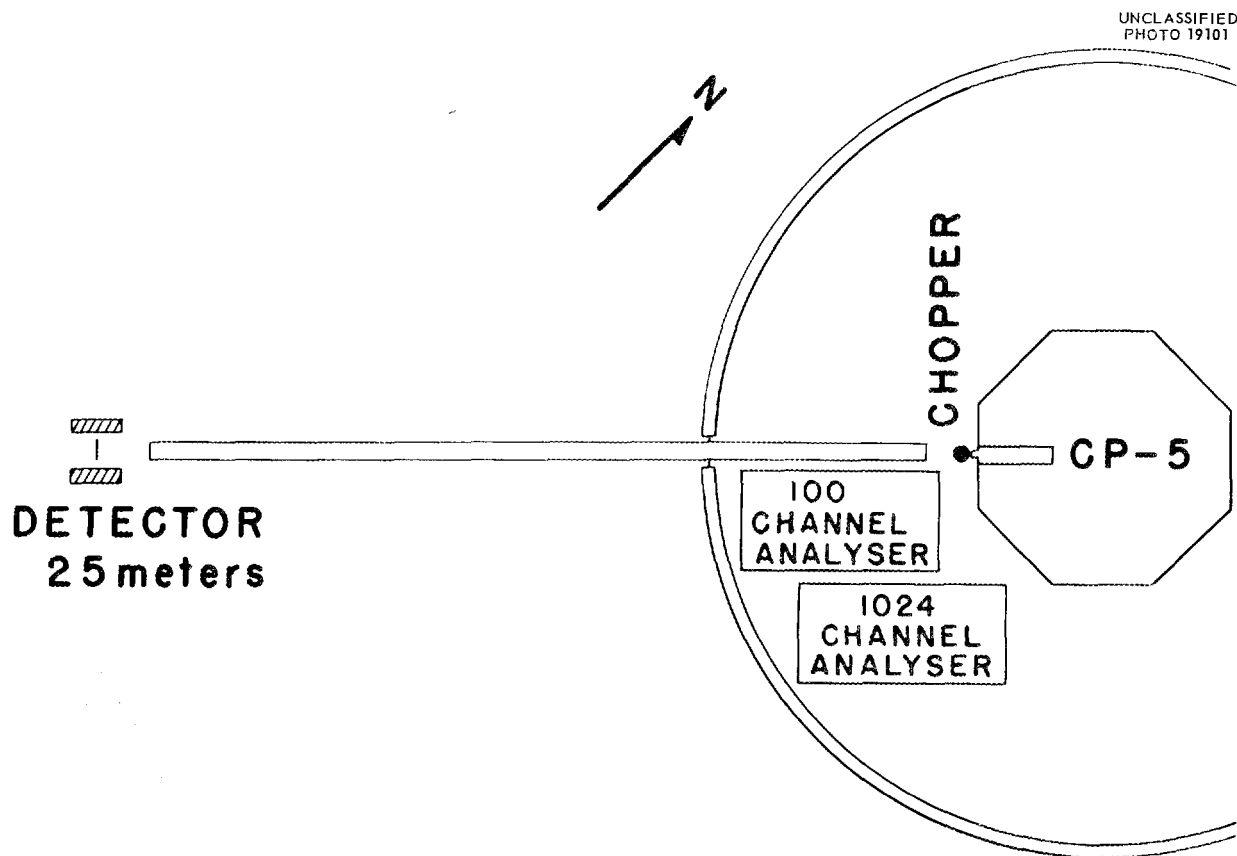
L. M. Bollinger
Argonne National Laboratory

L. M. BOLLINGER: What I would like to try to do in this talk is somewhat as follows: first, to describe for you some of what are really quite considerable advances in techniques for measuring cross sections of fissionable materials that have taken place during the past year; second, to illustrate these advances in terms of the plutonium cross-section data which we have obtained at Argonne, this work being done in collaboration with Bob Coté, Jim LeBlanc, who is now at Livermore, George Thomas, and for a short period Pierre Hubert, from Saclay; and third, to try to point out a few places where our present techniques are definitely lacking, in that they are not able to measure cross-section quantities which are of interest.

Let's start by writing down on the blackboard some quantities which we might like to measure,

because a problem will immediately show up. We would like to measure the total cross section, σ_T , the fission cross section, σ_F , the radiative-capture cross section, σ_γ , and the scattering cross section, σ_s . It is through this last item that we can immediately put an X, because I don't know anyone who thinks he knows how to measure the scattering cross section of fissionable materials. This is really too bad, because it takes away the most obvious way of measuring the J values for the states that are involved, and we must, therefore, go to other methods which are only in the idea stage at the present time.

Let's start off by discussing how we go about measuring some of these cross sections that we think we know how to measure. Consider first the fission cross section. Slide 1 is a schematic drawing of the equipment that is used in our



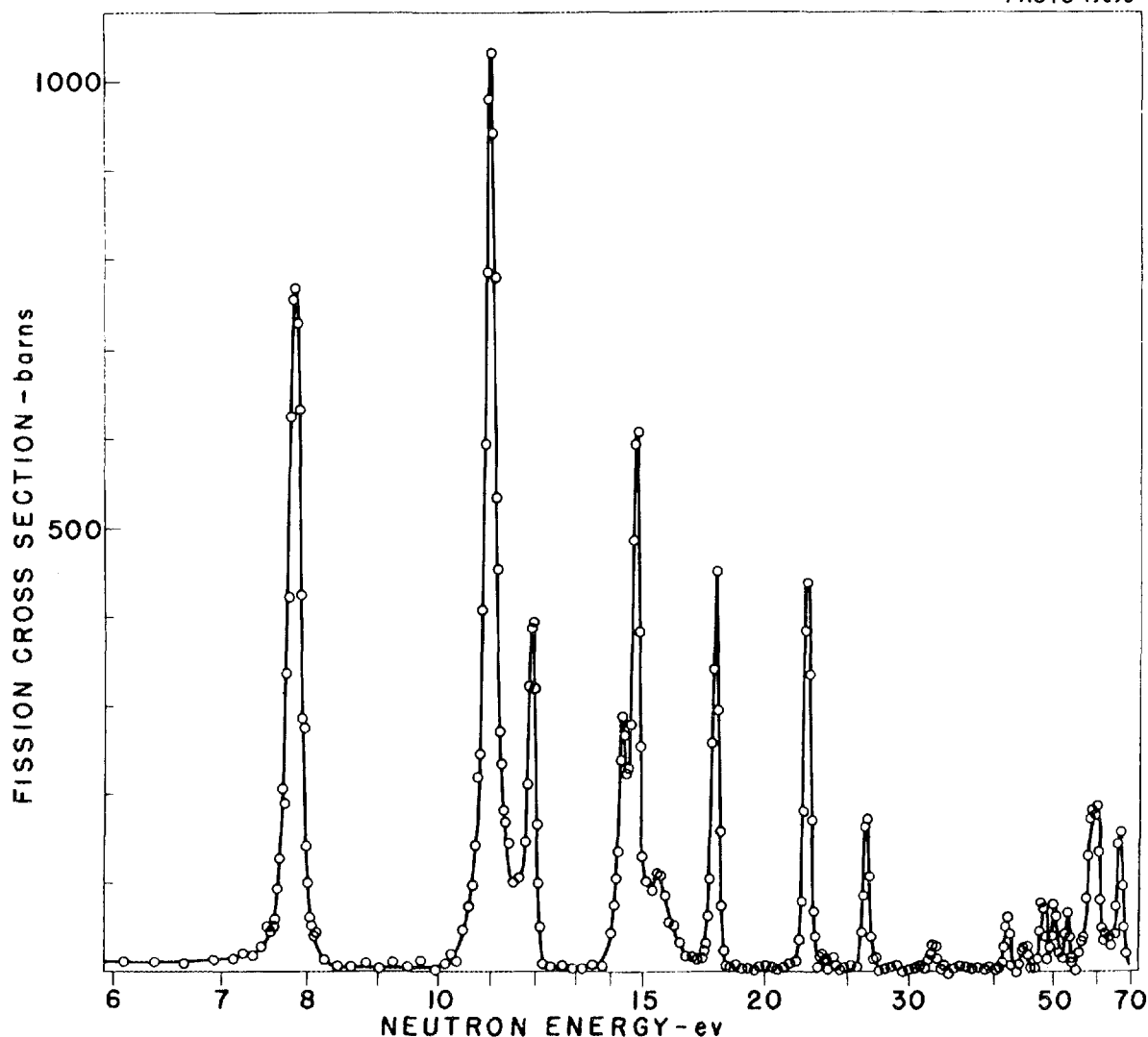
Slide 1. Schematic Diagram of Equipment Used in Fission Cross-Section Measurements.

partial-cross-section measurements at Argonne. You see the source of neutrons, the reactor CP-5, a fast chopper, a detector, which in this type of measurement is 25 m from the chopper, and two time analyzers, a somewhat old-fashioned 100-channel analyzer and a big, new 1024-channel analyzer.

Slide 2 shows the fission cross section of Pu^{239} as we measured it. These measurements were made by the classical method of detecting the fission event by detecting fission fragments. If

one compares this drawing with what would have been obtainable a year ago, one finds that there is really a very dramatic improvement in the quality of the data, particularly the resolution, and one may well ask just how this came to pass. The answer is that there has been a tremendous increase in flux. Taking our own case as an example of what has happened during the past $2\frac{1}{2}$ years, starting from the time we abandoned reactor CP-3, we have had the following increases in effective flux: a factor of 40 for the pile, a factor of 10 for the time analyzer, a factor of 15×8 for

UNCLASSIFIED
PHOTO 19093



Slide 2. Fission Cross Section of Pu^{239} vs Neutron Energy.

the chopper, and a factor of 10 in this measurement for the detector. This gives an over-all effective increase in flux of 480,000.

Of these many factors, I want to mention only one, and that is the detector. In the case of the isotope Pu^{239} , the primary detector problem is that the very high activity of the material causes the alpha-particle pulses, which are much smaller than the fission-fragment pulses, to rather frequently build up to a pulse-height level which is comparable with that of the fission fragment. This problem had limited chambers, in the past, in this type of work, to a total weight of the order of 10 mg of material. Rather recently, however, a new technique, using noble-gas scintillation as the light-producing element, has allowed one to get around this problem to some extent. The noble gases produce extremely fast pulses, so that one may now clip the pulses that are formed to a width of the order of a few millimicroseconds and thus to some extent inhibit the alpha pile-up phenomenon. I won't go into details as to the chamber we used but will just mention that, as compared with the order of 5 mg which had been used previously in this country, we were able to use 120 mg in our chamber.

Now, going on to a discussion as to the quality of the data of Slide 2, first let's see where they are not satisfactory. In general they are not satisfactory in low-cross-section regions, which usually are off-resonance regions. When plotted as in Slide 2, one does not observe this, but if one were to use a log-log scale it would be obvious that the cross sections near the base line are more or less meaningless. The problem is statistical in nature; we just don't have enough counts. So here is an indication that a new method of measurement is required, and I will suggest a way out and show an example of data obtained in a new way.

Although meaningless in regions of low cross section, the data of Slide 2 are useful for measuring a combination of resonance parameters, namely, the quantity $\sigma_0 \Gamma_F$, where σ_0 is the peak cross section and Γ_F is the fission width. The statistical accuracy of the areas that are involved in these peaks is of the order of 1% in the best cases and typically 3%, and therefore in those cases where one has clearly isolated peaks there seems no reason to doubt that the statistical accuracy of the quantity $\sigma_0 \Gamma_F$ is of the order of a few per cent.

One should mention, of course, that these data have to be normalized to thermal energy, so that any error which occurs in the absolute cross section of the material at thermal energy is carried over into the accuracy of the data at higher energy.

A second and newer approach in attempting to measure fission cross sections and related quantities is to register the occurrence of fission by detecting the fast neutrons produced. The first person to attempt to make measurements as a function of energy using these fission neutrons was Palevsky, at Brookhaven, who used a thick sample to measure directly the quantity η , the number of fission neutrons produced per incident neutron absorbed. Other people followed rapidly in this type of measurement. A number of different detectors were used: Hornyak buttons, hydrogen proportional counters, and BF_3 counters in a moderator. The difficulty with all of these detectors, particularly for time-of-flight work, is that they had an extremely low efficiency, of the order of 0.1%. Thus the measurement turned out to be quite tedious, and perhaps the possibility of error crept in just because the measurement did take so long.

In any case, at the time of the Geneva conference, just a little over a year ago, there were several sets of data giving results on U^{233} and U^{235} which gave values of η which were in very good agreement with the measured cross sections for the assumed constant value of ν , but there were also two sets of data on Pu^{239} which did not give this agreement. This anomaly for Pu^{239} suggested the extremely interesting possibility that ν varied from one resonance to another. Spurred on by the interest of Professors Wheeler, Bohr, and others, a race developed to make a direct measurement of ν for Pu^{239} .

The winners in this race were Auclair and Landon at Saclay. They found that ν was constant over the thermal energy range. Soon thereafter, four other groups also found it to be constant. The measurements were then extended into the resonance region by ourselves at Argonne, and ν was found to be constant from resonance to resonance.

I should like now to take the time to describe our measurement, because it gives an opportunity to describe several pieces of apparatus, an understanding of which is necessary for the presentation of some of the data that I have.

Slide 3 shows the detection system used in our study of the energy dependence of ν . One sees three counters, the fission chamber, which I mentioned before, in the center, and on the outside of it two large liquid scintillators. These liquid scintillators are for the purpose of detecting fast neutrons through the proton-recoil process; they are made insensitive to radiative-capture events by the lead surrounding the sample. To say that we have had a fission event, we require a twofold coincidence between the liquid counters, and we also require that the sum of the pulse heights be in a prescribed range, usually a relatively low pulse.

We have studied rather carefully the characteristics of this counting system and have found that the efficiency for the detection of a fission event is in the range of from 5 to 10%, depending on operating conditions.

Perhaps one of the biggest questions about the detection system is how insensitive it is to capture events. The detection efficiency for capture cannot be measured directly for a fissionable material. We have shown, however, that the ratio of

efficiencies for detecting capture in gold and fission in U^{235} is less than 0.0005. This ratio is small enough that it seems safe to assume that the detection system responds only to fission.

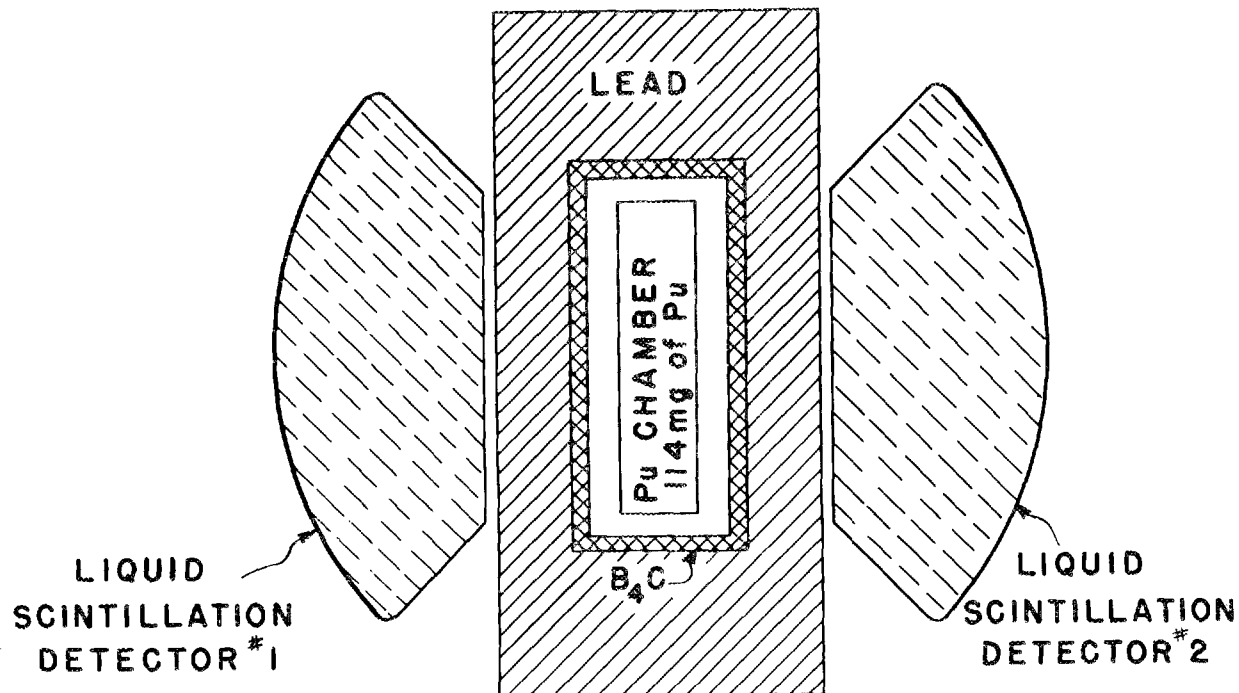
In the measurement to study the behavior of ν , we measure the single rate in the inner chamber and the threefold rate between the three chambers. The ratio of the coincidence to the single rate is proportional to the quantity $\nu(\nu - 1)$, where ν here refers to a particular event. For the known distribution in ν , the quantity $\nu(\nu - 1)$ is roughly equal to $\bar{\nu}^2$.

For our work on ν we were not particularly interested in just what was the exact relationship between $\bar{\nu}$ and $\nu(\nu - 1)$. We were looking for changes in ν , and, since we didn't find them, it was not important for us to know what the relationship was.

Now, going to the data themselves, Slide 4 gives the data obtained at thermal energy, and, as you can see, there is no perceptible variation in ν .

Now, at epithermal energies the main problem is one of counting rate. You can get some idea of this difficulty from Slide 5, which shows the raw

UNCLASSIFIED
PHOTO 19094



Slide 3. Detection System Used in the Study of ν vs Energy.

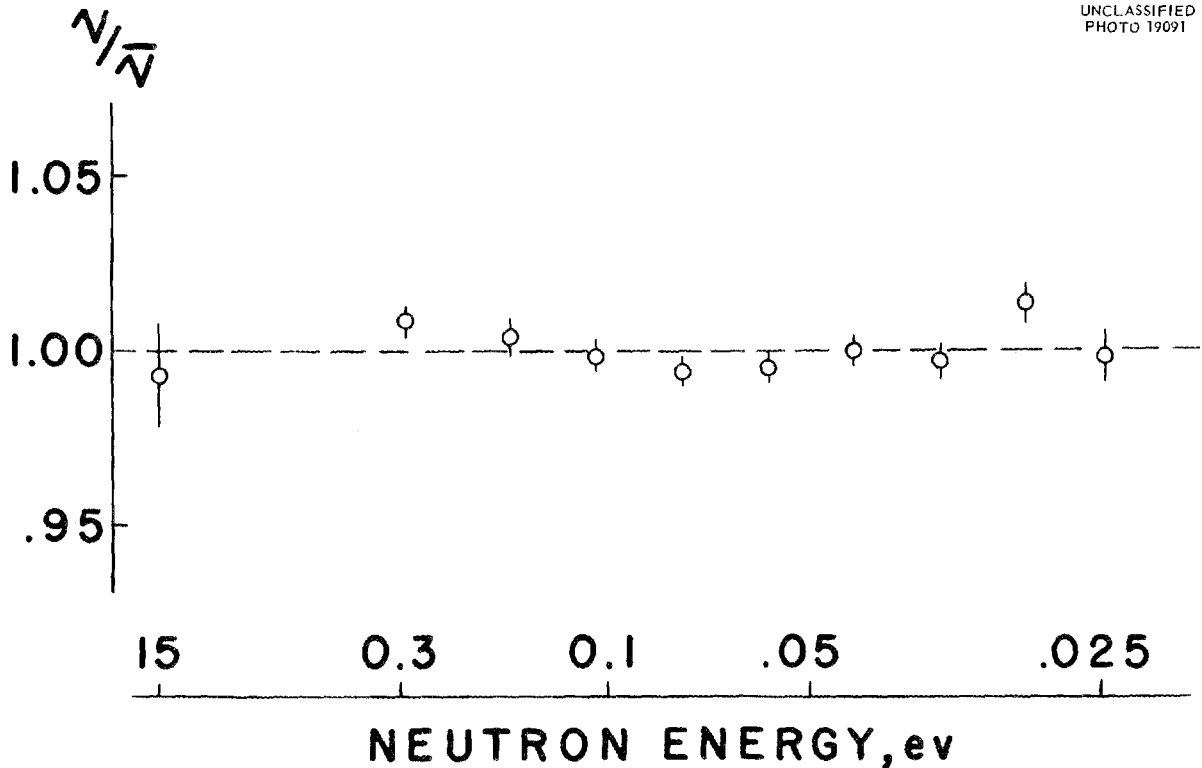
data obtained in one of many runs. Up above, one sees the number of coincidence counts obtained in 15 hr, and below are the single counts. Both of these two sets of data were obtained simultaneously and were recorded simultaneously in our 1024-channel analyzer. It is an obvious advantage in a low-counting-rate experiment of this kind, where one has to count over perhaps a period of one month altogether, to have the data recorded simultaneously, so as to eliminate the possibility of drifts in efficiency which might cause the results to be in doubt.

Table I gives a summary of the results on the measurement of ν for the various resonances; here again, to within a statistical accuracy of the order of 3 or 4%, there is no perceptible variation in ν .

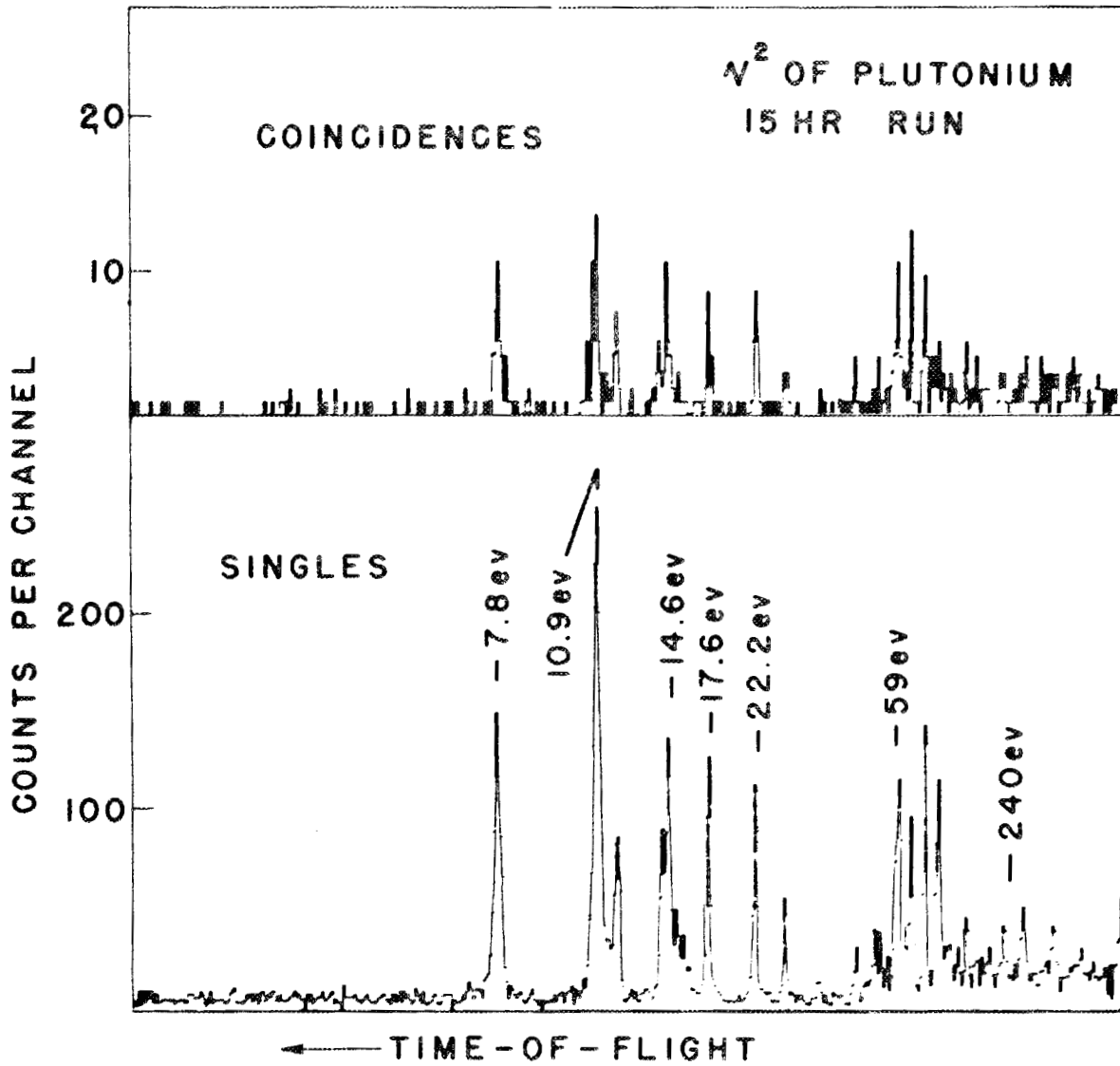
Having found this result, we could now with some confidence use the detection system for telling ourselves that a fission event had occurred and know that the detection efficiency was a constant which could be found by normalizing the quantity being measured to, say, thermal energy. The first

Table I. Numerical Value of ν for Pu^{239} as a Function of Energy

Resonance Energy (ev)	Relative ν	Standard Statistical Error (%)
Thermal	1.008	1.6
7.8	1.009	2.6
10.9	0.972	1.9
11.9	0.999	3.3
14.3	1.001	3.9
14.6	0.975	3.0
15.5	1.083	4.0
17.6	1.006	3.6
22.2	0.983	3.4
26.6	0.954	6.1
59	1.048	3.0
66	1.041	3.4
75	0.959	3.4
86	1.023	3.2
110-1700	0.991	2.7



Slide 4. Energy Dependence of ν for Pu^{239} .



Slide 5. Raw Data from Single Run for Measurement of v^2 of Plutonium.

experiment that it seemed desirable to do was to repeat the measurement of η for Pu^{239} in the thermal energy range. If we could not clear up the anomaly mentioned earlier for this case, there was very little point in trying to extend the measurement to the higher energy range.

If we have a block of material with a beam of neutrons coming into it and some kind of a neutron counter off to one side having an efficiency ϵ for the detection of a fission event, then the counting

rate R in the counter is

$$(1) \quad R = I\epsilon(1 - T) \left\{ \frac{\sigma_F}{\sigma} + \frac{\sigma_s}{\sigma} (1 - T') \left[\frac{\sigma'_F}{\sigma'} \dots \right] \right\},$$

where I is the neutron current into the sample, T is its transmission, T' the escape-without-interaction probability after one scattering, T'' the probability of escape after two scatterings, etc. This is obviously a very complicated expression if

one carries it all the way out. But the important point is that under favorable conditions the latter terms are small as compared with the first term, and one can therefore look for simplifying assumptions or simplifying experimental conditions which will allow one to handle it in a reasonable way.

In particular, if we make what is a rather general and reasonable assumption, that the ratios of cross sections are independent of the number of scatterings and that the probabilities of escape are the same for all scatterings, then Eq. 1 can be written in the form:

$$(2) \quad \frac{\eta}{\nu} = \frac{R}{\epsilon l} \frac{1 + (\sigma_s/\sigma_a)T'}{1 - T'}$$

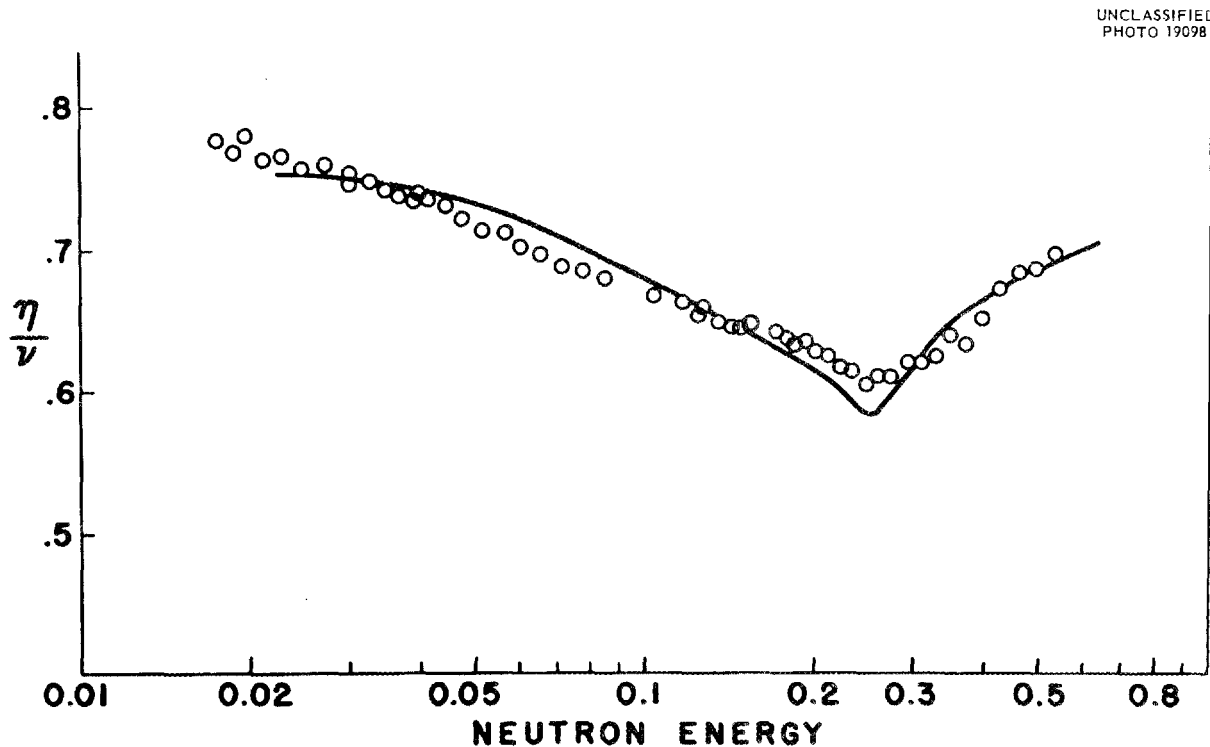
Now consider the case of incident neutrons of thermal energy. The term $(\sigma_s/\sigma_a)T'$ is in general less than 1%, and the sample can be thick enough so that the transmission is zero and T' is not far from zero. Thus we have a very simple relationship in which one can measure all the experimental quantities involved.

Slide 6 shows the results we have obtained near thermal energy. Here η/ν is plotted as a function

of neutron energy. The points are the directly measured values, whereas the solid line is the value calculated from cross sections which were measured at Argonne. As you see, within the experimental error there is good agreement.

Let me conclude this part by saying that these results convince us that we have measured the right value of η/ν . There still are two distinct sets of data for η of Pu^{239} , however: our results and Leonard's from Hanford, which are in very good agreement, and both of which are in agreement with the cross-section data; and the Brookhaven and the Harwell results, which are in distinct disagreement with our results, and yet seem to be of very good quality. As far as I know, no one can offer a reasonable explanation for this anomaly.

Having proved to our own satisfaction, at least, that we knew how to handle the technique of measurement by fast-neutron detection and that the technique gave correct answers, we then proceeded to attempt to push the technique to higher energies. Here things become more difficult, and not in this case because of the counting rate, because with



Slide 6. Graph of η/ν vs Neutron Energy for Plutonium.

our detector the counting rate is almost overwhelmingly high; rather, the measurement is harder because one must select favorable conditions in order to make sure that one knows what is being measured. As far as I can see, the main limitations which one must place upon the experimental conditions for the measurements are, first, that $\sigma_s \ll \sigma$ (and this is most important), and, second, that the resolution be reasonably good.

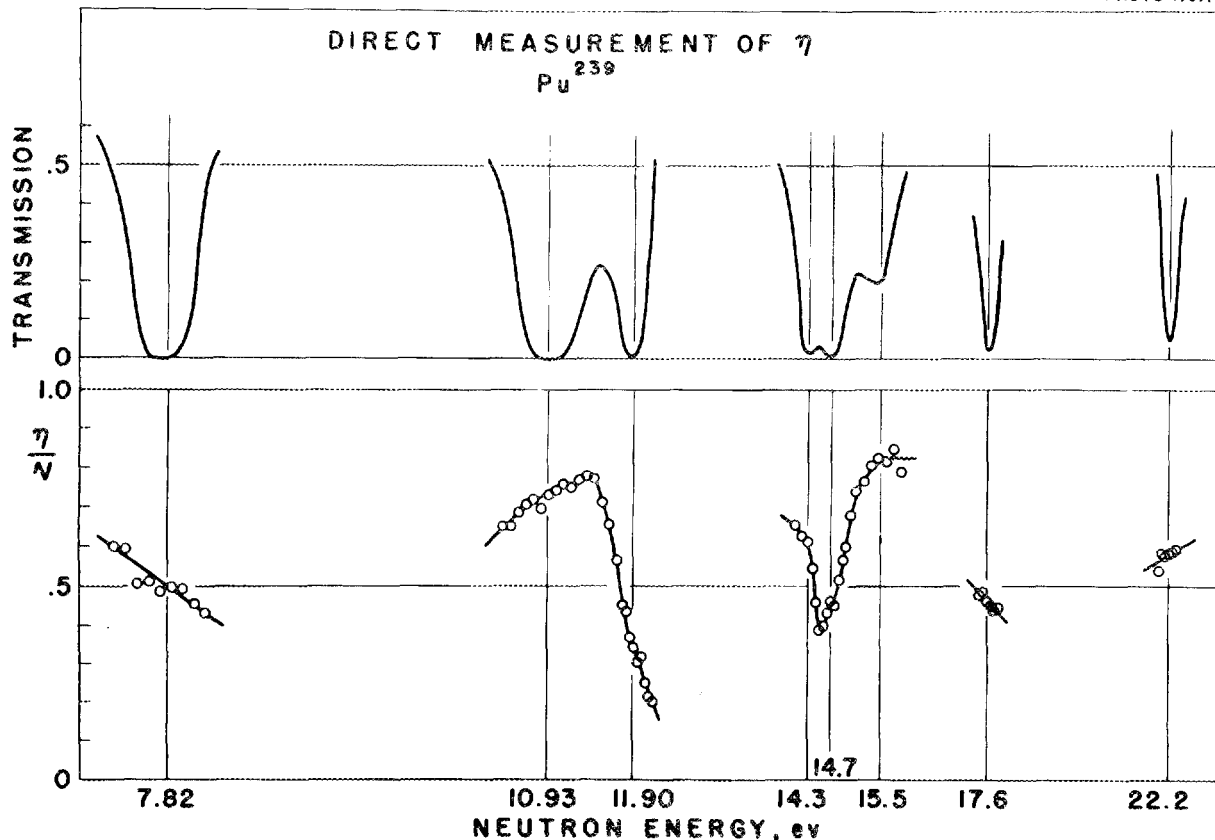
In the measurements which we made, the results of which are shown in Slide 7, we used a sample which was 3 mm thick, and for which we chose to use results only if the transmission was less than 50%. Now, you will observe that in the immediate neighborhood of most of the resonances at low energy the transmission is very close to zero and only rather small corrections had to be made. In general, the statistical accuracy is of the order of 1%, and for favorable resonances we don't see any reason to believe that there should be systematic

errors much larger than this; one must again mention, however, that the data were normalized to thermal energy, and there is some uncertainty in that.

Let us now consider the interpretation of the results for η/ν . We were surprised initially on getting the shapes given in the figure. If the resonances involved have single-level Breit-Wigner shapes, and we make a plot of η/ν as a function of energy, one would expect that in the immediate neighborhood of each resonance there would be a more-or-less plateau region, with a monotonic variation between levels. But, as you see in the figure, there are almost none of these plateau regions. Everywhere the variable is going either up or down, and at particular resonances, such as that at 11.9 ev, it is not really experimentally clear that there is a tendency to flatten at all.

If one interprets these curves in terms of asymmetry caused by interference between resonances,

UNCLASSIFIED
PHOTO 19097



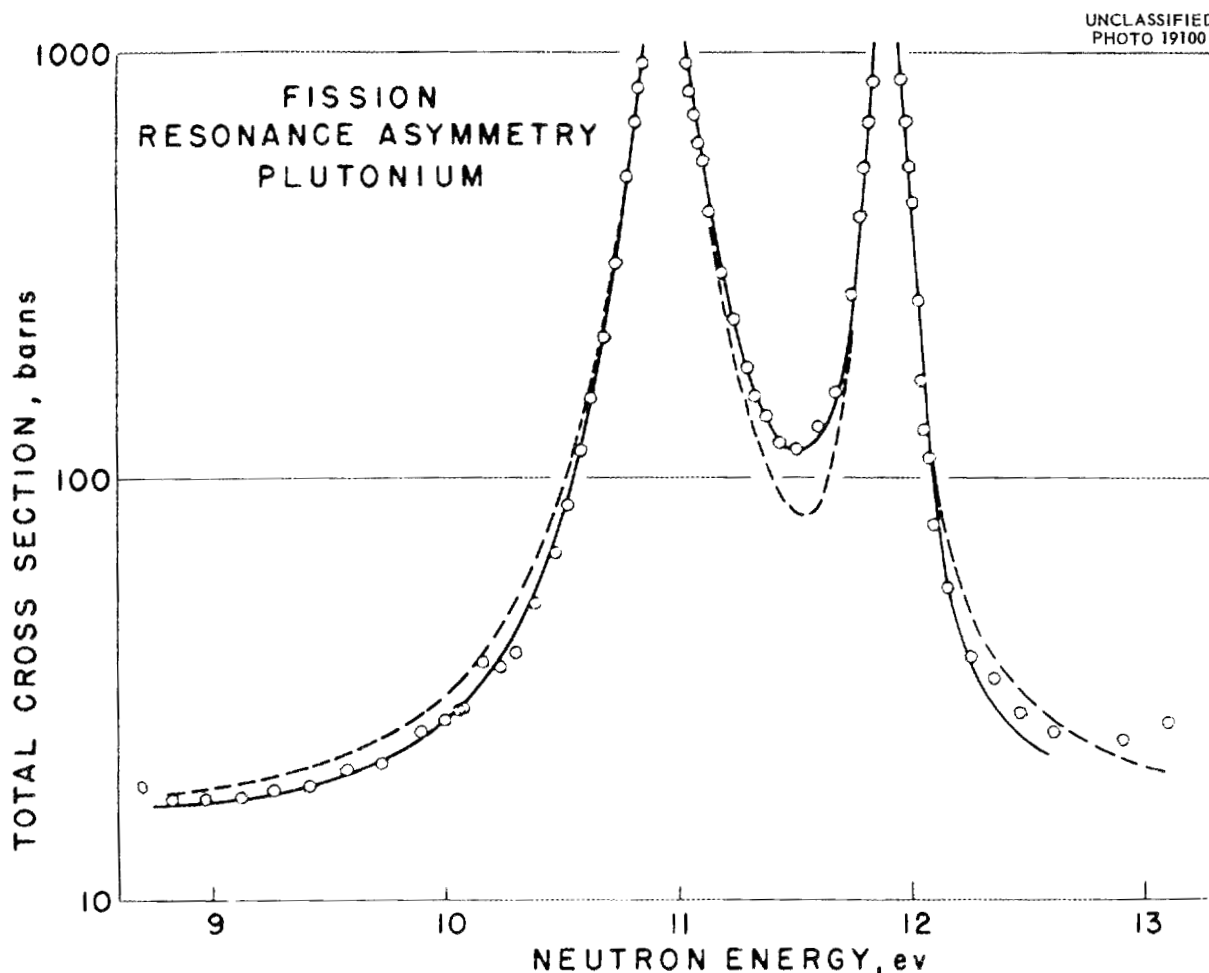
Slide 7. Transmission and η/ν vs Neutron Energy for Pu^{239} .

as Professor Wigner suggested was the normal thing to do in any case, all this difficulty disappears. In the most favorable case, the two resonances at 10.9 and 11.9 ev, we have been able to fit the η/ν data quantitatively using a multilevel formula and assuming that there is a single exit channel for fission.

Let me present another figure which bears on this point. Slide 8 shows the total-cross-section data obtained for this same system of resonances. The dashed line is the best fit that we could get using a single-level formula, whereas the solid line is the fit that we got using the multilevel formula. On this point, there seems to be some question among experimentalists as to just what multilevel formula should be used, and if any one in the audience feels competent to speak on it, I wish he would when I get through. The one that

we used is that to be found in the Appendix of the Feshbach-Porter-Weisskopf article. The fission cross section was calculated using this formula, and then the radiative-capture cross section was simply added to it as being an entirely independent quantity. We feel that the quality of the fit of the multilevel curve on Slide 8 and the fact that the η/ν data also agree with the multilevel interpretation are rather strong indications that the resonances are really asymmetric and that we should no longer attempt to explain all anomalies in the shapes of fission resonances in terms of little, unobserved resonances which are added here and there.

If, now, all of this convinces us that our measured values of η/ν are really meaningful, it provides a powerful tool for deducing resonance parameters, and I must now backtrack a little and



Slide 8. Total Cross Section vs Neutron Energy for Plutonium (See Text).

point out that measurements of this type were first done by Farley, at Harwell, and that with Egelstaff's aid he attempted to get some parameters for plutonium in much the same way that I am now suggesting.

From total-cross-section measurements, one can easily measure some combination of parameters, such as, for instance, $\sigma_0 \Gamma$. If, now, we can assume from some other knowledge a value of Γ_γ , and we have a measured value of $\eta/\nu = \Gamma_F / (\Gamma_\gamma + \Gamma_F)$, it is a very simple calculation to get independent parameters, and I will show a slide later which will show that under favorable conditions one seems to get parameters, using such a treatment, which are in very good agreement with those that one gets using other treatments.

Now let's see if we can use the technique of detecting fission neutrons for some other type of measurement. In the η/ν measurements, we felt that there were a number of resonances where the data were not useful because the resolution was not satisfactory, and we also felt that, in between resonances, the measurement was meaningless because we could not satisfy the criterion that the scattering cross section be small. However, between the resonances it seems quite possible to use fission-neutron detection to measure fission cross sections, and, if you recall, this is the very region where we could not measure fission cross sections by detecting fission fragments. Again, this approach was followed by Harwell in their work.

Returning to Eq. 1, we see that the fission cross section is related to measurable quantities by

$$(3) \quad \sigma_F = \frac{R}{\epsilon l} \left(\frac{\sigma}{1-T} \right) \left[1 - \frac{\sigma_s}{\sigma} (1-T') \right].$$

The important point here is that, for thin samples, the last factor may be made arbitrarily small and the ratio $\sigma/(1-T)$ approaches $1/n$, where n is the sample thickness. Thus σ_F is rather directly related to the measurable quantities R and l .

Slide 9 shows raw data obtained in a measurement of σ_F by detecting fission neutrons, as compared to data obtained when fission fragments are detected. The tremendous gain in the statistical accuracy given by the new method, caused by the much greater thickness of sample that can be used, is obvious without further comment.

For lack of time, I would like to omit a discussion of another special case of an application

of the method of fission-neutron detection and try to summarize what we feel we have learned about plutonium.

We have shown that ν is a constant.

We have observed that most resonances in plutonium appear to be asymmetric, and we have found what appears to be one reasonably convincing example of interference between levels.

We have found a list of average parameters which should be of use: $\bar{\Gamma}_\gamma = 0.040$ ev, the observed level spacing is 2.9 ev, $\bar{\Gamma}_n^0/D = 0.78 \times 10^{-4}$ ev^{-1/2} (assuming that resonances were observed for both spin states), and $\bar{\Gamma}_F = 0.084$ ev.

The value of $\bar{\Gamma}_F$ is of some interest as related to Professor Wheeler's talk, because it gives a value of N , the effective number of fission channels. Now, I don't quite know how to do this, but, if you assume that there is actually only one spin state involved, then you get a value of N that is 0.18, whereas if you assume there are two spin states it is half of that.

Finally, we have measured a fission width for each of the first 15 resonances and find that the results are consistent with either an exponential or a Porter-Thomas distribution.

There is one slide which I missed that is extremely important. This slide (Table 2) is one with which I wanted to convince you that the methods of measurement which I have been talking about are valid and give results that are in remarkably good agreement.

Let's first look at the values obtained for Γ_γ . One test of the data is the fact that these are rather close to being equal, although here I would like to make a comment in connection with the conversation that went on this morning, that in my opinion, at least, a certain subjective element enters an area analysis which gives a value of Γ_γ and, therefore, it is extremely dangerous to take such values and do a detailed statistical analysis of their scatter and from this try to come to a conclusion.

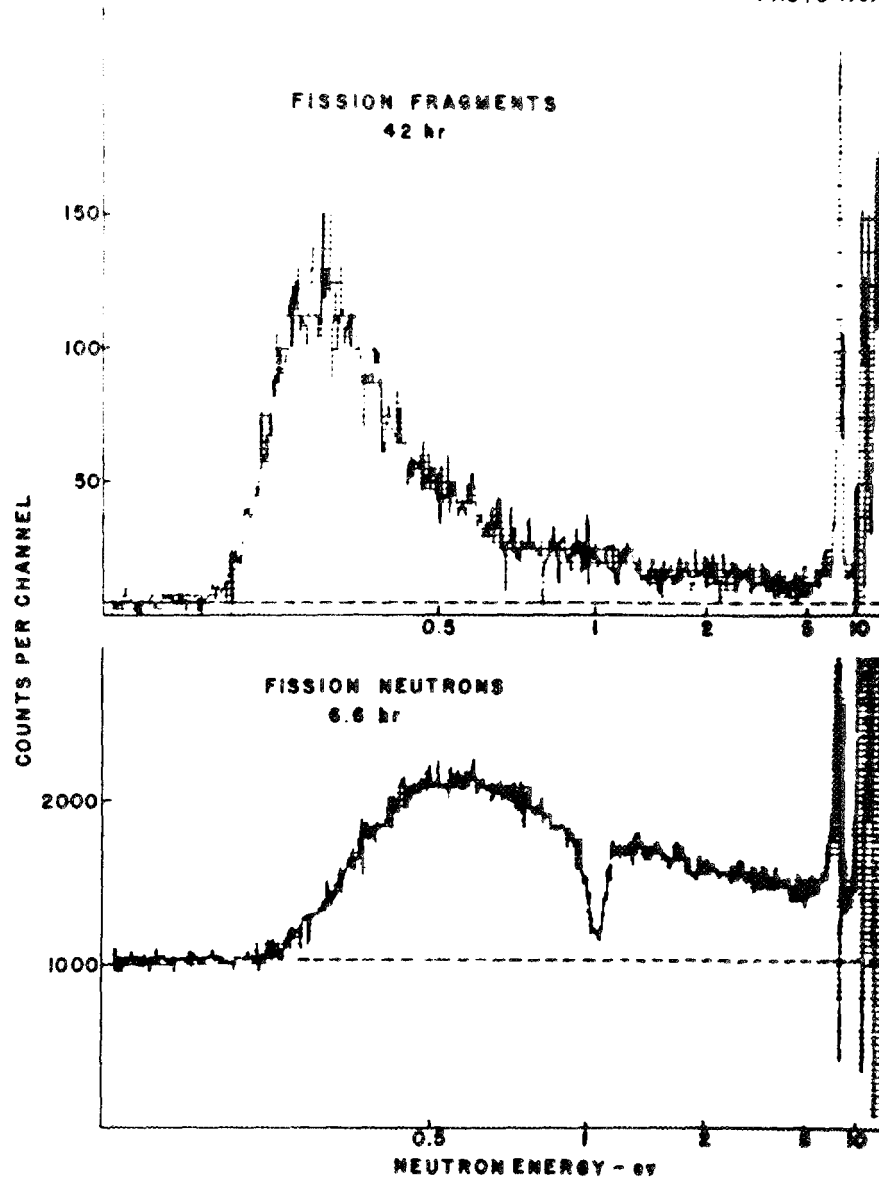
Let us go on now to the columns giving results for η/ν . I didn't discuss at all the intermediate-sample technique, and so I will omit it here. But in the third column we have values of the quantity η/ν deduced from the fission-fragment cross-section measurements and the transmission measurements, and in the fifth column we have the results from the direct, thick-sample measurements. As you see, all three sets of values are in remarkably good agreement.

P. A. EGELSTAFF: First let me say how impressed I am by this beautiful work which Dr. Bollinger has described. I think the work we reported a year ago is entirely insignificant against this series of experiments.

I would like to make just a few points. First, I don't agree with your statement that you have

shown that there is a place where you can say definitely there is interference. Personally, would like very much to believe in interference. I think it ought to follow from all we know at present, but I don't know of any place where I could really say I believe there is interference. I would like to say more about this when I give some of our measurements later in the evening.

UNCLASSIFIED
PHOTO 19090



Slide 9. Comparison of Raw Data Obtained in Fission Cross-Section Measurements by Fragment Detection and by Neutron Detection.

Table 2. Parameters for Pu²³⁹ Resonances

E_0 (ev)	Γ_γ (mev)	η/ν		
		Thin Sample	Intermediate Sample	Thick Sample
0.30	40	0.61	0.59	0.62
7.82	38	0.48	0.50	0.49
10.9	39	0.77	0.75	0.73
11.9	42	0.35	0.35	0.34
14.3			0.59	0.61
14.6		0.41	0.46	0.44
15.5		0.83		0.81
17.6		0.46	0.51	0.46
22.2	41	0.62	0.69	0.57

I would just like to have the details of the errors on some of the measurements, if you have them available.

L. M. BOLLINGER: In general, the errors of individual resonances have not been fully evaluated. For most of these average quantities, though, the main source of error comes from the small statistical sample which we have, and you can evaluate that as well as I. We have 15 resonances for which we have parameters.

P. A. EGELSTAFF: The last question is on the 7.8-ev resonance on your slide which shows the constancy of ν vs energy through that resonance. You have those two points in the wing which are way above the remainder of the points. Do you recall that?

L. M. BOLLINGER: For that particular resonance, the statistical accuracy is very much poorer than for the other.

P. A. EGELSTAFF: The question I wanted to ask was, is that difference significant?

L. M. BOLLINGER: It is my opinion that for the 7.8-ev resonance the difference is not significant, because the statistical accuracy there is poor.

P. A. EGELSTAFF: Would you be prepared in that case to draw a line, a sort of horizontal and another horizontal, that would fit the points?

L. M. BOLLINGER: That would fit the points, but it is no better than a large number of other lines.

J. A. WHEELER: I was impressed very much by these direct measurements of η and by the fact that, if there is a small resonance, and if amplitudes are involved as one has to deal with them in talking about these asymmetric resonances, then one might have a much greater sensitivity for detecting very weak resonances if we measure η as a function of energy rather than measuring the total cross section, because we would be adding the amplitude of the small level to the amplitude of the other larger levels rather than adding the intensities.

L. M. BOLLINGER: I am not quite sure that I understand your point. It seems to me the primary advantage of the η measurement is that one is to some extent eliminating the smearing out in sensitivity of measurement that one gets in a total-cross-section measurement because of the fact that one is piling the capture cross section on top of the fission cross section, and that one would be just as well off if one could with precision measure the fission cross section directly.

J. A. WHEELER: Right, I agree completely. In that case also, the measurement should give a contribution of a weak resonance which is proportional to the amplitude rather than the intensity of the weak resonance.

LOW-ENERGY FISSION MEASUREMENTS OF Pu^{240}

B. R. Leonard E. J. Seppi W. J. Friesen
Hanford Atomic Products Operation, General Electric Company

B. R. LEONARD: The work that I am going to report on now was done with a crystal spectrometer at Hanford. The audience has a right to know why crystal-spectrometer work is included in this time-of-flight meeting. I think the confusion arises from the Pu^{240} resonance we published back in June, which some crystal-spectrometer people insisted must be fast-chopper data. We now have better data.

In this business of the Pu^{240} fission cross section, the first positive result that was obtained on a subthreshold fission cross section was obtained by E. K. Hulet, of Livermore, and his co-workers, who obtained a thermal-fission cross-section value of 4.4 ± 0.5 barns. With that in mind, I will describe the method that we used to attack this problem.

We used a gas ionization chamber in which we had mounted a foil essentially of Pu^{240} back to back with a foil of mostly Pu^{239} . If one plots the ratio of the counting rates of these two foils, one gets a curve that is fairly flat at low energies and has a dip of about 4% at the 0.3-ev resonance. At this point the Pu^{239} fission completely dominates, and by taking a good ratio at this point one essentially normalizes to the relative weights of the foils. Then, as one comes back to lower energy, the primary effect of this increase in ratio is due to the Pu^{241} in the Pu^{240} foil, and this is the primary correction that has to be applied to the data.

One reason for reporting these data is that we have recently remeasured the fission cross section of Pu^{241} and have removed some of the uncertainties that were previously assigned to this cross section. We have also slightly renormalized the Pu^{239} and Pu^{241} fission cross sections as previously reported, and we have obtained two points with high statistical accuracy at neutron energies of 0.1 and 0.075 ev.

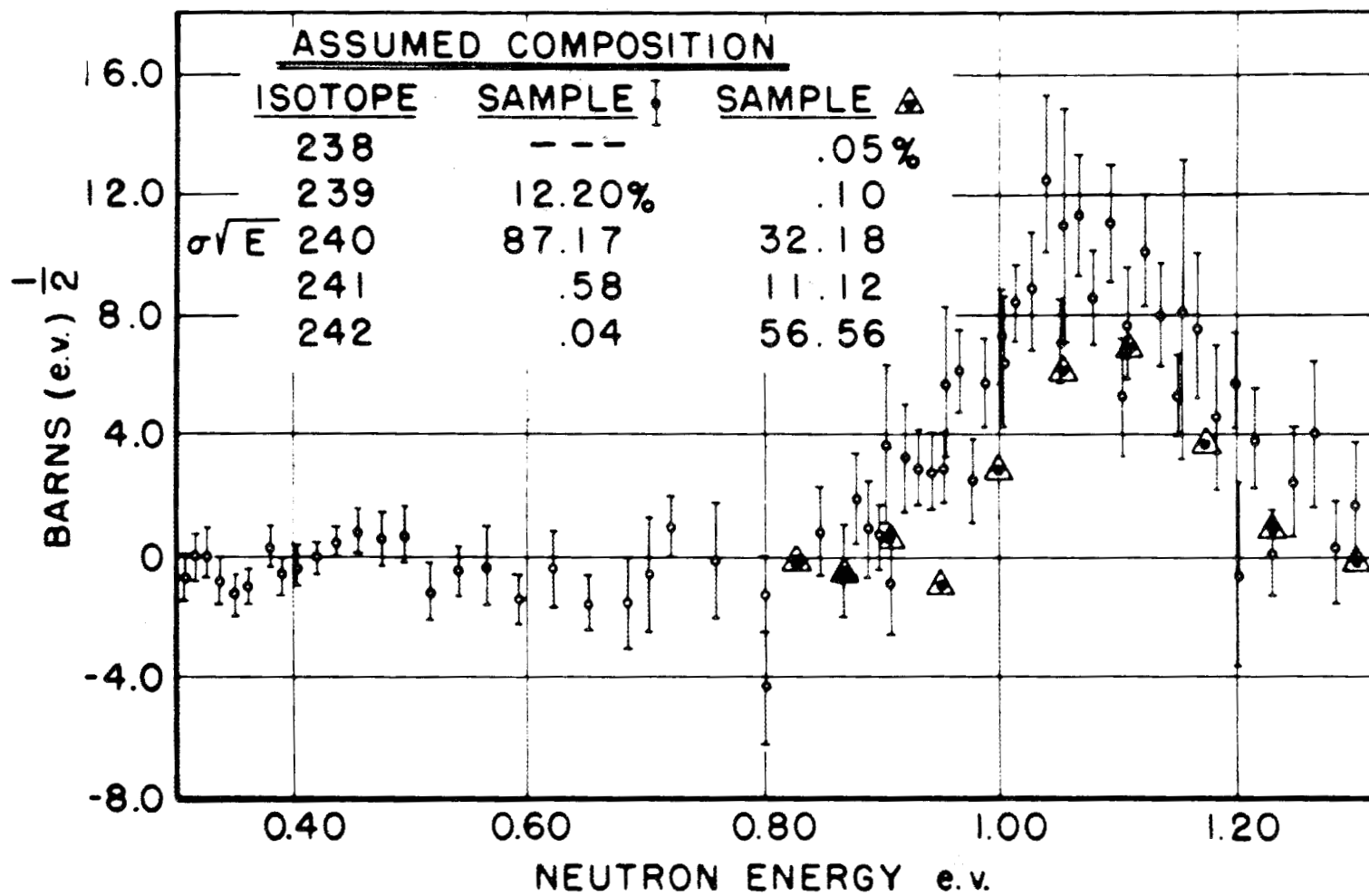
The results that we obtained trying to find a fission cross section of Pu^{240} at these energies are given below:

Neutron Energy (ev)	Fission Cross Section of Pu^{240} (barns)
0.075	0.43 ± 0.50 (statistical component ± 0.43)
0.10	0.21 ± 0.39 (statistical component ± 0.31)

You see that the fission cross section that we apparently observed is less than our statistical error, and our statistical error is already so low we think it should not be pushed any lower, due to other inherent uncertainties in the crystal-spectrometer method. These results, as quoted here, do not overlap the 4.4 barns as measured at Livermore. But they really do not prove anything about what the value of the cross section is.

Well, after we looked at this we decided that we should look at the 1-ev resonance, which is known to be very large in total cross section, and see if we could find fission in this resonance. We originally found what we thought was a fission component in this resonance and reported it as such. We have recently improved our spectrometer by putting an automatic data-taking and recording system on it, and we have much better data now, although the resolution has not been improved.

Slide 1 shows the results that we now have on this resonance region. The open-circle points were obtained with the same foil with which we did the low-energy work that we have previously reported. You can see that now there are a sufficient number of points so that this really does look like a resonance, even though the resolution width is greater than the actual width of the resonance. There are some other points plotted on this graph, the triangles being the size of the statistical uncertainty. Those points were obtained with a set of foils of quite different isotopic

Slide 1. Fission Cross Section of Pu²⁴⁰.

composition. The fact that we observed a resonance of about the same height and at about the same place tends to give increased reliability to our result that the resonance is in Pu^{240} .

I should point out that we have only calculated values of these isotopic contents, so that the small disagreement in the abscissa that we observe we do not consider to be very important. If one does an area analysis on this curve, although it is not strictly valid, one gets a true peak fission cross section of about 35 barns, and assuming that the 1-ev resonance is responsible for

all of the thermal fission cross section, as it is for the absorption cross section, this predicts a value of only 0.05 barn for the thermal fission cross section of Pu^{240} .

(Editors' Note: Dr. Leonard also spoke about recent Pu^{241} fission-cross-section measurements. However, since the conference, a mass-spectrometric analysis of the foil showed that there was an appreciable amount of Pu^{239} in the sample. Hence, the fission data must be corrected for the Pu^{239} contribution, and they are not included in this report.)

ASYMMETRY OF RESONANCE LEVELS IN FISSILE TARGET NUCLEI

P. A. Egelstaff N. Pattenden
Atomic Energy Research Establishment, Harwell

P. A. EGELSTAFF: The asymmetry of the resonance levels of fissile nuclei is explained either as the superposition of a number of levels of normal shapes or through interference between neighboring levels. Since we don't really know the distribution of spacings and widths and various other factors, we can mix levels together and get a fit to almost any shape we like. Thus the only way to get an answer to this problem on the shape basis is to do some kind of statistical analysis, whereby you hope to show that the probability of getting a particular shape is very low if you take symmetrical resonances and add them up, but it is high if you take interference. At the present stage of development we just don't have sufficient data with which to adopt this approach. The present experiments are designed to improve this situation, and I will give a progress report on them.

The probability that one is observing a single resonance is greatest if one looks at the very top of the resonance and confines the measurements

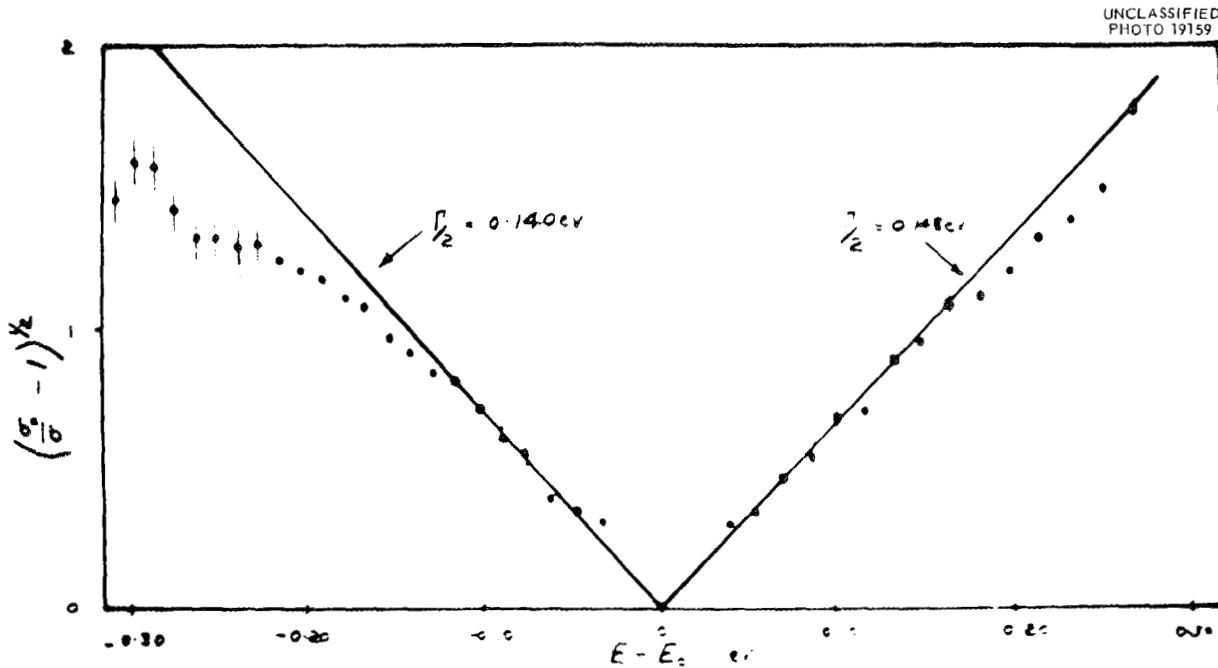
to as small a region as possible. Thus our method is to examine the cross section in great detail from $-\Gamma/2$ to $+\Gamma/2$. This is a region which has not been studied in great detail by other people. The observations are corrected for minor things, such as the $1/v$ variation, the Doppler effect, etc. Then we write the Breit-Wigner formula as:

$$(1) \quad \left(\frac{\sigma_0}{\sigma} - 1 \right)^{1/2} = \frac{2}{\Gamma} (E - E_0) .$$

You get two straight lines with equal slopes in the form of a V if you have a symmetric shape.

The results on the Pu^{239} resonance at 0.3 ev show two lines with equal slope, but the data outside the $\pm\Gamma/2$ range are up on the low-energy side and down on the high-energy side. There is thus some indication of a departure from the single-level Breit-Wigner shape.

Slide 1 shows a similar plot for the U^{233} 1.78-ev resonance. Here you can see that we get nice



Slide 1. "V-Plot" for the 1.78-ev Resonance of U^{233} . See text.

lines on the two sides through the points which are about $\Gamma/4$ away from the resonance. But the two lines give different values for Γ , and there is a very severe dip on the low-energy side. This checks with previous measurements of this cross section. We feel that in this case there is strong evidence for another resonance coming in at 1.53 ev, but there could well be substantial interference or maybe a third resonance.

To interpret the V-plots, a number of theoretical ones have been calculated. If, for example, you have a large and a small resonance so close that their sum has a single maximum, then you will get two lines with different slopes, but they will be straight lines to a fair approximation. If you have an interference term plus a normal Breit-Wigner term, then you get two lines of different slopes, but just outside the $\pm\Gamma/2$ range they bend over.

What one has to do is identify which is the most probable fit in as many cases as possible, and then do a statistical analysis to decide which, on the average, is the most reasonable explanation for the observed asymmetries.

As a check we have done the same thing for rhodium (1.26-ev level), and, in fact, the result

one gets is in excellent agreement with the Breit-Wigner formula.

H. H. LANDON: May I ask you how you have chosen E_0 for this?

P. A. EGELSTAFF: Due to the shortage of time I didn't explain this point in detail. Experimentally, σ_0 is defined as the maximum observed cross section and E_0 as the energy corresponding to it. The determination is made from the points within just a few per cent of the maximum cross section. Suppose you wish to compare the experimental V-plot with a theoretical one representing an interference case (say):

$$(2) \quad \sigma_i = \frac{1}{1+x^2} + \frac{x}{1+x^2} .$$

Then you work out the maximum value of σ_i and the energy corresponding to it. These theoretical values of σ_0 and E_0 , together with the values of σ_i from Eq. 2, are inserted into Eq. 1, and the theoretical V-plot is obtained. In a similar way a theoretical V-plot for two closely spaced levels is calculated.

INITIAL RESULTS ON THE FISSION CROSS SECTION OF U^{233}

L. G. Miller R. M. Brugger R. G. Fluharty
Phillips Petroleum Company

R. G. FLUHARTY: The work that I have to report tonight covers quite a large area, so I will try to go through it pretty rapidly.

We have been concentrating at MTR on the fission cross section of U^{233} using two instruments. We have a crystal spectrometer that goes up to 10 ev, and we have a fast chopper that extends the energy range to 5000 ev. The talk on the fast chopper represents a progress report on preliminary results. We are doing the fission cross section on both the chopper and crystal spectrometer, and η measurements on the crystal spectrometer. The fast-chopper fission measurements are being made with a resolution of 0.12 $\mu\text{sec}/\text{m}$. The crystal spectrometer has about 1.0 $\mu\text{sec}/\text{m}$ for the η data and 0.08 $\mu\text{sec}/\text{m}$ for fission.

I think the really interesting thing that we would like to discuss is interference. Our philosophy on this subject is a little different. We do not wish to argue about whether we are proving that we have interference or not, but only wish to try something to see how it works. We feel that one expects to see interference among the levels. Our point of view is based on the level spacing in those nuclei, particularly U^{235} and U^{233} , in which the width of some of the levels is of the order of 0.2 to 0.3 ev and the average distance between the levels is of the order of 0.7 ev. Also, we assume that the number of fission channels is limited. We feel that under these circumstances the Porter-Feshbach approximation is not valid, and particularly we feel that the single-level Breit-Wigner formula is not expected to be valid.

On this basis, C. W. Reich and M. S. Moore have started fitting the data using a multilevel formula based on the Wigner-Eisenbud formulation. This multilevel formula is programed for as many as 14 interfering levels on an IBM-650.

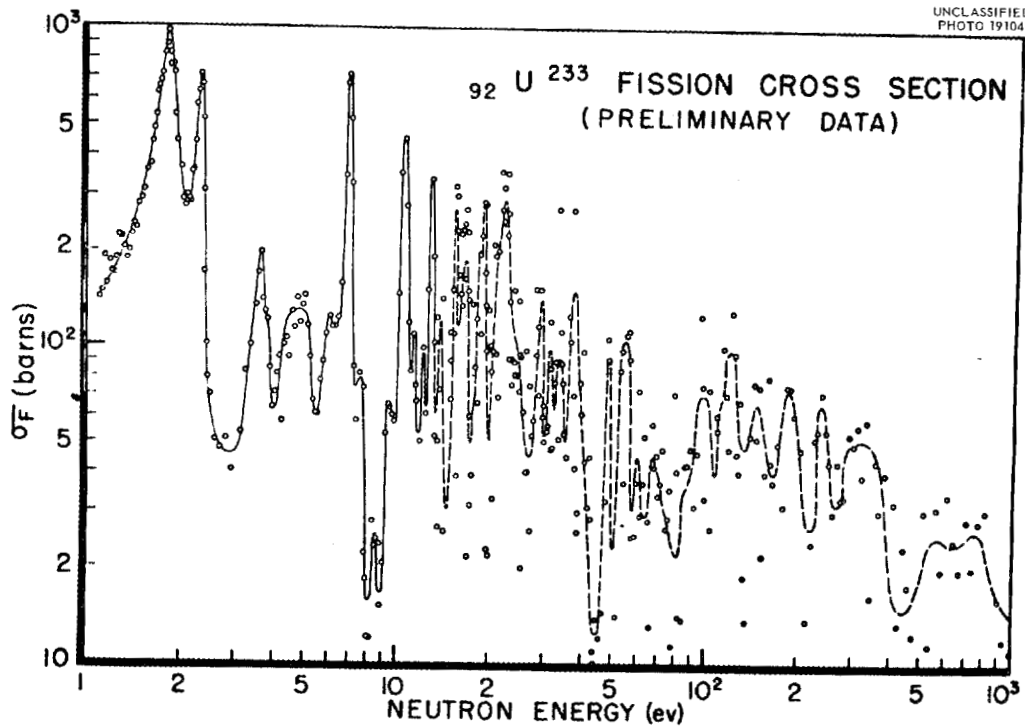
The first slide shows the fission cross section obtained on the fast chopper. The observed resonance energies are in good agreement with total-cross-section data reported by Sailor and by Harvey and Sanders.

A comparison between the crystal-spectrometer data and the chopper data is shown in Slide 2.

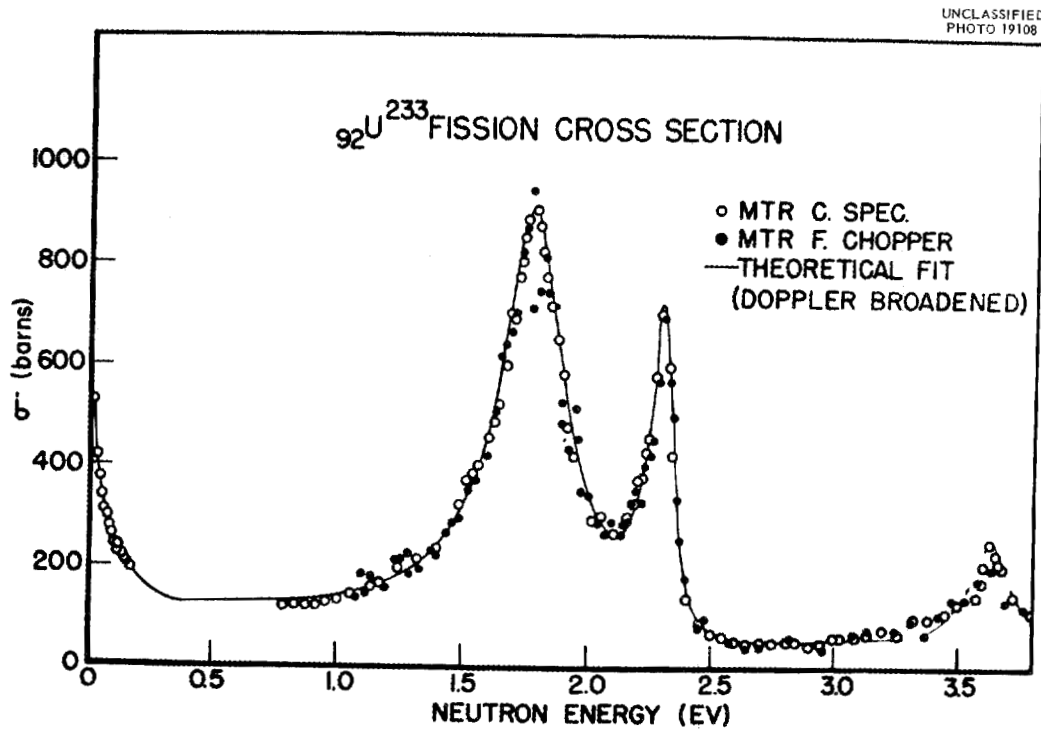
The agreement is considered to be within the errors. The chopper data are normalized to those of the crystal spectrometer between resonances. A thin BF_3 monitor is used to carry this normalization to other energies. The solid line is the theoretical fit (Doppler- and resolution-broadened) that has been obtained for the data using the multilevel formula. You can see that there is a slight disagreement in the 3.6-ev region. We have the impression that the fitting improves considerably the more levels one puts in, that is, the effects of a given level can be appreciable over an energy region large compared with the level spacing. The 1.8- and 2.3-ev levels are a typical case of interference between two levels, in that one observes a fullness between the levels and a drop-off on the high side of the 2.3-ev level. However, on the low-energy side of the 1.8-ev level there is a fullness which is not accounted for by the two-level interference as proposed. In order to account for this fullness, a weak interfering level is postulated at about 0.3 ev plus a very strong level at -5 ev.

There are some really puzzling things going on. There is a large thermal cross section, which still cannot be accounted for by any reasonable parameters that we have chosen for observed levels. This large cross section cannot be explained by any type of fitting, such as a single-level fitting, that has been done previously. It appears necessary to premise a very large negative energy level, and in this case it would be a non-interfering level. This might be more acceptable if the same situation did not exist in U^{235} and Pu^{239} .

The η data are being taken by J. R. Smith and E. H. Magleby on the crystal spectrometer. A combination of their data, data from Brookhaven (Palevsky), and data from Harwell (Sanders), which are unpublished, is shown in Slide 3. The solid curve is then predicted from the multilevel fit assumed. We feel that the dip in η at approximately 0.3 ev is explained by the weak level assumed. The theoretical fit to the higher-energy data is not very satisfactory. The multilevel fitting is preliminary, and the scattering corrections



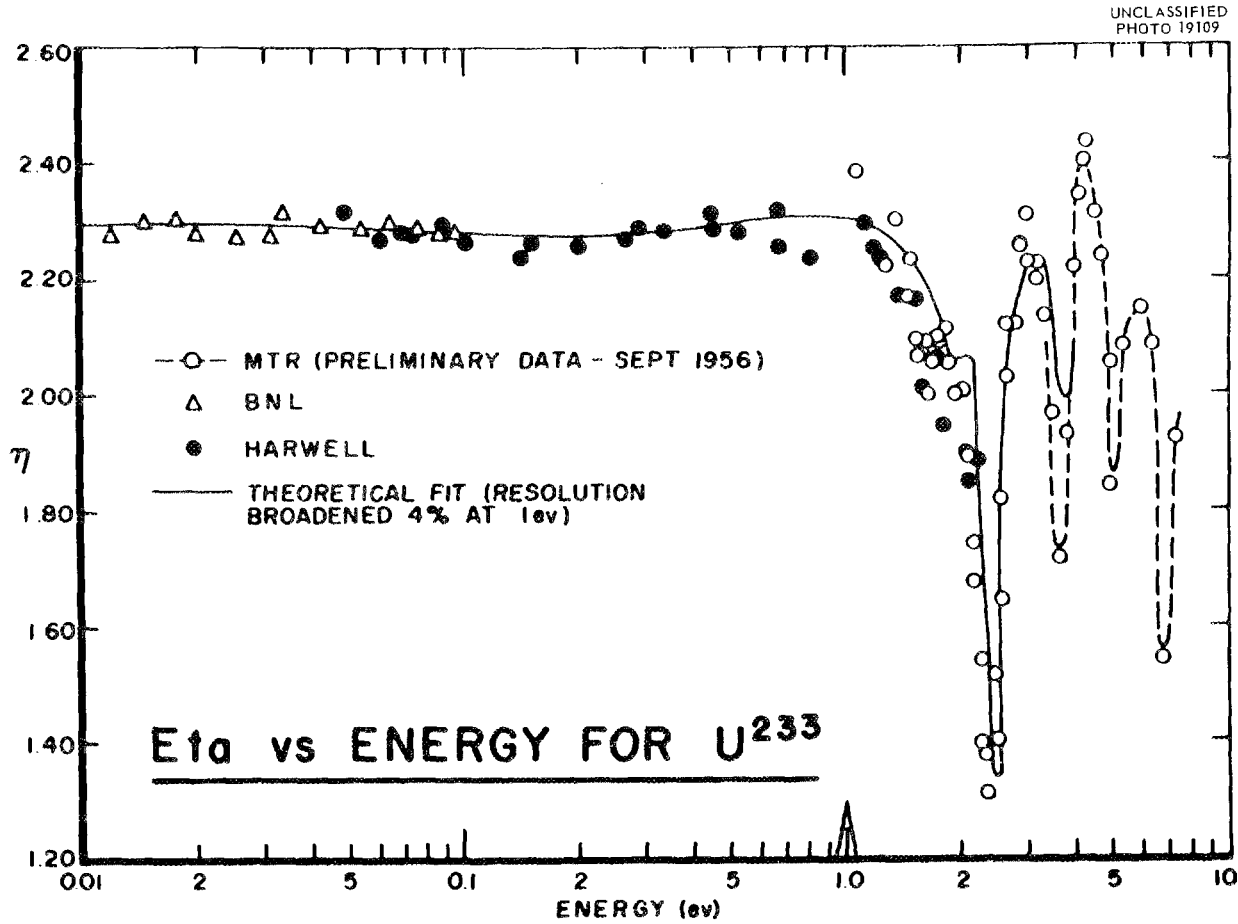
Slide 1. Fission Cross Section of U^{233} from Initial Runs on the MTR Fast Chopper, Taken with a Resolution of 0.12 sec/m.



Slide 2. Comparison of the Fission Cross Section of U^{233} Measured by the MTR Crystal Spectrometer and Fast Chopper.

required for η are fairly severe and add uncertainties. Note that in many cases η has a slope as it crosses E_0 . This is very easily explained if one assumes that interference is present in going across the level. In turn, the η data can be used as a basis for picking the relative sign of the amplitude of the scattering matrix that is used in the multilevel fit.

It has been said that if you are given enough parameters you can fit anything. To reduce arbitrariness, two extreme assumptions have been made. We have assumed one fission channel only, and we have assumed that all the levels are of the same spin state. We feel that this approach has great promise in accounting for the observed cross sections.



Slide 3. Eta Measurements from the MTR Crystal Spectrometer, Brookhaven (BNL-325) and Harwell (unpublished).

FISSION AND CAPTURE CROSS SECTION OF U^{235} FOR SLOW NEUTRONS

F. J. Shore V. L. Sailor
Brookhaven National Laboratory

H. MARSHAK: The Columbia University fission chamber is being used with the Brookhaven National Laboratory crystal spectrometer (resolution ≈ 0.17 $\mu\text{sec/m}$) to measure the fission cross section of U^{235} . The total cross section of U^{235} has previously been measured by V. L. Sailor on the same spectrometer with identical resolution.

Objectives of this experiment are, first, to study fission resonances with enough precision to see if their shape can be explained in terms of a single-level Breit-Wigner formula or in terms of a many-level formula; second, to determine by methods of shape analysis the basic parameters which enter the single-level-type formula, namely, E_0 , Γ , Γ_γ , $\Gamma_{F'}$, and σ_{0F} for as many resonances as practicable within the energy range studied. If a many-level formula is needed to fit the data, this would be evidence for interference between resonances, which would imply that a limited number of channels were available for fission in U^{235} .

Data have been accumulated on the ratio of the fission count rate to that in a thin BF_3 counter for incident neutrons of varying energy. At present the range from 0.25 to 10 ev has been studied using the reflections from the Be (1231) planes. For energies below 0.25 ev, the NaCl (240) planes will be used. The data are being analyzed, including corrections due to the effects of second-order contamination and of attenuation caused by material between the U^{235} and the incident-neutron beam.

Our uncorrected data are in good agreement with the fission data of B. Leonard *et al.* from 0.25 to 0.5 ev, when normalized at 0.30 ev. Using the

Hanford fission data from 0.1 to 0.5 ev, the total-cross-section data of Sailor, and the scattering data of H. Foote, one obtains by subtraction the capture cross section as a function of energy. Using the parameters of Sailor for the other capture resonances, their contribution can be estimated in this energy range. On subtraction there results the capture cross section for the 0.29-ev resonance, which on a plot of $\sigma_c\sqrt{E}$ is found to be symmetric, that is, Breit-Wigner, in shape.

By subtracting the fission contribution due to other resonances (as calculated from the parameters of Sailor) from the measured fission cross section, one obtains an asymmetrical curve. This curve, representing the 0.3-ev resonance, can further be decomposed into the sum of a symmetrical curve and an interference-type curve. Both the symmetrical fission and capture curves are centered at $E_0 = 0.286$ ev.

A similar analysis on the 1.14-ev resonance likewise shows asymmetry in the fission part, but symmetry in the capture part.

Since several small corrections have not yet been applied to the data, one hesitates to derive values for Γ_γ , $\Gamma_{F'}$, etc. However, the trend of the data suggests qualitatively that a multilevel formula must be invoked for the fission contribution to the total cross section.

Comparison of our raw data with the results of previous workers suggests substantial agreement in σ_F from 0.25 to 1.5 ev. At higher energies, we get higher values at the resonance peaks and lower values in the dips than Yeater, Mills, and Gaerttner did, for example.

VELOCITIES OF COINCIDENT PAIRS OF FRAGMENTS IN THE SPONTANEOUS FISSION OF Cf^{252}

J. S. Fraser J. C. D. Milton
Atomic Energy of Canada Limited, Chalk River

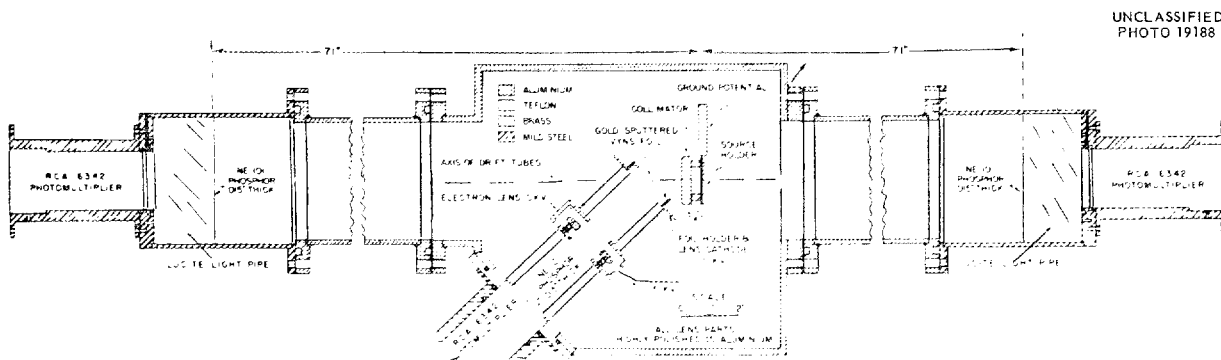
J. S. FRASER: The work I am going to describe is part of a program undertaken to study the energetics of fission with improved energy resolution. The results that I am going to show are of a preliminary nature, but I would like to outline the method and discuss the results that can be obtained from this sort of work.

A diagram of the apparatus is shown in the first slide. The source is mounted on a very thin plastic foil, so that fragments can emerge from both sides with negligible loss of energy. One of the difficulties with this type of measurement is to obtain a zero-time signal which is nonselective, that is to say, that does not select one type of fission mode in preference to another. An obvious way of getting a signal which is sufficiently prompt would be to detect fission neutrons or gamma rays. But it is the correlation of the probability of these radiations with fission mode that one wants to study. So following a suggestion by Leachman, of Los Alamos, we have developed a means of producing a fast zero-time signal which takes only a negligible amount of energy from one of the fragments. This involves detecting the secondary electrons ejected by the fragment as it passes through a thin foil. The secondary electrons, or delta rays, are accelerated to 10 keV and focused by a lens onto a thin plastic phosphor. The transit time in this lens system, which is about 6 in. long, is calculated to be about $4 \mu\text{sec}$. The fluctuation in the transit time should be small,

as we are using only the central portion of this foil.

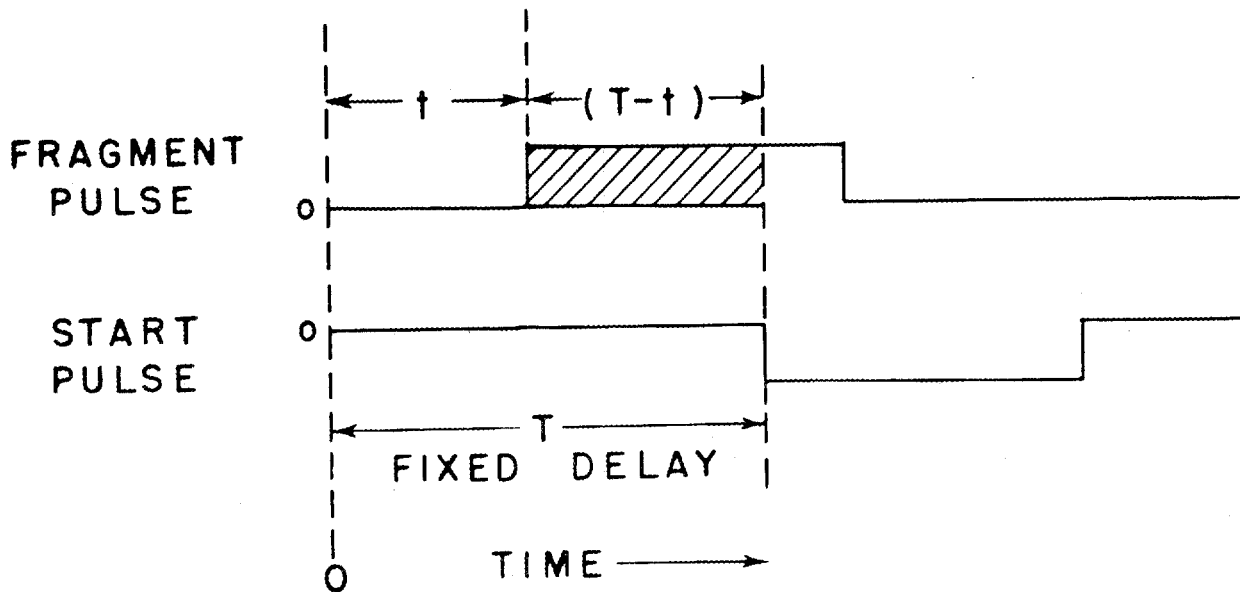
Fragments that pass through the foil then continue on down the tube and are detected in a 4-in.-dia phosphor. The complementary fragments penetrate the source backing and travel an equal distance to a similar detector. The time intervals, then, between this start pulse and the two detector pulses are converted to pulse amplitude. Slide 2 shows schematically how this is done. The start pulse is delayed a fixed time T and shaped into a negative pulse. The pulse from the remote counter is made positive and applied to one grid of a 6BN6 tube. Constant current flows until the delayed start pulse turns the current off. The pulse formed by integrating the anode current is, then, proportional to $(T - t)$, where t is the time of flight of the fragment. The presentation is on an inverse velocity scale. The observed time-resolution curve is about $7 \mu\text{sec}$ wide at half maximum.

Slide 3 shows our method of recording the data. The fast signals from the photomultipliers are fed into two time sorters - time analyzers - and in the work done to date we have observed gamma rays in coincidence with the velocity-selected fragments. The gamma rays are detected in a 4-in.-dia NaI crystal placed as close as possible to the spontaneous-fission source. The three pulse heights are measured on a 100-channel analyzer, and in order to preserve the correlation

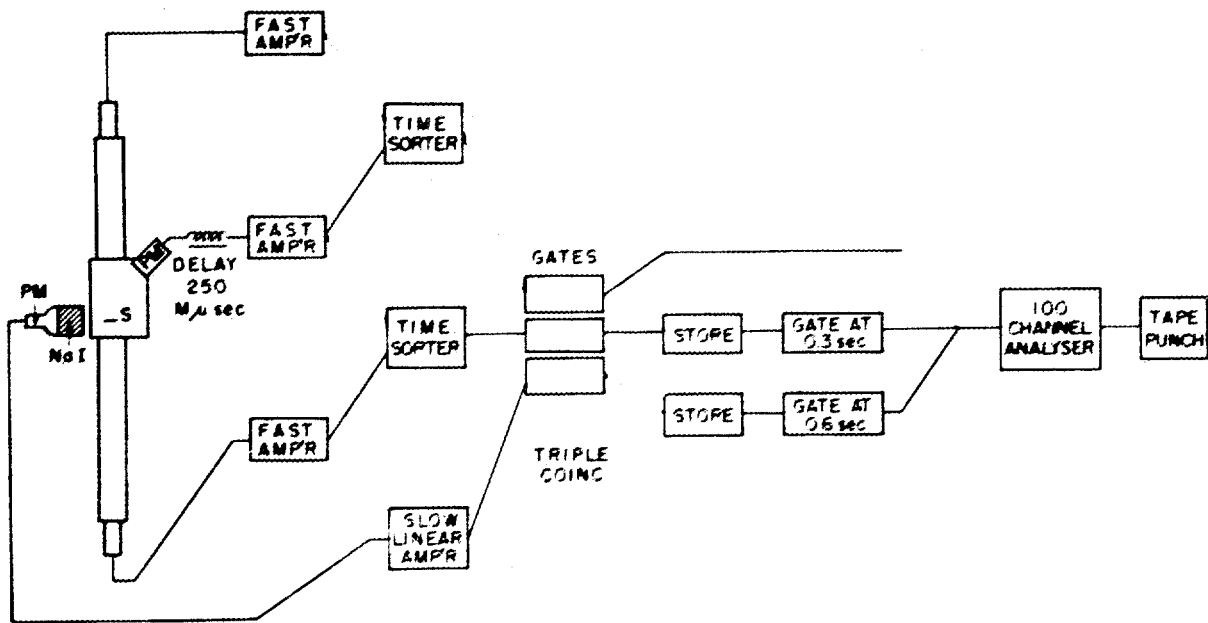


UNCLASSIFIED
PHOTO 19188

Slide 1. Apparatus for Fission Experiment.



Slide 2. Detector Pulses as Applied to 6BN6 Time-to-Height Converter.



FISSION FRAGMENT TIME-OF-FLIGHT & γ -RAY ENERGY

Slide 3. Block Diagram of Electronic Apparatus.

the three pulses are recorded in sequence on punched tape. The data then are transferred from the tape to cards for sorting and tabulating.

We have made provision for measuring neutron time-of-flight with this apparatus, and a third time sorter is available. The neutron time-of-flight involves a further solid-angle restriction, and since we have to date worked only with a spontaneous-fission source the counting rate is prohibitively low, but we have plans for this in the future.

Slide 4 shows a contour diagram or topographical map for Cf^{252} . From this plot one can obtain various quantities such as the most probable total energy, mass-ratio distribution, and so on.

In Slide 5 are shown some of the plots obtained from the complete set of data. The solid circles are the mass-ratio distribution. This curve is somewhat wider than that obtained by radiochemical analysis, but we feel quite sure the discrepancy is largely due to the thickness of the source. The X's show the variation of the average total kinetic

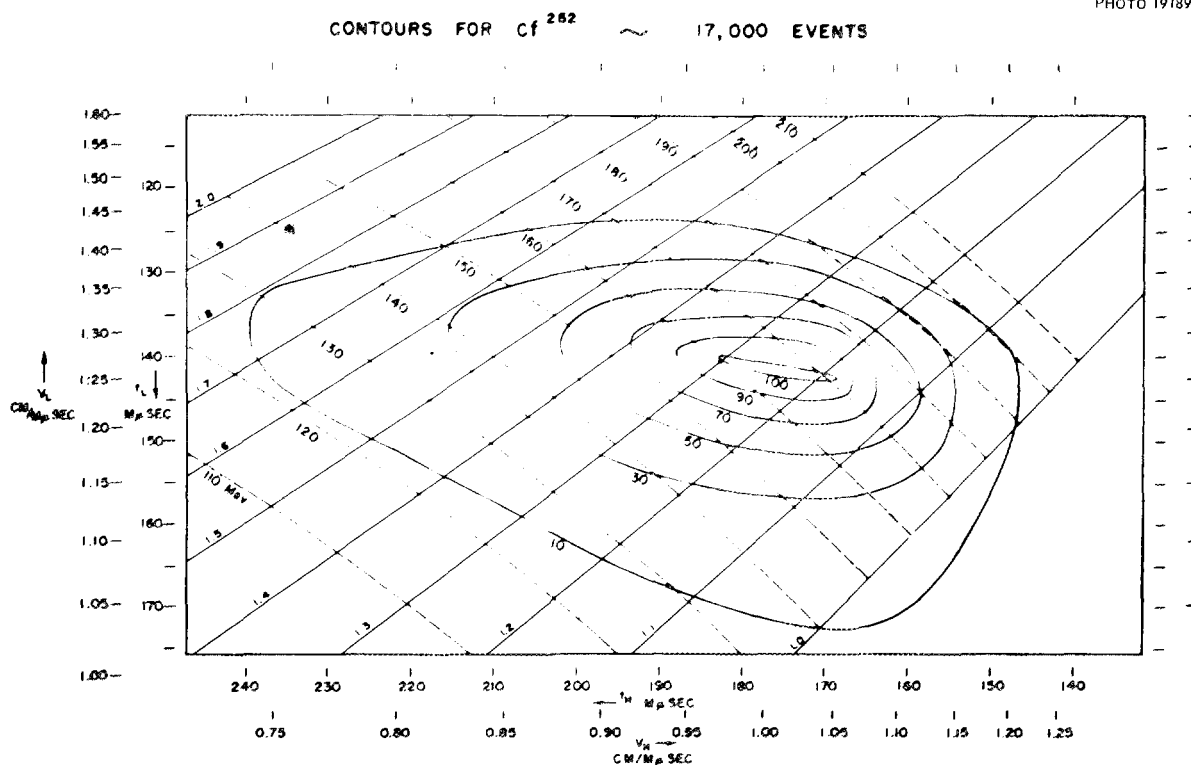
energy with mass ratio. The dip at low mass ratios that is usually found in ion-chamber measurements is not present here, but again we are not certain that this is a real effect.

In principle our method of taking the data would allow us, if we were patient enough, to obtain a gamma-ray spectrum for each resolved fission mode; but the number of events we have to date is too small to permit this. It is apparent, however, that the gamma-ray yield is independent of mass ratio. The ratios of number of gamma rays to fission events are plotted as open circles.

J. A. WHEELER: Is there any prospect of measuring the average total kinetic energy curve with other spontaneous-fissionable materials?

J. S. FRASER: One of the difficulties with that is that the alpha-to-fission ratio goes up very rapidly as one goes to lower-mass spontaneous-fission nuclei. One would probably have an intolerable background due to the alpha particles. However, if one had a detector which wasn't sensitive to alpha particles, this would be feasible,

UNCLASSIFIED
PHOTO 19189



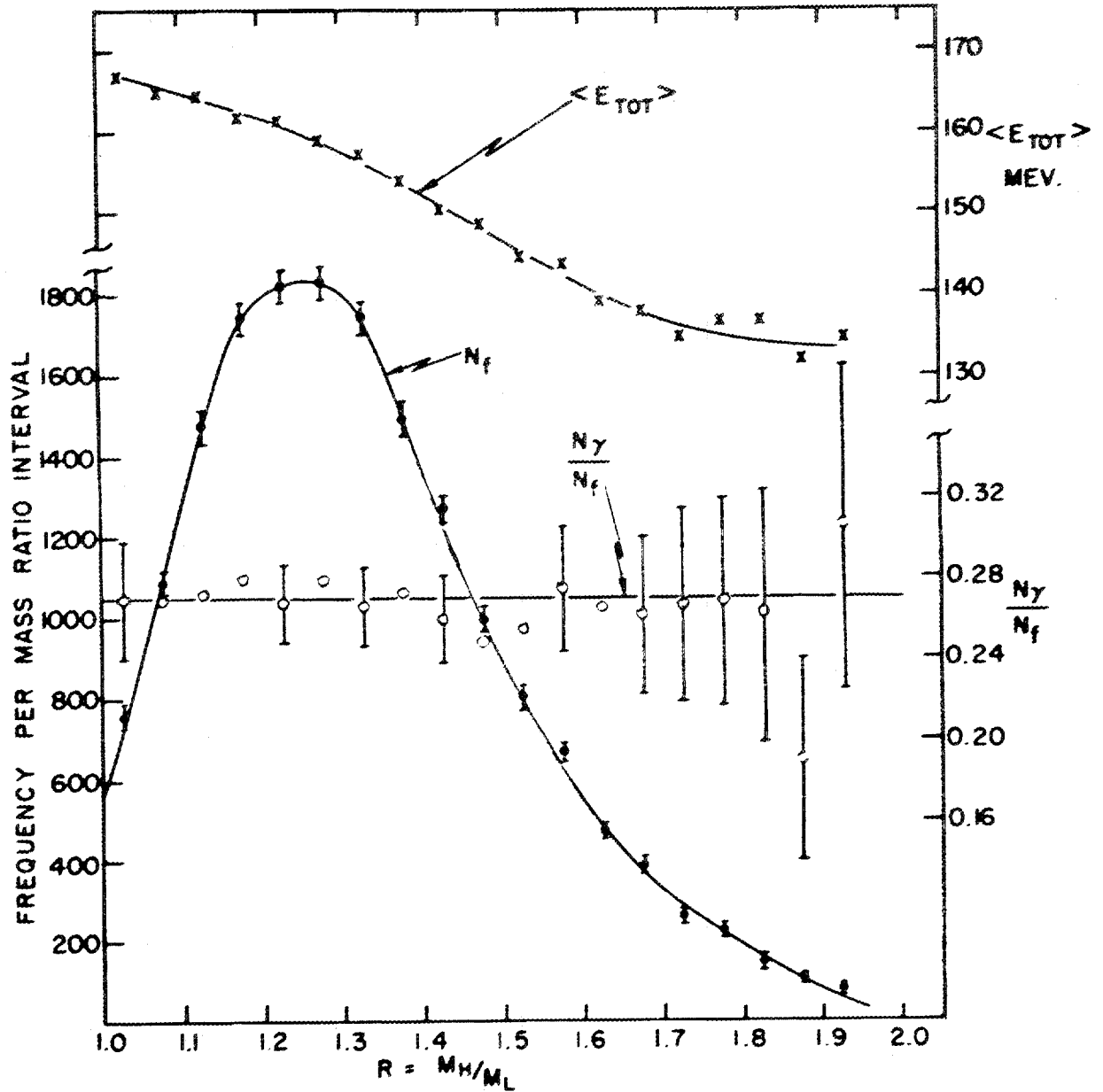
Slide 4. Fission Fragment Contour Diagram for Cf^{252} .

I think. The heavier nuclei have too short half lives for this type of work.

H. W. SCHMITT: Do you have a figure yet for the total gamma-ray energy liberated per fission?

J. S. FRASER: No, we have not measured this, but I believe that a measurement made at Livermore gives about 9 Mev for the total gamma-ray energy in californium.

UNCLASSIFIED
PHOTO 19186



Slide 5. Distributions for $\langle E_{tot} \rangle$, N_f , and N_γ/N_f vs M_H/M_L .

RESONANCE PARAMETERS OF U^{235}

R. B. Schwartz

Brookhaven National Laboratory

R. B. SCHWARTZ: I should like to give a brief rundown of the status of the resonance parameters of U^{235} . The general problem at Brookhaven was to determine parameters for as many levels as we reasonably could, using Brookhaven fast-chopper total data, and fission data from wherever we could get it. The first thing we had to do was to determine Γ_γ , the radiation width. This was done by analyzing both the total- and fission-cross-section data for those levels where precise measurements were available. Using data available to the Brookhaven Compilation Group from the United States, United Kingdom, and the Soviet Union, a "shape" method of analysis was used for the 0.3- and 1.1-ev levels, and area analysis was used for the 2.0- and 4.8-ev levels to get $2g\Gamma_n$, Γ_F , and Γ_γ for these levels. The weighted average Γ_γ turned out to be 33 ± 3 mev (milli-electron volts), which fits the general trend of Γ_γ 's for elements in this region.

The next thing that we had to do was determine Γ_F for as many levels as we could, and here all we could do with our own data was measure a total Γ and subtract the value of Γ_γ and Γ_n to get Γ_F . In this way, in addition to the values for the four low-lying levels, we were able to get Γ_F 's for another eight levels. The trouble with this method of getting Γ_F 's is that, if the Γ_F is small, say compared with Γ_γ , then you are subtracting two relatively large numbers to get a small number, and the error is relatively large. Fortunately, for four levels in U^{235} we were able to use some of the KAPL fission data. Their $\sigma_0\Gamma_F$ combines with our total Γ and $2g\Gamma_n$ in a multiplicative rather than an additive way, so that for small Γ_F 's the errors don't pile up quite so rapidly. It is encouraging to see that we get essentially the same results using KAPL data mixed in with our data as with just our own data. The best example is the 11.7-ev resonance in U^{235} , where using just the Brookhaven data we get a Γ_F of 6 ± 19 mev, which does not mean very much. Using the value for $\sigma_0\Gamma_F$ from KAPL we

get 6 ± 3 mev. So, all in all, by hook or by crook, we have 12 Γ_F 's, of which eight have probable errors of less than 50%.

Slide 1 shows the distribution of Γ_F 's, which seems to follow an exponential, with an average of 50 ± 15 mev.

Slide 2 shows the observed level spacing, and we multiply it by 2 to get the level spacing per spin state, assuming that both spins are present. The fact that the observed levels fall away from the straight line at about 20 ev is taken as an indication that above that energy we are starting to miss levels, and so parameters for levels above 20 ev are not taken into account in determining the distribution of Γ_F 's or Γ_n 's.

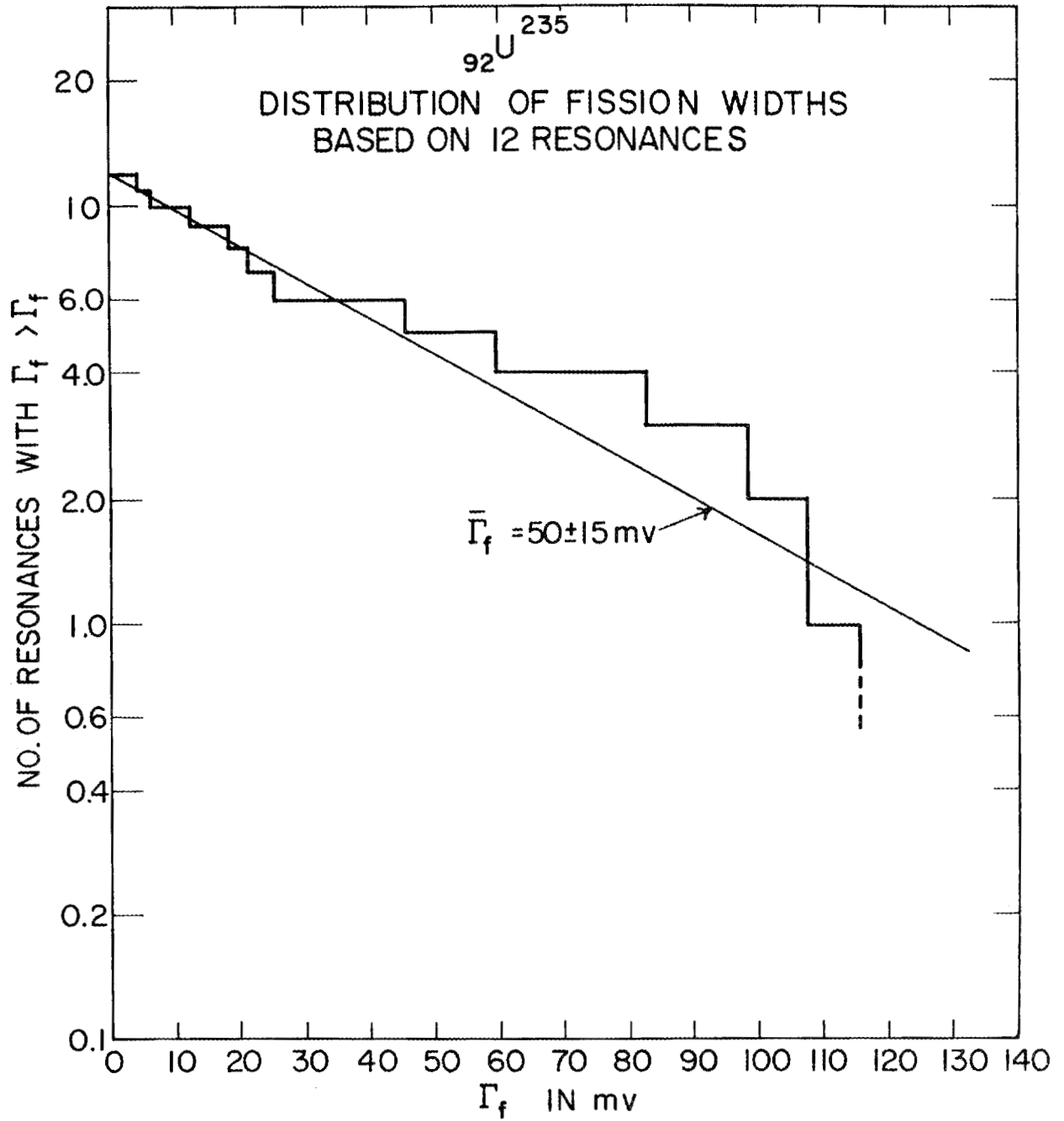
The Γ_n distribution follows close to an exponential with an average Γ_n of 0.09 ± 0.02 mev. The distribution does not follow an exponential quite as well as the Γ_n 's that have been measured for nonfissionable nuclei. There seems to be a surplus of both very small and very large levels, and it seems to be closer to a Porter-Thomas distribution.

Slide 3 shows the value of $\overline{\Gamma_n^0}/D$ obtained in the usual way. We get $(0.9 \pm 0.2) \times 10^{-4}$, which is in very good agreement with the $\overline{\Gamma_n^0}/D$ obtained by both this method and the averaging in the kilovolt region for all the isotopes of uranium, plutonium, or thorium.

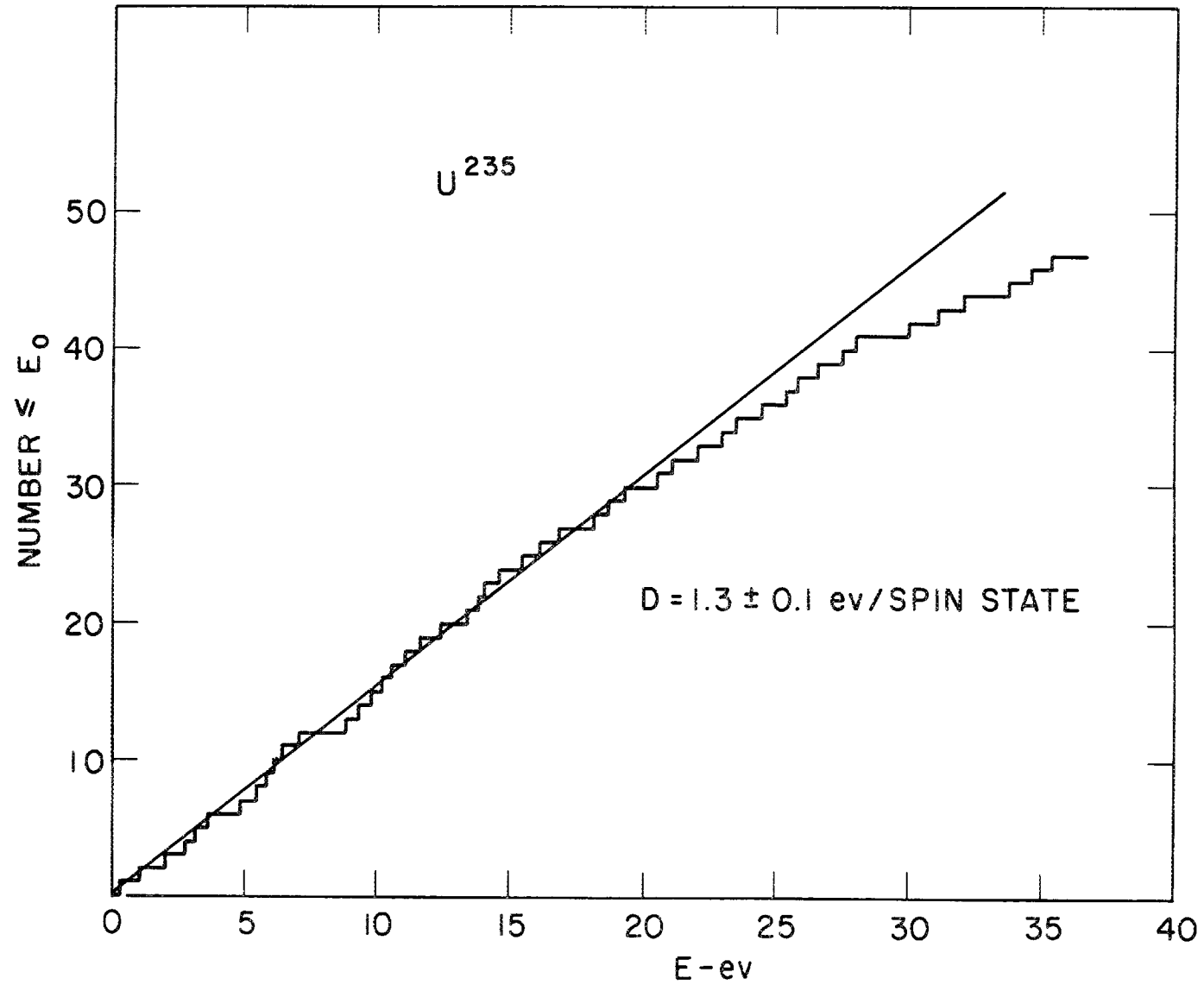
L. A. TURNER: I will take it upon myself to state what I am sure all the rest of you are thinking, namely, that we are extremely grateful to our hosts, Oak Ridge National Laboratory, for this excellent meeting. We appreciate the hard work that has gone into planning it and carrying it out.

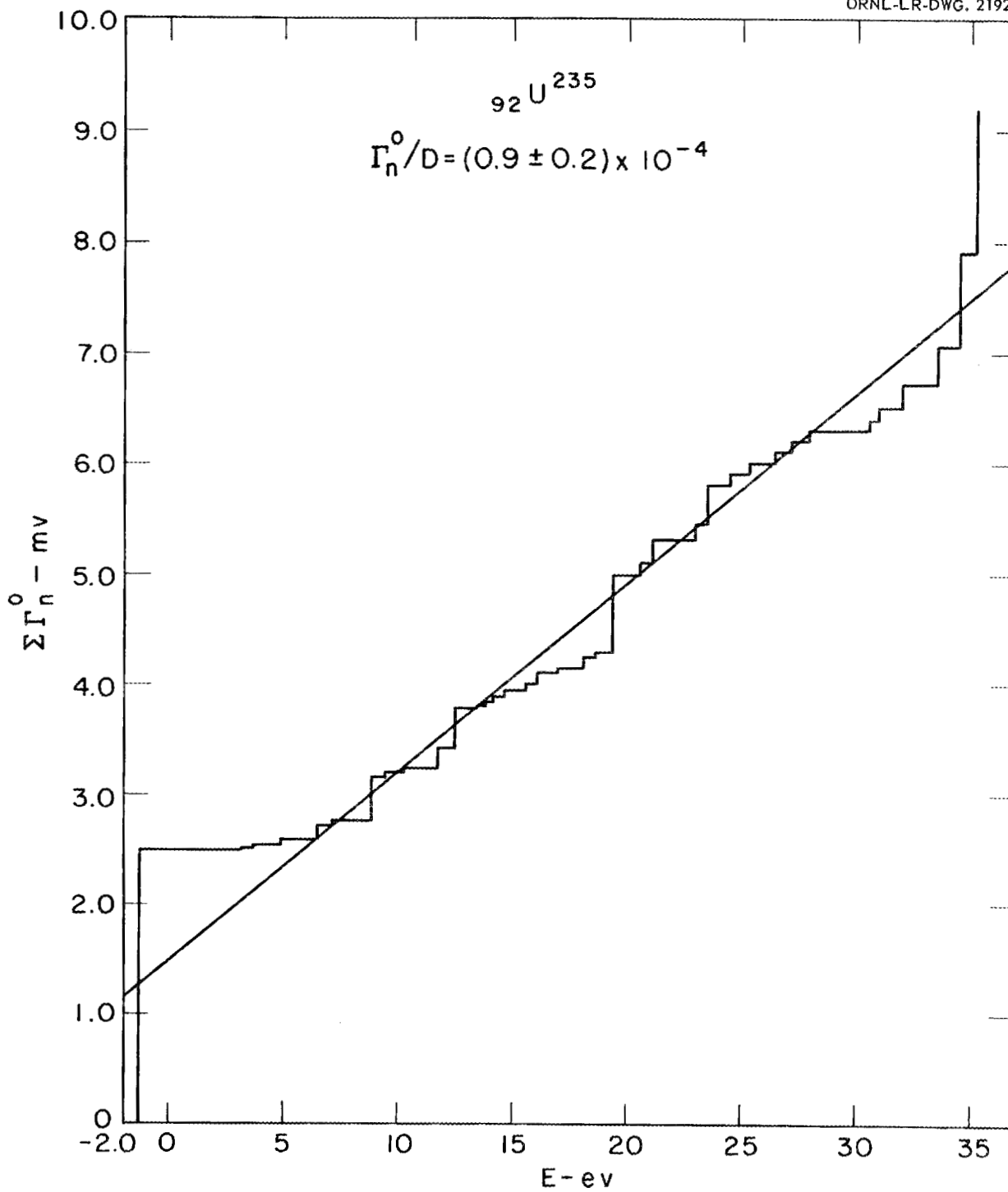
I think I remarked on a previous occasion here that it seems easy. They appear to do it effortlessly, but if you have ever tried it yourself you appreciate that it is a somewhat complicated job beautifully done.

We thank them very much for their hospitality.



Slide 1. Distribution of Fission Widths Based on 12 Resonances in ${}_{92}\text{U}^{235}$.

Slide 2. Level Spacing for U²³⁵.



Slide 3. Determination of Γ_n^0/D for U^{235} .

LIST OF PARTICIPANTS

C. P. Baker
Brookhaven National Laboratory
Upton, L.I., New York

C. A. Barnes
California Institute of Technology
Pasadena, California

R. L. Becker
University of Kentucky
Lexington, Kentucky

S. Bernstein
Oak Ridge National Laboratory
Post Office Box X
Oak Ridge, Tennessee

R. C. Block
Oak Ridge National Laboratory
Post Office Box X
Oak Ridge, Tennessee

C. K. Bockelman
Yale University
New Haven, Connecticut

L. M. Bollinger
Argonne National Laboratory
Post Office Box 299
Lemont, Illinois

R. Bondelid
Naval Research Laboratory
Washington 25, D.C.

E. Bretscher
Atomic Energy Research Establishment
Harwell, Didcot, Berkshire
England

R. M. Brugger
Phillips Petroleum Company
Idaho Falls, Idaho

E. C. Campbell
Oak Ridge National Laboratory
Post Office Box X
Oak Ridge, Tennessee

B. L. Cohen
Oak Ridge National Laboratory
Post Office Box X
Oak Ridge, Tennessee

L. Cohen
Naval Research Laboratory
Washington 25, D.C.

H. O. Cohn
Oak Ridge National Laboratory
Post Office Box X
Oak Ridge, Tennessee

R. E. Coté
Argonne National Laboratory
Post Office Box 299
Lemont, Illinois

L. Cranberg
Los Alamos Scientific Laboratory
Post Office Box 1663
Los Alamos, New Mexico

R. B. Day
Los Alamos Scientific Laboratory
Post Office Box 1663
Los Alamos, New Mexico

J. E. Draper
Yale University
New Haven, Connecticut

K. Dunning
Naval Research Laboratory
Washington 25, D.C.

P. A. Egelstaff
Atomic Energy Research Establishment
Harwell, Didcot, Berkshire
England

L. G. Elliott
Atomic Energy of Canada Limited
Chalk River
Ontario, Canada

W. K. Ergen
Oak Ridge National Laboratory
Post Office Box X
Oak Ridge, Tennessee

H. Feshbach
Massachusetts Institute of Technology
Cambridge 39, Massachusetts

R. G. Fluharty
Phillips Petroleum Company
Idaho Falls, Idaho

J. L. Fowler
Oak Ridge National Laboratory
Post Office Box X
Oak Ridge, Tennessee

J. S. Fraser
Atomic Energy of Canada Limited
Chalk River
Ontario, Canada

E. R. Gaertner
General Electric Company
Knolls Atomic Power Laboratory
Schenectady, New York

A. I. Galonsky
Oak Ridge National Laboratory
Post Office Box X
Oak Ridge, Tennessee

G. Gamow
University of Colorado
Boulder, Colorado

J. H. Gibbons
Oak Ridge National Laboratory
Post Office Box X
Oak Ridge, Tennessee

D. Gilbert
U.S. Atomic Energy Commission
Washington 25, D.C.

G. N. Glasoe
Brookhaven National Laboratory
Upton, L.I., New York

H. Goldstein
Nuclear Development Corporation of America
5 New Street
White Plains, New York

W. M. Good
Oak Ridge National Laboratory
Post Office Box X
Oak Ridge, Tennessee

C. D. Goodman
Oak Ridge National Laboratory
Post Office Box X
Oak Ridge, Tennessee

A. E. S. Green
Florida State University
Tallahassee, Florida

W. G. Guindon
Boston College
Chestnut Hill, Massachusetts

E. Guth
Oak Ridge National Laboratory
Post Office Box X
Oak Ridge, Tennessee

W. Haeberli
University of Wisconsin
Madison, Wisconsin

J. A. Harvey
Oak Ridge National Laboratory
Post Office Box X
Oak Ridge, Tennessee

W. W. Havens, Jr.
Columbia University
Pupin Physics Laboratory
New York 27, New York

R. E. Holland
Argonne National Laboratory
Post Office Box 299
Lemont, Illinois

D. J. Hughes
Brookhaven National Laboratory
Upton, L.I., New York

D. G. Hurst
Atomic Energy of Canada Limited
Chalk River
Ontario, Canada

R. Jastrow
Naval Research Laboratory
Washington 25, D.C.

C. H. Johnson
Oak Ridge National Laboratory
Post Office Box X
Oak Ridge, Tennessee

W. Y. Kato
Argonne National Laboratory
Post Office Box 299
Lemont, Illinois

B. D. Kern
University of Kentucky
Lexington, Kentucky

R. M. Kloepper
Los Alamos Scientific Laboratory
Post Office Box 1663
Los Alamos, New Mexico

W. Kofink
Oak Ridge National Laboratory
Post Office Box X
Oak Ridge, Tennessee

S. Krasner
Office of Naval Research
Washington 25, D.C.

E. Lampi
University of Minnesota
Minneapolis, Minnesota

H. H. Landon
Brookhaven National Laboratory
Upton, L.I., New York

A. M. Lane
Atomic Energy Research Establishment
Harwell, Didcot, Berkshire
England

J. LeBlanc
University of California
Radiation Laboratory
Livermore, California

H. W. Lefevre
General Electric Company
Hanford Atomic Products Operation
Richland, Washington

B. R. Leonard
General Electric Company
Hanford Atomic Products Operation
Richland, Washington

H. W. Lewis
Duke University
Durham, North Carolina

F. K. McGowan
Oak Ridge National Laboratory
Post Office Box X
Oak Ridge, Tennessee

R. L. Macklin
Oak Ridge National Laboratory
Post Office Box X
Oak Ridge, Tennessee

F. C. Maienschein
Oak Ridge National Laboratory
Post Office Box X
Oak Ridge, Tennessee

P. Malmberg
Naval Research Laboratory
Washington 25, D.C.

C. E. Mandeville
Bartol Research Foundation
Swarthmore, Pennsylvania

H. Marshak
Brookhaven National Laboratory
Upton, L.I., New York

E. Melkonian
Pupin Physics Laboratory
Columbia University
New York 27, New York

J. J. Meny
High Voltage Engineering Corporation
Cambridge, Massachusetts

C. D. Moak
Oak Ridge National Laboratory
Post Office Box X
Oak Ridge, Tennessee

R. C. Mobley
Louisiana State University
Baton Rouge, Louisiana

H. S. Morton
U.S. Atomic Energy Commission
Oak Ridge Operations
Oak Ridge, Tennessee

C. O. Muehlhause
Brookhaven National Laboratory
Upton, L.I., New York

M. P. Nakada
University of California
Radiation Laboratory
Livermore, California

J. H. Neiler
Oak Ridge National Laboratory
Post Office Box X
Oak Ridge, Tennessee

H. W. Newsom
Department of Physics
Duke University
Durham, North Carolina

S. Oleksa
Brookhaven National Laboratory
Upton, L.I., New York

H. Palevsky
Brookhaven National Laboratory
Upton, L.I., New York

W. C. Parkinson
University of Michigan
Ann Arbor, Michigan

R. W. Peelle
Oak Ridge National Laboratory
Post Office Box X
Oak Ridge, Tennessee

I. Pelah
Brookhaven National Laboratory
Upton, L.I., New York

A. M. Perry
Oak Ridge National Laboratory
Post Office Box X
Oak Ridge, Tennessee

D. D. Phillips
Los Alamos Scientific Laboratory
Post Office Box 1663
Los Alamos, New Mexico

L. A. Rayburn
Argonne National Laboratory
Post Office Box 299
Lemont, Illinois

G. L. Rogosa
U.S. Atomic Energy Commission
Washington 25, D.C.

M. E. Rose
Oak Ridge National Laboratory
Post Office Box X
Oak Ridge, Tennessee

M. A. Rothman
Bartol Research Foundation
Swarthmore, Pennsylvania

A. Saplakoglu
Argonne National Laboratory
Post Office Box 299
Lemont, Illinois

H. W. Schmitt
Oak Ridge National Laboratory
Post Office Box X
Oak Ridge, Tennessee

H. L. Schultz
Yale University
New Haven, Connecticut

R. B. Schwartz
Brookhaven National Laboratory
Upton, L.I., New York

R. E. Segel
Brookhaven National Laboratory
Upton, L.I., New York

K. K. Seth
Brookhaven National Laboratory
Upton, L.I., New York

E. F. Shrader
U.S. Atomic Energy Commission
Washington 25, D.C.

A. Simon
Oak Ridge National Laboratory
Post Office Box X
Oak Ridge, Tennessee

G. G. Slaughter
Oak Ridge National Laboratory
Post Office Box X
Oak Ridge, Tennessee

R. V. Smith
Westinghouse Research Laboratory
East Pittsburgh, Pennsylvania

W. H. Snedegar
University of Kentucky
Lexington, Kentucky

A. H. Snell
Oak Ridge National Laboratory
Post Office Box X
Oak Ridge, Tennessee

W. E. Stein
Los Alamos Scientific Laboratory
Post Office Box 1663
Los Alamos, New Mexico

P. H. Stelson
Oak Ridge National Laboratory
Post Office Box X
Oak Ridge, Tennessee

N. Tralli
Nuclear Development Corporation of America
5 New Street
White Plains, New York

L. A. Turner
Argonne National Laboratory
Post Office Box 299
Lemont, Illinois

M. Walt
Lockheed Aircraft
Palo Alto, California

B. Watt
Los Alamos Scientific Laboratory
Post Office Box 1663
Los Alamos, New Mexico

A. Wattenberg
Massachusetts Institute of Technology
Cambridge 39, Massachusetts

A. M. Weinberg
Oak Ridge National Laboratory
Post Office Box X
Oak Ridge, Tennessee

C. H. Westcott
Atomic Energy of Canada Limited
Chalk River
Ontario, Canada

J. A. Wheeler
Palmer Physics Laboratory
Princeton University
Princeton, New Jersey

E. P. Wigner
Palmer Physics Laboratory
Princeton University
Princeton, New Jersey

H. B. Willard
Oak Ridge National Laboratory
Post Office Box X
Oak Ridge, Tennessee

R. M. Williamson
Duke University
Durham, North Carolina

E. O. Wollan
Oak Ridge National Laboratory
Post Office Box X
Oak Ridge, Tennessee

C. Wong
University of California
Radiation Laboratory
Livermore, California

M. L. Yeater
General Electric Company
Knolls Atomic Power Laboratory
Schenectady, New York

I. F. Zartman
U.S. Atomic Energy Commission
Washington 25, D.C.

R. L. Zimmerman
Brookhaven National Laboratory
Upton, L.I., New York